DESIGN, SYNTHESIS, CHARACTERIZATION, AND APPLICATIONS OF FUNCTIONAL, POROUS, AND CROSSLINKED POLYMERS

Thesis Submitted to AcSIR For the Award of the Degree of

DOCTOR OF PHILOSOPHY

(In Chemistry)

By

SACHIN TANAJI MANE

(Registration Number: 10CC11J26095)

Under the guidance of

Dr. M. V. BADIGER

POLYMER SCIENCE AND ENGINEERING DIVISION

CSIR-NATIONAL CHEMICAL LABORATORY

PUNE-411008, INDIA

JULY 2015

CERTIFICATE

Certified that the work incorporated in this thesis entitled **"Design, Synthesis, Characterization, and Applications of Functional, Porous, and Crosslinked Polymers"** submitted by **Sachin Tanaji Mane** was carried out under my supervision. Such material obtained from other source has been duly acknowledged in this thesis.

July 2015

Pune

Dr. M. V. Badiger

(Research Guide)

Dr. S. Ponrathnam

(Co-Guide)

Dr. N. N. Chavan

(Co-Guide)

DECLARATION

I hereby declare that the thesis entitled **"Design, Synthesis, Characterization and Applications of Functional, Porous and Crosslinked Polymers"** submitted for the award of degree of **Doctor of Philosophy** in Chemistry to the Academy of Scientific and Innovative Research (AcSIR) has been carried out by me at the Polymer Science and Engineering Division of CSIR-National Chemical Laboratory, Pune under the supervision of Dr. M. V. Badiger. I also affirm that this work is original and has not been submitted in part or full by me for any other degree or diploma to this or any other university or institution.

Sachin T. Mane **July 2015**

CSIR-National Chemical Laboratory,

Pune

Acknowledgement

"Gratitude and affection sometimes cannot be expressed by mere words or sentences."

First and foremost, I am sincerely thankful to my research guide ***Dr. M. V. Badiger*** *for giving me opportunity to work under his guidance. His support helped me throughout during these years. Especially, I am thankful to my co-guide* ***Dr. S. Ponrathnam*** *and* ***Dr. N. N. Chavan*** *for his scientific guidance, suggestions, and encouragement related to this work. Besides this, I am extremely indebted to both for their kind care and concern in the laboratory. Most importantly, I would like to thank my* ***mother, father, and brothers.***

My deepest and sincere thanks go to ***Dr. C. R. Rajan*** *for his co-operation during the period of presented work. His meticulous approach to solving a problem was splendid. Working with him was always a pleasure. I wish to thank* ***Dr. D. Saini*** *for his valuable suggestions. I am sincerely thankful to* ***Dr. Smita Mule*** *and* ***Dr. Sunil Bhongale*** *for doing HPLC analysis. I am thankful to my senior lab members,* ***Dr. Sarika Deokar, Dr. R. Harikrishna, Dr. Abdul Wasif Shaikh, and Dr. R. V. Ghorpade.*** *I am also thankful to lab members* ***Ms. Archana Thorave, Ms. Sonali Bhosle, Mr. Kishor Rajdeo, and Ms. Asmita Thorave*** *and the people who helped me during Ph.D. work. I thank to* ***Mr. Shashikant Sathe*** *and* ***Mr. Lalan Giri*** *for their technical help. I especially thanks to my friends,* ***Khudbuddin Mulani, Mohasin Momin, Bhausaheb Tawade, and Nagnath Patil*** *for their help to complete this work.*

I wish to thank my external expert ***Dr. S. V. Lonikar, Solapur University*** *for giving valuable advice. I would like to thank DAC members,* ***Dr. Ravikumar, and Dr. S. Tambe, DAC chairman Dr. S. P. Chavan*** for their suggestions***.*** *I also gratefully acknowledge to the course work teachers,* ***Dr. S. K. Asha, Dr. A. V. Ambade, Dr. P. L. Dhepe, Dr. M. Shashidhar,*** *and* ***Dr. S. P. Chavan*** *for their knowledgeable and informative lectures.*

I would like to thank ***Dr. Mayadevi*** *for surface area analysis and* ***Mrs. D. A. Dhoble*** *for providing infrastructure like FTIR, thermal, UV analysis etc. I am greatly indebted to* ***Mr. Ketan*** *for SEM analysis.*

I would like to special thank to ***Dr. P. P. Wadgaonkar*** *for valuable discussions and suggestions during the period of this work.*

I am thankful to ***Dr. Ashish Lele,*** *Head, Polymer science and engineering division, National Chemical Laboratory, Pune.*

I am also thankful to Director, National Chemical Laboratory, Pune for providing infrastructure and permitting to submit the work in the form of thesis.

I feel very happy to express my sincere gratitude and appreciation to all the people who directly or indirectly contributed to my research work.

Finally, I would like to thanks University Grant Commission (UGC), New Delhi for the award of fellowship without which this research would not have been possible.

Sachin Tanaji Mane

DEDICATED TO,

MY MOTHER AND FATHER

TABLE OF CONTENTS

FIGURES

Chapter III

Chapter VI

Chapter VII

TABLES

ABSTRACT

Over the last two decades, crosslinked polymers with high porosity have received an increasing attention due to their interesting properties which make them for wide range of applications in different fields. Suspension polymerization is the best technique to synthesize the megaporous polymer bead for application as a support. A number of factors are attributes to obtain desired properties of polymer beads. Factors including monomer, crosslinker, crosslink density, type of porogen, porogen concentration, stirring speed, initiator, and polymerization temperature are an important parameters that decide the properties of beads. Crosslinker and porogen are very important parameter in controlling the properties of resulting polymers. These parameters are extensively affected to physical properties of polymers. Nowadays, different types of porogens are available to impart the porous properties into polymers. Porogens are classified depending on properties imparted by the porogens to the polymers. Generally, porogens are classified into three categories i.e. solvating (SOL), non-solvating (NONSOL), and POLY porogens. SOL porogens imparts the high surface area and less pore volume whereas NONSOL porogens imparts lower surface area and high pore volume into the polymer matrix. POLY porogens have the specific property to impart small surface area and pore volume.

Over the past few years, researchers have obtained the polymers in many different ways depending on the desired properties of polymers. Porous polymer is an ubiquitous material used as a support in research as well as in industry. This work is of specific interest due to providing the distinguishable porous materials with hydrophilic and hydrophobic properties. Number of polymerization methods such as suspension, emulsion, and dispersion can be used to produce micro, meso, or macroporous polymer beads. Emulsion polymerization technique can be used to obtain high porous material, but this method has some limitations. Major concern of emulsion polymerization method is that, polymer obtained by this technique has less strength, rigidity, stiffness, and traces of surfactant remaining in the polymer deteriorate the properties of polymer beads. Methyl methacrylate polymer can become a versatile support for adsorption technology or entrapment of an enzyme due to low cost, which is an important from technological view point.

Chapter 1. Introduction

This chapter deals with a brief introduction to micro, meso, and macroporous polymer and applications thereof in different fields such as racemic drug resolution, drug loading kinetics, and to support Lewis acids.

Chapter 2. Aims and objectives

This chapter deals with the broad introductory part of work done

Chapter 3. Synthesis and characterisation of microporous polymers using solvating porogens

This chapter deals with the synthesis of hydroxyl functionalized beaded microporous polymers of 2-hydroxy ethyl methacrylate by suspension polymerization using two different crosslinking agents (EDMA/DVB) and diluents (1,1,2,2-tetrachloroethane/1,2-dichlorobenzene). Microporous beads with high surface area were successfully obtained and characterized by different techniques. Maximum surface area obtained was 564 m^2/g bearing uniform, spherical, as well as non-aggregation images of beads. Thermal properties such as DTG and DSC revealed that, type of crosslinker (flexible/rigid) is a major while its concentration is a minor parameter that affects decomposition and softening temperature of polymer. Swelling ratio of polymer beads was examined as a function of crosslinker and crosslink density. Swelling behavior is in accordance with polymer–solvent interaction parameter.

Chapter 4. Synthesis and characterization of macroporous polymers using non-solvating porogens

This chapter deals with the synthesis of megaporous methyl methacrylate beaded microspheres using non-solvating, hydrophobic porogens by suspension polymerization. Objectives of the present work is to study the effect of non-solvating porogens on various properties including surface area, pore volume, pore size, thermal stability, and swelling behavior of synthesized polymers. Most importantly, greater hydrocarbon concentration in non-solvating porogens imparts megaporous properties and lower surface area to the polymers. On the other hand, as hydrocarbon concentration in the non-solvating porogens decreased, surface

area was increased whereas megaporosity decreased. In short, greater hydrocarbon concentration in a porogen is directly proportional to the megaporosity and inversely proportional to the surface area. Distinguishable porosity was obtained with n-decanol porogen whereas polymer obtained using cyclohexanol exhibits the maximum surface area. Interestingly, methyl methacrylate based polymer demonstrated the distinguishable pore size (5.47 μm) and pore volume (5.52 cc/g) for 100% crosslink density (CLD). Higher degree of swelling was observed for poly(MMA-*co*-DVB) when methanol as a swelling solvent and decreased for acetone as a swelling solvent. These properties are crucial during polymer support selection which spurred to use a macroporous polymer in different applications such as solid phase synthesis, solid phase extraction, adsorption, and entrapment technology.

Chapter 5. Synthesis and characterization of macroporous polymers varying concentration of non-solvating porogen

This chapter deals with synthesis of gigaporous polymers wherein effect of concentration and interfacial tension of non-solvating (n-butanol/n-hexanol) diluents and crosslinkers on polymer properties were evaluated. Polymers revealed the increased surface area with increasing concentration of crosslinker whereas surface area was decreased for increasing concentration of non-solvating diluents. Importantly, MEH-100 (1**:**3 v/v) demonstrated the highest pore volume and pore size of 4.33 cc/g and 0.87 μm, respectively whereas MDH-100 (1**:**2 v/v) displayed the highest pore volume and pore size of 3.56 cc/g and 0.68 μm, respectively. Notably, average particle sizes of all polymer series were decreased after 150% crosslink density (CLD). Higher concentration of rigid crosslinker or lower concentration of flexible crosslinkers substantially improves the thermal properties. Distinguishable porosity was obtained using higher concentration of n-hexanol diluent.

Chapter 6. Synthesis, characterization and applications of core-shell polymer supported chiral selector for racemic drug resolution

This chapter deals with the synthesis of core-shell polymer to obtain more reactive epoxy functionalized microsphere. For the core, acrylate based polymers were obtained varying

crosslinkers and porogens at different crosslink density (CLD). Owing to high surface area of poly(MMA-*co*-DVB) (554 m^2/g) synthesized using 1,2-dichlorobenzene was used as a core and low molecular weight poly(GMA) as a shell polymer (24,600 g/mol). They were successfully introduced in the core-shell polymer synthesis. The synthesis of core-shell polymer was characterized by FT-IR, ^{13}C NMR, scanning electron microscopy (SEM), surface area, particle size, and epoxy content determination. Average particle size of the core polymer was in the range of 15–75 μm. In order to evaluate the reactivity efficiency of core-shell polymer, epoxy content was determined which was 2.35 mmol/g. Importantly, epoxy content demonstrated the successful increasing reactive sites of core-shell polymer over conventional crosslinked hydroxyl polymer. Notably, surface area and pore volume is also higher, resulting more efficient core-shell polymer for applications. SEM demonstrated the spherical, uniform, and slightly conglomerated core-shell polymer. This core-shell polymer was modified by chiral selector, D-(-)-dibenzoyl tartaric acid. Racemic β-blocker drug (salbutamol) was resolved using a core-shell polymer supported D-(-)-dibenzoyl tartaric acid. An enantiomeric excess was reported at different time intervals by high performance liquid chromatography.

Chapter 7. Drug adsorption kinetics using polymer supported gold

This chapter deals with the synthesis of polymer supported gold and its application in selective drug adsorption kinetics. Acrylic acid based polymer was obtained using trimethylolpropane triacrylate as a crosslinker and chlorobenzene as a porogen at different crosslink density. Afterwards, poly(acrylic acid-*co*-trimethylolpropane triacrylate) for 10% crosslink density was selected to balance the reactivity as well as surface area for polymer modification with gold. Synthesis of base polymer and its modification was confirmed by FT-IR spectroscopy. Surface area, porosity, particle size, DSC, DTG, microanalysis, SEM, and EDX analysis of base polymer and polymer supported gold was evaluated. Drug adsorption selectivity of pantoprazole sodium and chloroquine was studied using polymer supported gold with respect to contact time, adsorption isotherm, and adsorption kinetics. Interestingly, results demonstrated that, pantoprazole sodium has exponential adsorption whereas chloroquine adsorb steadily on polymer supported gold. Adsorption study was carried out at room temperature. This study

provides an additional thermostability information of polymer supported gold. DTG and DSC were studied to confirm thermostability during catalytic applications.

Chapter 8. Polymer supported Lewis acids: Recyclable catalysts

This chapter deals with the synthesis of polymer supported Lewis acid which has potential applications over conventional Lewis acids. In the present work, allylamine based polymer was obtained using divinylbenzene as a crosslinker and cyclohexanol as a porogen at different crosslink density. Subsequently, polymer was post modified with various Lewis acids including $AlCl_3$, $SnCl_2$, and $HgCl_2$. These base and modified polymer was characterized by different techniques such as surface area, particle size, differential thermogravimetric analysis, differential scanning calorimetry, scanning electron microscopy, energy dispersive x-ray analysis, and swelling ratio. However, high surface area encourages the polymer efficiency whereas differential thermogravimetric analysis and differential scanning calorimetry revealed the degradation profile and polymer processing temperature, respectively. Moreover, swelling ratio helps to decide a suitable solvent medium during application in a reaction. More importantly, high loading of Lewis acid was obtained resulting more efficient polymer supported Lewis acid. The leakage problem of Lewis acid was solved by forming a strong co-ordinate bonding between amine based reactive polymer and Lewis acid. Polymer supported Lewis acids were successfully used in poly(imine) synthesis and recovered for reuse and recycle perspectives.

Chapter 9. Summary and conclusion

This chapter deals with the conclusion of overall work. Moreover, chapter includes a list of publications, patents, and conferences.

INTRODUCTION

1.1. Introduction

Polymer is an important class of material and is a part of life of human being. Polymers are existed in the nature from life began in the form of DNA, RNA, polysaccharides, and proteins which plays a pivotal role in living body. From an ancient time, human being has exploited the polymers for their needs such as clothing, tools, weapons, and many more. In the past, Charles Goodyear successfully improved the properties of the naturally occurring rubber using a vulcanization process.[1] However, real polymer industries started in nineteenth century. Backelite is the first synthetic polymer synthesized in 1909.[2] Hermann Staudinger is the pioneer of polymer chemistry who systematically studied the polymer.[3] In a simplistic way, polymer can be defined as combination effort of small units joined together to result in a large molecules. The small units also known as repeating units are called monomers and the resultant material of several monomer joined together is the polymer. The synthesized polymer consists in a one, two, or three-dimensional network structure. The three-dimensional network synthesized in nature cannot be melted by a process called as thermoset polymer. On the other hand, uni-dimensional or linear polymer can be easily melt and reprocessed are named as thermoplastics. Polymers are formed by chemical reaction known as polymerization. Polymerization reaction can be broadly classified into two categories based on mechanism namely chain growth and step growth polymerization. In chain growth polymerization, the chemical reaction takes place by addition of monomer units to form a polymer chains. On the other hand, step growth polymerization occurs by the reaction between functional groups. Repeated reaction from end groups leads to long chain. In condensation reaction, small molecules get eliminated and these need to be removed to shift the reaction equilibrium forward. Commonly, polymers are classifieds based on different parameters which are presented in **Table 1.1.**

Table 1.1. Polymer classification based on different parameters

Basis of classification	**Polymer Type**
Origin	Natural, Semi-synthetic, Synthetic
Thermal responses	Thermoplastic, Thermosetting
Mode of formation	Addition, Condensation
Line structure	Linear, Branched, Crosslinked
Application and physical properties	Rubber, Plastics, Fibers
Tacticity	Isotactic, Syndyotactic and Atactic
Crystallinity	Non-crystalline, Semi-crystalline, Crystalline
Polarity	Polar, Non-polar
Chain	Hetero, Homo

Generally, polymerization methods are broadly classified based on structure (chemical/geometrically) and mechanism. Based on structure, polymers are broadly classified into three main types.

(1) Linear polymer: If monomer joined together in a linear manner, then polymer is called as linear polymer. Generally, linear polymers are synthesized by addition polymerization (free radical polymerization).

(2) Branched polymer: If monomer units joined together in a branched manner, then polymer is called as branched polymer.

(3) Crosslinked polymer: In this type, monomer reacted with crosslinker to form insoluble polymer matrix. The concentration of a crosslinker may vary according to the desired properties of polymer support.

Based on mechanism, polymers are classified into three main types which are further classifieds into subtypes as represented in **Figure 1.1.**

Based on mechanism, polymers are broadly classified into three main types.

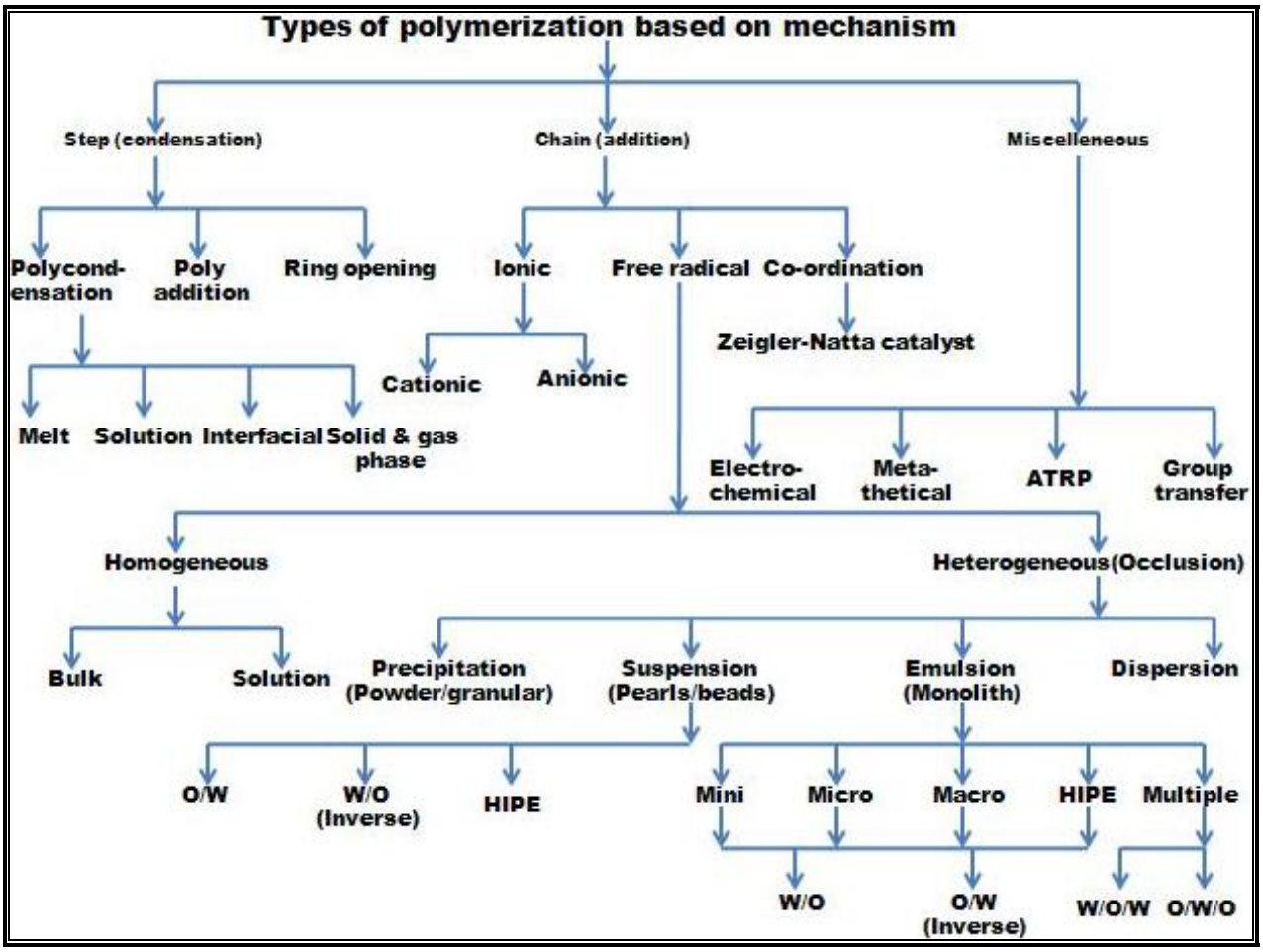

Figure 1.1. Schematic representation of types of polymerization based on mechanism

Our research work is focused on the synthesis of functional, porous, and crosslinked polymers which are applicable as a support for catalysis, drug delivery, metal chelation, enzyme immobilization etc. For these applications, polymer beads were prepared by suspension polymerization having technological importance. Thus, suspension polymerization as well as functionalization, porosity and crosslinking of polymers are illustrated below.

1.2. Suspension polymerization (General procedure)

Over the last two decades, suspension polymerization method was widely used to obtain the functional polymers with desired porosity (micro, meso, and macro). Some other methods like emulsion and dispersion can be used for porous polymer synthesis. However, these methods have limitations of loss of polymer strength. As a result, we used the suspension polymerization method to obtain the functional, porous (micro, meso, and macro) and crosslinked polymers for potential applications. Suspension polymerization comprises an aqueous (continuous) and organic (discontinuous) phase. An aqueous phase was prepared by dissolving the protective colloid (PVP) in deionized water whereas organic phase was prepared by mixing monomer, crosslinker, initiator, and pore generating solvent in a nitrogen atmosphere at room temperature. Synthesis of copolymers was conducted in a specially designed double walled cylindrical glass reactor. The reactor was equipped with a constant temperature water bath (thermostat), mechanical stirrer, reflux condenser, and nitrogen gas inlet. The organic (discontinuous) phase was added to the reactor containing aqueous (continuous) phase and under stirring speed of 500 rpm for 3 h in nitrogen atmosphere. The reaction temperature was raised to 70^{o}C. The copolymer beads obtained were thoroughly washed with water, methanol, and finally with acetone. Subsequently polymers were dried at 60^{o}C under reduced pressure. Synthesized polymer beads by suspension polymerization were further purified by methanol in a soxhlet extractor and dried at 60^{o}C for 8 h under reduced pressure.

Advantages of suspension polymerization

(i) Easy to control the reaction temperature due to the presence of a dispersion medium (water).

(ii) Reaction conditions are mild.

(iii) Low solubility of a continuous phase (monomers) into the discontinuous phase shows much higher product homogeneity.

(iv) Product obtained by suspension polymerization is more pure than product obtained by emulsion polymerization.

Disadvantage of suspension polymerization

(i) Specially designed reactor is needed. These reactors have low productivity due to the presence of high amount of dispersion medium.

(ii) Post treatment is needed to remove impurity such as pore generating solvent, protective colloid etc.

(iii) Different reactivity and solubility of monomers led to different interfacial tension with continuous phase (water) which attributes to difficulty in homogeneous copolymers synthesis.

1.3. Functional polymer synthesis

Functional and porous materials are unique materials and have attracted a lot of attention. Functional material may be organic, inorganic, or organic-inorganic (metal organic framework) material. Most widely used functional material is polymer. Functional polymer synthesis, polymer functionalization and polymer functional group conversion are dependent on nature of polymer matrix, degree of crosslinking, pore volume, pore size, porosity, hydrophilic-hydrophobic, solvation, and swelling behaviour of a polymer matrix. Polymer can be modified by physical or chemical method. Polymer design and synthesis are depending on the desired physical and chemical properties. Use of a polymer eliminates the major problems such as liability, toxicity, or odour of catalysts, reagents, substrates, and photosensitizer. During application, polymer provides a special environment based on polymer properties. From environmental view point, insoluble polymer supported toxic and corrosive compounds are more favorable and acceptable due to its recover, recycle, and reuse properties. In 1840, natural rubber was converted into a tough and elastic rubber by sulfur treatment.[4] In the past functional group addition and conversion was carried out. In 1847, cellulose was converted into nitrocellulose by exposing cellulose to nitric acid.[5] In 1948, Serniuk *et al.* used thiol-ene addition for butadiene functionalization.[6] In 1950s, chlorinated polystyrene-divinylbenzene beads were used for an ion exchange resin.[7,8] In the early 1960s, Iwakura used the pendant epoxy functionality for the post modification.[9] Polymer functionalization is classified depending on the method of functional polymer synthesis.[10] Functional polymer synthesis consists of two types, direct synthesis and post-polymerization modification.

(1) Direct polymerization: Functional monomer having pendant ester, hydroxyl, epoxy, amine, carboxylic acid, thiol, or aldehyde group can be polymerized directly to obtain functional polymer in the absence or in the presence of a crosslinker is called the direct synthesis.

(2) Post functionalization: This type of functionalization method can be used when the monomer functionality interfere into the direct polymerization. In this method, synthesis of non-functional, for instance, styrene-divinylbenzene polymer and subsequent modification can be carried out to obtain functional polymer. Some post functionalization methods are sulphonylation, chloromethylation, thiolation, alkylation, acylation, carboxylation, formylation, and esterification. However, number of post polymer modification methods is reported in the literature. Widely used post polymerization methods are given below.

(i) Thiol-ene addition, **(ii)** Epoxides, anhydrides, oxazolines and isocynates, **(iii)** Active esters, **(iv)** Thiol-disulfide exchange, **(v)** Diels-alder reactions, **(vi)** Michael type addition, **(vii)** Azide alkyne cycloadditions reaction, **(viii)** Ketones and aldehydes, and **(ix)** Other highly efficient. reactions Combination of above two processes can be used together to obtain desired functional polymer. This type of functionalization process can be used when particular functional polymer is difficult to synthesize in direct polymerization. In this method, non-desired functional polymer could be synthesized, subsequently this functionality converted into the desired functional polymer by functional group transformation such as oxidation, reduction, and so on.

1.4. Porous material

A porous matrix is a material containing pores or voids. The skeletal portion of the material is often referred as "matrix" or "frame". The pores are typically filled with liquid or gas to measure the porosity. Classically porous materials consist of organic, inorganic, or polymeric materials.[11] Owing to high surface area and tunable properties, polymers have potential applications in catalysis, adsorption, sensing, separation, and biotechnology.[12,13] Over a decade, porous polymer particles, especially the ones that are spherical in shape, have been utilized in numerous applications. Generally, suspension polymerization technique is able to provide polymers having particle size in the range of 5–200 μm.[14] Porous materials classifieds depending on the pore size and building framework as shown in **Figure 1.2.**

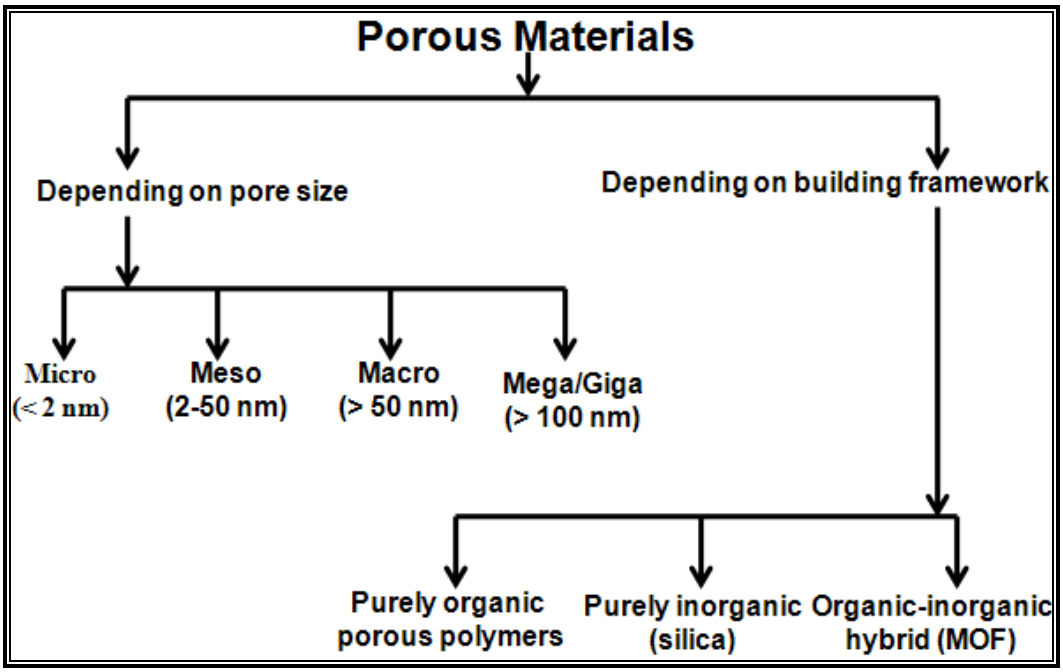

Figure 1.2. Classification of porous material based on pore size and building framework

Porous polymers in the form of spherical materials having average particle size in nano or in micron are preferred for the applications. Porous polymers synthesized may be micro, meso, or macroporous depending on the physico-chemical parameters. According to the IUPAC, pore size is classified into three main categories, micro (< 2 nm), meso (2–50 nm), and macro (> 50 nm).[15] Low crosslink density polymer is a suitable polymer matrix for covalent modification whereas high crosslink density polymer matrix is a suitable for adsorption or entrapment techniques. Emulsion polymerization can also produce porous material but polymer synthesized by this method has less strength compared to polymer synthesized by suspension polymerization. Even porosity can be controlled using different types of porogens.[16] Surface area, porosity, reactivity, and strength are the most crucial parameters considered during selection of a polymer matrix for specific applications. Moreover, porous materials can be classified depending on the constituent of porous materials. Porous materials may be purely organic (polymers, covalent organic frameworks), inorganic (silica, silicates, metal oxides, zeolites, and carbonates), and organic-inorganic hybrid (metal-organic framework and composites materials with metal/metal oxide particles).[17] Scanning electron micrograph of inorganic, organic, and organic-organic hybrid porous materials is represented in **Figure 1.3.**

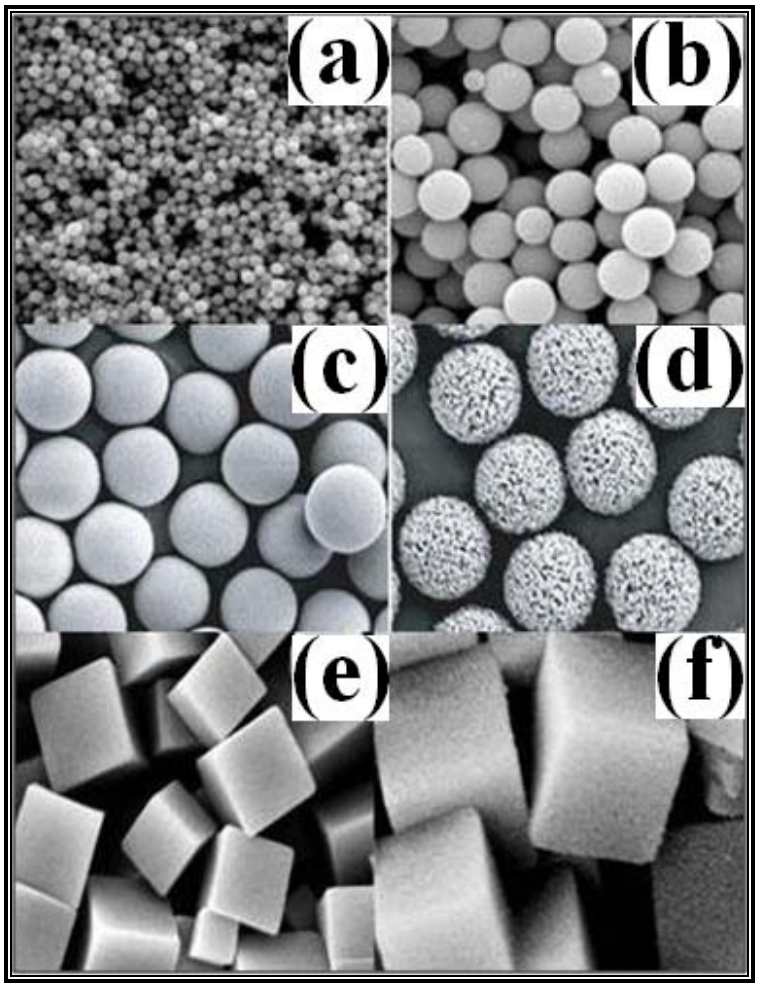

Figure 1.3. General SEM micrograph of (a,b) inorganic porous material, (c,d) organic porous polymers, and (e,f) organic-inorganic hybrid (metal organic framework)

1.4.1. Porogen selection

Porogen is the pore generating solvent which attributes for the polymer properties. However, porogen selection depends on the desired polymer properties for application and solubility parameter of monomer, polymer, and porogen. Three types of porogens can be used to generate the surface area and porosity in the polymer i.e. solvating, non-solvating, and polymeric porogens.[16] Surface area and pore volume varies according to the type of porogens. Solvating porogens like toluene and halogenated solvents are able to introduce surface area in the range of 50–500 m^2/g and comparatively low pore volume (upto 0.8 cc/g) for acrylate type polymer. Pore size distribution shown by solvating porogen is micro and mesopores in nature. Non-solvating

porogen like hydrocarbons and alcohols produces less surface area (10–100 m^2/g) and more pore volume (0.6–2.0 cc/g). Pore size distribution shown by non-solvating is meso and macropores. Polymeric porogen produces polymer having very small surface area (0.1 to 10 m^2/g) with less pore volume (upto 0.5 cc/g) and pore size (upto micrometer). Solubility parameter can be determined by the following **equation (1.1):**

$$\delta = C = \Delta H - RT \qquad \textbf{(1.1)}$$

where, δ is the solubility parameter, ΔH_V is the heat of vaporization, R is the universal gas constant, and T is the temperature in Kelvin.

Solubility parameter is a key parameter in porogen selection for polymer synthesis. Frequently, three approaches (one, two and three-dimensional solubility parameter) are used to determine the solubility parameter of porogenic solvent, monomer, and polymer.[18] Generally, solubility parameter is used to compare the solvation, miscibility, and swelling property of the interacting materials. Solubility parameter shows the good indication of the solubility of non-polar materials like polymers. In this study, we used the solubility parameter to evaluate the miscibility of a porogen and monomer mixture. However, solubility parameter of monomer and porogen helps to decide the property of the porogen as a solvating or non-solvating during polymer synthesis. The solubility parameter of monomer and porogen was determined by the following Hildebrand[19] **equation (1.2):**

$$\delta = \sqrt{\frac{D(\triangle H_V - RT)}{M}} \qquad \textbf{(1.2)}$$

where, δ is the solubility parameter, D is the density, ΔH_V is the heat of vaporization, R is the universal gas constant, T is the temperature in Kelvin, and M is the molecular weight.

Criteria for porogen selection

(i) Porogens must have high boiling point.

(ii) Porogen must not react chemically i.e. chemically inert.

Drawbacks of porogen in synthesis of porous material

(i) Proper selection is needed.

(ii) Sometime trial and error experiments are needed.

(iii) In some cases, it is difficult to remove porogen from the matrix.

1.4.2. Pore formation mechanism

Porosity is always expressed in percentage or fraction for the rock sample. In the present work, porosity of the beaded polymer was determined by mercury porosimetry. Porosity displays only total porous area; however, surface area and porosity are unable to display information regarding pore volume and pore size distribution and their degree of connectivity. Rock with same porosity has different properties. Pores with carbonate rocks are often unconnected resulting in lower permeability. Generally, porosity is classified by considering the rock porosity. Pore formation is controlled by the type and concentration of a porogen. Porogen substantially affects the surface area, pore size, pore size distribution (PSD), pore volume, and morphology of polymers. Moreover, phase separation is also an important parameter which affects the polymer porosity.[20] Solvating (good) porogens attributes for later-stage phase separation whereas non-solvating (bad) porogens attributes for early-stage phase separation. This is due to the fact that, solvating porogen has higher miscibility with monomer composition and inversely non-solvating porogen has less miscibility. The pores may be in single mode or in double mode. Single mode relates to the formation of micro, meso, or macro pores whereas bimodal porosity is the combination of micro-meso or meso-macro, or micro-macropores. In **Figure 1.4,** non-solvating porogen forms early-stage phase separation resulting into macroporous polymer. After extraction of non-solvating porogen, polymer forms unimodal pores **(a,b).** In another case, solvating porogen forms the microgel or micropores which on removal of porogen forms unimodal pores **(c,d).** However, the nature of these unimodal pores is micropores for solvating and macropores for non-solvating porogen. On the other hand, oligomer forms later-stage phase separation which forms micropores or microgel within macrogel whereas on removal of porogen, pore formation is bimodal (micro-meso, meso-macro, or micro-macro) **(e,f,g).** Pore formation mechanism into the polymer matrix is depicted in **Figure 1.4.**

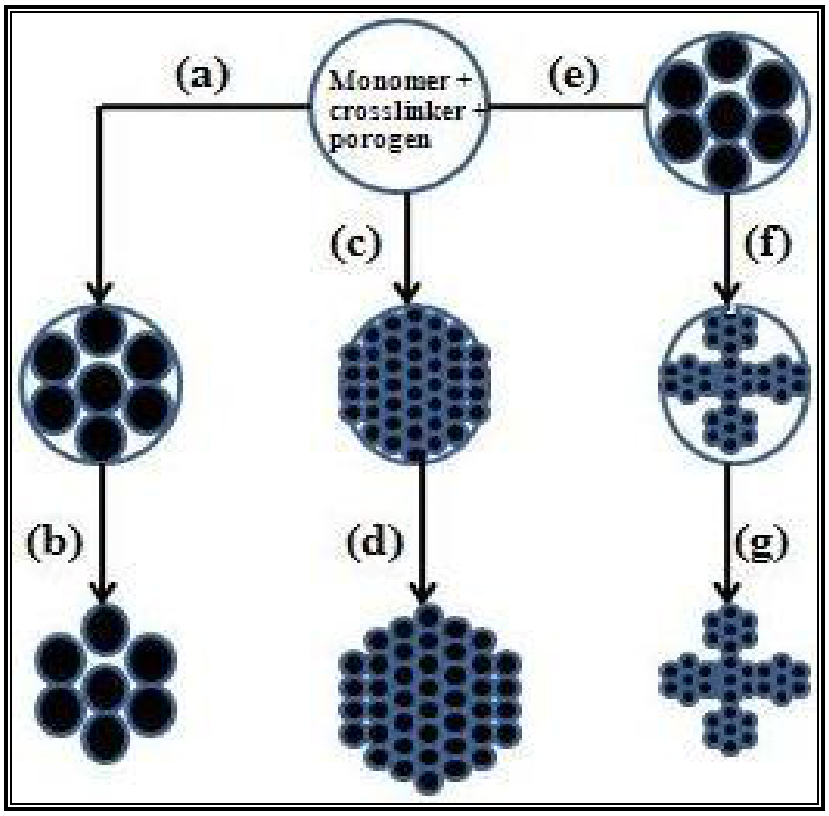

Figure 1.4. Schematic representation of pore formation mechanism

1.4.3. Types and shapes of porosity

Porosity is classified by considering the rock porosity.

- **Total porosity:** Total porosity is the unoccupied volume of the solid matter.
- **Connected porosity:** The ratio of the connected pore volume to the total volume is called as total porosity.
- **Effective porosity:** Effective porosity is nearly same like connected porosity.
- **Primary (main/original) porosity:** This porosity is the original depositional structure of rocks.
- **Secondary porosity:** This type of porosity results from diagenesis. This porosity enhances the overall porosity of rock and also referred as subsequent or separate porosity in rock.

- **Microporosity:** Pores with small sizes < 2 nm commonly called as microporosity.
- **Intergranular porosity:** The pore volume existed between the rock grains produces intergranular porosity.
- **Intragranular porosity:** Porosity originates due to voids within the rock grains.
- **Dissolution porosity:** Dissolution of rock grains results into dissolution porosity.
- **Fracture porosity:** This porosity considered as secondary porosity and created by fracture of rocks.
- **Intercrystal porosity:** Microporosity in intercrystalline boundaries especially in carbonate rocks referred as intercrystal porosity.
- **Moldic porosity:** This is a type of dissolution porosity in carbonate rocks resulting in molds of original grains or fossil remains.
- **Fenestral porosity:** This porosity relates to carbonate rocks usually called as fenestral porosity.
- **Vug porosity:** This is a secondary porosity and generated from dissolution of large features in the carbonate rocks leaving large holes or vugs. Porosity in the form of vugs or holes in carbonate rocks is called as vug porosity.

Types of pores: Different types of pores and shapes are associated with polymer matrix include,

(a) Closed pores **(b)** Open pores **(c)** Blind pores (dead-end or saccate), and **(d)** Through pores

Shape of pores: Above mentioned pores have various shapes and include,

(a) Cylindrical open **(b)** Cylindrical blind **(c)** Ink bottle shaped **(d)** Funnel shaped, and **(e)** Roughness

Types of pores and their shapes are depicted in **Figure 1.5.**

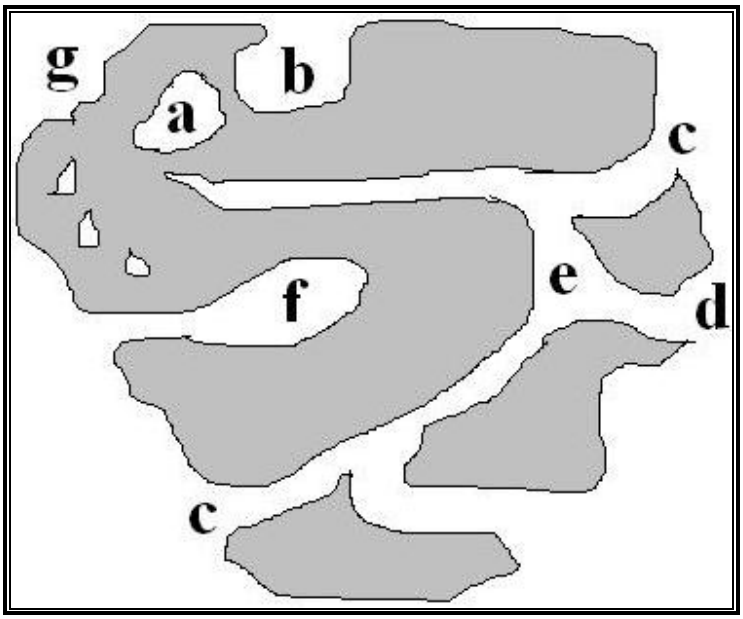

Figure 1.5. Types of pores **(a)** closed **(b,c,d,e,f)** open **(b,f)** blind or dead-end/saccate **(f)** through as well as shape of the pores **(b)** ink-bottle shaped **(c)** cylindrical open **(d)** funnel shaped **(f)** cylindrical blind, and **(g)** roughness

1.4.4. Measuring porosities

Number of methods is available to measure the porosity,[21] some of them are dependant on weight, length, and pressure measurement. However, some methods are able to measure open pores whereas some relates to closed pores.

(i) Direct measurement: This is a simple method and is useful to measure the total porosity. But this method has limitations in rocks porosity determination due to disaggregated nature of rocks.

(ii) Imbibition method: This method relates to the sample wetting with fluid. This is an accurate method, in which sample remains fully saturated which becomes ready for further petrophysical analysis.

(iii) Mercury injection: This method is mostly useful for connected porosity. In this method, sample first evacuated afterwards mercury immersed and slowly mercury pressure increased to fill the rock pores. Mercury displacement of rocks measures the volume of the rock. Small pores can not measured by mercury porosimetry. This method is considered as moderately accurate.

Advantage of this method is that, irregular samples can be analyzed whereas disposing of analyzed samples after analysis is needed from safety view point.

(iv) Gas expansion: This method depends on the ideal gas law or Boyle's law. This is rapid technique and useful for irregular samples also. Due to small size of helium molecules that penetrates smallest pores resulting higher porosity than imbibition and mercury injection method. This method is very accurate and sample available for further petrophysical tests.

(v) Density methods: If the density of the rock mineral is known, then pore volume and porosity can be calculated directly from the mineral density and the dry weight of the sample. This method is generally used for total porosity determination and not useful in petrophysics.

(vi) Petrographic methods: Two dimensional porosities usually determined by petrographic methods by point counting under an optical microscope, SEM, or image analysis. This method is suitable for total porosity. However, this method has limitation in rocks porosity.

(vii) Other techniques: Some other techniques are also available for porosity determination such as **(i)** evolved gas analysis **(ii)** CT scan method, and **(iii)** NMR techniques.

1.5. Crosslinked polymers

The polymer crosslinking depends on the desired polymer properties. Small crosslinked polymers are widely used as a solid support for covalent modification with catalysts, reagents, substrates, and so on. On the other hand, high crosslinked polymer can be potentially used for immobilization of an enzyme by entrapment or adsorption method. Effect of crosslinking on different polymer properties such as surface area, pore volume, pore size, particle size, thermal properties (thermal degradation/glass transition temperature), polymer swelling, and mechanical strength are described below.

The general trend of surface area is that, as crosslinking in a polymer increases, surface area also increases and vice-versa. However, surface area decreases after certain crosslink density which depends on monomer, crosslinker, porogen, and their concentration. Generally, pore volume and pore size increases with increase in crosslink density. Common trend of the pore volume is similar to surface area. As concentration of crosslinker (crosslink density)

increases, pore volume also increases. In contrast, pore size decreases with increase in crosslinker concentration (crosslink density). Pore volume and pore size are the most important parameters which can be controlled by varying physico-chemical parameters. Crosslink density and porogen are the most influencing parameter for the pore volume and pore size. Porosity may be unimodal or bimodal depending on the porogen or mixture of porogens. Solvating and non-solvating porogens have the property to impart unimodal porosity. Mostly, solvating porogen is used to obtain micro or mesoporous property whereas non-solvating porogen has the property to impart meso or macroporous property into the polymer matrix. Bimodal porosity can be generated using a mixture of porogens (solvating-non-solvating pair) and controlling their concentration. Bimodal porosity may be micro-meso, meso-macro or micro-macro. However, particle size of polymer depends on the method of polymerization as well as interfacial tension between aqueous and organic phase containing monomer, crosslinker, and porogen. Hydrophilicity/hydrophobicity of the crosslinker has a major role in the particle size distribution. Thermal properties are affected by the type and concentration of crosslinker. Type of crosslinker consists of rigidity, flexibility, elemental composition, and aromatic/aliphatic properties of a crosslinker. In most of the cases, rigidity and aromatic ring containing polymer are stable towards thermal action whereas polymer containing aliphatic and flexible crosslinker are less stable towards thermal action. Moreover, higher concentration of rigid crosslinker or lower concentration of flexible crosslinker produces thermostable polymers. Polymer swelling is the function of polymer crosslinking. Higher the polymer crosslinking, lower is the polymer swelling and vice-versa for lower crosslink polymer crosslinking. This is mainly because of lower crosslink polymer has a longer chain length and easy to expand. In contrast, in higher crosslink polymer, chain length is smaller and difficult to swell. Polymer strength depends on the polymer porosity. Higher the porosity, smaller is the polymer strength and vice-versa for low porosity polymer. Thus, polymer strength and porosity are inversely proportional to one another. Suspension polymerization is a method which produces less porous and high mechanical strength polymer whereas emulsion polymerization method produces polymer with greater porosity and little strength. Therefore, to balance these two properties is an important from application point of view.

1.6. Adsorption

Adsorption is a process of adhesion/accumulation of the atoms, ions, biomolecules, or molecules of solid, liquid, or gas onto the surface of another substance.[22,23] Adsorption is a process in which two substances are involved, adsorbate, and adsorbent. Adsorbent may be solid or liquid on which adsorption occurs. Adsorbate may be the gas, liquid or the solute from a solution which gets adsorbed on the surface.

Adsorbent: The substance on whose surface the adsorption occurs is known as adsorbent.

Adsorbate: The substance whose molecules get adsorbed on the surface of the adsorbent is known as adsorbate.

Adsorption and absorption are two different terms. In absorption, the molecules of substance are uniformly distributed in the bulk of the other material (liquid) whereas in adsorption, molecules of one substance adsorbed on the other molecule in higher concentration.

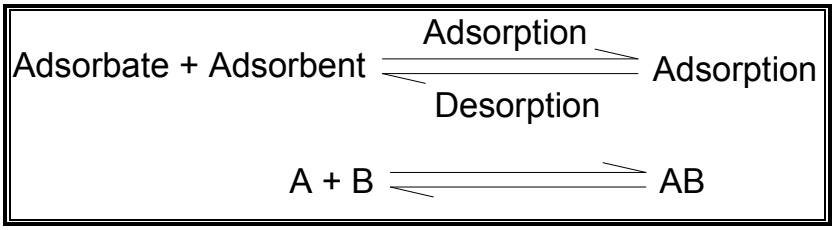

Examples

(1) Adsorption of gases like CO_2, SO_2, or Cl_2 on activated charcoal.

(2) Gas adsorbed on metals such as platinum or nickel.

(3) Acetic acid adsorbed on animal charcoal.

(4) Decolorization of molasses by activated charcoal.

1.6.1. Types of adsorption

Adsorption is classified into two types depending upon the forces of attraction between adsorbate and adsorbent.[24] If the attraction is weak Vander Walls forces then it is called as physical adsorption or physisorption. If the adsorption is strong chemical bond attraction, then it is called

as chemisorption or chemical attraction. Difference between physisorption and chemisorption is depicted in **Table 1.2.**

(A) Physical adsorption (physisorption): If the forces of attraction between adsorbent and adsorbate are weak i.e. Vander Waals attraction, then this adsorption is called as physical adsorption or physisorption. Usually, this adsorption takes place in multilayer form. Low temperature is favorable for this type of adsorption. High temperature decreases the physisorption. Due to weak attraction between adsorbent and adsorbate, physisorption can be reversed by heating or decreasing the pressure. The parameters affect to physi-sorption are mentioned below.

(i) Energetics and kinetics: Physisorption is exothermic process. This type of adsorption exists due to the presence of weak Vander Waals forces of attraction. Physisorption is a reversible process.

(ii) Temperature: According to Le-Chateliers principle, physisorption is exothermic process and it occurs at lower temperature whereas an increase in temperature decreases the physisorption.

(iii) Pressure: According to Le-Chateliers principle, physisorption increases with increase in pressure to a certain extent. However, further increase in the pressure decreases the physisorption.

(iv) Specificity: Vander Walls forces are universal. As a result, physisorption is not specific with respect to adsorbent.

(v) Nature of adsorbent: The extent of adsorption depends on nature of an adsorbent. Easily liquefiable gases having high critical temperature are readily adsorbed.

(vi) Surface area: As surface area increases, physisorption also increases. Therefore, porous materials such as polymer, inorganic, and metal-organic framework can work well.

(B) Chemical adsorption (chemisorption): If the forces between adsorbate and adsorbent are strong chemical bond attraction, then it is called as chemisorption. Due to strong forces of attraction, it is difficult to reverse the chemisorption. The parameters affects to chemi-sorption are mentioned below.

(i) Energetics and kinetics: Chemisorption is an exothermic and irreversible process. As temperature increases, chemisorption also increases upto a certain extent. But, adsorption decreases on further increase in temperature.

(ii) Temperature: Increase in temperature increases the chemical adsorption to a certain extent. However, further increase in temperature led towards decrease in adsorption or adsorption stabilization.

(iii) Pressure: High pressure is favorable for chemisorption. However, small change in pressure does not affect chemisorption.

(iv) High specificity: Chemisorption is highly specific and occurs only when chemical attraction exists between adsorbent and adsorbate.

(v) Surface area: Chemisorption increases with increase in surface area same like physisorption

Table 1.2. Comparison between physisorption and chemisorption

No.	Physisorption	Chemisorption
1.	Heat of adsorption is in the range of 20–40 kJ mol^{-1}	Heat of adsorption is in the range of 40–400 kJ mol^{-1}
2.	Force of attraction are Vander Waals forces	Forces of attraction are chemical bond forces
3.	It takes place at low temperature	It takes place at high temperature
4.	It is reversible process	It is irreversible process
5.	Sorption related to liquefaction of the gas	Sorption not related to liquefaction of the gas
6.	Sorption is not very specific	Sorption is highly specific
7.	Multi-molecular layers formation of an adsorbent	Monomolecular layer formation of an adsorbent
8.	It does not require any activation energy	It requires activation energy

1.6.2. Adsorption isotherm

Adsorption process is usually studied using a Langmuir and Freundlich adsorption isotherm.

Langmuir adsorption isotherm

In 1916, Irving Langmuir isotherm model assume that, dynamic equilibrium exists between adsorbed gaseous molecules and the free gaseous molecules.[25] Langmuir adsorption is based on four assumptions as follows:

(1) Uniform surface with all equivalent sites of adsorbent is needed.

(2) Adsorbed molecules do not interact with each other.

(3) Same mechanism is applicable to all adsorptions.

(4) Langmuir adsorption relates to the monolayer adsorption and considering the adsorbate molecules do not adsorb on the previously adsorbed molecules means each molecule adsorb on free space.

Langmuir suggested that, adsorption takes place through following mechanism:

$$A(g) + B(S) \underset{\text{Desorption}}{\overset{\text{Adsorption}}{\rightleftharpoons}} AB$$

where, A(g) is the unadsorbed gaseous molecule, B(s) is the unoccupied adsorbent surface, and AB is the adsorbed gaseous molecule.

Langmuir derived an equation which describes the relationship between number of active sites of the surface that undergo adsorption and pressure. This equation is called Langmuir[26] **equation (1.3):**

$$\theta = \frac{KP}{1 + KP} \qquad \textbf{(1.3)}$$

where, θ is the number of sites of the surface which are covered with gaseous molecule, P is the pressure, and K is the equilibrium constant for distribution of adsorbate between the surface and the gaseous phase.

Langmuir adsorption equation is valid at low pressure only. At lower pressure, KP becomes small, whereas factor (1+KP) in denominator becomes negligible. So Langmuir equation is written as,

$$\theta = KP$$

At high pressure KP is large and comparable; therefore factor (1+KP) in denominator is nearly equal to KP. So Langmuir equation is written as,

$$\theta = \frac{KP}{KP} = 1$$

Freundlich adsorption isotherm

In 1909, Freundlich expressed an empirical equation to represent the isothermal variation of adsorption pressure. This equation is commonly called as Freundlich adsorption isotherm or Freundlich adsorption equation or simply Freundlich isotherm[27] **equation (1.4):**

$$\frac{x}{m} = kP^{1/n} \quad \textbf{(1.4)}$$

where, x/m is the adsorption per gram of adsorbent which is obtained by dividing the amount of adsorbate (x) by the weight of the adsorbent (m), P is the pressure, and k and n are the constants whose values depend upon adsorbent and gas at a particular temperature.

Freundlich adsorption isotherm is represented in **Figure 1.6a.** Subsequently, taking the logarithms of both sides, equation (1.4) becomes **equation (1.5):**

$$\frac{\log(x)}{m} = \log k + \frac{1}{n}\log p \quad \textbf{(1.5)}$$

A plot of log x/m versus log p reveals a linear plot with an intercept **(Figure 1.6b).** Plot shows that, slope equal to 1/n and the value of intercept equal to log k can be obtained. Thus, Freundlich adsorption isotherm followed this system.

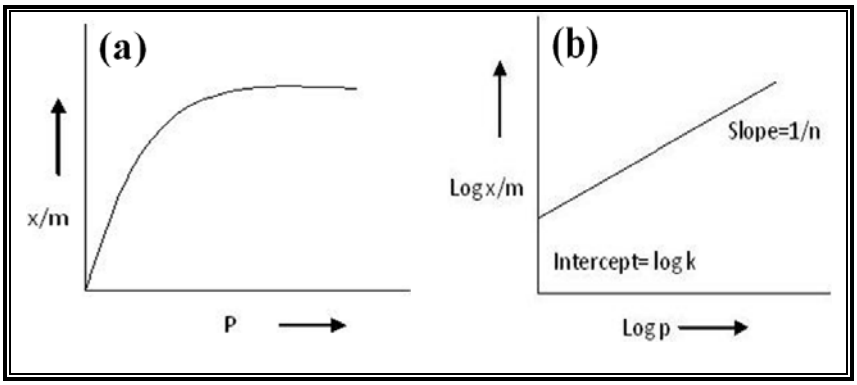

Figure 1.6. Freundlich adsorption isotherm (a) non-linear form, and (b) linear form

1.6.3. Adsorbent properties

(1) Adsorbent may be in the form of spherical pellets, rods, or monoliths.

(2) Adsorbent must have abrasion resistance, high thermal stability, and small pore diameters which allow to increase the surface area and obviously high adsorption.

(3) An adsorbent must have a distinct pore structure which allows fast transport of the gaseous vapors.

Most industrial adsorbents fall into one of three classes

(1) Oxygen-containing compounds having hydrophilic and polar properties, e.g. silica gel and zeolites.

(2) Carbon-based compounds having hydrophobic and non-polar properties, e.g. activated carbon and graphite.

(3) Polymer-based compounds having polar or non-polar functional groups, e.g. porous polymer matrix with or without a functional group.

Adsorption mechanism of an adsorbent and adsorbate is represented in **Figure 1.7.**

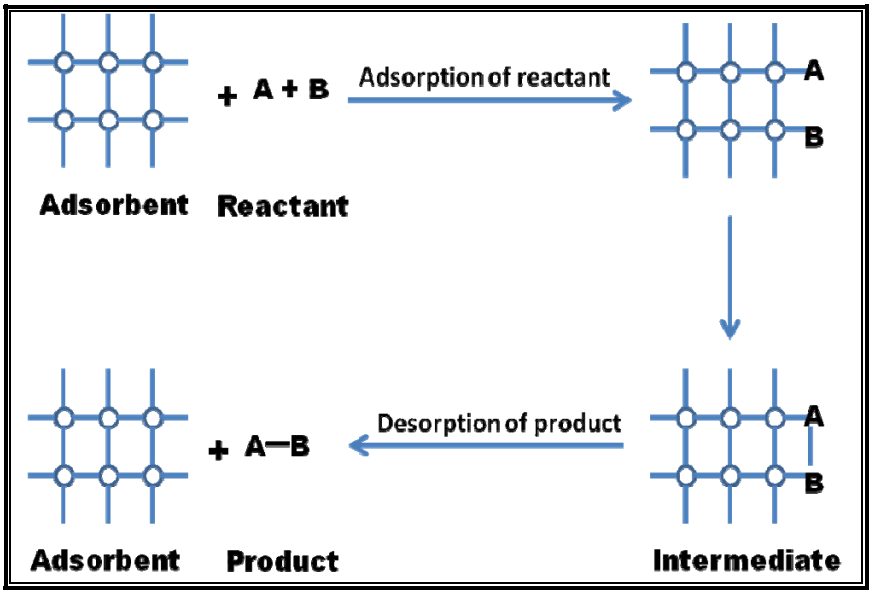

Figure 1.7. Adsorption mechanism between reacting molecules and an adsorbent

Adsorption process depends on the following factors

(i) Surface area of the adsorbent: The main factor attributes to adsorption is the surface area. The surface area is the tunable property which can be controlled by changing physico-chemical parameters.

(ii) Nature of the adsorbent: Adsorption also depends on the adsorbent nature i.e. solubility, and polarity. Highly soluble adsorbent has less capacity to adsorb an adsorbate whereas compound having less solubility into the solvent has more capacity to adsorb onto the adsorbent.

(iii) pH of the solution: pH of the solution can also affect the adsorption because the hydrogen and hydroxide ions adsorbed quite strongly.

(iv) Temperature: Small change in temperature does not affect the adsorption. Large variation in temperature significantly affects an adsorption.

(v) Nature of the adsorbate: Nature of adsorbent also affects the adsorption. Physico-chemical parameters of an adsorbent significantly affect the selectivity, capacity, and adsorption rate of the adsorbent.

1.6.4. Applications of an adsorption

The adsorption process used in number of applications such as,[28]

(i) Heterogeneous catalysis.

(ii) Masking of poisonous gases by activated charcoal.

(iii) Petroleum refining and discoloring of cane juice.

(iv) Gases can be adsorbed by activated charcoal that is useful in creating vacuum

(v) Usually, silica gel is used in chromatography to separate compounds based on different adsorption capacity of different analytes.

(vi) Silica gel adsorbs moisture that helps to control the humidity.

1.7. Applications of polymers in different fields

Porous beaded microsphere has received an increasing attention due to their wide range of applications in various fields[29,30] and ubiquitous properties including surface area, pore volume, pore size, reactivity, and particle size. However, these properties can be controlled by changing physico-chemical parameters. Physical parameters[31] such as stirring speed, reactor dimension, and temperature whereas chemical parameter like monomer, crosslinker, crosslink density, as well as type and concentration of porogens are able to control the properties of the beaded polymer. In the present work, micro and macroporous beaded polymers were synthesized for application as a polymer support in chiral drug separation, metal recovery, drug loading, and for modification with Lewis acids and applications thereof. Recently, in so many applications polymers were used as a solid support in solid phase synthesis and solid phase extraction. In most of the cases, beaded crosslinked polymers were used to support the catalyst, regent, substrate, protecting groups, chiral selector, and so on. Industrially, these polymers are widely used due to their recovery, recycle, and reuse properties which make them economical and environmentally benign.[32] Polymer applications in different fields are represented in **Figure 1.8.**

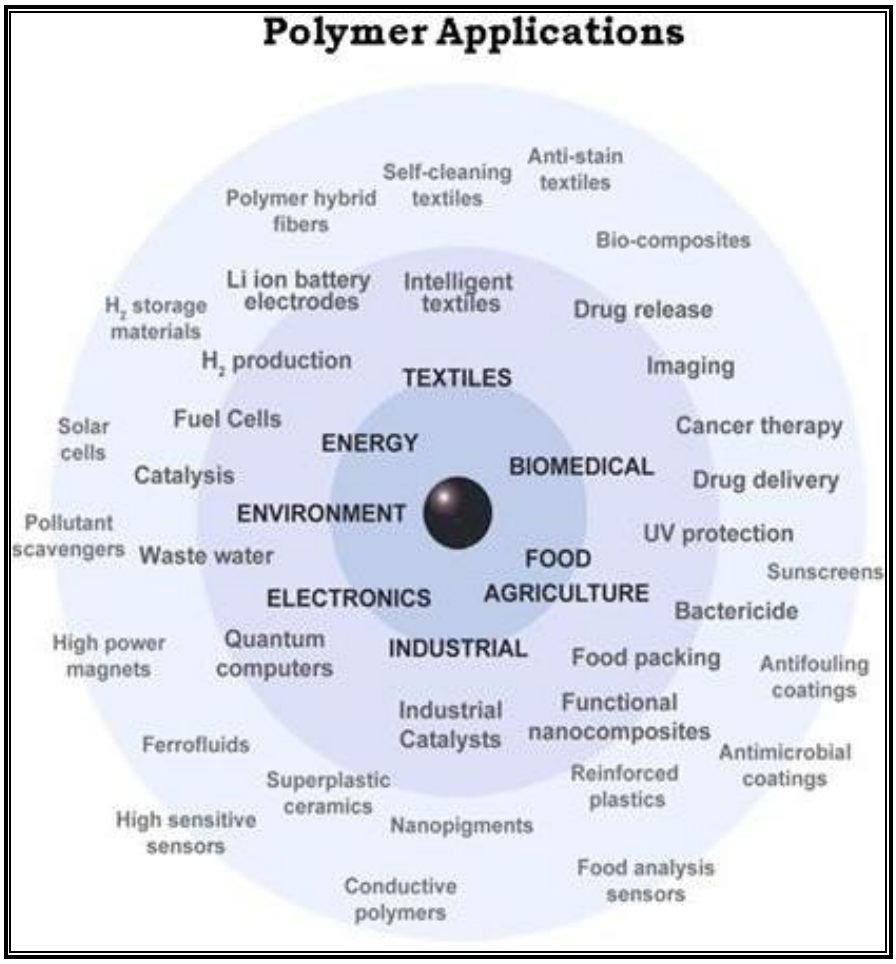

Figure 1.8. Applications of polymers in different fields

1.8. Polymer applications in racemic drug resolution

Pasteur discovered that, paratartaric acid exists in 'D' and 'L' tartaric acids in the form of racemic mixture.[33] This is the first report which describes that, a single compound can exist in two isomeric forms having same physical and chemical properties but different optical properties. According to Pasteur, this is due to asymmetric tetrahedral arrangement of atoms. Vant Hoff and Le Bel also discovered[34] the tetrahedral carbon atoms bounded to four different groups which attributes to origin of chirality e.g. tartaric acid. Tartaric acid has two chiral centers resulting in four stereoisomers. Two stereoisomers are left handed and other two are right handed stereoisomers. Moreover, mesotartaric acid also exists which contains two chiral centers but still isomer is optically inactive due to the presence of plane of symmetry (internal compensation).

Most of the biomolecules exist in optically pure form either 'S' or 'R' form. These two forms are present in two non-superimposable mirror images of each other and called as enantiomers or optical isomers. Naturally occurring amino acids in the protein exist in 'S' form (left handed)[35] whereas sugars in DNA and RNA exist in 'R' form (right handed).[36] The mixture of chirally pure but optically or stereochemically opposite compound in equal proportion produces racemic mixture. One isomer produces left handed rotation while opposite isomer produces right handed rotation and consequently mixture becomes optically inactive due to an external compensation.[37] On the other hand, sometimes compound containing chiral center also shows optically inactive property, due to the presence of plane of symmetry, center of symmetry, axis of symmetry, or alternating axis of symmetry in the molecule. This is mainly due to an internal compensation.[38] To resolve the racemic compounds (external compensation compounds) into optically pure enantiomer, chirally pure isomer is needed since interacting properties of racemic compound with chirally pure compounds (chiral selector) are different. Chiral selector often forms diastereomers with both enantiomers of racemic compounds. These formed diastereomers have different physical and chemical properties and become easy to separate. Three-dimensional structure of chiral molecule is represented in **Figure 1.9.**

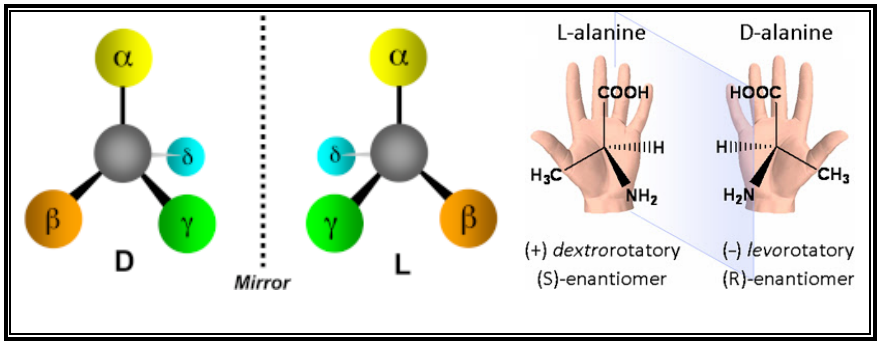

Figure 1.9. Schematic representation of D and L or R and S configuration of chiral molecules

1.8.1. Wallach's rule

In 1895, Otto Wallach[39] proposed that, racemic crystal tends towards denser than their pure enantiomer. As a result, chirally pure compound can be synthesized by the use of chiral compounds such as catalysts and reagents which tends to produce chirally pure product or in the enantiomeric excess form which is expensive.

1.8.2. Importance of chiral resolution

When one enantiomer is converted into another type of enantiomer then there is small change in structure but significant difference in properties.[40] In nature, biomolecules like proteins and nucleic acids are chiral.[41] Biological systems are controlled by proteins whereas information required for proteins is stored and carried out by DNA and RNA molecules, respectively. Thus, each enantiomer has their specific interaction response with living bodies. For instance, one enantiomer of limonene has orange smell whereas opposite enantiomer gives lemon smell. Chirality is an extremely important in drug synthesis. Thalidomide tragedy is the case that underlines an importance of chirally pure compounds.[42] Thalidomide was widely used in the treatment of morning sickness in pregnant women. One isomer of thalidomide has pharmaceutical effect. Unfortunately, its opposite isomer produces birth defect in newly born child. Another example is that, penicillamine is anti-arthritic agent but this activity resides with only one enantiomer whereas opposite enantiomer has highly toxic activity.[43]

1.8.3. Principles of chiral recognition by chiral stationary phases (CSPs)

Chiral liquid chromatography depends on the formation of diastereomeric complexes between a chiral selector and enantiomer analytes. Mobile phase (pH, solvent polarity) selection is the crucial factor that allows favoring the specific interaction. In 1952, Dalglish[44] proposed three-point interaction theory. Different types of interactions such as ionic, hydrophobic, hydrogen bonding, and π-π □interactions are possible between CSP and chiral analyte. In order to obtain a chiral separation, one of the enantiomers must form a weaker complex with the chiral selector than the other (K1>K2 or K1<K2). Ogsten's theory[45] explains that, chiral resolution does not require all three interactions to be attractive or bonding. Repulsive steric interactions with at least one attractive interaction can explain the chiral recognition. Three point rule[46] defines that, "Chiral recognition requires three simultaneous interactions between the CSP and chiral analyte with at least one stereochemically interaction.

1.8.4. Chromatographic methods

The first successful resolution of a racemic compound was performed by Louis Pasteur, who separated the crystals of a conglomerate. The separation of a racemate into its pure

enantiomers is called a chiral resolution. Various methods are available for chiral resolution such as crystallization, chromatography, and an enzymatic resolution. The chromatographic methods are fast, easy, and provide qualitative and quantitative separation. Two main approaches[47] i.e. direct and indirect are associated with chromatographic methods. In indirect method, chiral derivatizing agents are used to separate enantiomers whereas in direct method chiral stationary phases or chiral mobile phase additives can be used to separate the enantiomer.

Indirect chromatographic methods

In this method, chiral reagent used to separate the enantiomers from the racemic mixture. Both 'R' and 'S' enantiomer are allowed to interact with chiral reagent to form a diastereomer which then passes through achiral column. Due to difference in stability of diastereomers allowed separating them by achiral column.[48] Sometimes derivatization may led to side reactions like racemization. For instance, tartaric acid and its derivatives can be useful for resolution of racemic mixture of amine based compound. The formation of diastereomer between chiral selector and an analyte is represented in **Figure 1.10.**

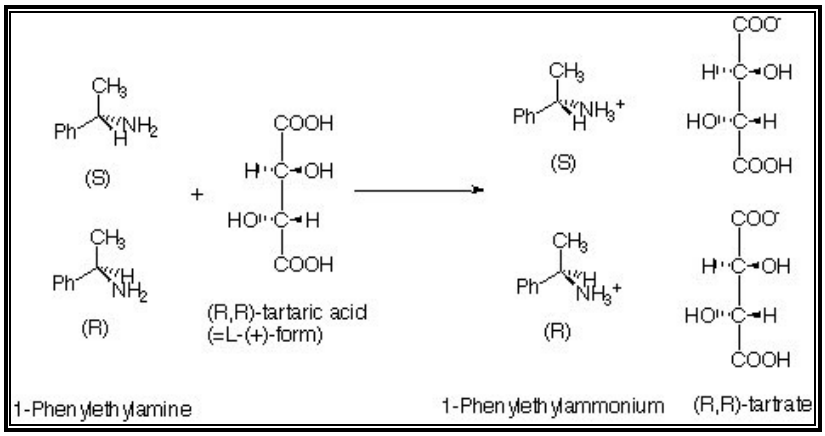

Figure 1.10. Chiral compound separation by formation of diastereomeric salt between chiral selector (tartaric acid) and racemic compound (1-phenylethylamine)

Direct chromatographic methods

Dalglish proposed three point interactions model.[44] This model states that, three interactions with at least one chiral interaction is needed for chiral separation. Direct separation is classified into two main categories, in first, chiral selector present in the form of stationary

phase which interacts with analyte in mobile phase. Second type consist of chiral selector may be added in the mobile phase which interacts with analyte and can be separated on achiral column.

Chiral stationary phases (CSP)

In this method, stationary phase made with chiral molecules containing large number of chiral centers acts as a support. Racemic mixtures are separated based on the ability of the complex formation of an enantiomer with chiral stationary phase.

Chiral mobile phase additives (CMPA)

In this method, racemic drug resolved using achiral column wherein chiral additives are added to form diastereomer with an enantiomers, subsequently they can be separated on achiral column owing to the different physical and chemical properties of the diastereomers. Analyte separation occurs based on the different stability of diastereomeric complexes, solvation effects of the mobile phase, as well as interaction with achiral column. In the past, α, β, and γ cyclodextrins[49,50] have been successfully used as a chiral mobile phase additives and they are represented in **Figure 1.11.**

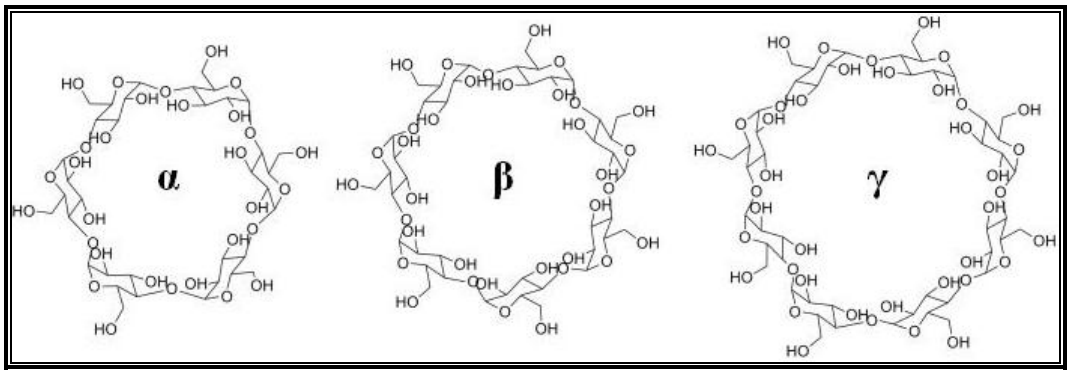

Figure 1.11. Macrocyclic chiral mobile phase additives (α, β, and γ forms of cyclodextrin)

1.8.5. Types of chiral stationary phases (CSPs)

No universal chiral selector is available for resolution of all compounds. Over the last decade, much attention has been paid for chiral separation based on analytical and preparative scale. Different chromatographic techniques such as high performance liquid chromatography, gas chromatography, thin-layer chromatography, supercritical fluid chromatography are

developed as powerful techniques. For the chiral separation, only an ionic interaction is not sufficient and some additional interactions like dipole-dipole or π-π-interactions must take part during resolution. Dobashi and Hara prepared[51] the HPLC phase based on amino acids and amides as a chiral selector which works on the principle of formation of multiple hydrogen bonds. In 1966, Gil-Av *et al.*[52] developed the chiral stationary phase for gas chromatography applications that works on the principle of formation of hydrogen bonds between CSP and an analyte. The chiral stationary phases (CSPs) can be divided into six major classes as follows,

(i) Pirkle/brush type CSPs (π donor and π acceptor)
(ii) Polysaccharide and derivatised polysaccharide based
(iii) Inclusion type
(iv) Ligand exchange
(v) Protein based columns
(vi) Macrocyclic antibiotic based columns

(i) Pirkle type CSPs

In 1979, Pirkle and House discovered[53] the chiral stationary phase having π-donors and π-acceptors characteristics between CSP and an analyte. In addition to π-π, dipole-dipole, hydrogen bonds, steric, and hydrophobic interaction also contributes for resolution. Pirkle type of stationary phase is potentially used in different techniques such as HPLC, GC, CE, CEC, and so on. The compounds containing alkyl, aryl, carbinols, hydantoins, lactams, succinimides, phthalides, sulphoxides, and sulphides functionality can be easily separated by Pirkle type of CSPs.

(ii) Polysaccharide CSPs

In 1952, Dalgliesh successfully resolved the racemic amino acids into chirally pure enantiomers on cellulose based TLC.[44] Native polysaccharides (cellulose) have five chiral centers but still cannot be used for chromatographic separation. This is due to highly polar hydroxyl groups that make some non-stereoselective interaction with racemic analyte resulting decrease in an enantiomeric excess. On the other hand, triacetate derivate of cellulose is widely used to separate the racemic compounds. Nowadays, cellulose based CSPs are commercially available and can separate a wide variety of compounds. Recently, researchers also work on

some other interesting chiral compounds such as chitosan, chitin, amylopectin, maltodextrins, and dextrans as a chiral material. Structures of polysaccharide type of chiral stationary phases are represented in **Figure 1.12.**

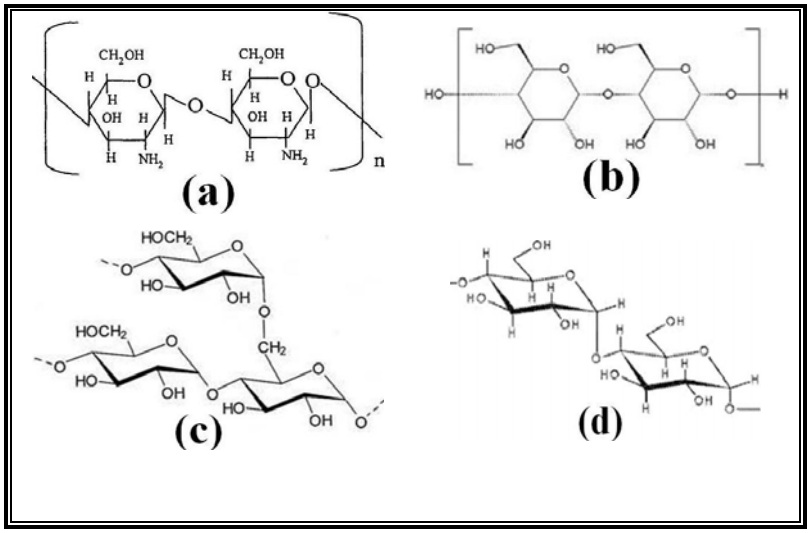

Figure 1.12. Polysaccharide type chiral stationary phases of (a) chitosan, (b) maltodextrin, (c) amylopectin, and (d) dextrans

(iii) Inclusion type CSPs

This type of CSPs work on the principle of host-guest type of mechanism wherein the host is the chiral CSP and guest is the racemic analyte. In this type, guest analyte inserted into the cavity of host CSP. Commonly used CSPs are chiral crown ether and cyclodextrins (CD). Chiral crown ethers are well-known macrocyclic compounds that work on the principle of host-guest inclusion complex formation. Kuhn *et al.*[54] first described the applications of crown ether in capillary electrophoresis. Nowadays, more literature is available for the separation of amino acids using crown ether based CSP. In 1986, Armstrong *et al.*[55] first developed the cyclodextrin containing chiral stationary phase. In nature, cyclodextrin is available in three different forms such as α, β, and γ-form. Potentially used cyclodextrin is the β form. The α form contains six, β form contains seven, and γ-form contains eight numbers of chiral centers. Inclusion type of CSPs have been potentially used in different chromatographic methods such as HPLC, GC, SFC, TLC, CE, CEC, and so on. Most preferable mechanism is the inclusion of the bulky hydrophobic group into the hydrophobic cavity of the CD. In addition to inclusion interaction, hydrogen bonding or dipole-dipole interactions between the CD and an analyte also attributes for resolution. Recently, derivatives of β-CD, such as heptakis(2,3,6-tri-O-methyl) or hydroxyalkyl-β-cyclodextrin are

widely used to separate the enantiomers. Different sizes of crown ethers[56,57] are also used widely as inclusion type of chiral stationary phases which are shown in **Figure 1.13.**

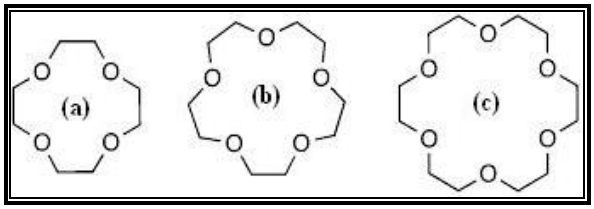

Figure 1.13. Inclusion type of chiral stationary phases (a) 12-crown-4, (b) 15-crown-5, and (c) 18-crown-6 polyether

(iv) Ligand exchange CSPs

In 1971, Davankov *et al.*[58] developed the ligand exchange CSPs based on the concept of ternary mixed metal complexes formation between bidentate analyte/divalent metal ion and ligand immobilized stationary phase. Generally, transition metal ions such as Cu^{2+} and chiral amino acids are used in Ligand exchange CSPs. Factors such as pH, ionic strength, and column temperature significantly influence to enantioseparation.

(v) Protein CSPs

A protein is made up of number of chiral amino acids and is well-known for racemic compound resolution.[59] For example, silica supported bovine serum albumin or human serum albumin is used as a chiral selector in chiral column and TLC. In addition to this, Chiral-AGP and Chiral-HAS comprises of α1-acid glycoprotein and human serum albumins, respectively and silica modified with these chiral compounds is used as a stationary phase. Different physico-chemical forces such as dipole-dipole interactions, hydrogen bonds, and hydrophobic interactions attribute for separation of racemic drug into optically pure compounds.

(vi) Macrocyclic antibiotics

Armstrong developed[60] the macrocyclic antibiotics as chiral selectors. These selectors have been potentially used in different applications such as HPLC, TLC, and capillary electrophoresis. Macrocyclic antibiotics are divided into two major classes i.e. ansamycins and glycopeptides. Ansamycins type consists of rifamycin B and rifamycin SV whereas

glycopeptides type consists of vancomycin, ristocetin, teicoplanin, and avoparcin. Rifamycin B is widely used for enantioseparation of basic compounds while rifamycin SV and the glycopeptides antibiotics are used for the enantioseparation of acidic compounds. However, Teicoplanin[61] is widely used for research as well as in industry due to higher selectivity. The structure of macrocyclic antibiotics (Teicoplanin) is depicted in **Figure 1.14.**

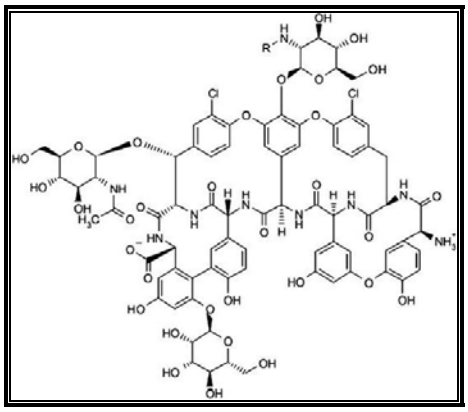

Figure 1.14. Structure of macrocyclic antibiotics (Teicoplanin)

1.8.6. Types of racemates

Racemic mixture contains equal proportion of left and right handed enantiomers of the chiral molecules. Louis Pasteur found[62] that, racemic tartaric acid contain both R and S forms. Racemic compound is a mixture of two enantiomers which rotate plane polarized light in equal and opposite direction, consequently racemic compound is optically inactive. However, two pure enantiomers have same physical properties except optical rotation. In general, racemates can be classified into four different types. Out of four methods, three were discovered by H. W. B. Roozeboom in 1899.[63]

(i) Conglomerate (racemic conglomerate)

It consists of mechanical mixture of two pure and opposite enantiomers. Especially, molecules with same enantiomer have more affinity instead of opposite. Melting point of racemic conglomerate is lower than pure enantiomer whereas addition of one enantiomer to racemic conglomerate increases the melting point.

(ii) Racemic compound (true racemate)

Molecules in true racemate have greater affinity towards opposite enantiomer than same. Enantiomers in the crystals are arranged in the order of 1:1 ratio. Small amount of one enantiomer addition decreases the melting point of racemic compound. Pure enantiomer have higher or lower melting point than racemic compounds.

(iii) Pseudoracemate (racemic solid solution)

In this type, there is no big difference between same and opposite enantiomers unlike conglomerate or racemic compound. Crystals formed by equal proportion of both enantiomers. There may be small change or no change after addition of the pure enantiomer to the racemate.

(iv) Quasiracemate

Quasiracemate relates to the mixture of two similar or opposite compounds, in which, one isomer is left handed and opposite isomer is right handed. In 1853, Pasteur studied this type of racemate which relates to 1:2 mixture of the bisammonium salt of (+)-tartaric acid and the bisammonium salt of (−)-malic acid in water.

1.9. Polymers for drug delivery

Drug delivery is the process of approaches, formulations, technologies, and systems for transporting a pharmaceutical compound into the body as needed to safely achieve its desired therapeutic effect. Drug delivery study relate to the development of drug release profile, absorption, distribution, and elimination to improve the product efficacy, safety, convenience, as well as compliance to patient. Drug can be released by different methods including diffusion, degradation, swelling, or affinity mechanisms. Natural and synthetic polymers became more successful as a carrier for drug delivery.[64] Targeted drug delivery is useful for a longer period drug profiling. In recent years, considerable attention has been paid to develop the nanoparticle for the application perspectives in drug loading/delivery. Researchers developed polymer having balanced system of hydrophilic-hydrophobic, reactivity, high surface area, and porosity. Nanoparticles have been used in the drug delivery such as targeted, controlled, and sustained drug delivery.[40,65] However, nano and micron sized particles have their own merits and demerits

with their properties. Nowadays, number of drug delivery materials is available. It can be classified depending on their composition.

1.9.1. Drug delivery materials

(i) Inorganic nanoparticles[66]

(a) Metal nanoparticles **(b)** Mesoporous silica nanoparticles

(ii) Polymers in drug delivery[67]

(a) Polymeric micelles **(b)** Polymeric nanoparticles

(iii) Dendrimers[68]

(iv) Carbon nanotube[69]

Most common factors attributing to drug delivery are mentioned below

(i) Adsorbent concentration **(ii)** Adsorbent properties (hydrophilic, hydrophobic, surface area, pore volume, pore size and porosity) **(iii)** Solubility of drug **(iv)** pH of the drug solution **(v)** Adsorbent-adsorbate contact time **(vi)** Temperature, and **(vii)** Drug solution concentration

1.9.2. Major types of drug delivery

(i) Controlled drug delivery: In this method, drug delivered with predetermined rate, locally or systematically for a specific period of time.

(ii) Targeted (smart) drug delivery: In this method, drug delivered to the patient in such a way that the concentration of the drug in the particular part of the body is higher relative to other body part. This type of drug delivery is mostly used in cardiovascular and diabetes. This drug delivery is widely used to treat cancerous tumors.

(iii) Sustained drug delivery: In this method, drug delivered at a predetermined rate in order to maintain a constant drug concentration for a specific period of time with minimum side effects. This drug delivery is also referred as “long acting” or “delayed release.”

(iv) Transdermal drug delivery: In this method, drug delivered to the body part across the skin for systemic distribution. Most widely used transdermal methods are transdermal patches and transdermal gel.

Drug delivery is related to two concepts

(i) *In vitro*: Study of drug delivery outside the living body

(ii) *In vivo:* Study of drug delivery inside the living body

Drug delivery material and its requirements

Mostly, drug delivery is carried out using biodegradable polymer, however, these types of polymers must follow the specific requirements.

(i) Polymer and their degradation product must be biocompatible

(ii) Drug carrier must have enough mechanical strength

(iii) Processability with simple equipment

(iv) Drug solubility in different solvents

(v) Drug delivery route must be inexpensive

(vi) Drug delivery material and route must be approved by USFDA or European Medicine Evaluation Agency (EMEA).

Drug delivery system and its requirements

(i) High efficiency **(ii)** More efficacy **(iii)** Less side effects **(iv)** Continuous and slow release,

(v) Easy handling **(vi)** High mobility**(vii)** Inexpensive, and **(vii)** Non-hazardous

1.9.3. Advantages of controlled drug delivery

(i) Convenient method **(ii)** Side effects can be reduced **(iii)** Minimum dose concentration is sufficient, and **(iv)** Reduction in cost due to minimized dose concentration

1.9.4. Disadvantages of controlled drug delivery

(i) Less applicability between *in vitro* and *in vivo* delivery

(ii) Once drug applied it can not be removed

(iii) Drug formulation increases cost

1.9.5. Applications of drug delivery

(i) Optimum dose at right time and at right location attributes to avoid the side effects
(ii) Effective use of expensive ingredients, reduction in production and costs
(iii) Beneficial to patients, better therapy, improved comfort, and standard of living

1.10. Polymer supported Lewis acids: Recyclable catalysts

Catalysis is an active and highly applicable research area of chemistry. However, Lewis acids are widely used in catalytic process for functional group conversion. Conventional unsupported Lewis acids are very old method for application in organic reactions and functional group transformation. Lewis acids such as $AlCl_3$, BF_3, $SnCl_2$, $HgCl_2$, $Cu(OTf)_2$, and $Sn(OTf)_2$ have potential applications in various fields.[70] The efficiency of polymer supported catalysts, reagents, substrates, scavenger, protecting group, and enzyme depends on the polymer properties such as surface area, pore volume, pore size, porosity, hydrophilic/hydrophobic and reactivity of a polymer. Polymer selection depends on the desired properties of a polymer support. Polymer properties can be tuned in such a way to balance crosslinking, porosity, and functionality. The non-crosslinked polymer (homopolymer) can swell to a certain extent depends on the solvent and polymer type or structure whereas crosslinked polymer is difficult to swell. In solid phase synthesis, feasibility of the polymer supported catalysts depend on the selection of resin. Increased crosslinker concentration, increases the mechanical strength, however, decreases the polymer swelling and functionality. Moreover, non-crosslinked polymer increases the swelling and functionality but reduces the polymer strength. This problem can be overcome by selection of proper monomer composition in copolymer resin. However, 1–2% of crosslinked polymers are widely used to obtain suitable polymer support for covalent modification. Porosity and surface area are highly influencing parameters that substantially affect the polymer application wherein we can control the micro, meso, and macroporous properties of polymer by selecting a suitable porogenic solvent. Eventhough, the large number of functional polymers were synthesized in the past, polystyrene was potentially used as a support in many solid phase synthesis. In 1970s, Neckers and co-workers[71] reported the polymer protected aluminium trichloride having potential applications in various fields. Lewis acids have been used in alkylation, acylation, sulfonylation, and hydroxylation. Currently, Lewis acids are widely used

for Diels-Alder reaction. Moreover, Ran *et al.*[72] reported the synthesis of polymer supported Lewis acid and applications thereof.

Solid support (polymer) and its required properties

It is difficult to synthesize the polymer bearing all the following properties. Therefore, synthesis of polymer containing maximum desired properties is an essential.[73]

(i) Mechanically robust, **(ii)** Stable towards temperature variation, **(iii)** Well-solvated and catalysts accessible sites, **(iv)** Uniform and acceptable particle size (nano/micron), **(v)** Stable towards acidic, basic, oxidizing, and reducing agents, **(vi)** Swelling in broad range of solvents, **(vii)** Compatible towards radical, carbene, carbanion, carbocation, and carbenium ions, **(viii)** Swelling in buffer, and **(ix)** Acceptable loading/immobilization

Most commonly used immobilization techniques are

(i) Adsorption **(ii)** Entrapment **(iii)** Covalent binding, and **(iv)** Membrane confinement

Effect of different parameters on polymer applications are described below

To balance all properties in a single type of resin is difficult. Therefore, selection of polymer resin with desired properties is needed. Properties of different types of immobilization techniques are given in **Table 1.3.**

Table 1.3. Properties of different types of immobilization techniques

Characteristics	Adsorption	Covalent binding	Entrapment	Membrane confinement
Preparation	Simple	Difficult	Difficult	Simple
Cost	Low	High	Moderate	High
Binding force	Variable	Strong	Weak	Strong
Leakage problem	Yes	No	Yes	No
Applicability	Wide	Selective	Wide	Very wide
Reuse property	High	Low	High	high
Matrix effect	Yes	Yes	Yes	No

1.10.1. Advantages of polymer supported Lewis acids

Polymer supported Lewis acids have wide applications due to their unique properties as presented below.

(i) Simple filtration to isolate and recover the catalyst[74]
(ii) Simplification of product work-up, separation and isolation
(iii) Odorous and harmful substances can be handled easily
(iv) Avoids product contamination
(v) Industrially economical
(vi) Environmentally benign[75]
(vii) Reusable[76]
(viii) Highly tunable properties by changing physico-chemical parameters to obtain desired polymer resin

1.10.2. Applications of Lewis acids

Over the last two decades, polymer resins were potentially used in number of applications. However, some common applications are: **(i)** C–C bond (alkylation and acylation) formation is the most attractive application of the Lewis acid[77] **(ii)** Diels-Alder reaction[78] **(iii)** Biginelli Reaction[79] **(iv)** Acylation of alcohols, thiols, and sugars **(v)** Baylis-Hillman reaction,[80] and **(vi)** Hydrocarbon conversion.

References

[1] Goodyear C., Improvement in India-rubber fabrics, 1859, **US Pat. No. 26360 A,** 1–2.

[2] Baekeland L. H., Method of making insoluble products of phenol and formaldehyde, 1909, **US Pat No. 942699 A,** 1–3.

[3] Staundinger H., *Uber Polym.,* 2006, **53,** 1073–1085.

[4] Cunningham W. A., *J. Chem. Educ.,* 1935, **12(3),** 120–124.

[5] Oesper R. E., *J. Chem. Educ.,* 1929, **6,** 677.

[6] Serniuk G. E., Banes F. W., and Swaney M. W., *J. Am. Chem. Soc.,* 1948, **70,** 1804–1808.

[7] Pepper K. W., Paisley H. M., and Young M. A., *J. Am. Chem. Soc.,* 1953, 4097–4105.

[8] Merrifield R. B., *J. Am. Chem. Soc.,*1963, **85,** 2149–2154.

[9] Iwakura Y., Kurosaki T., Ariga N. and Ito T., *Makromol. Chem.,* 1966, **97,** 128–138.

[10] Subbiah R., Veerapandian M. and Yun K. S., *Curr. Med. Chem.,* 2010, **17,** 4559–4577.

[11] Jones B. H. and Lodge T. P., *Polym. J.,* 2012, **44,** 131–146.

[12] Kann N., *Molecules,* 2010, **15(9),** 6306–6331.

[13] Alexandratos S. D. and Darrell Crick W., *Ind. Eng. Chem. Res.,* 1996, **35,** 635–644.

[14] Mane S., Ponrathnam S. and Chavan N., *Eur. Polym. J.,* 2014, **59,** 46–58.

[15] Costacurta S., Biasetto L., Pippel E. and Woltersdorf J., *J. Am. Ceram. Soc.,* 2007, **90(7),** 2172–2177.

[16] Oliveira M. B. and Mano J. F., *Biotechnol. Process,* 2011, **27,** 1–16.

[17] Pal N. and A. Haumik A., *Adv. Colloid Interface Sci.,* 2013, **189–190,** 21–41.

[18] Belmares M., Blanco, M., Goddard W. A., Ross R. B., Caldwell G., Chou S. H., Pham J., Olofson P. M. and Thomas C., *J. Comput. Chem.,* 2004, **25(15),** 1814–1826.

[19] Weast R. C., Handbook of Chemistry and Physics, 56th edition, *CRC Press, Inc. U.S.A.,* 1974–**75,** C-720(D).

[20] Feng C., Wang R., Shi B., Li G. and Wu Y., *J. Membr. Sci.,* 2006, **277(1–2),** 55–64.

[21] Uleva G. A. and Kim V. A., *Coke Chem.,* 2012, **55(5),** 167–171.

[22] Bajpai A. K. and Rajpoot M., *J. Sci. Ind. Res.,* 1999, **58,** 844–860.

[23] Katsikogianni M. and Missirlis Y. F., *Eur. Cells Mater.,* 2004, **8,** 37–57.

[24] Yang C. H., Goodwin J. G., *J. Catal.,* 1982, **78(1),** 182–187.

[25] Asha G. and Sham sunder K. M., *Int. J. Sci. Technol.,* 2014, **2(9),** 22–28.

[26] Singh R., Kulkarni K. and Kulkarni A. D., *Chem. Mater. Res.,* 2011, **1(2),** 16–21.

[27] Sharma V. and Sharma A., *Int. J. Enhanced Res. Sci. Technol. Eng.,* 2012, **1(2),** 1–8. ISSN: 2319–7463.

[28] Rao K. U and Satyanarayana S. V. V., Physical chemistry for the JEE and other engineering entrance examinations, Chapter 14: Surface Chemistry, 14.1–14.70. ISBN: 9788131787618.

[29] Hollis O. L., *Anal. Chem.,* 1966, **38(2),** 309–316.

[30] Ampon K., Basri M., Salleh A. B., Wan Yunus W. M. Z. and Razak A. C. N., *Biocatal. Biotransform.,* 1994, **10(1–4),** 341–351.

[31] Wood C. D. and Cooper A. I., *Macromolecules,* 2001, **34,** 5–8.

[32] Molla R. L., Ghosh K., Tuhina K. and Islam S. M., *New J. Chem.* 2015, **39,** 921–930.

[33] Barnett J. A., *Yeast,* 2000, **16,** 755–771.

[34] Blackmond D. G., *Cold Spring Harbor Perspective. Biol.,* 2010, **2(5),** a002147.

[35] Bai L., Sheeley S. and Sweedler J. V., *Bioanal Rev.,* 2009, **1(1),** 7–24.

[36] Hussain M. R. M., Din N., Hassan M., Razaq A. and Iqbal Z., *Arabian J. Chem.,* 2011. DOI: 10.1016/j.arabjc.2011.06.028.

[37] Kipping F. and Pope W. J., *J. Chem. Soc. Trans.,* 1909, **95,** 103–108.

[38] Ōki M., *Proc. Jpn. Acad. Ser. B,* 2010, **86(9),** 867–883.

[39] Wallach O., *Liebigs Ann. Chem.,* 1895, **286,** 90–143.

[40] Van Vlerken L. E. and Amiji M. M., *Expert Opin. Drug Dev.,* 2006, **3(2),** 205–216.

[41] Gonzalez-Campo A. and Amabilino D. B., *Top. Curr. Chem.,* 2013, **333,** 109–156.

[42] Kim J. H. and Scialli A. R., *Toxicol. Sci.,* 2011, **122,** 1–6.

[43] Sharma B., *J. Xenobiotics,* 2014, **4,** 2272–2290.

[44] Li B. and Haynie D. T., *Encycl. Chem. Process.,* 449–458. DOI: 10.1081/E-ECHP-120039232.

[45] Pirkle W. H. and Pochapsky T. C., *Chem. Rev.,* 1989, **89,** 347–362

[46] Huhnerfuss H. and Shah M. R., *J. Chromatogr. A,* 2009, **1216,** 481–502.

[47] Nguyen L. A., He H. and Pham-Huy C., *Int. J. Biomed. Sci.* 2006, **2(2),** 85–100.

[48] Hoffmann R. W. and Bewersdorf M., *Ann. Chem. Pharm.,* 1992, **6,** 643–653.

[49] Gazdag M., Szepesi G. and Huszar L., *J. Chromatogr. A,* 1988, **436,** 31–38.

[50] Vıctor G. Z., Leon A. G., Olives A. I., Martin M. A. and Menendez J. C., *Green Chem.,* 2011, **13,** 115–126.

[51] Dobashi Y. and Hara S., *Tetrahedron Lett.,* 1985, **26(35),** 4217–4220.

[52] Gil-Av E., Feibush B. and Charles-Sigler R., *Tetrahedron Lett.,* 1966, **10,** 1009.

[53] Pirkle W. H. and House D. W., *J. Org. Chem.,* 1979, **44,** 1957–1960.

[54] Kuhn R., Stoecklin E. and Erni E., *Chromatogr.,*1992, **33(112),** 32–36.

[55] Armstrong D. W., Ward T. J., Armstrong R. D. and Beesley T. E., *Science,* 1986, **232(4754),** 1132–1135.

[56] Paik M. J., Kang J. S., Huang B. S., Carey J. R. and Lee W., *J. Chromatogr. A,* 2013, **1274,** 1– 5.

[57] Choi H. J. and Hyun M. H., *J. Liq. Chromatogr. Related Technol.,* 2007, **30,** 853–875.

[58] Davankov V. A. and Rogozhin S. V., *J. Chromatogr.,* 1971, **60,** 280.

[59] Dang B., Kubota T., Mandal K., Bezanilla F. and Kent S. B. H., *J. Am. Chem. Soc.,* 2013, **135,** 11911−11919.

[60] Armstrong D. W., Tang Y., Chen S., Zhou Y., Bagwill C. and Chen J. R., *Anal. Chem.,* 1994, **66,** 1473–1484.

[61] Ward T. J. and Farris III A. B., *J. Chromatogr. A,* 2001, **906,** 73–89.

[62] Singh M. D. and Singh K. B., *J. Chem. Pharm. Res.,* 2012, **4(2),** 1123–1129

[63] Roozeboom H. W. B., *Z. Phys. Chem.,* 1899, **28,** 494.

[64] Shaik M. R., Korsapati M. and Panati D. D., *Int. J. Pharm. Sci.,* 2012, **2(4),** 112–116.

[65] Behera A. L., Patil S. V., Sahoo S. K. and Sahoo S. K., *Der Pharmacia Sin.,* 2010, **1(1),** 20–28.

[66] Liong M. M., Lu J., Kovochich M., Xia T., Ruehm S. G., Nel A. E., Tamanoi F. and Zink J. I., *ACS Nano,* 2008, **2(5),** 889–896.

[67] William B. Liechty W. B, Kryscio D. R., Slaughter B. V. and PeppasAnnu N. A., *Rev. Chem. Biomol. Eng.* 2010, **1,** 149–173.

[68] Tripathy S. and Das M. K., *J. Appl. Pharm. Sci.,* 2013, **3(9),** 142–149.

[69] Elhissi A. M. A., Ahmed W., Hassan I. U., Dhanak V. R. and Demanuele A., *J. Drug Delivery,* 2012, **837327,** 1–10.

[70] Chandra K. L., Saravanan P., Singh R. K. and Singh V. K., *Tetrahedron,* 2002, **58(7),** 1369–1374.

[71] Neckers D. C., Kooistra D. A. and Green G. W., *J. Am. Chem. Soc.,* 1972, **94(26),** 9284–9285.

[72] Ran R. and Fu D., *Chin. J. Polym. Sci.,* 1991, **9(1),** 79–85.

[73] Subbiah R., Veerapandian M. and Yun K. S., *Curr. Med. Chem.,* 2010, **17,** 4559–4577.

[74] Bandini M., Fagioli M, Melloni A. and Achille U. R., *Adv. Synth. Catal.,* 2004, **346,** 573–578.

[75] Dadiboyena S. and Hamme A. T., *Eur. J. Org. Chem.,* 2013, **33,** 7567–7574.

[76] Yamazaki O., Hao X., Yoshida A. and Nishikido J., *Tetrahedron Lett.,* 2003, **44(49),** 8791–8795.

[77] Friedel C. and Crafts J. M., *Compt. Rend.,* 1877, **84,** 1392 and 1450.

[78] Dias L. C., *J. Braz. Chem. Soc.,* 1997, **8(4),** 289–332.

[79] Ramos L. M., Tobio A. P. L., Santos M. R., Oliveira H. C. B., Gomes A. F., Gozzo F. C., Oliveira A. L. and Neto B. A. D., *J. Org. Chem.,* 2012, **77,** 10184−10193.

[80] Yang K. S., Lee W. D., Pan J. F. and Kwunmin Chen K., *J. Org. Chem.,* 2003, **68,** 915–919.

AIMS & OBJECTIVES

2.1. Synthesis of microporous polymers using solvating porogens

Over the last decade, crosslinked polymers are widely used as a support in column material, polymer supported catalysts, reagents, scavenger, enzymes, chelating agent and so on. Hydroxyl functionalized copolymers with high surface area and micropores would be synthesized by suspension polymerization varying monomer, crosslinker (ethylene dimethacrylate or divinylbenzene), pore generating solvent (1,1,2,2-tetrachloroethane or 1,2-dichlorobenzene), stirring speed, protective colloid concentration, and crosslink density to obtain the desired polymer properties for application perspectives. Thermogravimetry, differential scanning calorimetry, and swelling ratio of polymer beads would be examined as a function of crosslinker and crosslink density. Thus, copolymers could be scanned on the basis of surface area, pore volume, particle size, and swelling behavior to be suitable as solid supports for column chromatography, catalysis, and solid phase synthesis.

2.2. Synthesis of macroporous polymers using non-solvating porogens

Megaporous methyl methacrylate beaded microspheres would be synthesized using non-solvating, hydrophobic porogens by a suspension polymerization. Surface area, pore volume, pore size, thermal stability, and swelling behavior of the synthesized polymers could be studied. Moreover, effect of non-solvating porogens on polymer properties would be evaluated. We can obtain the distinguishable porosity and surface area using non-solvating porogens. Indeed, porous polymers are substantially recognized as a support for adsorption and entrapment technology. Swelling behaviour of polymer in different solvents could be evaluated. Polymer properties are crucial during polymer support selection. In the past, macroporous polymers were used in different applications such as solid phase synthesis, solid phase extraction, and biomedical applications.

2.3. Synthesis of macroporous polymers by varying concentration of non-solvating porogens

Gigaporous polymers would be synthesized by varying concentration of non-solvating (n-cyclohexanol, n-octanol, or n-decanol) porogens and crosslinkers. Effect of concentration of non-solvating porogens on polymer properties such as surface area, particle size, thermal, and

swelling behaviour can be evaluated. Indeed, porosity is a key parameter for enzyme immobilization as a support. Thermal properties can be studied as a function of rigidity and flexibility of the crosslinker in the polymer matrix. Thermostable polymer would be obtained by varying type and concentration of crosslinker. Distinguishable porosity would be obtained using the higher concentration of n-hexanol.

2.4. Synthesis of core-shell polymer for application in racemic drug resolution

Racemic drug resolution is one of the prominent research areas. Racemic drug salbutamol would be resolved using polymer supported chiral selector which can be evaluated by high performance liquid chromatography. β_2-adrenergic receptor agonist are widely used for the relief of bronchospasm in the conditions such as asthma and chronic obstructive pulmonary disease. Salbutamol is a highly selective adrenergic stimulant used in the treatment of bronchial asthma and other forms of reversible airways obstructive disease. Salbutamol sulphate has pharmaceutical R(+) form and adverse S(-) form (inactive form) which would be resolved by core-shell polymer. For core-shell polymer, poly(MMA-*co*-DVB) can be obtained as a core and poly(GMA) may be synthesized as a shell. Suspension polymerization is the suitable technique for obtaining the core polymer and solution polymerization is a suitable technique for shell polymer synthesis. This core-shell polymer could be used as polymer support for D-(-)-dibenzoyl tartaric acid as a chiral selector. Chirobiotic-T (Teicoplanin) chiral column would be used for the separation of an enantiomers of racemic drugs. An enantiomeric excess of racemic drug can be determined by the peak area of the individual enantiomers.

2.5. Synthesis of polymer supported metal for application in drug loading kinetics

Acrylate based polymer would be synthesized and modified with gold by simple aqueous reduction method for drug loading application perspectives in a suitable medium. Although, surface area, particle size, acid content (reactivity), scanning electron microscopy, and energy dispersive X-ray analysis of the base polymer and polymer supported metal is need to be performed. Pantoprazole sodium and chloroquine would be the drugs to be evaluated. Physico-chemical characterization, contact time, adsorption isotherm and adsorption kinetics would be evaluated. Langmuir adsorption isotherm, pseudo-first, and pseudo-second order kinetics would

be evaluated. Differential thermogravimetric analysis and differential scanning calorimetry can be studied to confirm polymer thermostability and processing temperature during catalytic applications in thermal reactions. In addition, polymer supported gold can be used in catalytic activity for functional group transformations.

2.6. Synthesis of polymer supported Lewis acids and application thereof

Moisture-insensitive polymer supported Lewis acids have potential applications over conventional Lewis acids. In the present work, poly(allylamine-*co*-divinylbenzene) would be synthesized using cyclohexanol as a porogen at different crosslink densities. Subsequently, polymer can be modified with various Lewis acids including $AlCl_3$, $SnCl_2$, and $HgCl_2$. These base and modified polymers can be characterized by different techniques such as surface area, particle size, thermogravimetric analysis, scanning electron microscopy, energy dispersive X-ray analysis, and swelling ratio. Recovery, recycle and reuse properties would be evaluated.

MICROPOROUS POLYMER: SOLVATING POROGENS

3.1. Introduction

In 1963, Merrifield invented the polymer supported chemistry for solid phase peptide synthesis.[1] Over the past few years, polymers with high surface area have increased attention due to their interesting properties such as hydrophilic/hydrophobic interaction, reactivity, porosity which make them potentially useful in different fields.[2–7] Mostly, in solid phase synthesis, polymers were used as a support for substrate,[8–10] reagents,[11] catalysts,[12,13] enzymes,[14] scavengers, protecting groups, and photosensitizers. Number of compounds can be immobilized on polymer support by covalent, ionic, adsorption, or entrapment methods. Industrially, the use of polymer as a support in asymmetric synthesis[15] and chiral resolution has become more successful.[16] Crosslinked polymer provides reliability in use, recovery, and reuse characteristics. Surface area of polymer is an important parameter to bind an organic compound while pore volume is a key parameter for enzyme immobilization. IUPAC classified the pores based on their width as a micro (< 2 nm), meso (2–50 nm), and macroporous (> 50 nm).

Suspension polymerization method is useful for synthesis of polymers in the form of beads with sizes ranging from 5–200 μm. In this method, protective colloid is added to stabilize the monomer droplets which are generally insoluble in water. The well-known polymerization methods such as suspension, emulsion, and dispersion were used to prepare microspheres. However, suspension polymerization is a unique method to prepare crosslinked polymer beads in the range of 10–200 μm. Investigation of porous properties is very crucial due to covalent binding of organic compounds and entrapment or adsorption of an enzyme into the polymer support. Polymers have been potentially used as a support in high temperature reactions also.[17] As a result, study of thermal properties like decomposition, and softening temperature is an essential. Furthermore, swelling behavior is helpful to decide the compatibility of polymer with solvent during application. Indeed, more swelling solvent exquisitely provides better results in solid phase synthesis. In 2004, Vianna-Soares and his coworkers[18] showed the surface area of 2-hydroxyethyl methacrylate copolymer is 31 m^2/g but this surface area is very small for industrial use or any other applications. This study was mainly focused on the synthesis of microporous polymer beads possessing high surface area.

In the present work, hydroxyl functionalized porous, crosslinked polymers of 2-hydroxyethyl methacrylate were synthesized using ethylene dimethacrylate/divinylbenzene as a

crosslinker in the presence of 1,1,2,2-tetrachloroethane/1,2-dichlorobenzene as a porogen. Present work demonstrated the synthesis and evaluation of porous, thermal, and swelling properties of the crosslinked polymers.

3.2. Experimental

3.2.1. Materials

2-Hydroxyethyl methacrylate:- Make: Sigma-Aldrich; Molecular formula: $C_6H_{10}O_3$; Molecular weight (g/mol): 130.14; Specific gravity/density (g/cm^3): 1.073; Boiling point (^{o}C): 205–208; Physical state: colorless liquid.

Ethylene dimethacrylate:- Make: Sigma-Aldrich; Molecular formula: $C_{10}H_{14}O_4$; Molecular weight (g/mol): 198.22; Specific gravity/density (g/cm^3): 1.051; Boiling point (^{o}C): 98–100; Physical state: colorless liquid.

1,4-Divinylbenzene (85%):- Make: Sigma-Aldrich; Molecular formula: $C_{10}H_{10}$, Molecular weight (g/mol): 130.19; Specific gravity/density (g/cm^3): 0.914; Boiling point (^{o}C): 195; Physical state: colorless liquid.

Azobisisobutyronitrile (AIBN):- Make: SAS Chemicals Pvt. Ltd. Mumbai; Molecular formula: $C_8H_{12}N_4$; Molecular weight (g/mol): 164.21; Specific gravity/density (g/cm^3): 1.1; Melting point (^{o}C): 103–105; Physical state: white solid.

1,1,2,2-Tetrachloroethane:- Make: Loba Chemie; Molecular formula: $C_2H_2Cl_4$; Molecular weight (g/mol): 167.85; Specific gravity/density (g/cm^3): 1.59; Boiling point (^{o}C): 146.5; Physical state: colorless liquid.

1,2-Dichlorobenzene:- Make: Loba Chemie; Molecular formula: $C_6H_4Cl_2$; Molecular weight (g/mol): 147.01; Specific gravity/density (g/cm^3): 1.30; Boiling point (^{o}C): 180.5; Physical state: colorless liquid.

Poly(vinyl)pyrrolidone:- Make: Fluka; Molecular formula: $(C_6H_9NO)_n$; Molecular weight (g/mol): 360,000 g/mol; Physical state: white powder.

Methanol:- Make: Loba Chemie; Molecular formula: CH_4O; Molecular weight (g/mol): 32.04; Specific gravity/density (g/cm^3): 0.7918; Boiling point (^{o}C): 34.7; Physical state: colorless liquid.

Toluene:- Make: Loba Chemie; Molecular formula: C_7H_8; Molecular weight (g/mol): 92.14; Specific gravity/density (g/cm^3): 0.87; Boiling point (^{o}C) : 111; Physical state: colorless liquid.

Dimethylformamide:- Make: Loba Chemie; Molecular formula: C_3H_7NO; Molecular weight (g/mol): 73.09; Specific gravity/density (g/cm^3): 0.948; Boiling point (^{o}C): 152–154; Physical state: colorless liquid.

3.2.2. Synthesis of microporous polymer

The aqueous phase (5 wt%) was prepared by dissolving the protective colloid (PVP) in deionised water whereas organic phase was prepared by mixing monomer (2-hydroxyethyl methacrylate), crosslinker (ethylene dimethacrylate/divinylbenzene), initiator (2,2'-azobisisobutyronitrile), and pore generating solvent (1,1,2,2-tetrachloroethane/1,2-dichlorobenzene) in a nitrogen atmosphere at room temperature. Synthesis of copolymers was conducted in a specially designed double walled cylindrical glass reactor. The reactor was equipped with a constant temperature water bath (thermostat), mechanical stirrer, reflux condenser, and nitrogen gas inlet. Inlet and outlet for hot water circulation was also provided in the form of outer jacket to the reactor as shown in **Figure 3.1.** The organic (discontinuous) phase was added to the aqueous (continuous) phase and stirred at 500 rpm under nitrogen atmosphere. The reaction temperature was raised to 70^{o}C and stirred for 3 h. The copolymer beads obtained were thoroughly washed with water, methanol, finally with acetone, and dried at 60^{o}C under reduced pressure. The copolymer beads obtained by suspension polymerization were further purified with methanol in a soxhlet extractor[19] and dried at 60^{o}C under reduced pressure for 8 h. Poly(HEMA-*co*-EDMA) series synthesized in the presence of 1,1,2,2,-tetrachloroethane and 1,2-dichlorobenzene are abbreviated as HET and HED series, similarly poly(HEMA-*co*-DVB) synthesized in the presence of 1,1,2,2,-tetrachloroethane and 1,2-dichlorobenzene are abbreviated as HDT and HDD, respectively. Schematic representation of suspension polymerization is depicted in **Figure 3.1.**

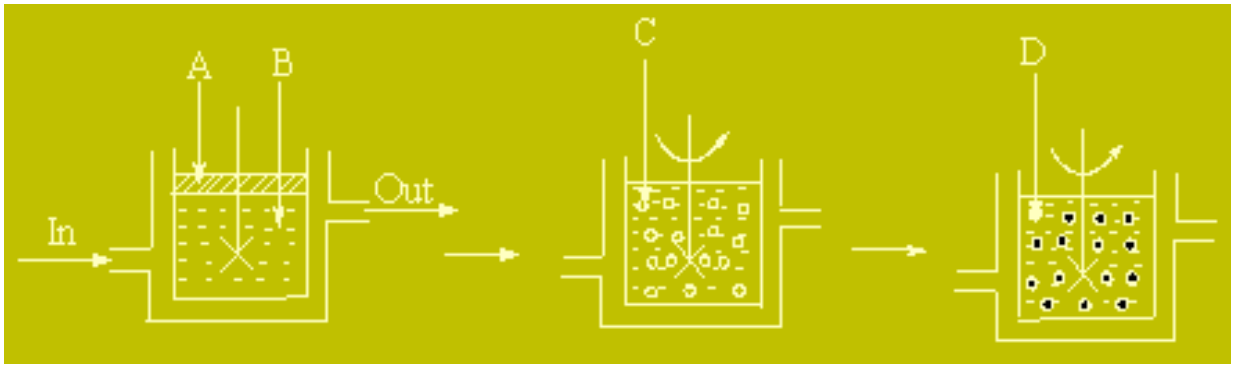

A – Organic (discontinuous) phase, B – Aqueous (continuous) phase, C – Formation of liquid droplets of monomer in aqueous phase, D – Thermal polymerization (70°C) of monomers to form solid copolymers

Figure 3.1. Schematic representation of suspension polymerization

Polymer synthesis scheme

Synthesis of poly(HEMA-*co*-EDMA) and poly(HEMA-*co*-DVB) by suspension polymerization is presented in **Scheme 3.1 and 3.2,** respectively.

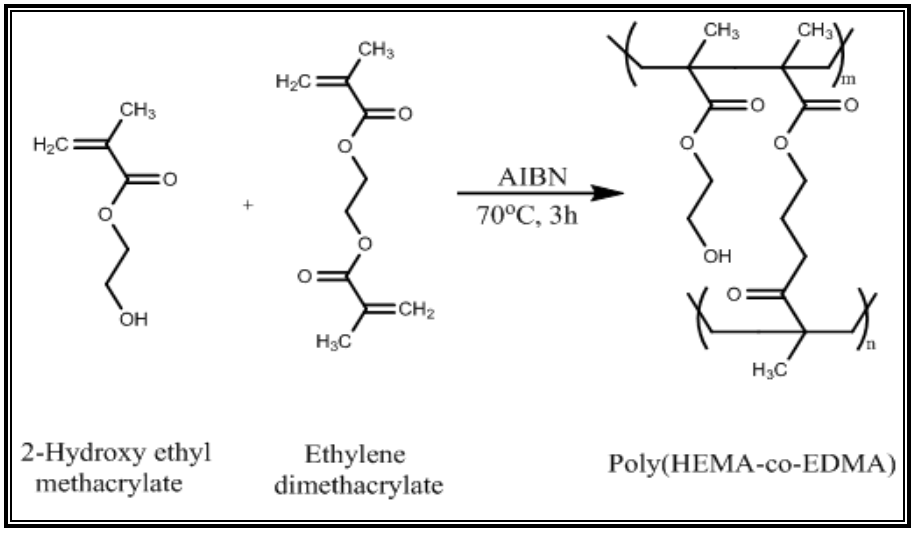

Scheme 3.1. Synthesis of poly(HEMA-*co*-EDMA) by suspension polymerization

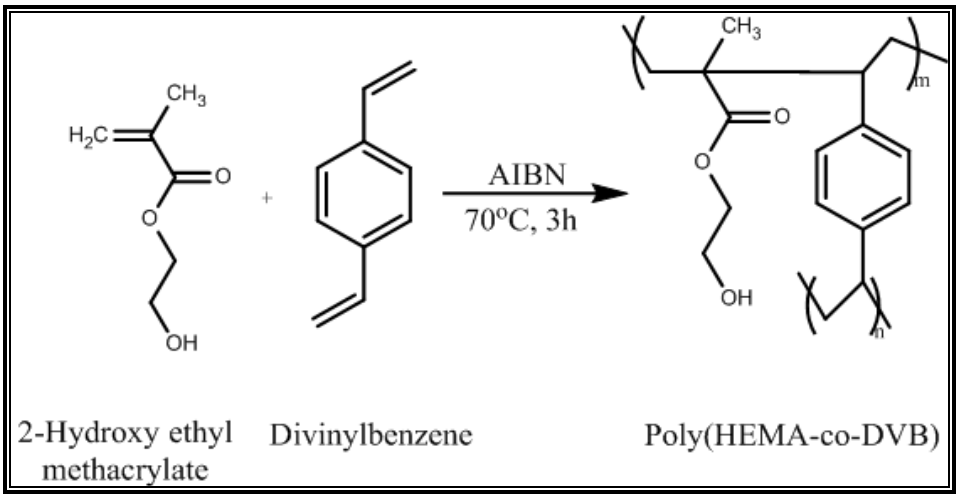

Scheme 3.2. Synthesis of poly(HEMA-*co*-DVB) by suspension polymerization

3.2.3. Characterization

FT-IR spectra were recorded on Perkin Elmer spectrophotometer (Model: Spectrum GX). The samples were prepared after drying the polymers at 80^{o}C for 8 h. Surface area of copolymers were determined from the adsorption/desorption isotherm by BET (Nitrogen adsorption) method using surface analyzer NOVA 2000e, Quantachrome. Microporous properties (pore volume and the pore size) were determined by Barrett–Joyner–Halenda (BJH) method via nitrogen adsorption-desorption method. Average particle diameter was measured using Accusizer 780 (model LE 2500-20) PSS.NICOMP particle sizing system, Santa Barbara, California, USA. Hydroxyl content was determined by acetic anhydride in pyridine using titrimetric method. Thermal stability (DTG) of polymers was studied by simultaneous thermal analysis (STA, Perkin Elmer), while glass transition temperature was studied by differential scanning calorimetry Q10 (Thermal analysis). Swelling ratio of polymers was determined by wt/wt ratio. Scanning electron microscopy (SEM) was used for external morphology and practical visualization which was performed by Quanta 200-3D with dual beam ESEM microscope wherein an electron source was thermionic emission tungsten filament.

3.3. Results and discussion

Microporous poly(HEMA-*co*-EDMA) and poly(HEMA-*co*-DVB) were synthesized by suspension polymerization varying crosslink density to obtain hydrophilic/hydrophobic properties of beads. Two different crosslinkers and two different porogens were used to obtain polymers exhibiting wide range of surface area. The crosslink density (CLD) defines the percent moles of crosslinker relative to the moles of monomer. The monomer-crosslinker feed composition and reaction conditions of poly(HEMA-*co*-EDMA) and poly(HEMA-*co*-DVB) used in suspension polymerization is depicted in **Table 3.1.** The concentration of monomer and crosslinker was determined by the **equation (3.1):**

$$A = \frac{\text{Mol wt. of M}}{\text{Density of M}} X + \frac{\text{Mol wt. of C}}{\text{Density of C}} X \text{ CLD} \quad \textbf{(3.1)}$$

where, A is the batch size, M is the monomer, C is the crosslinker, CLD is the crosslink density, and X is the determination factor.

Table 3.1. Monomer-crosslinker feed composition of polymer synthesized by suspension polymerization

Monomer system	Units	Crosslink density (%)					
		25	50	75	100	150	200
HEMA:EDMA	mol	0.047 : 0.012	0.037 : 0.018	0.030 : 0.023	0.026 : 0.026	0.020 : 0.030	0.016 : 0.032
	g	6.181 : 2.353	4.829 : 3.677	3.962 : 4.526	3.360 : 5.117	2.575 : 5.884	2.088 : 6.362
HEMA:DVB	mol	0.051 : 0.013	0.039 : 0.021	0.035 : 0.029	0.030 : 0.030	0.024 : 0.036	0.020 : 0.039
	g	6.636 : 1.660	5.040 : 2.705	4.564 : 3.747	3.948 : 3.949	3.108 : 4.664	2.563 : 5.129

Reaction conditions: Batch size: 8 mL; 2,2'-azobisisobutyronitrile: 2.5 mol%; stirring speed: 500 rpm; reaction time: 3 h; outer phase: H_2O; protective colloid: PVP; concentration of PVP: 5 wt%; porogens: 1,1,2,2-tetrachloroethane/1,2-dichlorobenzene; porogen conc.: 24 mL (monomer: porogen ratio, 1:3 v/v).

3.3.1. Fourier transform infrared (FT-IR) spectroscopy

FT-IR analysis is helpful for assigning functional groups present in the polymers. FT-IR spectrum (KBr pellet, cm^{-1}) of poly(HEMA-*co*-EDMA) elucidated the absorption peak for –OH functionality at 3534, aliphatic C–H stretching at 2957, ester functionality at 1731, methyl C–H asymmetrical bending at 1457, C–O–C stretching at 1263 and 1160, and –OH out-of-plane bending at 756. FT-IR spectrum (KBr pellet, cm^{-1}) of poly(HEMA-*co*-DVB) showed the absorption peak of –OH functionality at 3456, aliphatic C–H stretching at 2937, ester functionality at 1727, methyl C–H asymmetrical bending at 1455, C=C stretching at 1604, C–O–C stretching at 1250, aromatic C–H out-of-plane bending at 906 and 797, –OH out-of-plane bending at 711 and disubstituted ring at *para* position[20] at 832. FT-IR spectra of microporous poly(HEMA-*co*-EDMA) and poly(HEMA-*co*-DVB) are presented in **Figure 3.2.**

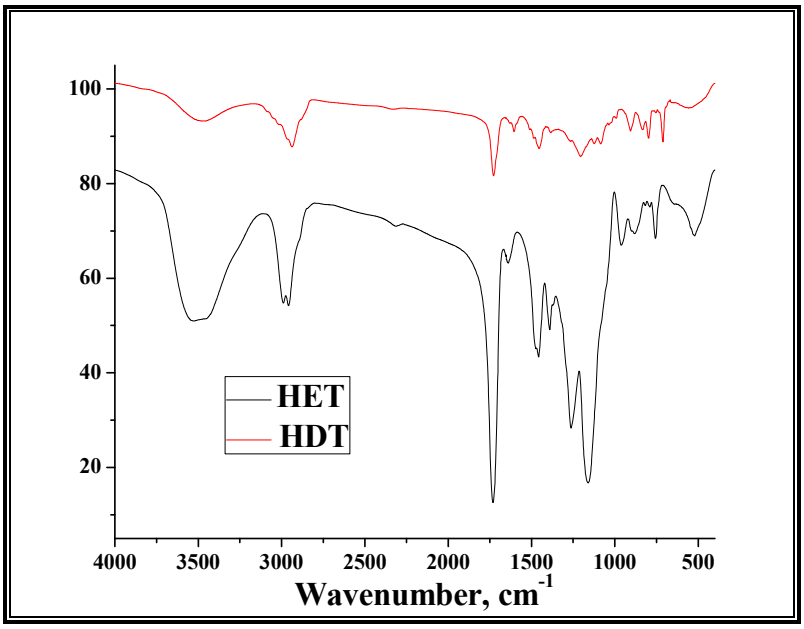

Figure 3.2. FT-IR spectrum of poly(HEMA-*co*-EDMA) and poly(HEMA-*co*-DVB) for 25% crosslink density

3.3.2. Surface area, pore volume, and pore size determination

Effects of several parameters like type of crosslinkers, porogens, and concentration of crosslinkers on the physical properties of the polymers were investigated. In general, three types of porogens can be used to generate the surface area and porosity into the polymer matrix[21] i.e. solvating (SOL), non-solvating (NONSOL), and polymeric (POLY) porogen. The porogen selection depends on desired properties of polymer. Qu *et al.*[22] reported the surface area of poly(HEMA-*co*-EDMA) prepared by emulsification method are in the range of 38–129 m^2/g. In the present work, effect of crosslinkers and porogens on different physical properties of poly(HEMA-*co*-EDMA) and poly(HEMA-*co*-DVB) obtained by suspension polymerization were studied. This investigation provides the high surface area poly(HEMA-*co*-EDMA) and it was in the range of 9–144 m^2/g. In addition, this study also demonstrated the high surface area of poly(HEMA-*co*-DVB) and was in the range of 22–564 m^2/g.

Surface tension of an aqueous and organic phase plays a pivotal role to generate surface area of polymers prepared by suspension polymerization. Surface tension of water, 1,1,2,2,-tetrachloroethane, and 1,2-dichlorobenzene are 72.8, 35.58, and 38.75 dynes/cm, respectively at room temperature (25^oC). However, if the surface tension difference between porogen (1,2-dichlorobenzene) and aqueous phase is lower, then attractive forces between aqueous phase and porogen also decreases resulting the separation of a porogen from an aqueous phase become easy and thus formed micropores leads towards high surface area. Miscibility of porogen in water is also an important which decides the porous properties of polymers. Miscibility of 1,1,2,2-tetrachloroethane and 1,2-dichlororbenzene in water is 2900 and 140 mg/L, respectively. If the miscibility of porogen in water is higher, then it is difficult to separate porogen from water as a result burst phenomena was followed and provides the bigger pore size. If the miscibility of porogen in water is lower, then it is easy to separate porogen from water, resulting release of porogen become uniform and provides smaller pore size. Thus, HET and HDT series showed bigger pore size than HED and HDD, respectively.

3.3.2.1. Effect of crosslinker

Concentration of crosslinker is the major while type of crosslinker (hydrophilic-hydrophobic) is the minor parameter that attributes to properties like surface area,[22] pore volume, and pore size of the beaded polymer.[23] In all four HEMA series, specific surface area was increased with increasing concentration of crosslinker.[24] Poly(HEMA-*co*-DVB) series showed the high surface area compared to poly(HEMA-*co*-EDMA) series due to increased hydrophobicity of DVB. Since, EDMA has polar as well as slight hydrophilic properties consequently more affinity towards aqueous phase, inversely DVB has non-polar and highly hydrophobic properties obviously more affinity towards organic phase. In all four copolymer series, HET, HED, HDT, and HDD, the surface area and pore volume was increased as crosslink density increased. This implied that, there is a particular trend in surface area as well as pore volume with crosslink density and these two properties are directly proportional to each other. However, phase separation occurs due to difference in the cohesive force between organic and aqueous phase during polymer synthesis that attributes for high surface area and porous property of polymer matrix.[25] At lower concentration of crosslinker, the higher meso and macropores formation took place resulting is lower surface area. No particular trend was observed in pore size, but in general, pore size was decreased with increasing crosslink density. This is because, as the crosslink density increased, network structure of polymer becomes rigid resulting reduction in pores size. Another problem associated with BET (Brunauer-Emmett-Teller) method is that, it has limitation to determine pore size between 0.3–300 nm by nitrogen adsorption-desorption i.e. smaller pore size of polymer can be only determined. To determine larger pore size (3 nm–200 μm) mercury porosimetry is a useful technique.[26]

3.3.2.2. Effect of porogens

Most important factors which control the surface area, pore volume, and pore size of the micro and macroporous properties of the polymer are the type of porogens and crosslinking density. Generally, solvating porogens produce small pores whereas non-solvating porogen produce large pores. In suspension polymerization, porogens are attributed to impart porous properties to the polymer beads. In poly(HEMA-*co*-EDMA), HED series exhibited the high surface area and pore volume compared to HET series. This is based on the solubility parameter

difference between water and porogens. Solubility parameter of 1,2-dichlorobenzene, 1,1,2,2-tetrachloroethane, and water are 10.0, 9.7, and 23.5 $(cal/cm^3)^{1/2}$, respectively. If the solubility parameter difference between water and porogens is low, the porogen remains in aqueous phase for a longer time and release slowly resulting small pores and vice-versa. Maximum surface area obtained for HED and HET series was 144 and 117.3 m^2/g for 200% crosslink density, respectively. Maximum pore volume for HED and HET series was 0.15 and 0.14 cm^3/g for 200% crosslink density, respectively. Both properties (surface area and pore volume) increased with increase in concentration of EDMA crosslinker. In case of poly(HEMA-*co*-DVB), maximum surface area was obtained with 1,2-dichlorobenzene porogen (564 m^2/g) for HDD, whereas equal volume of 1,1,2,2-tetrachloroethane showed only 399 m^2/g for same (200%) crosslink density. Maximum pore volume for HDD series was 0.56 cm^3/g whereas pore volume for HDT series was only 0.37 cm^3/g. However, no definite trend was observed in pore size distribution relative to crosslink density but 1,2-dichlorobenzene porogen showed lower pore size compared to 1,1,2,2-tetrachloroethane. These results clearly indicated that, 1,2-dichlorobenzene is able to impart more porous properties of polymer than 1,1,2,2-tetrachloroethane.[27] The BET isotherm plots of all four series for 200% crosslink density are shown in **Figure 3.3.** Surface area, pore volume and pore size for different crosslink density are displayed in **Figure 3.4** and labeled as a, b, and c, respectively. The results of surface area, pore volume, and pore size are reported in **Table 3.2.**

Table 3.2. Porous properties of poly(HEMA-*co*-EDMA) and poly(HEMA-*co*-DVB) series

Polymer series code	CLD (%)	SA (m^2/g) by BET	PV (cm^3/g) by BJH	PS (A^o) by BJH	APS (μm) By PSS	Expt. HC (mmol/g)
HET	25	9.6	0.01	43.46	18.66	1.57
	50	15.1	0.05	45.18	20.89	1.24
	75	86.2	0.11	52.81	21.89	0.79
	100	88.1	0.11	48.81	23.95	0.33
	150	112.0	0.12	38.59	28.37	0.20
	200	117.3	0.14	37.91	29.67	0.09
HED	25	27.0	ND	ND	18.94	1.76
	50	39.7	0.04	29.49	23.57	1.48
	75	91.7	0.09	57.90	24.40	0.94
	100	85.33	0.10	22.50	27.48	0.59
	150	93.3	0.12	52.35	34.47	0.47
	200	144.0	0.15	40.36	41.63	0.28
HDT	25	22.64	ND	ND	17.06	1.94
	50	141.1	0.20	57.14	17.97	1.61
	75	224.0	0.28	49.90	18.11	1.03
	100	246.0	0.29	47.43	21.56	0.73
	150	353.0	0.31	34.91	29.65	0.51
	200	399.0	0.37	37.47	30.58	0.33
HDD	25	37.65	ND	ND	17.21	1.95
	50	173.2	0.17	38.76	21.84	1.69
	75	250.5	0.23	37.23	46.02	1.17
	100	406.1	0.38	37.03	53.52	0.80
	150	549.0	0.54	39.30	65.18	0.65
	200	564.0	0.56	39.56	87.05	0.43

Abbreviations: **Poly(HEMA-*co*-EDMA):- HET (series 1):** HEMA-EDMA as monomer system and 1,1,2,2-tetrachloroethane as porogen; **HED (series 2):** HEMA-EDMA as monomer system and 1,2-dichlorobenzene as porogens; **Poly(HEMA-*co*-DVB):- HDT (series 3):** HEMA-DVB as monomer system and 1,1,2,2-tetrachloroethane as porogens; **HDD (series 4):** HEMA-DVB as monomer system and 1,2-dichlorobenzene as porogens; **CLD:** Crosslink density; **SA:** Surface area; **PV:** Pore volume; **PS:** Pore size; **APS:** Average particle size; **HC:** Hydroxyl content; **ND:** Not determined.

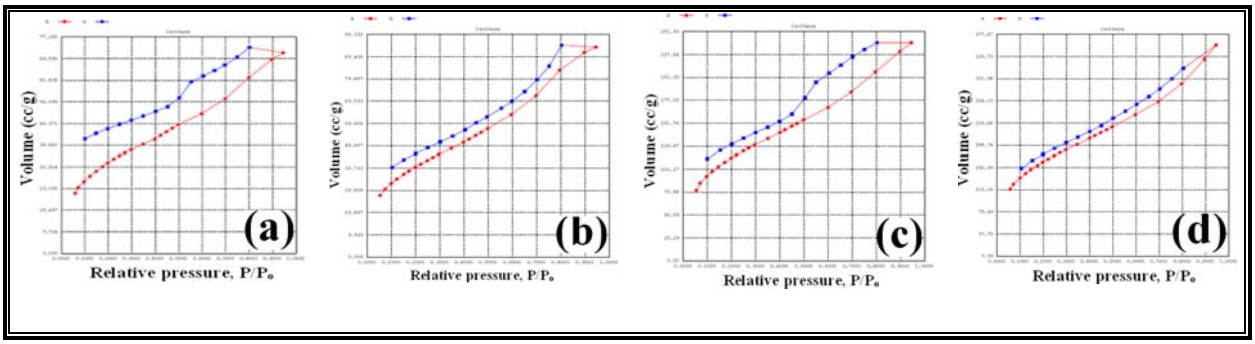

Figure 3.3. BET isotherm plots of polymer series (a) HET, (b) HED, (c) HDT, and (d) HDD for 200% crosslink density

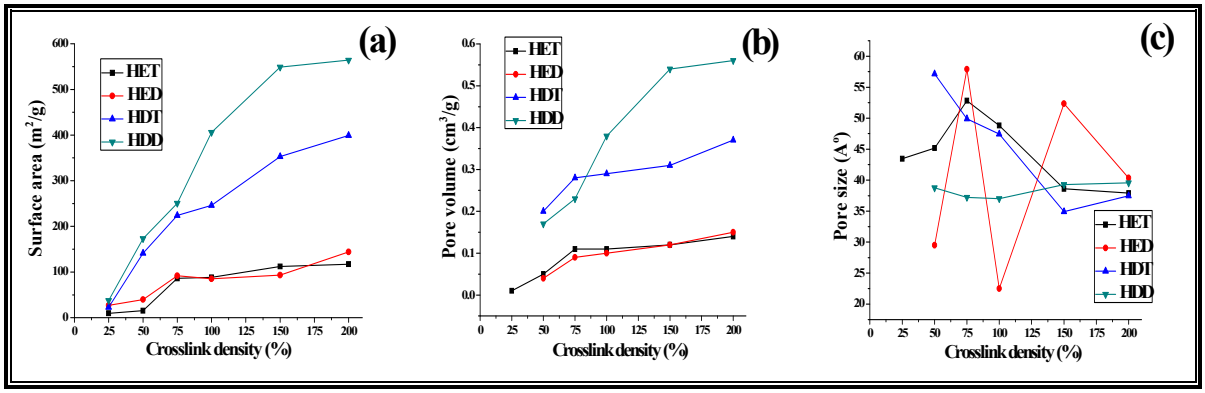

Figure 3.4. Comparison plots of (a) surface area, (b) pore volume, and (c) pore size for HET, HED, HDT, and HDD polymers

3.3.3. Particle size distribution

Average particle size of macroporous poly(HEMA-*co*-EDMA) and poly(HEMA-*co*-DVB) were evaluated. Copolymers synthesized by suspension polymerization, generally, have a particle size in the range of 5–200 μm. The particle size distribution of poly(HEMA-*co*-EDMA) and poly(HEMA-*co*-DVB) synthesized at 70°C was studied as a function of crosslink density and variation in porogens as illustrated in **Table 3.2.** The graphical representation of particle size distribution of HET, HED, HDT, and HDD polymer series for 25% crosslink density is shown in **Figure 3.5** and labeled as a, b, c, and d, respectively.

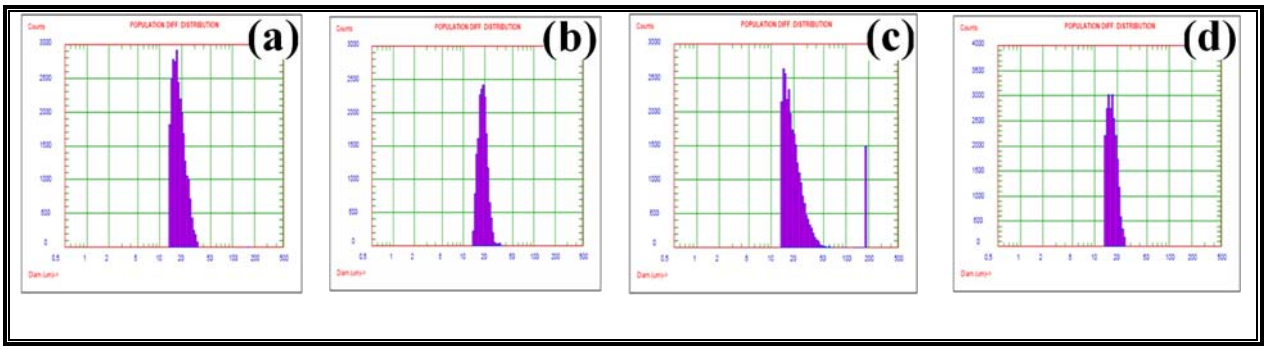

Figure 3.5. Particle size distribution of polymers (a) HET, (b) HED, (c) HDT, and (d) HDD for 25% crosslink density

Effect of crosslink density and porogens on average particle sizes was evaluated. In general, particle size increases with increase in the concentration of crosslinker. A similar observation was reported by Gong *et al.*[28,29] This phenomenon is probably due to increased interfacial tension between aqueous and organic phase which substantially affects the particle diameter. In reality, interfacial tension of HEMA-EDMA monomer mixture is much lower than HEMA-DVB due to variation in hydrophobicity. Average particle size of poly(HEMA-*co*-EDMA) and poly(HEMA-*co*-DVB) at different crosslink densities is represented in **Figure 3.6.**

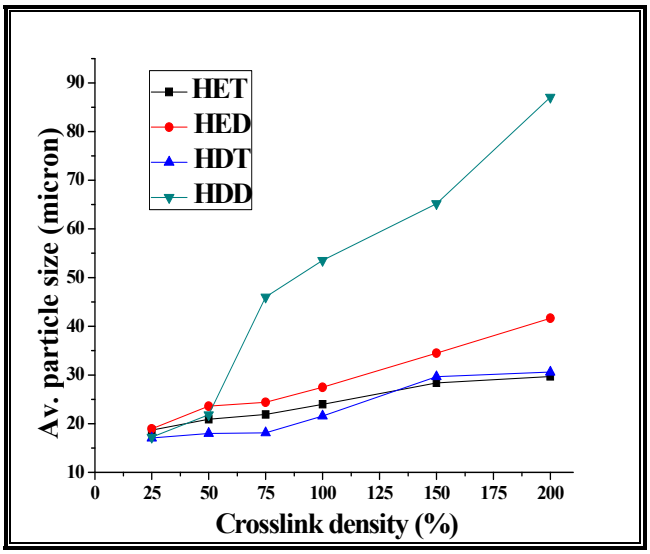

Figure 3.6. Average particle size of poly(HEMA-*co*-EDMA) and poly(HEMA-*co*-DVB) for different crosslink density

Comparatively, HET and HDT series synthesized using 1,1,2,2-tetrachloroethane as a porogen showed small average particle size than HED and HDD series synthesized using 1,2-dichlorobenzene as a porogen. This is mainly due to the high miscibility of 1,1,2,2-tetrachloroethane (2900 mg/L) than 1,2-dichlorobenzene (140 mg/L) in water resulting release of porogen easily in an aqueous phase. However, hydrophobic effect of crosslinker (DVB) produces more interfacial tension[30,31] than hydrophilic crosslinker (EDMA) which allowed increasing average particle size of HDD series than HED series. Generally, polymers synthesized by suspension polymerization displayed the average particle size in range of 15 – 100 μm. Both poly(HEMA-*co*-EDMA) and poly(HEMA-*co*-DVB) series demonstrated considerably larger particle size with 1,2-dichlorobenzene than 1,1,2,2-tetrachloroethane as a porogen. Nevertheless, HDD series demonstrated the higher particle size compared with other three series, because of hydrophobic property of DVB unlike EDMA as a crosslinker and less miscibility of 1,2-dichlorobenzene compared with 1,1,2,2-tetrachloroethane as a porogen. Particle size is dictated primarily by agitation[32] and density differences between organic and aqueous phase. The small density difference and higher agitation led to smaller particles. The particle size distribution of the four series was studied as a function of population difference and diameter of particles were in the range of 17 – 87 μm which is the characteristic feature of suspension polymerization.

3.3.4. Surface hydroxyl content

The surface hydroxyl contents of the dried polymers were determined using acetic anhydride in pyridine method, titrimetrically.[33] The hydroxyl content illustrated that, experimental values are much lower than theoretical due to large number of functional groups being buried within the bulk of the polymer matrix and hence are not available for titrimetric determination. At low crosslink density, hydroxyl content is high which indicates that polymer has more reactive sites. This is mainly due to the decreased concentration of 2-hydroxyethyl methacrylate monomer with increasing crosslink density. The theoretical hydroxyl content of polymer was determined using **equation (3.2):**

$$\text{Hydroxyl content (Theoretical)} = \frac{\text{Moles of HEMA monomer}}{\text{Total wt. of HEMA monomer and crosslinker}} \qquad \textbf{(3.2)}$$

Among the four series, HDD series demonstrated the highest surface hydroxyl content (1.95 mmol/g), whereas HET series revealed the lowest surface hydroxyl content (1.57 mmol/g) for 25% crosslink density. This is mainly due to the high surface area of HDD series compared to other series at same crosslink density. The other two series, HDT and HED showed 1.94 and 1.76 mmol/g, respectively at same crosslink density. Importantly, HDD series has high surface area resulting in more hydroxyl content followed by HDT, HED, and HET series. The hydroxyl contents (HC) are reported in **Table 3.2** (observed) and **Table 3.3** (theoretical) while theoretical and observed HC depicted in **Figure 3.7 (a) and (b),** respectively.

Table 3.3. Theoretical hydroxyl content of polymers

Polymer series code	Crosslink density (%)	Hydroxyl content (mmol/g)
Poly(HEMA-*co*-EDMA) HET/HED	25	5.5542
	50	4.3616
	75	3.5815
	100	3.0448
	150	2.3289
	200	1.8935
Poly(HEMA-*co*-DVB) HDT/HDD	25	6.1457
	50	4.9992
	75	4.2188
	100	3.8407
	150	3.0621
	200	2.5599

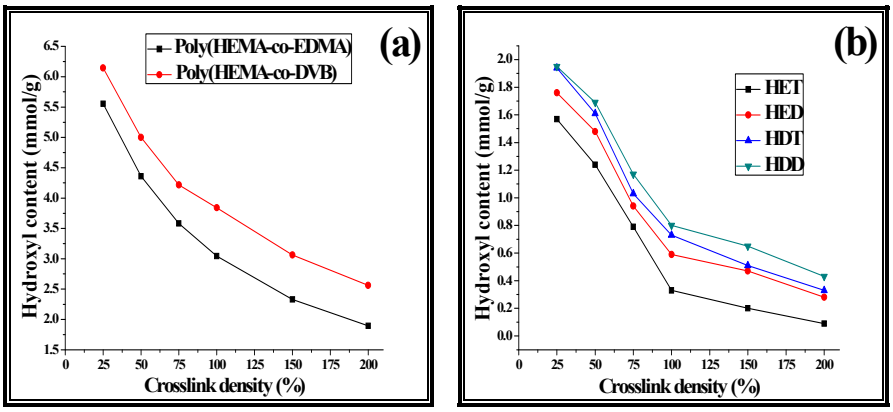

Figure 3.7. Hydroxyl content of polymers (a) theoretical, and (b) observed

3.3.5. Thermogravimetric analysis

The microporous polymers are widely used as a support for catalyst, reagent, substrate, protecting group, as well as for enzyme immobilization. These polymer supported moieties can be used in organic reactions at different temperatures depending on the reaction conditions.[34] Therefore, evaluation of polymer thermostability study is an essential. Thermogravimetric analysis was performed to study the decomposition temperature (Tmax) of polymers at different crosslink densities. The differential thermogravimetric (DTG) analysis of poly(HEMA-*co*-EDMA) and poly(HEMA-*co*-DVB) was studied by simultaneous thermal analyzer (STA-6000) in the temperature range of 50–800^{o}C at heating rate 10^{o}C/min. It was observed that, maximum decomposition temperature (Tmax) of poly(HEMA-*co*-EDMA) and poly(HEMA-*co*-DVB) was 321 and 413^{o}C for 25% CLD whereas 296 and 442^{o}C for 200% CLD, respectively. This is mainly due to the more flexible property of EDMA crosslinker unlike DVB. The maximum decomposition temperature (Tmax) of poly(HEMA-*co*-EDMA) and poly(HEMA-*co*-DVB) for 25 and 200% crosslink density is displayed in **Figure 3.8.**

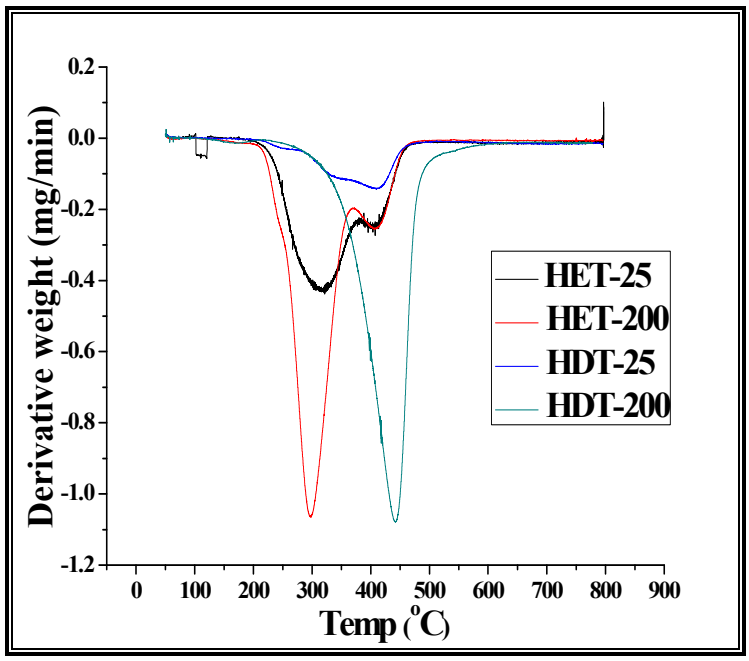

Figure 3.8. Differential thermogravimetric analysis of poly(HEMA-*co*-EDMA) and poly(HEMA-*co*-DVB) for 25 and 200% crosslink density

3.3.6. Differential scanning calorimetry

Differential scanning calorimetry illustrated that, glass transition temperature (T_g) of the poly(HEMA-*co*-EDMA) and poly(HEMA-*co*-DVB) for 25% crosslink density is 254 and 335^oC, respectively, whereas Tg of poly(HEMA-*co*-EDMA) and poly(HEMA-*co*-DVB) for 200% crosslink density is 240 and 343^oC, respectively. Poly(HEMA-*co*-EDMA) has lower T_g than poly(HEMA-*co*-DVB). It is worth noting that, as concentration of rigid crosslinker increased, glass transition (T_g) temperature was also increased and vice-versa. Particularly, in case of poly(HEMA-*co*-EDMA), if the concentration of crosslinker increased, polymer softens at slightly lower temperature inversely if the concentration of DVB increased in poly(HEMA-*co*-DVB), polymer softens at slightly higher temperature. More importantly, higher the DVB or lower the EDMA concentration imparts better thermal properties to the polymer. This is due to the thermal properties of the polymer depends on basic monomeric structure of monomer or crosslinker.[35] Divinylbenzene contains aromatic ring, whereas EDMA comprises aliphatic unit. Aromatic ring enhances the thermal stability as well as glass transition temperature due to Π – Π bonding. Type of crosslinker (rigid/flexible) is highly influenced to T_g while concentration of crosslinker influenced marginally. This shifting of glass transition temperature is mainly due to rigid and flexible property of the crosslinkers. In fact, glass transition temperature for poly(HEMA-*co*-EDMA) and poly(HEMA-*co*-DVB) is 225 and 325^oC, respectively. Thus, poly(HEMA-*co*-DVB) is a suitable polymer support in thermal reactions due to higher surface area and thermal stability. The DSC thermogram of polymers for 25 and 200% crosslink density is depicted in **Figure 3.9.**

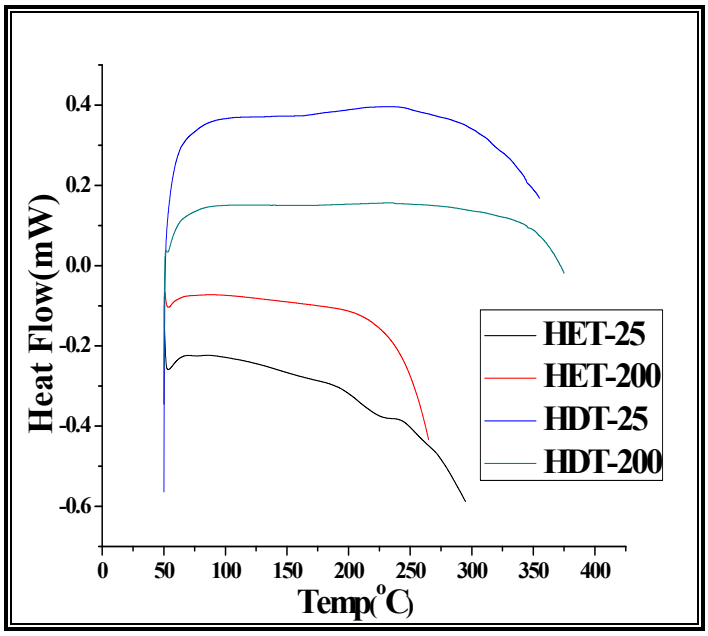

Figure 3.9. DSC thermograms of poly(HEMA-*co*-EDMA) and poly(HEMA-*co*-DVB) for 25 and 200% crosslink density

3.3.7. Swelling ratio

Swelling ratio of microporous, poly(HEMA-*co*-EDMA) and poly(HEMA-*co*-DVB) were carried out. Degree of polymer swelling depends on the porosity, solubility parameter of polymer, crosslink density, and interaction between polymer-swelling solvent. When a solvent enters into the polymer network, the polymer gets expand, reaches to equilibrium with maximum swelling. Degree of crosslinking and degree of swelling are inversely related to one another. Generally, homopolymer of HEMA monomer initially swell and finally dissolve in polar solvent. However, crosslinked polymers experience through swelling but not dissolve in polar or non-polar solvents. Solvent for swelling ratio was selected according to solubility parameter of polymer. The solubility parameter values of copolymers (calculated) and solvents[36] are reported in **Table 3.4.** The solubility parameter[36] of poly(HEMA-*co*-EDMA) and poly(HEMA-*co*-DVB) were determined by the **equation (3.3):**

$$\delta = \frac{D\Sigma G}{M} \qquad \textbf{(3.3)}$$

where, D is the density of monomer and crosslinker; ΣG is the summation of Small's molar attraction constant, and M is the molecular weight.

Table 3.4. Solubility parameter of polymers and swelling solvents

Copolymer and swelling solvent	Solubility parameter (δ) $(cal/cm^3)^{1/2}$
Poly(HEMA-*co*-EDMA)	14.23
Poly(HEMA-*co*-DVB)	13.72
Toluene	8.91
Dimethylformamide	12.14

Swelling ratio can be studied by binary or ternary system depending on solvent used for swelling purpose. In binary system, polymer and a single solvent interact with each other, whereas in ternary system, polymer interacts with a mixture of two solvents. Polymer-solvent interaction parameter (χ) depends on the crosslink density of polymer instead of molecular weight. However, polymer-solvent interaction parameter is directly proportional to the molar volume of the solvent and square of the difference between solubility parameter of solvent and polymer. The polymer-solvent interaction parameter (χ) was determined by Bristo and Watson semi empirical[37] **equation (3.4):**

$$\chi = \beta_1 + \frac{V_s}{RT}(\delta s - \delta p)^2 \qquad \textbf{(3.4)}$$

where, β_1 is the Lattice constant, usually about 0.34, V_s is the molar volume of solvent, R is the Universal gas constant, T is the absolute temperature in Kelvin, δ_s is the solubility parameter of solvent, and δ_p is the solubility parameter of copolymer.

Molar volume (Vs) of solvent was determined by equation.

$$Vs = \frac{M}{d}$$

where, M is the molecular weight of solvent, and d is the density of solvent.

Polymer-solvent interaction parameters are reported in **Table 3.5.** Swelling ratio was calculated by mass swell ratio[38] **equation (3.5):**

$$Ds = \frac{Ws - Wd}{Wd} \qquad \textbf{(3.5)}$$

where, D_S is the degree of swelling, W_S is the weight of swollen polymer at a given time and W_d is the weight of dried polymer.

Table 3.5. Polymer-solvent interaction parameter

Copolymer	Solvent	Polymer-solvent interaction parameter (χ)
Poly(HEMA-*co*-EDMA)	Toluene	5.39
	DMF	0.61
Poly(HEMA-*co*-DVB)	Toluene	4.47
	DMF	0.66

Swelling measurements[39] were carried out in a small 30 mL capacity glass bottles by storing 0.5 g of polymer sample which was immersed in 10 mL of toluene/DMF solvent at room temperature for 72 h to ensure equilibrium swelling of polymer. Then, sample was removed, blotted with tissue paper, and was transferred to a weighing bottle. The weight of the swollen polymer was recorded. Thereafter, swelling ratio of crosslinked polymers was determined by measuring weight of the polymer after equilibrium swelling in solvent (W_s) and after drying (W_d) of the polymers.

Swelling ratio depends on the crosslink density of the polymer and polymer-solvent interaction parameter. As to be expected, swelling ratio is higher at low crosslink density whereas decreased with increasing crosslink density. This is due to the small chains in highly crosslinked polymers adversely affects to polymer swelling while in lower crosslinked polymer swelling is higher due to long chain length. Swelling ratio is thus based on crosslink density of polymer.[40–42] However, solubility parameter of DMF is closer to both poly(HEMA-*co*-EDMA) and poly(HEMA-*co*-DVB) rather than toluene. In both solvents, poly(HEMA-*co*-DVB) series showed the higher swelling ratio than poly(HEMA-*co*-EDMA). Interestingly, it was observed that, swelling ratio was in accordance to polymer-solvent interaction parameter (χ). **Figure 3.10** illustrated that, polymers have the higher swelling ratio in DMF than in toluene. This is because of polymer has polymer-solvent interaction parameter (χ) in the range of 4–6 for toluene whereas χ for DMF is in the range of 0–1. HDD series displayed the highest swelling ratio which was

1.80 and 1.28 with DMF and toluene, respectively for 25% crosslink density. Swelling behavior of polymer is a key parameter for polymer applications in pharmaceutical and biomedical sciences. Moreover, swelling ratio also depends on the mobility and wettability of a polymer which is useful to select polymer-solvent pair in solid phase synthesis. Swelling ratio of polymers with different solvents and for different crosslink densities are represented in **Figure 3.10.**

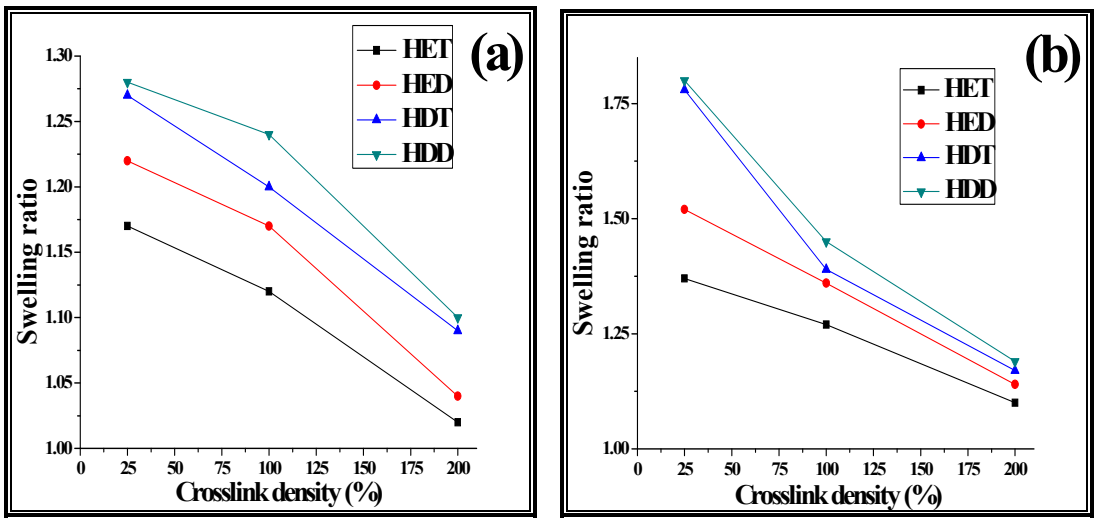

Figure 3.10. Swelling ratio of poly(HEMA-*co*-EDMA) and poly(HEMA-*co*-DVB) with (a) toluene, and (b) DMF for different crosslink density

3.3.8. Scanning electron microscopy

SEM images of microporous, poly(HEMA-*co*-EDMA) and poly(HEMA-*co*-DVB) were scanned for 150 and 500X magnification as shown in **Figures 3.11 (a-d) and (e-h),** respectively. **Figure 3.11 (a-d)** displayed uniform and spherical polymer beads for 150X magnification whereas **Figure 3.11 (e-h)** displayed the surface morphology of the polymer beads for 500X magnification. Interestingly, polymer synthesized from 1,2-dichlorobenzene revealed relatively higher porous properties as compared to polymer obtained from 1,1,2,2-tetrachloroethane at same crosslink density. However, SEM images revealed the non-aggregation of polymer beads.[43]

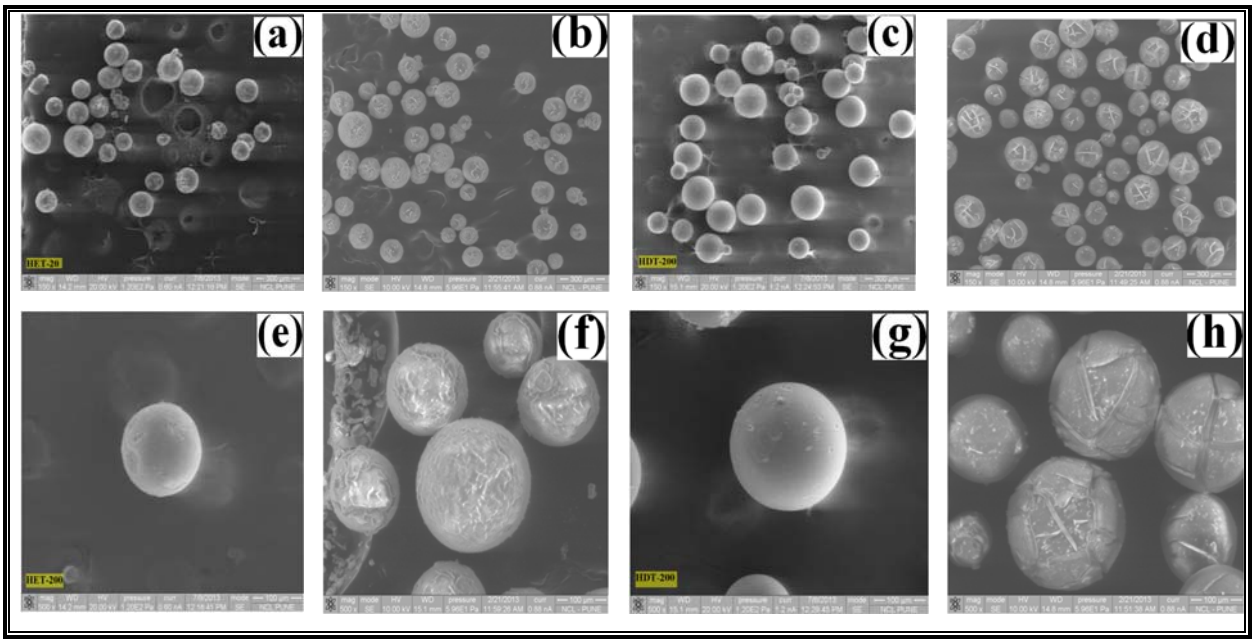

Figure 3.11. SEM images of polymers: a, b, c, d and e, f, g, h of HET, HED, HDT, and HDD with 150 and 500X magnification for 200% crosslink density

3.4. Conclusion

High surface area crosslinked polymer beads were synthesized successfully. Present study implied that, surface area increased and hydroxyl content decreased with increase in crosslink density. Consequently, low crosslink density polymers are suitable supports for covalent modification with organic compounds. In contrast, high crosslink density polymers are useful for entrapment of an enzyme as a polymer supported catalyst. Maximum surface area (564 m^2/g) was obtained with poly(HEMA-*co*-DVB) using 1,2-dichlorobenzene as a porogen for 200% crosslink density. Average particle size of the polymers ranged from 15–80 μm and this particle size is promisingly applicable for column chromatography as well as support for catalysts, reagents, substrate, and scavengers. Differential thermogravimetric analysis (DTG) and differential scanning calorimetry (DSC) study assists in polymer selection as a support in high temperature solid phase synthesis. Rigid crosslinker and its higher concentration encourage polymer properties whereas flexible crosslinker and its higher concentration attributed for decreased thermal properties (thermal degradation and glass transition temperature). Poly(HEMA-*co*-DVB) showed the higher swelling ratio than poly(HEMA-*co*-EDMA) with both

porogens due to variation in polymer-solvent interaction parameter and hydrophobic nature of poly(HEMA-*co*-DVB) compared to poly(HEMA-*co*-EDMA). Swelling ratio plays pivotal role in suitable solvent selection during application in solid phase synthesis. Thus, poly(HEMA-*co*-DVB) for 200% crosslink density is a suitable polymer support for adsorption and entrapment technology because of its high surface area, more thermostability and hydrophobic properties whereas poly(HEMA-*co*-DVB) for 25% crosslink density can be used as a covalent binding support, because of its more reactivity, high thermostability, and hydrophobicity. This work also promises to provide ubiquitous microporous polymer. Moreover, high surface area poly(HEMA-*co*-DVB) beads are not only suitable matrix in chiral resolution but can be used as a core in synthesis of core-shell polymers.

References

[1] Merrifield R. B., *J. Am. Chem. Soc.,* 1963, **85,** 2149–2154.

[2] Gokmen M. T. and Du Prez F. E., *Prog. Polym. Sci.,* 2012, **37,** 365–405.

[3] Ahuja G. and Pathak K., *Indian J. Pharm. Sci.,* 2009, **71(6),** 599–607.

[4] Speybrouck S., Beelen R., Casselman F., Maene L., Bouckenooghe I. and Degrieck I., *EJVES Extra,* 2012, **24,** e5–e6.

[5] Gruttadauria M. and Giacalone F., *Wiley,* 2011, **3,** 177–208.

[6] Sherrington D. C., *Chem. Commun.,* 1998, 2275–2286.

[7] Akelah A. and Sherington D. C., *Chem. Review,* 1983, **24,** 1369–1386.

[8] Guibal E., *Prog. Polym. Sci.,* 2005, **30,** 71–109.

[9] Clapham B., Reger T. S. and Janda K. D., *Tetrahedron,* 2001, **50,** 4637–4662.

[10] Singh R. G. and Chauhan S. M. S., *J. Braz. Chem. Soc.,* 2006, **17,** 421–425.

[11] Drewry D. H., Coe D. M. and Poon S., *John Wiley Sons, Inc,* 1999, 97–148.

[12] Sherrington D. C., *J. Pure. Appl. Chem.,* 1988, **60,** 401–414.

[13] Adjidjonou K. and Caze C., *Eur. Polym. J.,* 1994, **30,** 395–398.

[14] Marconi W., *Brit. Polym. J.,* 1984, **16**, 222–224.

[15] Stille J. K., *J. Macromol. Sci. Chem.,* 1981, **A21,** 1689–1693.

[16] Lenev D. A., Lyssenkob K. A. and Kostyanovsky R. G., *New J. Chem.,* 2010, **34,** 403–404.

[17] Isabel C. U., Frank S., Josep F., Azael F., Agusti F. and Christophe B., *Rec. Prog. Genie Des. Procedes,* 2007, **94,** 1–8.

[18] Vianna-Soares C. D., Kim C. J., Ciftci K. and Borenstein M. R., *Mater. Res.,* 2004, **7(3),** 473–477.

[19] Luque De Castro M. D. and Garco a-Ayuso L. E., *Anal. Chim. Acta,* 1998, **369,** 1–10.

[20] Bartholin M., *Makromol. Chem.,* 1981, **182,** 2075–2085.

[21] Rabelo D. and Coutinho F. M. B., *Polym. Bull.,* 1994, **33,** 479–486.

[22] Qu H., Gong F., Ma G. and Su Z., *J. Appl. Polym. Sci.,* 2007, **105,** 1632–1641.

[23] Verweij P. D. and Sherrington D. C., *J. Mater. Chem.,* 1991, **1,** 371–374.

[24] Kotha A., Rajan C. R., Ponrathnam S., Kumar K. K. and Shewale J. G., *Appl. Biochem. Biotech.,* 1998, **74,** 191–203.

[25] Kotha A., Rajan R. C., Ponrathnam S. and Shewale J. G., *React. Funct. Polym.,* 1996, **28,** 227–233.

[26] Westermarck S., Thesis, Use of mercury porosimetry and nitrogen adsorption in characterisation of the pore structure of mannitol and microcrystalline cellulose powders, granules and tablets. Pharm Technol Div Dept Pharm Helsinki Univ. Finland, Helsinki 2002, 20.

[27] Donahue D. J. and Bartell F.E., *J. Phys. Chem.,* 1952, **56(4),** 480–484.

[28] Gong T. and Wang C. C., *J. Mater. Sci.,* 2008, **43,** 1926–1932.

[29] Gooch J. W., Emulsification and polymerization of alkyd resins, 2002, **XXII,** 28.

[30] Fanun M., *Colloids in drug delivery,* 2010, **148,** 76–77.

[31] Mayoral E. and Achar E. N., *J. Chem. Phys.,* 2012, **137(19),** 1–11.

[32] Baudonnet L., Grossiord J. L. and Rodriguez F., *J. Dispersion Sci. Technol.,* 2004, **25(2),** 183–192.

[33] Vogel A. I., Elementary practical organic chemistry, Part-III, Quantitative Organic Analysis, (Lond.), 1958, **Chapter XVI,** 667–671.

[34] Zhao C., Shi S., Mir D., Hurst D., Li R., Xiao X. Y., Lillig J. and Czarnik A. W., *J. Comb. Chem.,* 1999, **1,** 91–95.

[35] Vroman I. and Tighzert L., *Mater.,* 2009, **2,** 307–344.

[36] Clarisse M., Queiros Y., Barbosa C., Barbosa L. and Lucas E., *Chem. Chem. Technol.,* 2012, **6,** 145–152.

[37] Barlkani M. and Hepburn C., *Iran. J. Polym. Sci. Tech.,* 1992, **1,** 1–5.

[38] Brundha B. A. and Pazhanisamy P., *Int. J. Chem. Tech. Res.,* 2010, **2,** 2192–2197.

[39] Choi J., Kwak S. Y., Kang S., Lee S. S., Park M., Lim S., Kim J., Choe C. R. and Hong S. I., *J. Polym. Sci. A: Polym. Chem.,* 2002, **40,** 4368–4377.

[40] Yildiz U. and Hazer B., *Macromol. Chem. Phys.,* 1998, **199,** 163–168.

[41] Okay O., *Hydrogel Sens. Actuators,* 2010, **6,** 1–14.

[42] Pal K., Banthia A. K. and Majumdar D. K., *Des Monomers Polym.,* 2009, **12,** 197–220.

[43] Hwang M. L., Lee Y. S., Kim T. G., Yang G. S., Park T. S. and Lee Y. S., *Bull. Korean Chem. Soc.,* 2010, **31(8),** 2395–2398.

MACROPOROUS POLYMER: NON-SOLVATING POROGENS

4.1. Introduction

Porous polymers have attracted a lot of attention due to their ubiquitous applications[1] in the fields like enzyme immobilization, catalysts, adsorbents, chromatography, and separation science. Industrially, the use of porous polymers is increased from last two decades.[2] The porous properties such as surface area, pore volume, pore size, and swelling behavior of polymers are depending on the various physico-chemical parameters including monomer, porogen, crosslink density (CLD), stirring speed and temperature.[3] Sederel *et al.*[4] showed the effect of porogen, crosslinker, temperature, initiator, CLD, and stirring speed on polymer properties. Present study demonstrates that, non-solvating porogens and crosslinkers (rigidity/flexibility) are the major parameters that influences to surface area, porosity, and other properties of polymers. Nowadays, different types of porogens like organic solvents, inorganic, and polymeric materials are available to introduce the porosity.[5] In general, organic porogens are low molecular weight solvents, inorganic porogens are solutions of inorganic material like potassium chloride, sodium bicarbonate,[6] whereas homopolymer like poly(ethylene glycol) and poly(propylene) can be used as polymeric porogen.

In 2012, Rahman *et al.*[7] reported the toluene-n-heptane as a non-solvating porogen in terpolymer synthesis wherein they reported that surface area decreases, inversely pore volume and pore size increases with increasing concentration of porogen. The present study reports the higher porosity with acrylate copolymer using single non-solvating porogen instead of pair. Generally aliphatic alcoholic porogens having carbon number ranging from 4 to 12 are known as hydrophobic porogens.[8] Highly porous property of the materials is the characteristics for effective enzyme immobilization by entrapment. Small loading of enzymes is the major concern with available porous material. Non-solvating (NONSOL) porogens are able to impart porous properties to the polymers. Indeed, large pore volume and small surface area is the characteristic property of the non-solvating porogens.[9] In fact, hydrophobicity of the porogen substantially affects the properties like surface area, pore volume, and pore size of the beaded microsphere. Beads formed using solvating (SOL) porogens have limitations due to inserting microporous properties into the polymer matrix. Unfortunately, these polymers cannot be employed for an enzyme immobilization since large structure property of various enzymes. The beads obtained by suspension polymerization using non-solvating, hydrophobic alcoholic porogens have

megaporous properties. Furthermore, different types of immobilization techniques such as covalent, ionic, adsorption, and entrapment are available to anchor the enzymes.[10] However, adsorption and entrapment techniques are useful in most of the applications of porous polymers. Thus, porous material containing large number of pores having more pore volume is the best candidate to entrap an enzyme. Mostly, acrylate copolymers employed as a solid support, pharmaceutical and biomedical applications as well as formulation of bone cement.[11] This wide applicability of the polymers has attracted a lot of attention towards acrylate porous polymer synthesis.

Recently, Todorovic *et al.*[12] synthesized the methyl methacrylate copolymer to immobilize the enzymes. They reported the highest pore volume of 3.25 cc/g. In 2007, Chen *et al.*[13] showed the pore size of polystyrene in the range of 0.03 to 0.1 μm for *Candida Antarctica* Lipase B (CALB) adsorption which is again small. However, present study implied the pore volume and pore size of 5.52 cc/g and 5.47 μm, respectively resulting much higher porous materials. In the present work, hydrophobic interfacial tensions are inversely functioning towards surface area and megaporosity which are studied in details. In this study, non-solvating porogens i.e. cyclohexanol, n-octanol, and n-decanol were used to obtain the megaporous beaded polymer. In this work, we reported the crosslinked polyacrylates with improved porosity, thermal stability and swelling behavior.

4.2. Experimental

4.2.1. Materials

Methyl methacrylate:- Make: Loba Chemie, Molecular formula: $C_5H_8O_2$; Molecular weight (g/mol): 100.12; Specific gravity/density (g/cm^3): 0.94; Boiling point (^{o}C): 101; Physical state: colorless liquid.

Ethylene dimethacrylate:- Make: Sigma-Aldrich; Molecular formula: $C_{10}H_{14}O_4$; Molecular weight (g/mol): 198.22; Specific gravity/density (g/cm^3): 1.051; Boiling point (^{o}C): 98–100; Physical state: colorless liquid.

1,4-Divinylbenzene (85%):- Make: Sigma-Aldrich; Molecular formula: $C_{10}H_{10}$; Molecular weight (g/mol): 130.19; Specific gravity/density (g/cm^3): 0.914; Boiling point (^{o}C): 195; Physical state: colorless liquid.

Cyclohexanol:- Make: Loba Chemie; Molecular formula: $C_6H_{12}O$; Molecular weight (g/mol): 100.158; Specific gravity/density (g/cm^3): 0.9624; Boiling point (^{o}C): 161.84; Physical state: colorless, viscous liquid (hygroscopic).

n-Octanol:- Make: Loba Chemie; Molecular formula: $C_8H_{18}O$; Molecular weight (g/mol): 130.23; Specific gravity/density (g/cm^3): 0.824; Boiling point (^{o}C): 195; Physical state: colorless liquid.

n-Decanol:- Make: Loba Chemie; Molecular formula: $C_{10}H_{22}O$; Molecular weight (g/mol): 158.28; Specific gravity/density (g/cm^3): 0.8297; Boiling point (^{o}C): 232.9; Physical state: colorless, viscous liquid.

Poly(vinyl)pyrrolidone:- Make: Fluka; Molecular formula: $(C_6H_9NO)_n$; Molecular weight (g/mol): 360,000 g/mol; Physical state: white powder.

2,2'-Azobisisobutyronitrile (AIBN):- Make: SAS Chemicals Pvt. Ltd. Mumbai; Molecular formula: $C_8H_{12}N_4$; Molecular weight (g/mol): 164.21; Specific gravity/density (g/cm^3): 1.1; Melting point (^{o}C): 103–105; Physical state: white solid.

Methanol:- Make: Loba Chemie; Molecular formula: CH_4O; Molecular weight (g/mol): 32.04; Specific gravity/density (g/cm^3): 0.7918; Boiling point (^{o}C): 34.7; Physical state: colorless liquid.

Acetone:- Make: Loba Chemie; Molecular formula: C_3H_6O; Molecular weight (g/mol): 58.08; Specific gravity/density (g/cm^3): 0.791; Boiling point (^{o}C): 56; Physical state: colorless liquid.

Dimethyl sulfoxide:- Make: Merck; Molecular formula: C_2H_6OS; Molecular weight (g/mol): 78.13; Specific gravity/density (g/cm^3): 1.1; Boiling point (^{o}C): 189; Physical state: colorless liquid.

Methyl ethyl ketone:- Make: Merck; Molecular formula: C_4H_8O; Molecular weight (g/mol): 72.11; Specific gravity/density (g/cm^3): 0.8050; Boiling point (^{o}C): 79.64; Physical state: colorless liquid.

4.2.2. Synthesis of crosslinked polymers

The aqueous phase was prepared by dissolving protective colloid poly(vinylpyrrolidone) in deionized water (1 wt%). Moreover, organic phase was prepared by mixing monomer (MMA), crosslinker (EDMA/DVB), initiator (AIBN) and pore generating solvent (cyclohexanol/n-octanol/n-decanol) in nitrogen atmosphere at ambient temperature. Polymer synthesis was conducted in a double walled cylindrical polymerization reactor. The reactor was equipped with a thermostat, mechanical stirrer and a condenser. The prepared aqueous (continuous) phase was added to the reactor. Subsequently, the prepared organic (discontinuous) phase was slowly added to the reactor containing aqueous (continuous) phase with continuous stirring at 300 rpm under nitrogen atmosphere. The reaction temperature was raised to 70^{o}C and maintained for 3 h. Thus, polymer beads obtained were thoroughly washed with water, methanol, and finally with acetone. These beads were dried at 60^{o}C under reduced pressure. The polymers obtained by suspension polymerization were further purified by a soxhlet extraction method. However, poly(MMA-*co*-EDMA) and poly(MMA-*co*-DVB) of differing crosslink densities (CLDs) were synthesized. In the present work, poly(MMA-*co*-EDMA) was obtained using cyclohexanol, n-octanol, and n-decanol as porogens and they were abbreviated as **MEC** (MMA–EDMA–cyclohexanol), **MEO** (MMA–EDMA–n-octanol) and **MEDe** (MMA–EDMA–n-decanol), respectively. In another, poly(MMA-*co*-DVB) obtained using cyclohexanol, n-octanol, and n-decanol as porogens and they were abbreviated as **MDC** (MMA–DVB–cyclohexanol), **MDO** (MMA–DVB–n-octanol), and **MDDe** (MMA–DVB–n-decanol), respectively. The CLD defines the percent moles of crosslinking agent (ethylene dimethacrylate/divinylbenzene) relative to the moles of methyl methacrylate monomer. The concentration of monomer and crosslinkers were determined by **equation (3.1).** Monomer-crosslinker feed composition of poly(MMA-*co*-EDMA) and poly(MMA-*co*-DVB) at different CLDs and reaction conditions are reported in **Table 4.1** whereas synthesis of poly(MMA-*co*-EDMA) and poly(MMA-*co*-DVB) are depicted in **Schemes 4.1 and 4.2,** respectively.

Table 4.1. Monomer-crosslinker feed composition of polymer synthesized by suspension polymerization

Monomer system	Units	Crosslink density (%)					
		25	50	75	100	150	200
MMA:EDMA	mol	0.104: 0.026	0.080: 0.040	0.065: 0.048	0.054: 0.054	0.041: 0.062	0.033: 0.066
	g	10.448: 5.171	7.990: 7.910	6.469: 9.605	5.434: 10.759	4.117: 12.227	3.314: 13.122
MMA:DVB	mol	0.113: 0.028	0.090: 0.045	0.075: 0.056	0.064: 0.064	0.050: 0.075	0.041: 0.082
	g	11.298: 3.672	9.030: 5.871	7.520: 7.334	6.443: 8.378	5.008: 9.769	4.096: 10.653

Reaction conditions: Batch size: 16 mL; 2,2'-azobisisobutyronitrile: 2.5 mol%; stirring speed: 300 rpm; reaction time: 3 h; outer phase: H_2O; protective colloid: poly(vinylpyrrolidone); concentration of protective colloid: 1 wt%; porogen: cyclohexanol, n-octanol, and n-decanol; porogen concentration: 48 mL (monomer: porogen ratio, 1:3 v/v).

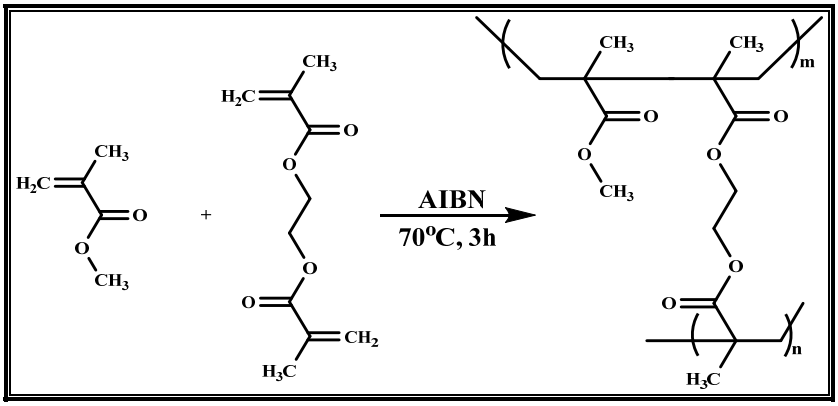

Methyl methacrylate **Ethylene dimethacrylate** **Poly(MMA-*co*-EDMA)**

Scheme 4.1. Synthesis of poly(MMA-*co*-EDMA) by suspension polymerization

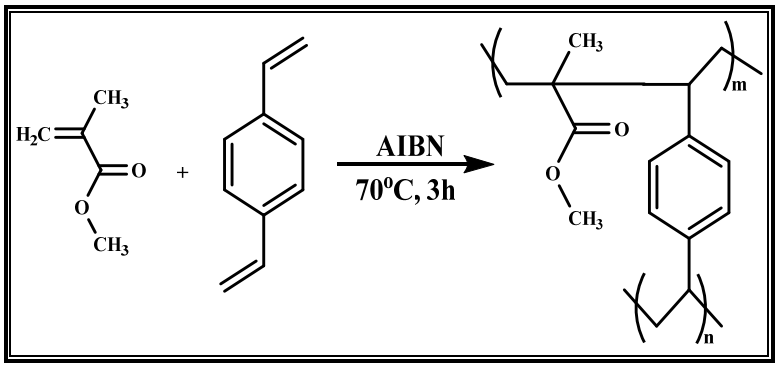

Methyl methacrylate **Divinylbenzene** **Poly(MMA-*co*-DVB)**

Scheme 4.2. Synthesis of poly(MMA-*co*-DVB) by suspension polymerization

4.2.3. Characterization

Synthesis of polymers was confirmed by FT-IR spectrometer (Perkin Elmer, USA). The sample was mixed with potassium bromide (KBr) to make pellets for FT-IR study. Surface area of polymer beads was determined using a surface area analyzer (NOVA 2000e Quantachrome instruments, Boynton, FL-33426) by BET (nitrogen adsorption) method. Pore volume and pore size was determined by mercury porosimetry (Quantachrome, automated mercury intrusion porosimeter, PM-60-7) and was carried out for the samples of poly(MMA-*co*-EDMA) and poly(MMA-*co*-DVB) for 100% CLD. However, samples dried at 80^{o}C under reduced pressure for 6 h were used for pore size and pore volume determination using a mercury porosimetry by nitrogen adsorption-desorption method. Swelling ratio of the polymers was determined by wt/wt ratio and morphology was observed by scanning electron microscope (Quanta 200 3D dual beam ESEM, Netherland) wherein an electron source for ESEM was thermionic emission tungsten filament.

4.3. Results and discussion

In 1963, Merrifield *et al.*[14] invented the solid state chemistry i.e. to use the polymer as a support in solid phase synthesis. Therefore, study of physical properties like surface area, pore volume, pore size, swelling behavior, and surface morphology is an essential to the obtain desired properties before application of polymer as a support.

4.3.1. Fourier transform infrared (FT-IR) spectroscopy

Synthesis of poly(MMA-*co*-EDMA) and poly(MMA-*co*-DVB) were confirmed by FT-IR (KBr) spectroscopy using their respective initial reactions for 25% CLD. FT-IR spectra were recorded on Perkin Elmer instrument having Spectrum GX model and serial number is 69229. The number of scans was 10 with resolution 4 cm^{-1} and interval was 1. Poly(MMA-*co*-EDMA) revealed the peak at 1732 cm^{-1} which attributes to the presence of ester functionality, 2952 cm^{-1} assigned to the aliphatic –CH stretching whereas 1389 (sym.) and 1455 cm^{-1} (antisym.) corresponds to aliphatic $–CH_3$ bending **(Figure 4.1).** In another, poly(MMA-*co*-DVB) demonstrates the peak at 1731 cm^{-1} which indicates the presence of an ester functionality, 2950 cm^{-1} for aliphatic –CH stretching, 905 cm^{-1} corresponds to disubstituted benzene ring and 841 cm^{-1} assigned to *p*-disubstituted benzene ring in the polymer matrix[15] **(Figure 4.1).**

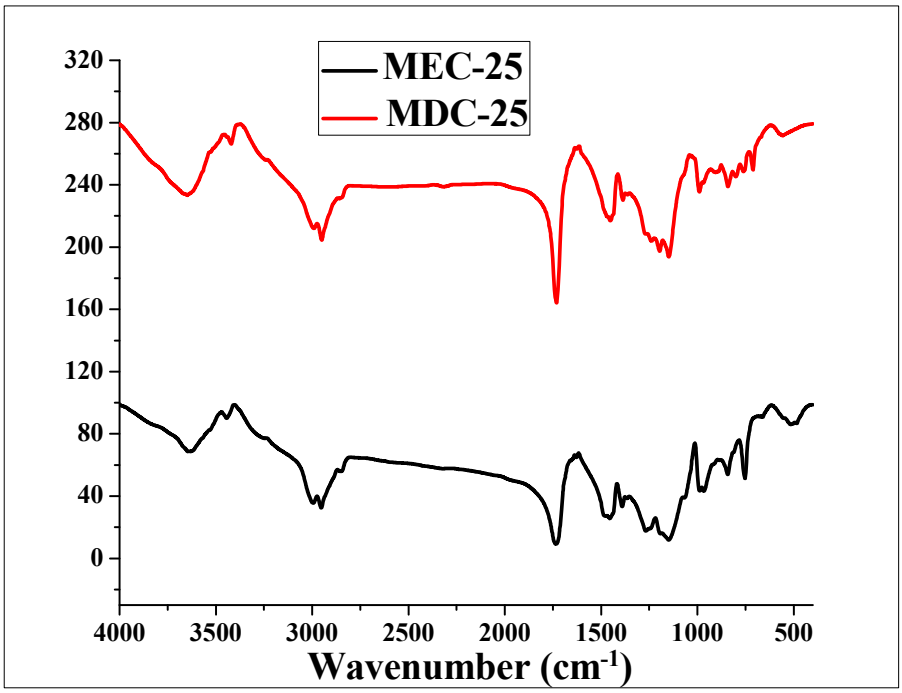

Figure 4.1. FT-IR spectrum of poly(MMA-*co*-EDMA) and poly(MMA-*co*-DVB) for 25% CLD

4.3.2. Surface area

Overall, six series of methyl methacrylate copolymers were obtained varying crosslinkers, CLD, and porogens to evaluate the effect of different parameters on the properties of crosslinked microbeads. However, non-solvating and hydrophobic porogens were selected to

obtain megaporous microbeads. According to theory, hydrophobic porogens imparts high pore volume and pore size whereas lower surface area compared to hydrophilic porogens. In this work, cyclohexanol porogen imparts surface area in the range of 94 – 300 m^2/g for MEC series whereas 94 – 244 m^2/g for MDC series. Moreover, polymer obtained from n-octanol revealed the surface area in the range of 3 – 11 m^2/g for MEO whereas 3 – 33 m^2/g for MDO series. Furthermore, polymers obtained from n-decanol demonstrated the surface area in the range of 5.5 – 15 m^2/g for MEDe series whereas 3 – 11 m^2/g for MDDe series.

Recently, Clarisse *et al.*[16] reported the surface area of poly(MMA-*co*-DVB) using a mixture of porogens. However, in the present study we reported the nearly same surface area as well as higher porosity with single porogen instead of mixture of porogens. Poly(MMA-*co*-EDMA) showed the higher surface area than poly(MMA-*co*-DVB) for the reported series. Furthermore, cyclohexanol imparted the greater surface area to the polymers than n-octanol and n-decanol porogens. Poly(MMA-*co*-EDMA) revealed 94.7 and 294.5 m^2/g whereas poly(MMA-*co*-DVB) illustrates the surface area of 94.3 and 196.3 m^2/g for 25 and 200% CLD, respectively with cyclohexanol porogen which were significantly decreases for n-octanol and n-decanol porogens. This is possibly due to the solubility parameter difference between polymer and cyclohexanol is lower than other porogens. The surface area was decreased with increasing difference between solubility parameter of polymer and porogen.[17–19] Solubility parameter $[(cal/cm^3)^{1/2}]$ of poly(MMA-*co*-EDMA) (14.18) and poly(MMA-*co*-DVB) (14.70) was calculated (see swelling ratio) whereas solubility parameters of cyclohexanol (11.4), n-octanol (9.30), and n-decanol (8.30) were referred.[17]

Interestingly, surface area was increased upto 150% CLD and later on decreased for both cyclohexanol series. On the other hand, the remaining four series (MEO, MDO, MEDe, and MDDe) showed the lower surface area compared to cyclohexanol series wherein surface area increased up to 75% CLD afterwards decreased steadily even though CLD increases. According to Xie *et al.*[20] the aliphatic alcoholic porogens containing carbon numbers C_4–C_6 showed increasing surface area whereas porogen containing C_8–C_{10} carbon numbers attributes for decreasing surface area. This is probably due to the fact that higher hydrophobicity of porogen increases interfacial tension between aqueous and organic phase resulting lower surface area.[1,21] In this study, aliphatic carbon content of a porogen increases in the sequence of cyclohexanol, n-

octanol, and n-decanol consequently surface area goes on decreasing in the same sequence. Surface area of copolymers at different CLD is illustrated in **Table 4.2 and Figure 4.2.**

Table 4.2. Surface area of poly(MMA-*co*-EDMA) and poly(MMA-*co*-DVB) at different CLD using cyclohexanol, n-octanol, and n-decanol as porogens

Polymer code	Crosslink density (%)					
	25	50	75	100	150	200
MEC	94.7	130.1	185.3	221.3	300.9	294.5
MDC	94.3	162.6	203.7	207.4	244.9	196.3
MEO	2.9	8.1	11.00	7.9	6.7	5.7
MDO	8.7	11.6	33.2	12.8	10.5	2.9
MEDe	5.5	7.1	13.3	13.1	15.1	10.7
MDDe	2.8	5.6	11.3	7.6	7.1	6.9

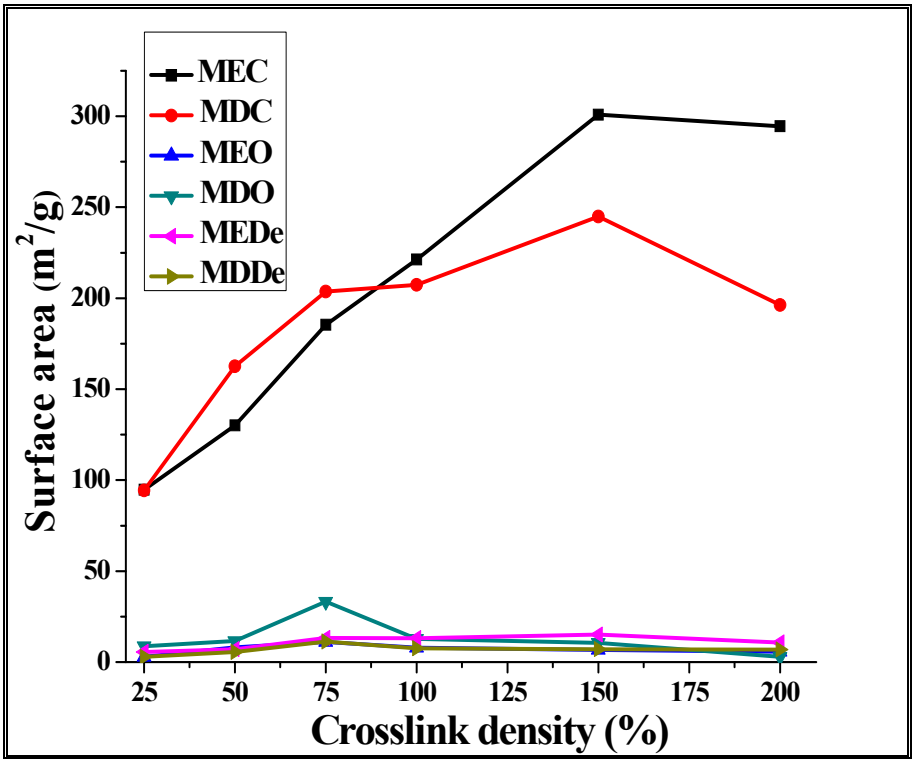

Figure 4.2. Surface area of poly(MMA-*co*-EDMA) and poly(MMA-*co*-DVB) using cyclohexanol, n-octanol, and n-decanol as porogens

4.3.3. Pore volume and pore size determination

IUPAC classifieds the pores based on their width.[22] The pores classified as micro (<20 Å), meso (20–50 Å), and macropores (>500 Å). Commonly pore size in the range of 10 – 100 nm referred as macropores whereas pore size >100 nm considered as mega or gigapores materials.[23] Effect of crosslinkers and porogens on the pore volume and pore size for 100% CLD was studied.

In suspension polymerization, the phase separation will occur at much later stage if porogen is solvating.[24] On the other hand, non-solvating porogen has poor miscibility with monomer composition consequently phase separation occurs at early stage in polymerization process. If non-solvating porogen is used in polymerization, polymer beads fuse together and aggregate into larger clusters resulting into higher pore volume and smaller surface area.[25,26] Although, solvating porogen delays phase separation, as a result polymer beads retain their individual identity unlike non-solvating porogen. This leads to a decreasing pore sizes and high surface area of a polymer.[7,27] According to the solubility parameter, n-decanol is not a good solvent for polymers such as poly(MMA-*co*-EDMA) or poly(MMA-*co*-DVB) and acts as a precipitant during polymerization. Thus, n-decanol causes the phase separation of the system before polymerization due to the polymer – solvent incompatibility. As a result, n-decanol introduces greater pore diameter and led towards the lower surface area.[18]

In 2014, Ezzati *et al.*[28] reported the pore volume of 1.6 cc/g which attributes to small loading of enzyme, which decreases polymer efficiency. On the other hand, present work provides much higher pore volume of 5.52 cc/g, which increases polymer efficiency. Kucuk *et al.*[19] reported the pore volume of poly(MMA-*co*-EDMA) wherein toluene and cyclohexane was porogens. Poly(MMA-*co*-EDMA) revealed the pore diameter of 0.10, 0.71, and 1.47 μm and pore volume of 3.17, 4.19, and 5.23 cc/g whereas poly(MMA-*co*-DVB) demonstrated the pore diameter of 0.22, 1.73, and 5.47 μm and pore volume of 5.31, 4.54, and 5.52 cc/g using cyclohexanol, n-octanol, and n-decanol porogens, respectively for 100% CLD. **Figure 4.3** displayed the increased pore volume with increasing hydrophobicity of porogen. Importantly, polymer containing DVB as a crosslinker illustrated the higher pore volume and large pore size than polymer containing EDMA as a crosslinker. Moreover, pore diameter of microsphere was increased with increasing hydrophobicity of the porogens. Thus, polymers obtained from non-

solvating porogens have megaporous properties. Indeed, the porogen has more impact on pore volume and pore size than any other physico-chemical parameter. Hydrophobicity of porogen increased in the sequence of cyclohexanol, n-octanol, and n-decanol porogen. Moreover, polymers containing DVB as a crosslinker produces additional interfacial tension facilitating formation of higher pore volume and pore size than polymers containing EDMA as a crosslinker.[29,30] Pore volume and pore diameter is presented in **Figure 4.3.**

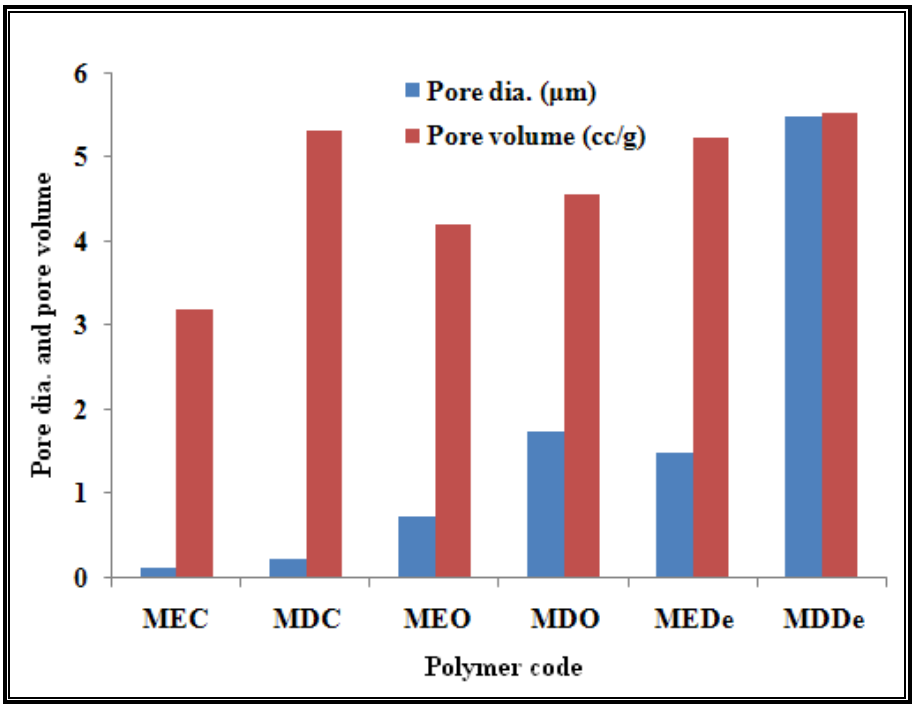

Figure 4.3. Pore diameter and pore volume of poly(MMA-*co*-EDMA) and poly(MMA-*co*-DVB) using cyclohexanol, n-octanol, and n-decanol porogen at 100% CLD

4.3.4. Thermogravimetric analysis

Recently, polymer supported materials such as catalysts, reagents, and substrates are potentially employed for high temperature reactions, consequently, thermostability evaluation of synthesized polymers become essential.[31] However, thermostability plays pivotal role during the selection of polymer as a support for application perspectives.[32] Therefore, differential thermal analysis of polymer microspheres at different CLDs were performed by simultaneous thermal analysis (Perkin Elmer) from 50–800^{o}C temperature under nitrogen atmosphere using heating

rate of 10^{o}C/min. Polymer systems selected for analysis was poly(MMA-*co*-EDMA) and poly(MMA-*co*-DVB) for 25 and 200% CLD.

Cooper *et al.*[33] showed the effect of concentration of DVB crosslinker on the decomposition temperature of polymer. Moreover, present study reported the effect of type (flexible/rigid) and concentration of crosslinkers on decomposition temperature of polymer matrix. It was observed that, maximum decomposition temperature (Tmax) of poly(MMA-*co*-EDMA) was 350 and 318^{o}C for 25 and 200% CLD, respectively. In another polymer series, poly(MMA-DVB) demonstrated the decomposition temperature (Tmax) of 400 and 444^{o}C for 25 and 200% CLD, respectively. This study revealed that, Tmax was higher for poly(MMA-*co*-DVB) than poly(MMA-*co*-EDMA). Results conclude that, polymers containing rigid crosslinker (divinylbenzene) possess higher Tmax due to the presence of aromatic ring (non-flexible part). However, higher concentration of rigid crosslinker (200% CLD) further increased decomposition temperature compared to lower concentration of rigid crosslinker (25% CLD). On the contrary, polymer containing flexible crosslinker (ethylene dimethacrylate) showed the lower Tmax due to the presence of a flexible aliphatic chain. Moreover, higher concentration (200% CLD) of flexible crosslinker further decreased the polymer decomposition temperature compared to lower concentration of flexible crosslinker (25% CLD). The graphical representation of differential thermogravimetric analysis **(**DTG) of poly(MMA-*co*-EDMA) and poly(MMA-*co*-DVB) for 25 and 200% CLD is represented in **Figure 4.4.**

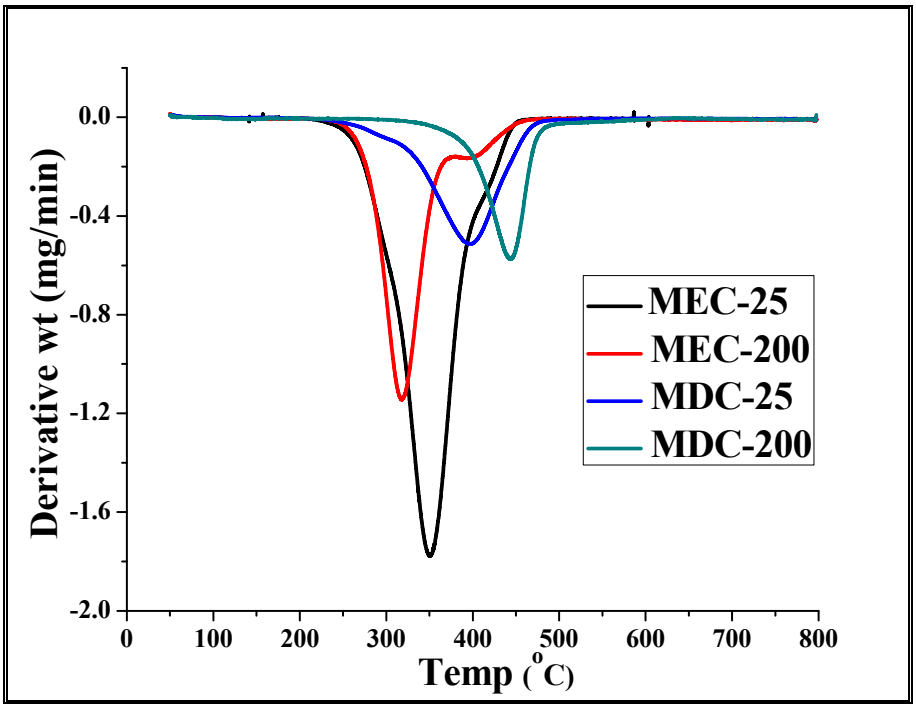

Figure 4.4. Thermogravimetric analysis (DTG) of poly(MMA-*co*-EDMA) and poly(MMA-*co*-DVB) for 25 and 200% CLD

4.3.5. Differential scanning calorimetry

Polymer beads as a support should be used below the glass transition (Tg) temperature. If polymer used at or above Tg, there is a possibility of physical/chemical interaction of polymer and reaction medium or reactant. As a consequence, Tg helps to decide the processing (safe) temperature of polymer as a support. DSC study showed that, glass transition temperature (Tg) of poly(MMA-*co*-EDMA) is 275 and 240^{o}C for 25 and 200% CLD, respectively. In another polymer series, poly(MMA-*co*-DVB) demonstrated the Tg of 278 and 314^{o}C for 25 and 200% CLD, respectively. In case of crosslinker, polymer containing DVB crosslinker revealed the higher Tg than polymer containing EDMA crosslinker. This is mainly due to the high rigidity of DVB crosslinker than EDMA. Moreover, concentration effect demonstrated that, higher concentration (CLD) of rigid crosslinker (DVB) increases Tg, since DVB based copolymer contains aromatic unit which increases rigidity. In contrast, higher concentration of flexible (EDMA) crosslinker lowers the polymer Tg due to increasing flexible composition in the polymer matrix. In short, higher concentration of rigid crosslinker or lower concentration of

flexible crosslinker imparts the greater Tg to the beaded microsphere. The trend of results observed for glass transition temperature (Tg) was similar to DTG analysis. Thus, it was concluded that, the same factors envisaged in DTG were also attributes for Tg variation. Moreover, rigidity and its higher concentration increased Tg whereas flexibility and its higher concentration decreased Tg of the polymer beads.[34] Glass transition temperature (Tg) of poly(MMA-*co*-EDMA) and poly(MMA-*co*-DVB) for 25 and 200% CLD is depicted in **Figure 4.5.**

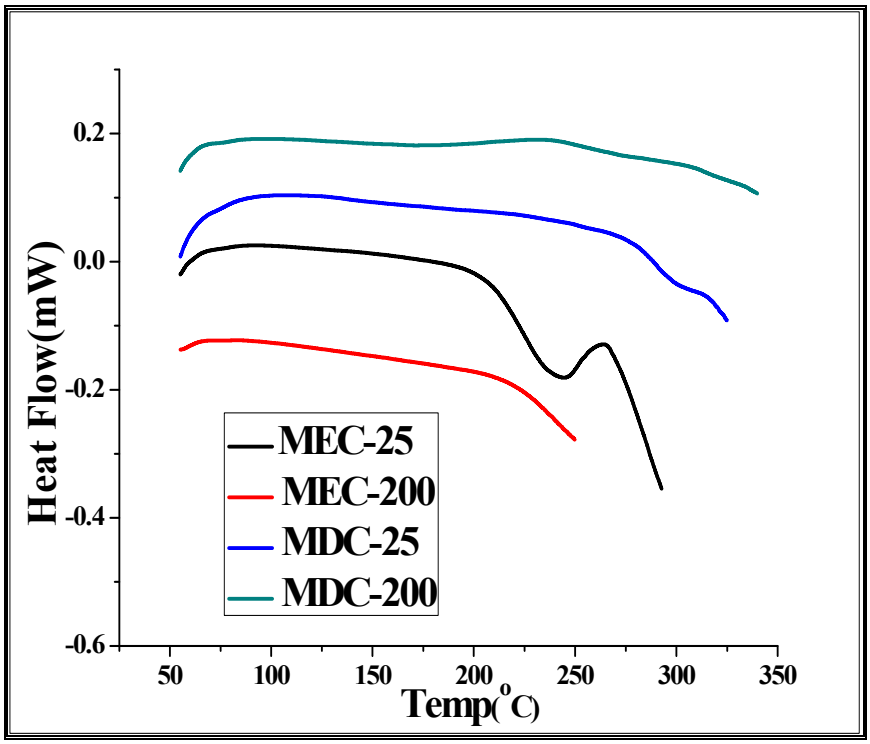

Figure 4.5. Differential scanning calorimetry of poly(MMA-*co*-EDMA) and poly(MMA-*co*-DVB) for 25 and 200% CLD

4.3.6. Swelling ratio

Generally, each solvent has capability to swell the polymer to a certain extent; however, this extent of swelling depends on porosity, degree of crosslinking, and closeness of the solubility parameter (SP) of polymer – swelling solvent. Maximum swelling can be observed with same or nearly same solubility parameter and for less crosslinked polymer. The solvents for swelling ratio were selected according to the solubility parameter of polymer. Solubility parameter of

polymers (calculated) and solvents (referred) are reported in **Table 4.3.** SP of poly(MMA-*co*-EDMA) and poly(MMA-*co*-DVB) was determined[19] by the **equation (3.3).**

Table 4.3. Solubility parameter of poly(MMA-*co*-EDMA), poly(MMA-*co*-DVB), methanol, and acetone

Polymer	Swelling solvent	Solubility parameter (δ) $(cal/cm^3)^{1/2}$
Poly(MMA-*co*-EDMA)		14.70
Poly(MMA-*co*-DVB)		14.18
	Methanol	14.28
	Acetone	9.77

The polymer-solvent interaction parameter (χ) is directly proportional to the molar volume of solvent and square of the difference between solubility parameter of solvent and polymer. The calculated polymer – solvent interaction parameters are reported in **Table 4.4** which were determined by Bristo and Watson[36] semi empirical **equation (3.4).**

Table 4.4. Polymer-solvent interaction parameter

Polymer	Solvent	Polymer-solvent interaction parameter (χ)
Poly(MMA-*co*-EDMA)	Methanol	0.35
	Acetone	3.35
Poly(MMA-*co*-DVB)	Methanol	0.34
	Acetone	2.75

In the present work, swelling measurements[38] were carried out by storing 0.5 g of polymer matrix into 20 mL of methanol/acetone swelling solvent at room temperature for 24 h to obtain equilibrium swelling. The swelling ratio of crosslinked polymers were determined by measuring the weight of the polymer after equilibrium swelling in solvent (W_s) and after drying (W_d) of polymers. Swelling ratio was calculated by the mass swell ratio[37] **equation (3.5).**

Poly(MMA-*co*-DVB) demonstrated the swelling ratio of 1.71, 1.79, and 2.15 whereas poly(MMA-*co*-EDMA) revealed the swelling ratio of 1.63, 1.58, and 1.81 in methanol swelling solvent wherein cyclohexanol, n-octanol and n-decanol was the porogens, respectively for 25% CLD. Poly(MMA-*co*-DVB) revealed the swelling ratio of 1.38, 1.37, and 1.53 whereas poly(MMA-*co*-EDMA) demonstrates swelling ratio of 1.38, 1.36, and 1.42 in acetone swelling solvent using cyclohexanol, n-octanol and n-decanol was the porogens, respectively at 25% CLD. Swelling ratio was measured as a function of polymer – solvent interaction parameter, CLD, and porosity of the polymer. Solubility parameter of methanol is closer to both poly(MMA-*co*-EDMA) and poly(MMA-*co*-DVB) than acetone. Thus, all six series of polymers showed the higher swelling in methanol compared to acetone as a swelling solvent. Further, it can be also justified by polymer – solvent interaction parameter. Smaller the polymer – solvent interaction parameter more is the polymer swelling. This is because at smaller interaction parameter difference there is no force to oppose the solvent to penetrate the matrix. The results also confirmed that, swelling ratio is dependent on the CLD. Higher crosslinked polymer attributes to lower swelling perhaps due to the small chains in high CLD polymer makes it difficult to swell the polymer, while in low CLD polymer long chain length expand to give swollen polymer[39,40] Swelling ratio is thus a measure of polymer CLD. Polymer synthesized from n-decanol and n-octanol revealed nearly equal swelling ratio perhaps due to nearly same porosity generated by both porogens and porosity decreased for polymer obtained from cyclohexanol. Swelling ration is displayed in **Figure 4.6.**

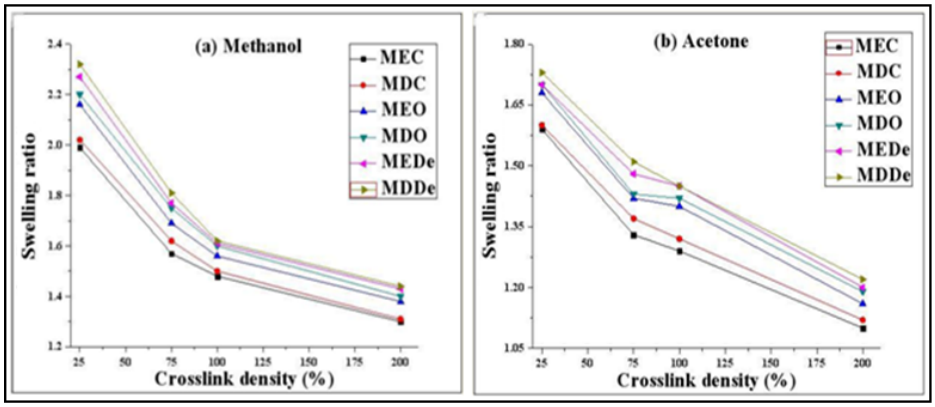

Figure 4.6. Swelling ratio of poly(MMA-*co*-EDMA) and poly(MMA-*co*-DVB) using (a) methanol, and (b) acetone

4.3.7. External morphology

An important characteristic of the polymers obtained by suspension polymerization is the morphology of the inside as well as external surface of the polymer. Polymers are produced in the form of beads, which can be hard or soft depending on the monomer and crosslinker composition. Solubility parameter difference of the monomers and porogens also affect the morphological structure of the polymers. The particle morphology significantly affects by the porogens which decides porogens may be good or bad for polymer synthesis. Careful choice of the porogen, concentration, and type of crosslinker can produce a large porosity range in the polymer beads.[41] In the present work, SEM was used to study the external morphology of the polymer beads. All SEM images were scanned to view pore size distribution, particle size distribution, and surface morphology. Typically, copolymer formed by cyclohexanol porogen showed the comparatively mesoporous and higher surface area beads,[42] whereas polymer obtained from n-octanol and n-decanol porogens displayed the cauliflower morphology having brusted pores and forms megaporous morphology, resulting lower surface area. These observations can be easily understood since solubility parameters of both porogen (n-octanol/n-decanol) and polymer is different which affect significantly. Copolymers obtained for 25% CLD were subjected to SEM analysis (10000X magnifications) and are represented in **Figure 4.7.**

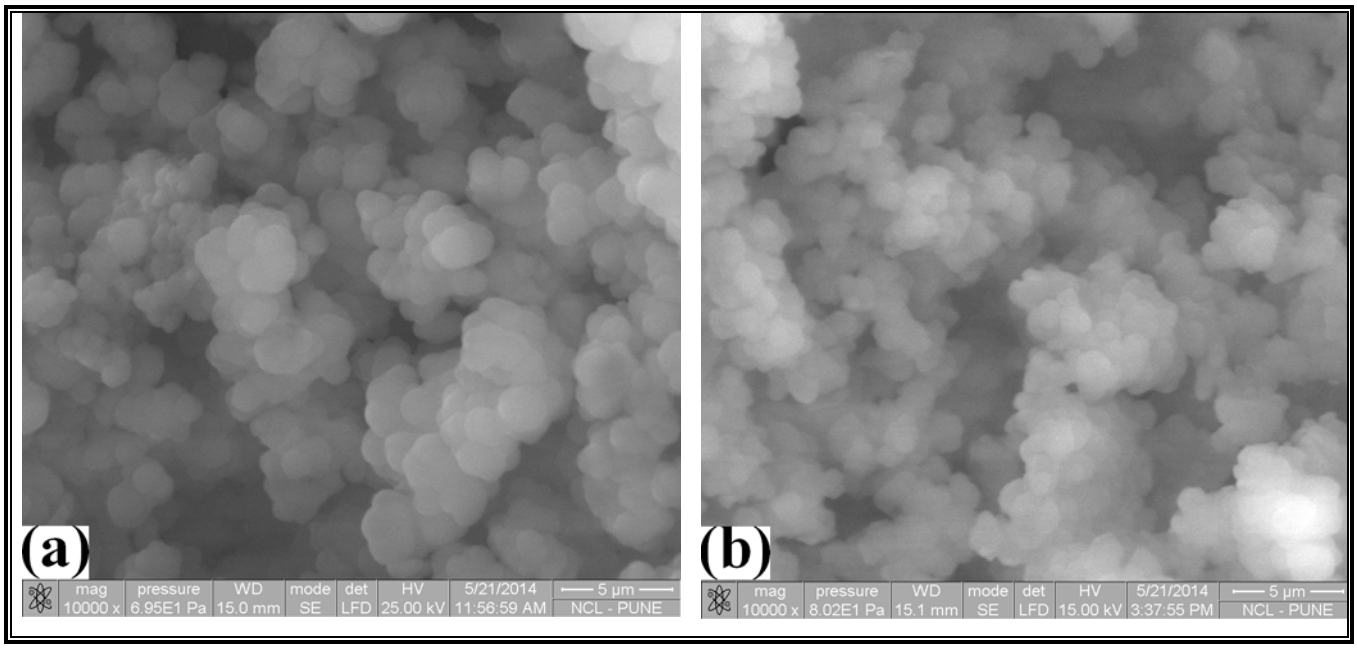

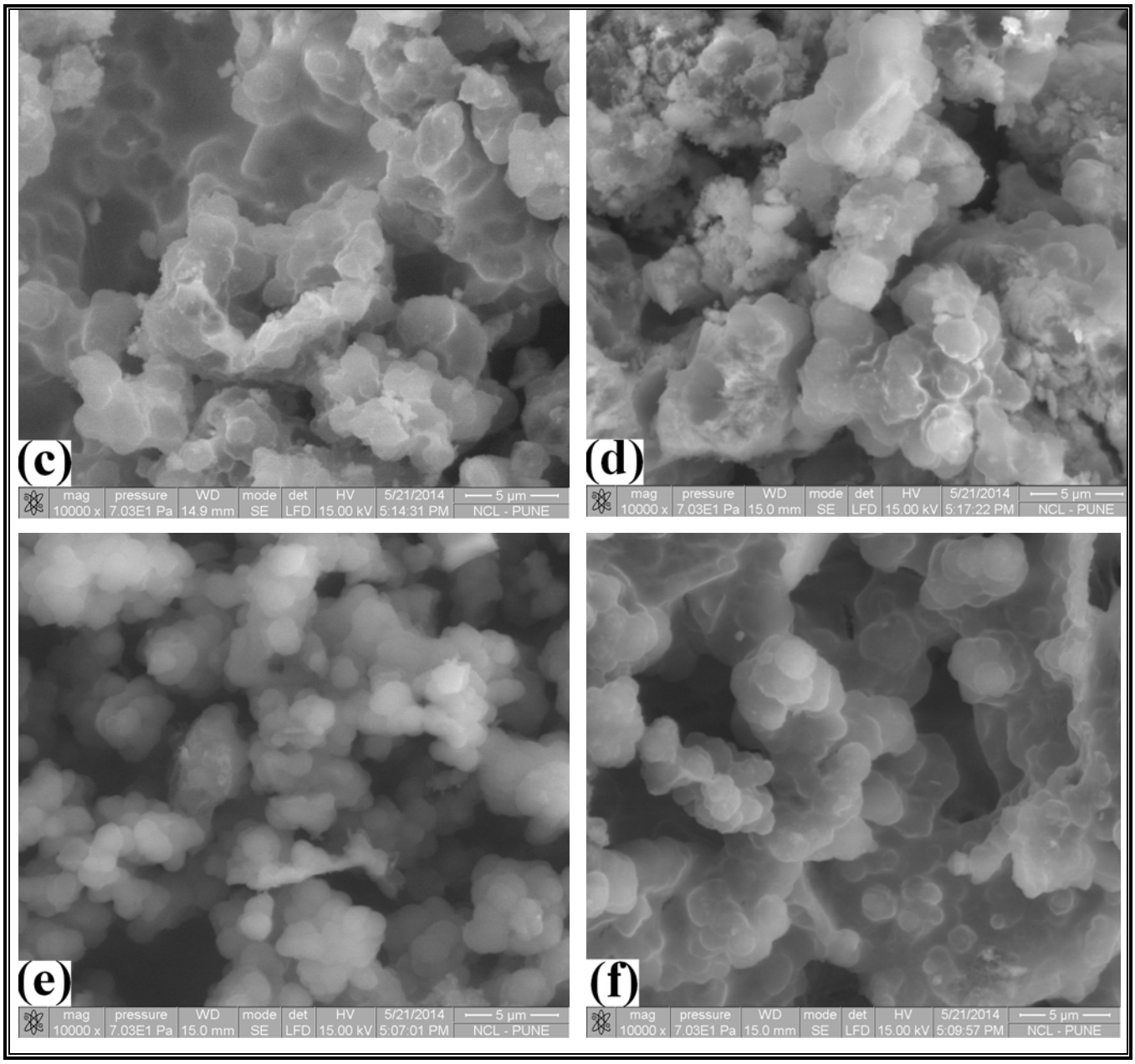

Figure 4.7. SEM images of poly(MMA-*co*-EDMA) and poly(MMA-*co*-DVB) for 25% CLD (a) MEC, (b) MDC, (c) MEO, (d) MDO, (e) MEDe, and (f) MDDe for 10000X magnification

4.4. Conclusion

Notably, non-solvating porogen in an organic phase are inversely functioning toward surface area and megaporosity of hyper-cross-linked microbeads. It is worth noting that, surface area was attenuated inversely pore volume and pore size increased with increasing aliphatic carbon content in porogens. It must be pointed out that, surface area is higher for polymers obtained by cyclohexanol and attenuated for n-octanol and further for n-decanol. In contrast, pore volume and pore size is higher for polymers obtained by n-decanol and attenuated for n-octanol and further for cyclohexanol. Poly(MMA-*co*-EDMA) revealed a surface area of 94.7 and 294.5 m^2/g whereas poly(MMA-*co*-DVB) demonstrated the surface area of 94.3 and 196.3 m^2/g for 25 and 200% cross-link density, respectively with cyclohexanol porogen which were significantly attenuates for n-octanol and further for n-decanol. Interestingly, much higher pore size (5.47 μm) and pore volume (5.52 cc/g) was obtained with inexpensive n-decanol porogen whereas porous properties significantly attenuate for n-octanol and further for cyclohexanol. Thus, aliphatic carbon content of porogen is directly proportional to megaporosity whereas inversely proportional to surface area. Importantly, higher rigidity of cross-linker (DVB) and its concentration increased the decomposition temperature of polymers. Opposite to this, higher flexibility of cross-linker (EDMA) and its concentration attenuated the decomposition temperature as well as glass transition temperature of the microbeads. Observation revealed that, smaller the difference in polymer – solvent interaction parameter greater is the swelling ratio of polymer and vice-versa. Swelling ratio is in accordance to polymer-solvent interaction parameter. However, polymer demonstrated the higher swelling in methanol compared to acetone. Owing to less cross-linking, small cross-link density polymer showed the greater degree of swelling compared to high cross-linked microbeads. Scanning electron microscopy images clearly demonstrated the porous nature of polymer beads. More importantly, it was concluded that, cyclohexanol is the porogen which guarantees the pores with greater surface area and pore volume.

References

[1] Gokmen M. T. and Du Preg F. E., *Prog. Polym. Sci.,* 2012, **37,** 365–405.

[2] Ahmed E. M., *J. Adv. Res.,* 2015, **6,** 105–121.

[3] Badyal J. P., Cameron A. M., Cameron N. R., Oates L. J., Oyea G., Steel P. G., Davis B. G., Coe D. M. and Cox R. A., *Polymer,* 2004, **45,** 2185–2192.

[4] Sederel W. L. and De Jong G. J., *J. Appl. Polym. Sci.,* 1973, **17,** 2835–2846.

[5] Okay O., *Prog. Polym. Sci.,* 2000, **25,** 711–779.

[6] Mohamed M. H. and Wilson L. D., *Nanomaterials,* 2012, **2,** 163–186.

[7] Rahman A. U., Iqbal M., Rahman F. U., Dayan F. D., Yaseen M. L. Y., Omer M., Garver M., Yang L. and Tan T., *J. Appl. Polym. Sci.,* 2012, **124,** 915–926.

[8] Levkin P. A., Svec F. and Frechet J. M. J., *Adv. Funct. Mater.,* 2009, **19,** 1993–1998.

[9] Si T., Wanga Y., Wei W., Lv P., Ma G. and Su Z., *React. Funct. Polym.,* 2011, **71,** 728–735.

[10] Nisha S., Arun K. S. and Gobi N., *Chem. Sci. Rev. Lett.,* 2012, **1,** 148–155.

[11] Morejon L., Mendizabal E., Delgado J. A., Davidenko N., Lopez-Dellamary F., Manriquez R., Ginebra N. P., Gil F. J. and Planell J. A., *Lat. Am. Appl. Res.,* 2005, **35,** 175–182.

[12] Todorovic Z. S., Nikolic L. B., Nikolic V. D., Vukovic Z. M., Mladenovic-Ranisavljevic I. I. and Takic L. M., *Adv. Technol.,* 2012, **1,** 11–19.

[13] Chen B., Miller M. E. and Gross R. A., *Langmuir,* 2007, **23,** 6467–6474.

[14] Merrifield R. B., *J. Am. Chem. Soc.,* 1963, **85,** 2149–2154.

[15] Bartholin M., Boissier G. and Dubois J., *J. Macromol. Chem.,* 1981, **182,** 2075–2085.

[16] Clarisse M., Queiros Y., Barbosa C., Barbosa L. and Lucas E., *Chem. Chem. Tech.,* 2012, **6,** 145–152.

[17] Weast R. C., Handbook of chemistry and physics, 56th edition, *CRC Press, Inc. U.S.A.* 1974–75, PP. C-720(D).

[18] Zhao X., Wang X. and Yan J., *J. Appl. Polym. Sci.,* 2004, **92,** 997–1004.

[19] Kucuk I., Kuyulu A. and Okay O., *Polym. Bull.,* 1995, **35,** 511–516.

[20] Xie S., Svec F. and Frechet J. M. J., *J. Polym. Sci. A: Polym. Chem.,* 1997, **35,** 1013–1021.

[21] Arrua R. D., Strumia M. C. and Igarzabal C. I. A., *Materials,* 2009, **2,** 2429–2466.

[22] Sing K. S. W., Everett D. H., Haul R. A. W., Moscou L., Pierotti R. A., Rouquerol J. and Siemieniewska T., *Pure Appl. Chem.,* 1985, **57,** 603–619.

[23] Chan C. H., Chia C. H. and Thomas S., Physical chemistry of macromolecules: macro to nanoscales; molecular characterization of synthetic polymers, *Taylor and Francis,* 2014, PP. 271.

[24] Hammed M. A., Nahed R., Fuzail and Rehman E., *Eur. Polym. J.,* 1999, **35,** 1799–1811.

[25] Ortiz-Palacios J., Cardoso J. and Manero O., *J. Appl. Polym. Sci.,* 2008, **107,** 2203–2210.

[26] Matsuno R., Yamamoto K., Otsuka H. and Takahara A., *Macromolecules,* 2004, **37,** 2203–2209.

[27] Westermarck S., Thesis, Use of mercury porosimetry and nitrogen adsorption in characterisation of the pore structure of mannitol and microcrystalline cellulose powders, granules and tablets. Pharm. Technol. Div., Dept. Pharm., *Helsinki Univ. Finland, Helsinki,* 2002, PP. 20.

[28] Ezzati P., Ghasemi I., Karrabi M., Azizi H. and Fortelny I., *Iran. Polym. J.,* 2014, **23,** 757–766.

[29] Espeso J. F., De La Campa J. G., Lozano A. E. and Abajo J. D., *J. Polym. Sci. A: Polym. Chem.,* 2000, **38,** 1014–1023.

[30] Arkles B., Hydrophobicity: hydrophilicity and silanes issue of paint and coatings Industry magazine, Oct. 2006.

[31] Isabel C. U., Josep F., Azael F., Agusti F. and Christophe B., Rec. *Prog. Genie Des. Procedes,* 2007, **94,** 1–8.

[32] Gajiwala H. M. and Zand R., *Polymer,* 2000, **41,** 2009–2015.

[33] Cooper A. I., Hems W. P. and Holmes A. P., *Macromolecules,* 1999, **32,** 2156–2166.

[34] Tagle L. H., Diaz F. R. and Opazo A., *Bull. Soc. Chil. Chem.,* 2001, **46,** 1. ISSN 0366–1644.

[35] Okay O. and Gurun C., *J. Appl. Polym. Sci.,* 1992, **46,** 401–410.

[36] Barlkani M. and Hepburn C., *Iran. J. Polym. Sci. Tech.,* 1992, **1,** 1–5.

[37] Brundha B. A. and Pazhanisamy P., *Int. J. Chem. Tech. Res.,* 2010, **2,** 2192–2197.

[38] Yildiz U. and Hazer B., *Macromol. Chem. Phys.,* 1998, **199,** 163–168.

[39] Pal K., Banthia A. K. and Majumdar D. K., *Des. Monomers Polym.,* 2009, **12,** 197–220.

[40] Mane S., Ponrathnam S. and Chavan N., *Eur. Polym., J.* 2014, **59,** 46–58.

[41] Yu S., Ng F. L., Ma K. C. C., Mon A. A., Ng F. L. and Ng Y. Y., *J. Appl. Polym. Sci.,* 2013, **127,** 2641–2647.

[42] Yang C., Guan Y., Xing J., Shan G. and Liu H., *J. Polym. Sci. A: Polym. Chem.,* 2008, **46,** 203–210.

MACROPOROUS POLYMER: NON-SOLVATING POROGENS CONCENTRATION

5.1. Introduction

Over the last two decades, crosslinked polymers with high porosity have received an increasing attention due to their interesting properties which make them suitable for a wide range of applications in different fields.[1–3] Suspension polymerization is the best technique to synthesize the gigaporous beaded polymers for use as a support. A number of factors attribute to obtain suitable properties of beaded polymers.[4,5] Factors including monomer, crosslinker, crosslink density (CLD), type of porogen, porogen concentration, stirring speed, initiator, and polymerization temperature are an important parameters that decides the properties of the beads. Physico-chemical parameters like crosslinkers and porogens are playing a pivotal role in controlling the properties of resulting polymers.[6–9] Over the past few years, researchers have synthesized the polymers in many different ways to obtain desired polymer properties. Porous polymer is a unique material employed as a support in research as well as in industry. This work is of specifically interested in providing the distinguishable porous materials with hydrophilic and hydrophobic properties.

Over a decade, number of polymerization methods such as suspension, emulsion, dispersion etc. was used to obtain porous material. Emulsion polymerization technique can be used to obtain highly porous polymers; however, this method has some limitations. Most important problem of emulsion polymerization method is that, the polymers obtained by this technique have no strength, rigidity, stiffness and traces of surfactant remaining in the polymer deteriorate the properties. Methyl methacrylate polymer can become a versatile support for adsorption and entrapment of an enzyme due to low cost, which is an important from the technological view point. In the present work, gigaporous poly(MMA-*co*-EDMA) and poly(MMA-*co*-DVB) were obtained by suspension polymerization and can be employed in wide range of applications. Microporous beads were widely used as a column material in chromatography.[10–12] However, small pore size beaded polymers have slow diffusion rate during passing through stationary phase.[13] Main drawback of these types of polymers is the low porosity. This problem can be overcome to a remarkable extent using non-solvating porogens. However, porosity can be controlled by varying porogens and their concentrations. The porous polymers, particularly with large pore size have potential applications. Currently, different types of porogens are available to obtain the porous beads. Porogens are classifieds in accordance with

the properties imparted by the porogens to the polymers. Generally, porogens are classified into three main categories i.e. solvating, non-solvating, and poly porogens.[14,15] Solvating porogens are known to provide high surface area and less pore volume whereas non-solvating porogens provide the polymers with low surface area and high pore volume. Poly porogens have specific property to impart the small surface area and pore volume. The use of a polymer support at high temperature is an intensively growing area; therefore, thermostability study of the polymers is an essential. Polymers are employed as a support in different areas such as chemical technology, medicinal chemistry, and solid phase synthesis to support the catalysts, reagents, scavengers, protecting groups etc.[16–18] Industrially, polymer supported reactions are economical due to recyclable and reusable properties.

Recently, Rahman *et al.*[19] reported the mixture of toluene-n-heptane as a porogen for poly(glycidyl methacrylate-triallylisocyanurate-ethylene glycol dimethacrylate) terpolymer synthesis wherein they reported the surface area, pore volume, and pore size using a pair of porogen. In the present investigation, gigaporous beaded materials were obtained using a single non-solvating porogen instead of pair. Low porosity is the major concern with polymer beads. As a result, present work is focused to obtain improved polymer properties such as surface area, pore volume, and pore size by employing hydrophobic non-solvating porogens. In this work, we tried to overcome the less porosity concern. Despite the use of an inexpensive, non-hazardous, and easily available non-solvating porogens, present work promises to provide unique gigaporous material.

5.2. Experimental

5.2.1. Materials

Methyl methacrylate:- Make: Loba Chemie, Molecular formula: $C_5H_8O_2$; Molecular weight (g/mol): 100.12; Specific gravity/density (g/cm^3): 0.94; Boiling point (^{o}C): 101; Physical state: colorless liquid.

Ethylene dimethacrylate:- Make: Sigma-Aldrich; Molecular formula: $C_{10}H_{14}O_4$; Molecular weight (g/mol): 198.22; Specific gravity/density (g/cm^3): 1.051; Boiling point (^{o}C): 98–100; Physical state: colorless liquid.

1,4-Divinylbenzene (85%):- Make: Sigma-Aldrich; Molecular formula: $C_{10}H_{10}$; Molecular weight (g/mol): 130.19; Specific gravity/density (g/cm^3): 0.914; Boiling point (^{o}C): 195; Physical state: colorless liquid.

n-Butanol:- Make: Merck; Molecular formula: $C_4H_{10}O$; Molecular weight (g/mol): 74.12; Specific gravity/density (g/cm^3): 0.81; Boiling point (^{o}C): 117.7; Physical state: colorless liquid.

n-Hexanol:- Make: Loba Chemie; Molecular formula: $C_6H_{10}O$; Molecular weight (g/mol): 102.17; Specific gravity/density (g/cm^3): 0.8136; Boiling point (^{o}C): 155–159; Physical state: colorless liquid.

Poly(vinyl)pyrrolidone:- Make: Fluka; Molecular formula: $(C_6H_9NO)_n$; Molecular weight (g/mol): 360,000 g/mol; Physical state: white powder.

2,2'-Azobisisobutyronitrile (AIBN):- Make: SAS Chemicals Pvt. Ltd. Mumbai; Molecular formula: $C_8H_{12}N_4$; Molecular weight (g/mol): 164.21; Specific gravity/density (g/cm^3): 1.1; Melting point (^{o}C): 103–105; Physical state: white solid.

Methanol:- Make: Loba Chemie; Molecular formula: CH_4O; Molecular weight (g/mol): 32.04; Specific gravity/density (g/cm^3): 0.7918; Boiling point (^{o}C): 34.7; Physical state: colorless liquid.

Acetone:- Make: Loba Chemie; Molecular formula: C_3H_6O; Molecular weight (g/mol): 58.08; Specific gravity/density (g/cm^3): 0.791; Boiling point (^{o}C): 56; Physical state: colorless liquid.

Dimethyl sulfoxide:- Make: Merck; Molecular formula: C_2H_6OS; Molecular weight (g/mol): 78.13; Specific gravity/density (g/cm^3): 1.1004; Boiling point (^{o}C): 189; Physical state: colorless liquid.

Methyl ethyl ketone:- Make: Merck; Molecular formula: C_4H_8O; Molecular weight (g/mol): 72.11; Specific gravity/density (g/cm^3): 0.8050; Boiling point (^{o}C): 79.64; Physical state: colorless liquid.

5.2.2. Synthesis of polymers

An aqueous phase (1 wt. %) was prepared by dissolving the protective colloid poly(vinylpyrrolidone) in deionized water. The organic phase was prepared by mixing the monomer (methyl methacrylate), crosslinker (ethylene dimethacrylate/divinylbenzene), initiator (2,2'-azobisisobutyronitrile) and non-solvating porogen (n-butanol/n-hexanol) in a nitrogen atmosphere at room temperature. Synthesis of beaded polymers was conducted in a double walled cylindrical polymerization reactor of 11 cm diameter and 15 cm of height. Polymerization reactor was equipped with a thermostat, nitrogen inlet, overhead stirrer, and condenser. Then, prepared organic (discontinuous) phase was added in a dropwise manner to the polymerization reactor containing aqueous (continuous) phase under stirring at a speed of 300 rotations per min in nitrogen overlay. Subsequently, temperature was raised to 70^{o}C and maintained for 3 h to obtain crosslinked gigaporous beads. Polymer beads obtained were thoroughly washed with water, methanol, and finally with acetone. The beads were dried at 60^{o}C under reduced pressure for 8 h. Poly(MMA-*co*-EDMA) and poly(MMA-*co*-DVB) having different crosslink densities (50, 100, 150, and 200%) were obtained by varying monomer-crosslinker feed composition. Beaded polymer obtained by suspension polymerization was further purified by soxhlet extraction using methanol as an extracting solvent.[20] Poly(MMA-*co*-EDMA) was obtained using n-butanol and n-hexanol as porogens and were abbreviated as **MEB** and **MEH,** respectively whereas poly(MMA-*co*-DVB) obtained using n-butanol and n-hexanol porogens were abbreviated as **MDB** and **MDH,** respectively. Crosslink density defines the percent moles of crosslinking agent (EDMA/DVB) relative to the moles of methyl methacrylate. Concentration of monomer and crosslinkers were determined by **equation (3.1).** Monomer-crosslinker feed composition and reaction conditions are presented in **Table 5.1.** Synthesis of poly(MMA-*co*-EDMA) and poly(MMA-*co*-DVB) is depicted in **Schemes 5.1 and 5.2**, respectively.

Table 5.1. Monomer-crosslinker feed composition of polymers synthesized by suspension polymerization

Monomer system	Units	Crosslink density (%)			
		50	100	150	200
MMA:EDMA	mol	0.080: 0.040	0.054: 0.054	0.041: 0.062	0.033: 0.066
	g	7.990: 7.910	5.434: 10.759	4.117: 12.227	3.314: 13.122
MMA:DVB	mol	0.090: 0.045	0.064: 0.064	0.050: 0.075	0.041: 0.082
	g	9.030: 5.871	6.443: 8.378	5.008: 9.769	4.096: 10.653

Reaction conditions: Batch size: 16 mL; 2,2'-azobisisobutyronitrile: 2.5 mol%; stirring speed: 300 rpm; reaction time: 3 h; outer phase: H_2O; protective colloid: poly(vinylpyrrolidone); protective colloid conc.: 1 wt%; porogens: n-butanol and n-hexanol; porogen concentration: 16/32/48 mL (monomer: porogen ratio, 1:1, 1:2, and 1:3 v/v).

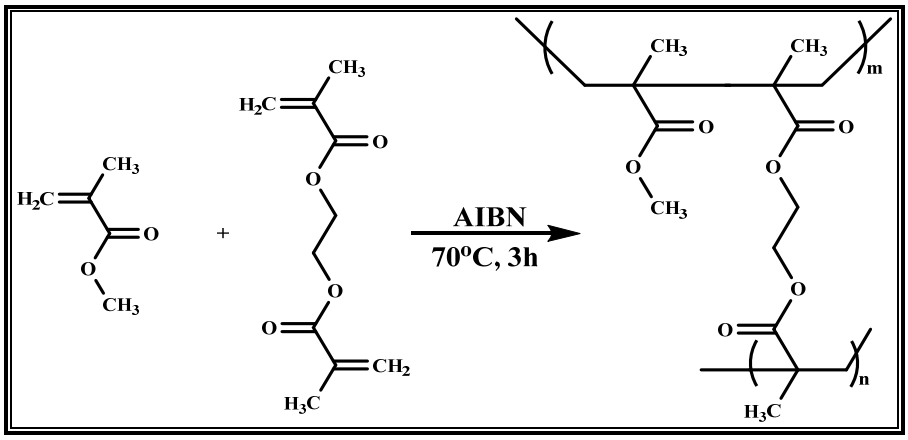

Methyl methacrylate **Ethylene dimethacrylate** **Poly(MMA-*co*-EDMA)**

Scheme 5.1. Synthesis of poly(MMA-*co*-EDMA) by suspension polymerization

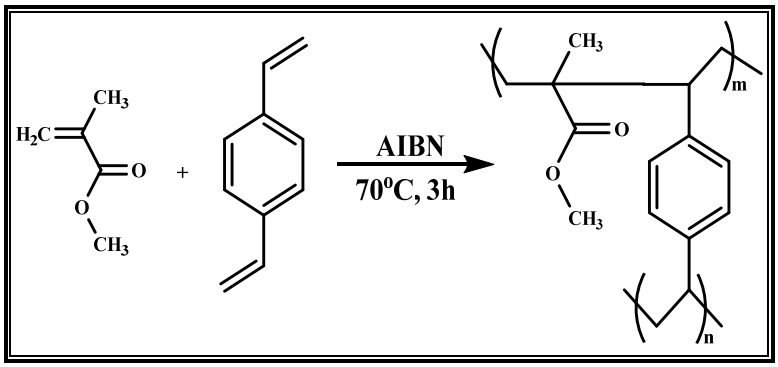

Methyl methacrylate **Divinylbenzene** **Poly(MMA-*co*-DVB)**

Scheme 5.2. Synthesis of poly(MMA-*co*-DVB) by suspension polymerization

5.2.3. Characterization

Polymers purified by soxhlet extraction and dried under reduced pressure at 60^{o}C were used for characterization. Synthesis of polymers was confirmed by FT-IR spectrometer (Perkin Elmer). Surface area of polymer beads was measured by BET (nitrogen adsorption) method using a surface area analyzer (NOVA 2000e surface area analyzer, Quantachrome, Boynton, FL-33426). Pore volume and pore size were determined using a mercury porosimetry (Quantachrome, automated mercury intrusion porosimetry, PM-60-7). Particle size distribution was evaluated by an Accusizer 780, particle sizing system, (PSS.NICOMP particle sizing system, Santa Barbara, California, USA). Thermal stability of polymers was studied by simultaneous thermal analysis (STA Perkin Elmer). Furthermore, swelling ratio of polymers was determined by wt/wt ratio. Morphology of polymers were observed by scanning electron microscope (Quanta 200-3D, dual beam ESEM microscope) wherein an electron source was thermionic emission tungsten filament.

5.3. Results and discussion

5.3.1. Fourier transform infra-red (FT-IR) spectroscopy

Synthesis of poly(MMA-*co*-EDMA) and poly(MMA-*co*-DVB) was confirmed by FT-IR (KBr pellet, cm^{-1}) spectroscopy. FT-IR spectra were recorded for initial reactions (50% CLD). FT-IR spectrum of poly(MMA-*co*-EDMA) illustrates the presence of an ester functionality at

1732 and aliphatic –C–H str. at 2952. Moreover, aliphatic $–CH_3$ sym. bend. at 1380 and antisym. bending at 1455. In another, synthesis of poly(MMA-*co*-DVB) was also confirmed by FT-IR spectrum (KBr pellet, cm^{-1}). FT-IR demonstrates the presence of an ester functionality at 1730, aliphatic –CH stretching at 2950, disubstituted benzene ring[21] corresponds to 905 and *para*-disubstituted benzene ring assigned by 841. FT-IR spectrum of poly(MMA-*co*-EDMA) and poly(MMA-*co*-DVB) is represented in **Figure 5.1.**

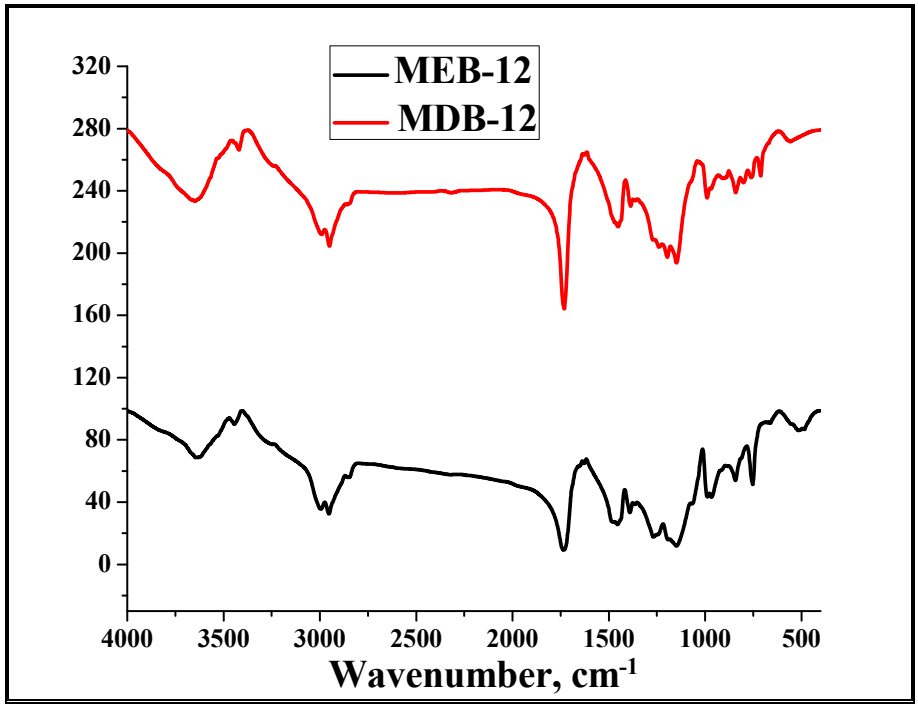

Figure 5.1. FT-IR spectrum of poly(MMA-*co*-EDMA) and poly(MMA-*co*-DVB) for 50% CLD and 1:1 monomer: porogen ratio

5.3.2. Surface area

Four polymer series (MEB, MEH, MDB, and MDH) of methyl methacrylate monomer were obtained by varying crosslinkers (EDMA/DVB), concentration of crosslinkers, porogens (n-butanol/n-hexanol) and monomer**:** porogen ratio (1:1, 1:2 and 1:3 v/v) at four different crosslink densities (50, 100, 150, and 200%) by suspension polymerization. Desirable properties such as surface area, pore volume, and pore size are highly tunable by changing porogen (type and concentration), crosslink density (CLD), polymerization temperature, and type of initiator.[22]

In the present work, effect of the reaction composition variables on surface area and porosity of crosslinked beaded microspheres were studied.

5.3.2.1. Effect of crosslinkers and crosslink density on surface area

Type of crosslinker significantly affects the physical properties of the polymers. Ethylene dimethacrylate and divinylbenzene were used as crosslinkers whereas CLD was varied from 50 to 200%. Ethylene dimethacrylate based polymers showed higher surface area than divinylbenzene. This is mainly due to the fact that, basic structure of monomers such as methyl methacrylate and dimer of ethyl methacrylate (i.e. EDMA) is almost similar, thus, miscibility of these monomers is higher. On the contrary, miscibility of methyl methacrylate into the divinylbenzene is lower due to the different type of monomeric structure resulting in lower surface area. MEH series exhibited the higher surface area than MDH in all monomer**:** porogen ratios (1:1, 1:2, and 1:3). Solubility of an ethylene dimethacrylate in water (1.086 g/L) is much higher than divinylbenzene (0.005 g/L) at 20^{o}C. Thus, EDMA has higher affinity towards aqueous phase and thus remains in water for a longer period and forms smaller pores resulting high surface area. The polymers synthesized using n-butanol as a porogen exhibited much higher surface area compared to n-hexanol. This is also again due to the solubility of n-butanol in water (80 g/L) being higher than n-hexanol (5.9 g/L) at 20^{o}C. Thus, n-butanol remains in an aqueous phase for a longer period and forms smaller pores resulting high surface area.

In this work, MDB series demonstrates the surface area of 110.3, 8.8, and 1.3 m^2/g for 50% CLD which was significantly increased to 178.6, 46.8, and 32.9 m^2/g for 200% CLD using 1:1, 1:2 and 1:3 (M:P) ratio, respectively. Notably, same trends were observed for remaining three series. Crosslink density was also played pivotal role in crosslinked polymers since it not only affects the chemical composition of resulting polymer but also influences the physical properties. Variation in concentration of crosslinker led to the polymer with different chemical composition as a result different characteristics. It was concluded that, surface area increased with increasing CLD (concentration of crosslinker) whereas substantially decreased with increasing porogen concentration. This is due to a decreased pore size inside the nuclei of bead resulting into smaller pores which generates the higher surface area.[8] As to be expected, four series demonstrated an increase in surface area with increasing CLD at all monomer: porogen ratio.[19] Furthermore, particular concentration of monomer and porogen pass through a critical

value[23] at a particular CLD. As a result, all series revealed increasing surface area from 50 to 150% CLD whereas surface area gets decreased above 150% CLD for 1:3 (M:P) ratio (shown in figure by red arrow). As concentration of porogen was increased, surface area was decreased inversely pore volume was increased because non-solvating porogen allowed increasing phase separation between aqueous and organic phase.

5.3.2.2. Effect of type and concentration of porogens on surface area

Undoubtedly, surface area and porous properties of the beaded polymers depends on the type and concentration of porogens. In the present work, poly(MMA-*co*-EDMA) exhibited the higher surface area with n-butanol than n-hexanol at 1:2 and 1:3 (M:P) ratio, inversely, surface area was decreased for MEB than MEH at 1:1 (M:P) ratio. This is probably due to the crosslinker and porogen passing through a critical hydrophilic-hydrophobic concentration at a particular CLD. Copolymer series MDB, MEH, and MDH revealed a decrease in surface area with increasing porogen concentration. This is due to the non-solvating porogens have the property to decreasing surface area and increasing pore volume with higher concentration of porogen since at lower concentration of monomer a large number of nuclei formed randomly which tend to grow through each other and eventually resulted in lower surface area.[24] Overall, poly(MMA-*co*-EDMA) displayed the higher surface with n-butanol whereas poly(MMA-*co*-DVB) displayed the higher surface area with n-hexanol (1:2 and 1:3 v/v). Surface area of all four series are reported in **Tables 5.2, 5.3** and are depicted in **Figure 5.2.**

Table 5.2. Surface area of poly(MMA-*co*-EDMA) and poly(MMA-*co*-DVB) at different CLD using n-butanol porogen

Property	Monomer: Porogen ratio	**MEB (Series 1)**				**MDB (Series 2)**			
		Crosslink density (%)							
		50	100	150	200	50	100	150	200
Surface area (m^2/g)	1:1	41.94	75.8	92.9	103.3	110.3	113.6	128.9	178.6
	1:2	72.73	117.5	112.6	128.9	8.8	17.14	35.9	46.8
	1:3	59.80	92.2	97.2	85.2	1.3	8.2	35.8	32.9

Table 5.3. Surface area of poly(MMA-*co*-EDMA) and poly(MMA-*co*-DVB) at different CLD using n-hexanol porogen

Property	Monomer: Porogen ratio	MEH (Series 3)				MDH (Series 4)			
		Crosslink density (%)							
		50	100	150	200	50	100	150	200
Surface area (m^2/g)	1:1	76.9	144.5	154.8	184.9	43.6	112.8	118.5	125.1
	1:2	54.2	101.7	112.4	126.4	24.4	28.6	47.5	88.1
	1:3	12.3	19.9	113.3	92.4	10.9	17.8	127.1	75.8

Abbreviations: MEB – MMA-EDMA-n-butanol; MDB – MMA-DVB-n-butanol; MEH – MMA-EDMA-n-hexanol; MDH – MMA-DVB-n-hexanol; PV – Pore volume; CLD: crosslink density; Porogen concentration (X**:**Y) – monomer**:** porogen ratio; Tmax – Maximum decomposition temperature; M:P – Monomer**:** porogen ratio.

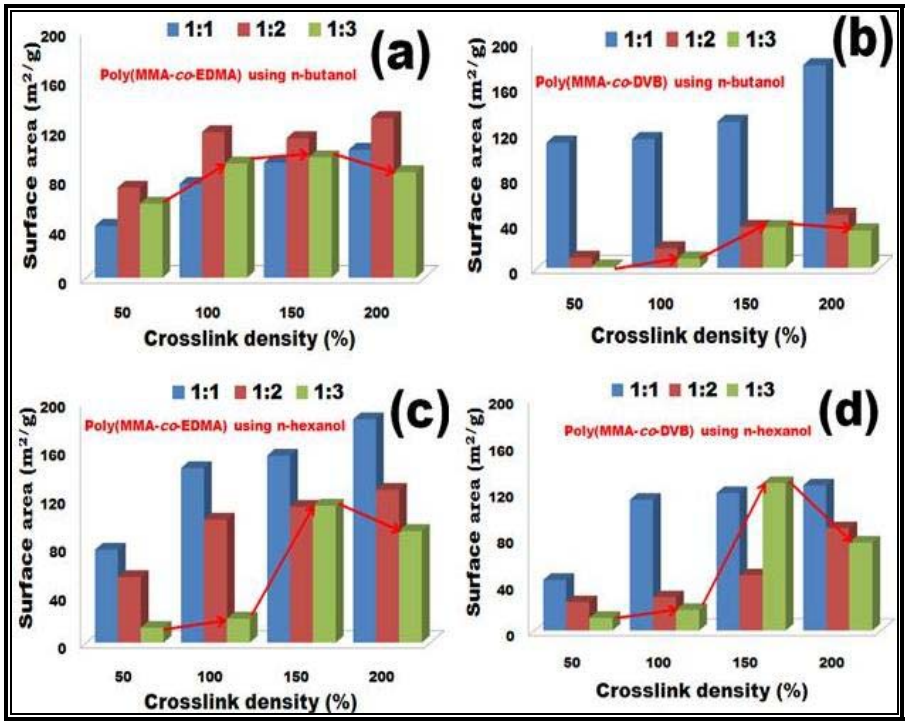

Figure 5.2. Surface area of poly(MMA-*co*-EDMA) and poly(MMA-*co*-DVB) using with (a,b) n-butanol, and (c,d) n-hexanol porogen, respectively

5.3.3. Pore volume and pore size determination

According to the IUPAC pores are classifieds based on their width as micro (<0.002 μm), meso (0.002 – 0.05 μm), and macropores (>0.05 μm).[25] Commonly pore size in the range of 0.01 – 0.1 μm is referred as macropores whereas pore size >0.1 μm are considered as mega or gigapores materials.[26] Effects of crosslinkers and porogens (type and concentration) on pore volume and pore size for 100% CLD were studied.

5.3.3.1. Effect of porogens and crosslinkers on pore volume

Pore volume (PV) or porosity is a measure of the void spaces in the polymer and is a fraction of the volume of voids over the total volume of polymer matrix. Interestingly, MEB, MDB, MEH and MDH series revealed the highest pore volume of 0.44, 0.22, 0.87 and 0.466 μm and pore size of 3.75, 3.36, 4.33 and 3.310 cc/g using 1:3 (monomer: porogen) ratio. Furthermore, this pore volume and pore size was decreased for 1:2 and further for 1:1 (monomer: porogen) ratio and 100% CLD. Poly(MMA-*co*-EDMA) demonstrated the high pore volume with n-hexanol as compared to n-butanol as a porogen. This is probably due to the polarity of the porogens. Indeed, n-hexanol is less polar and less miscible with MMA-EDMA monomer systems that led to porous polymer beads. Poly(MMA-*co*-DVB) revealed the high pore volume with n-butanol as compared to n-hexanol. This is mainly due to more polar and less miscible n-butanol with MMA-DVB monomer system that led to highly porous poly(MMA-*co*-DVB).[27] Furthermore, poly(MMA-*co*-DVB) revealed the higher pore volume than poly(MMA-*co*-EDMA). Porogen concentration study revealed that, pore volume (PV) of poly(MMA-*co*-EDMA) increased with increasing concentration of porogen (n-butanol or n-hexanol) because of higher concentration of hydrophobic alcoholic porogen in comparatively hydrophilic MMA-EDMA monomer system leading to larger pores,[28] consequently resulting in more porous polymer matrix. Interestingly, poly(MMA-*co*-EDMA) illustrates the larger PV for 1:3 (M:P) ratio with both (n-butanol/n-hexanol) porogens. On the other hand, poly(MMA-*co*-DVB) displayed the larger PV for 1:2 (M:P) ratio and PV was decreased with change in M:P ratio for both (n-butanol/n-hexanol) porogens. This may happen due to the less miscibility of a hydrophobic porogen with MMA-EDMA system and more miscibility with MMA-DVB system.

5.3.3.2. Effect of porogens and crosslinkers on pore size

Pore size decides the applicability of the polymer, however, larger pore sized polymers have been efficiently employed in applications such as pharmaceuticals, ceramics, biomedical, metallurgy and engineering fields. Indeed, solvating porogens have the property to impart more surface area, and microporosity. On the contrary, non-solvating porogens have the property to impart lower surface area and gigaporosity. Pore diameter is an important criterion for enzyme immobilization due its large structure property. Particular monomer**:** porogen concentration introduces the larger pore size into the polymer matrix.

Importantly, pore size demonstrates the similar observation like pore volume with n-butanol and n-hexanol porogens. Porogens effect revealed that, poly(MMA-*co*-EDMA) and poly(MMA-*co*-DVB) have larger pore size with n-hexanol than n-butanol porogen at all monomer: porogen ratio. This is mainly due to the increased chain length of an aliphatic porogen from C4 to C6 allow increase in pore size.[29] Poly(MMA-*co*-EDMA) exhibited larger pore size with both porogens using 1:3 monomer**:** porogen ratio due to increased concentration of a porogen led to larger pore diameter.[22,30] This observation was demonstrated by all polymer series. In addition, poly(MMA-*co*-DVB) displayed larger pore size at 1:2 monomer**:** porogen ratio whereas change in monomer: porogen concentration led towards smaller pore size. The reason may be same as aforementioned in pore volume. Thus, maximum pore volume and pore size was obtained for poly(MMA-*co*-DVB) at 1:2 (M:P) ratio. Recently, Costae *et al.*[31] reported the surface area, pore volume, and pore size of poly(MMA-*co*-DVB) which is lower for industrial or any other applications. However, polymer synthesized in the present work by non-solvating porogens is a paradigm of polymer porosity. Overall, polymer synthesized using non-solvating porogens revealed the excellent porosity than earlier reported. Thus, aim of the gigaporous polymer synthesis was successfully achieved. Pore volume and pore diameter of polymers at 100% CLD using different crosslinkers, porogens, and monomer: porogen ratio is reported in **Table 5.4** and is depicted in **Figure 5.3.**

Table 5.4. Pore diameter and pore volume of MEB, MDB, MEH, and MDH for 100% CLD with different monomer: crosslinker ratios (1:1, 1:2, and 1:3 v/v)

Monomer: Porogen ratio	Polymer	**MEB**	**MDB**	**MEH**	**MDH**
1:1	Pore diameter (μm)	0.024	0.058	0.12	0.09
	Pore volume (cc/g)	0.680	2.320	2.70	1.80
1:2	Pore diameter (μm)	0.066	0.35	0.17	0.68
	Pore volume (cc/g)	2.430	3.64	2.85	3.56
1:3	Pore diameter (μm)	0.44	0.22	0.87	0.466
	Pore volume (cc/g)	3.75	3.36	4.33	3.310

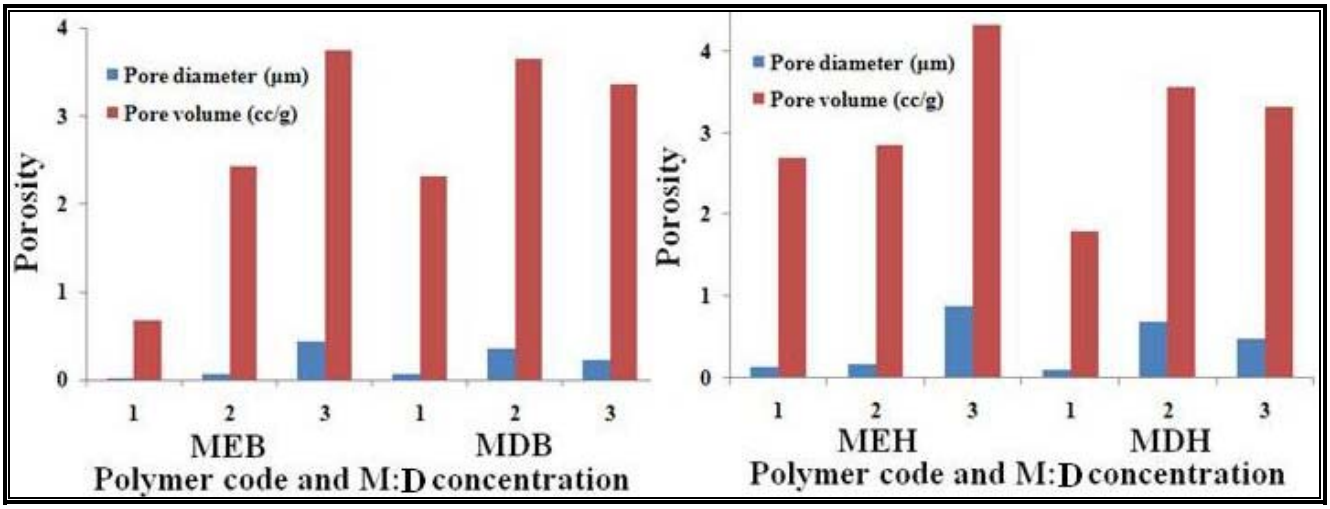

Figure 5.3. Pore volume and pore size of poly(MMA-*co*-EDMA) and poly(MMA-*co*-DVB) using n-butanol, and n-hexanol porogen, respectively for 100% CLD

5.3.4. Particle size distribution

Particle size is also one of the most important properties that substantially influences to the efficiency of a beaded polymer. Average particle size of the polymer revealed a particular trend with CLD and concentration of porogen. It noteworthy that, particle size was slightly increased with increasing CLD whereas decreased with increasing porogens concentration. In other words, as concentration of crosslinker increased, average particle size was also increased

due to higher vander Waals interaction of crosslinker.[32] Larger particle size is related with particular monomer to crosslinker concentration and type of porogen (solvating/non-solvating) Slight changes in these factors led to change in the average particle diameter. These results were shown by all four different polymer series i.e. MEB, MDB, MEH and MDH.

Herein, MEB series revealed the average particle size of 35.6, 34.9, and 28.0 μm for 50% CLD which was increased to 76.1, 38.2, and 30.4 μm for 200% CLD at 1:1, 1:2 and 1:3 (M:P) ratio, respectively. This observation clearly showed that, particle size was increased with increasing CLD whereas decreased with increasing monomer: porogen concentration. Similar observation was demonstrated by remaining three series. Interfacial tension between aqueous and organic phase played a pivotal role in deciding the average particle size of polymers. Indeed, DVB has more hydrophobicity than EDMA as a crosslinker, whereas n-hexanol porogen has more hydrophobicity than n-butanol as a porogen. As a result, n-hexanol has the property to create more interfacial tension than n-butanol between aqueous and organic phase. Consequently, polymer obtained by n-hexanol porogen revealed the larger average particle size than n-butanol porogen at all monomer:porogen (M:P) ratio. This is because of increased hydrophobicity of an organic phase due to porogen and its concentration decreases the interfacial tension resulting into larger particle size. Both hydrophobic porogens impart comparatively smaller particle size to polymer containing DVB crosslinker than polymer containing EDMA as a crosslinker due to the more compatibility of DVB with n-butanol/n-hexanol porogens. Most importantly, average particle sizes of poly(MMA-*co*-EDMA) and poly(MMA-*co*-DVB) was decreased with increasing M:P ratio perhaps due to higher concentration of hydrophobic porogen allowing to decrease the vander Waals interaction which allowed synthesizing small sized particles. Interestingly, particle size was decreased after 150% CLD with all series and all M:P ratios. Average particle sizes shown by the polymers were in the range of 25–120 μm which is the characteristic feature of suspension polymerization. Average particle sizes of the polymers are depicted in **Tables 5.5, 5.6** and in **Figure 5.4 (a, b).**

Table 5.5. Average particle size (APS) of poly(MMA-*co*-EDMA) and poly(MMA-*co*-DVB) at different CLD using n-butanol porogen

Polymer	Monomer: Porogen ratio	**MEB (Series 1)**				**MDB (Series 2)**			
		Crosslink density (%)							
		50	100	150	200	50	100	150	200
Average particle size (μm)	1:1	35.6	49.9	85.4	76.1	30.99	43.62	63.2	46.4
	1:2	34.9	46.6	49.9	38.2	30.4	34.9	46.5	33.8
	1:3	28.0	37.7	39.9	30.4	27.7	30.6	32.4	29.72

Table 5.6. Average particle size (APS) of poly(MMA-*co*-EDMA) and poly(MMA-*co*-DVB) at different CLD using n-hexanol porogen

Polymer	Monomer: Porogen ratio	**MEH (Series 3)**				**MDH (Series 4)**			
		Crosslink density (%)							
		50	100	150	200	50	100	150	200
Average particle size (μm)	1	68.9	73.3	115.3	73.4	59.1	70.2	76.3	68.0
	2	66.5	91.5	94.3	39.6	29.3	32.5	43.8	42.6
	3	50.2	60.5	64.4	46.9	26.3	26.9	32.0	31.2

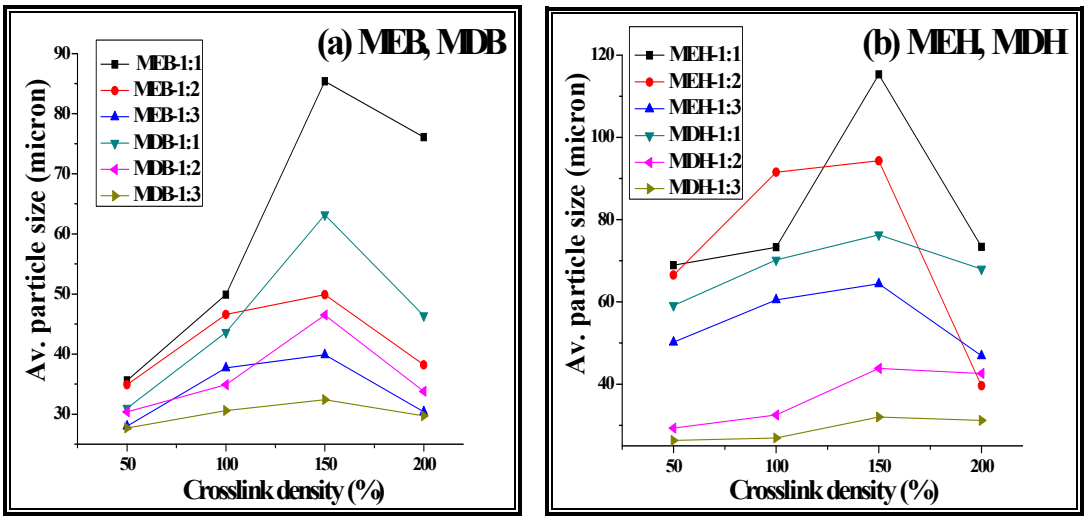

Figure 5.4. Average particle size of poly(MMA-*co*-EDMA) and poly(MMA-*co*-DVB) using (a) n-butanol, and (b) n-hexanol porogen

5.3.5. Thermogravimetric analysis

Typically, crosslinked polymer obligates as a support for adsorption and entrapment. However, crosslinked gigaporous beaded polymers were potentially used for entrapment of an enzymes. Polymer supported enzymes is a paradigm for chiral resolution and biotransformation at room temperature only. Despite restriction of room temperature, polymer supported species can be used for higher temperature solid phase synthesis depending on the reaction conditions. As a result, thermal stability evaluation of a polymer is an essential. Thermogravimetric (TGA) analysis of polymers were studied by simultaneous thermal analysis (STA, Perkin Elmer) in the temperature range of 50–800^{o}C under nitrogen atmosphere at heating rate of 10^{o}C per min. It was observed that, maximum decomposition temperature (Tmax) of poly(MMA-*co*-EDMA) is 323 and 318^{o}C whereas poly(MMA-*co*-DVB) showed the Tmax of 418 and 443^{o}C for 50 and 200% CLD, respectively.

Poly(MMA-*co*-DVB) displayed the higher Tmax for 200% CLD due to the presence of bulky aromatic ring in the basic polymeric structure which attributes for higher thermal stability. On the contrary, poly(MMA-*co*-EDMA) displayed the much lower Tmax than poly(MMA-*co*-DVB) due to increased flexibility in polymeric structure. In conclusion, aromatic (rigid) part in the polymer is the major parameter that decides the Tmax of a polymer.[33] Crosslinking is also

plays an important role in thermal stability of the polymers. In 1999, Cooper *et al.*[34] reported the Tmax of polymers containing DVB as a crosslinker. Present work not only reports the comparative effect of crosslinker (rigid and flexible) but also the effect of concentration of crosslinker on thermostability of gigaporous material. Result clearly showed that, increasing concentration of a rigid (DVB) crosslinker and decreased concentration of a flexible (EDMA) crosslinker allowed increasing Tmax. Differential thermogravimetric (DTG) curves are depicted in **Figure 5.5.**

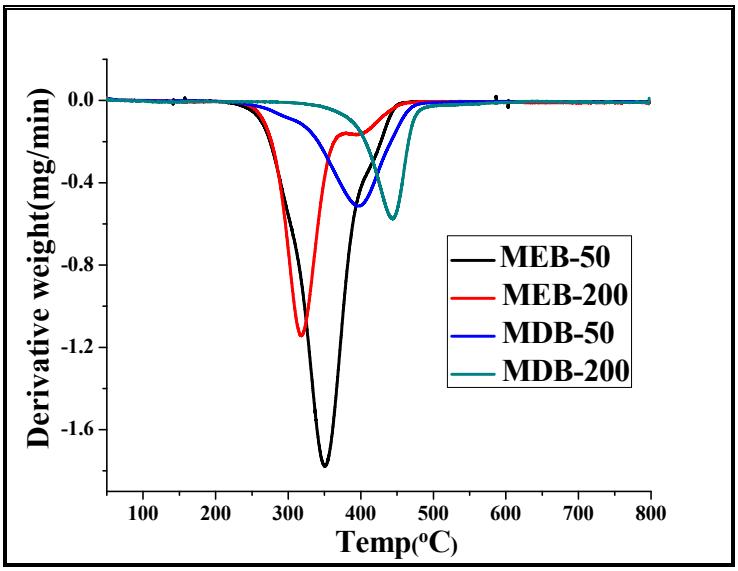

Figure 5.5. Differential thermogravimetry (DTG) curves of poly(MMA-*co*-EDMA) and poly(MMA-*co*-DVB) for 25 and 200% CLD

5.3.6. Swelling ratio

When crosslinked polymer is contacted with swelling solvent, the solvent enters into the pores of polymer matrix and attains a maximum swelling but not dissolve. However, swelling ratio and rate depends on the CLD, pore size, and the polymer-solvent interaction. Solubility parameter of polymer is useful to predict the polymer behavior in various solvents. In reality, closer the solubility parameter of the polymer and swelling solvent; more is the polymer swelling and vice-versa. Two swelling solvents were selected to evaluate the swelling behavior of polymers. Solubility parameter of the polymers and swelling solvents are reported in **Table 5.7.**

Table 5.7. Solubility parameter of polymers and swelling solvents

Copolymer/Swelling solvent	Solubility parameter (δ) $(cal/cm^3)^{1/2}$
Poly(MMA-*co*-EDMA)	14.70
Poly(MMA-*co*-DVB)	14.18
Dimethyl sulfoxide	12.93
Methyl ethyl ketone	9.27

Nevertheless, higher the solubility parameter difference between polymer and swelling solvent, more is the polymer-solvent interaction, ultimately this solvent is bad for swelling purpose and vice versa for good solvent. Polymer-solvent interaction parameter (χ) was determined by Bristo and Watson[35] semi empirical **equation (3.4)** and reported in **Table 5.8.**

Table 5.8. Polymer-solvent interaction parameter

Polymer	Solvent	Polymer-solvent interaction parameter (χ)
Poly(MMA-*co*-EDMA)	DMSO	0.71
	MEK	4.79
Poly(MMA-*co*-DVB)	DMSO	0.53
	MEK	3.98

Swelling ratio[36] was carried out in 30 mL glass vials by adding 0.5 g of polymer beads in 20 mL of DMSO/MEK as a swelling solvent. Polymer beads were placed at an ambient temperature for a period of 24 h to obtain equilibrium swelling. Later on, polymers were removed, blotted with tissue paper, and weighed. Weight of the polymers was measured after swelling (W_s) and after drying (W_d). Swelling ratio is depicted in **Figure 5.6** which were calculated by mass swell ratio[37] **equation (3.5).**

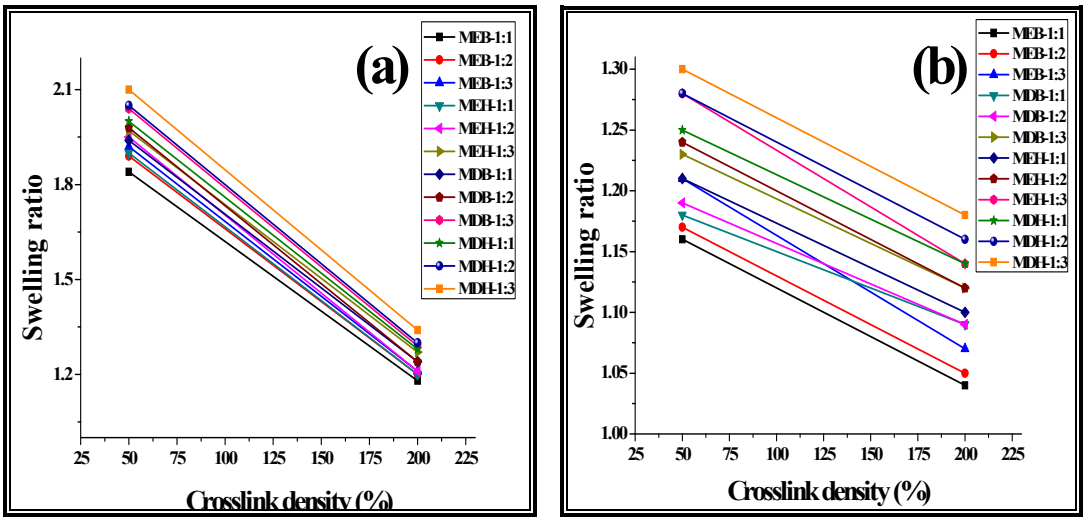

Figure 5.6. Swelling ratio of poly(MMA-*co*-EDMA) and poly(MMA-*co*-DVB) using (a) DMSO, and (b) methyl ethyl ketone

All polymer series demonstrated the maximum swelling in dimethyl sulfoxide over methyl ethyl ketone. Most importantly, polymer synthesized using 1:3 (monomer: porogen) ratio revealed the highest porosity which was decreased for 1:2 and further for 1:1 (monomer: porogen) ratio. All series demonstrated the higher swelling ratio for lower CLD (50%) whereas significantly decreased for higher CLD (200%). Notably, MDH, MDB, MEH, and MEB series illustrate the swelling ratio of 2.10, 2.04, 1.97, and 1.92 for 50% CLD which were decreased to 1.34, 1.29, 1.27, and 1.21, respectively for 200% CLD. Recently, Clarisse *et al.*[38] reported, the swelling behavior of poly(MMA-*co*-DVB) in different solvents. In the present work, poly(MMA-*co*-DVB) showed the more swelling in DMSO than earlier reported solvents. This is due to the polymer-solvent interaction parameter being much lower for DMSO as a swelling solvent. In addition, this study was also explained the swelling ratio of poly(MMA-*co*-EDMA) with respect to dimethylformamide and methyl ethyl ketone. Indeed, swelling ratio depends on CLD, porosity, and polymer-solvent interaction parameter. However, swelling ratio was much higher for low CLD polymer and it was decreased for higher CLD. This is mainly due to low CLD polymer has longer chains in polymer matrix that can easily swell, inversely high CLD polymer has smaller chains in polymer and difficult to swell. Thus, swelling ratio is the measure of CLD of polymer matrix. Poly(MMA-*co*-DVB) showed the more swelling than poly(MMA-*co*-EDMA) in both swelling solvents which indicates the more porous nature of poly(MMA-*co*-

DVB). Besides, polymer-solvent interaction parameter for DMSO is between 0–1 and for MEK it is 3–5, consequently polymer revealed the more swelling ratio in DMSO than MEK at same CLD.

5.3.7. External morphology

Scanning electron microscopy (SEM) is the powerful tool to visualize the morphology of porous beads as well as for particle size observation. SEM images of poly(MMA-*co*-DVB) were obtained for 200% CLD at 1:3 monomer**:**diluent ratio (200x and 10000x) magnification. Poly(MMA-*co*-DVB) showed the uniform beads at 200% CLD. Indeed, poly(MMA-*co*-DVB) demonstrated more porosity especially greater pore size for 1:3 monomer:diluent ratio. Lower magnification images (200x) clearly demonstrated the uniform and spherical beads whereas higher magnification (10000x) revealed the porous properties of the beaded microsphere. Interestingly, the pore size of polymer beads was increased with increase in monomer:diluent ratio which can be observed in SEM images (10000x magnification). SEM images of poly(MMA-*co*-DVB) for 1:1, 1:2, and 1:3 ratio are represented in **Figure 5.7 6 a, b, and c** (200x) and **Figure 5.7 d, e, and f** (10000x) at 200% CLD.

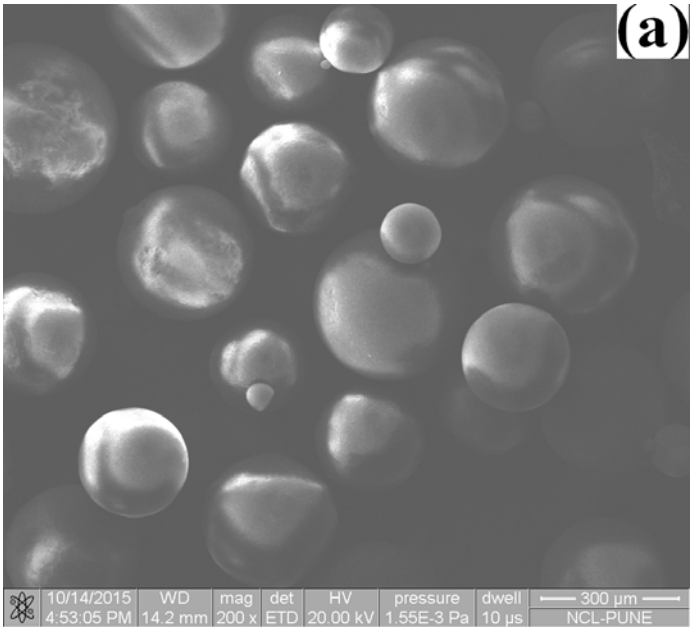
(a)
10/14/2015 4:53:05 PM
WD 14.2 mm
mag 200 x
det ETD
HV 20.00 kV
pressure 1.55E-3 Pa
dwell 10 µs
300 µm
NCL-PUNE

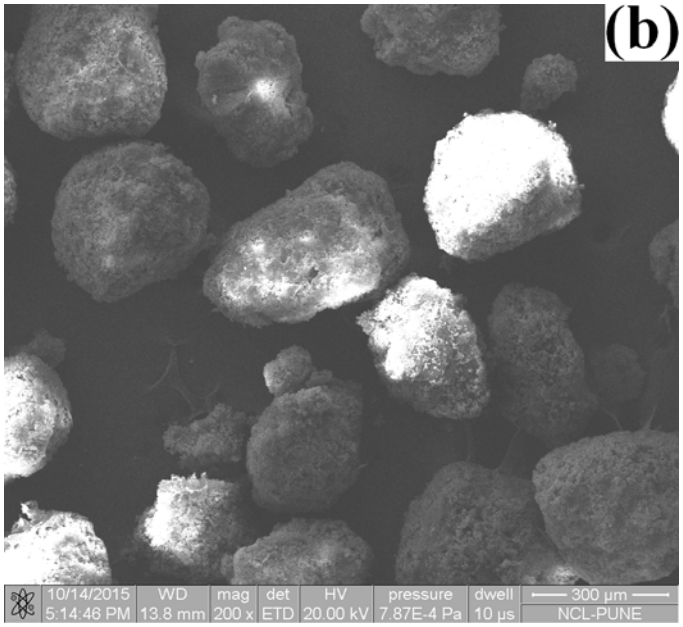
(b)
10/14/2015 5:14:46 PM
WD 13.8 mm
mag 200 x
det ETD
HV 20.00 kV
pressure 7.87E-4 Pa
dwell 10 µs
300 µm
NCL-PUNE

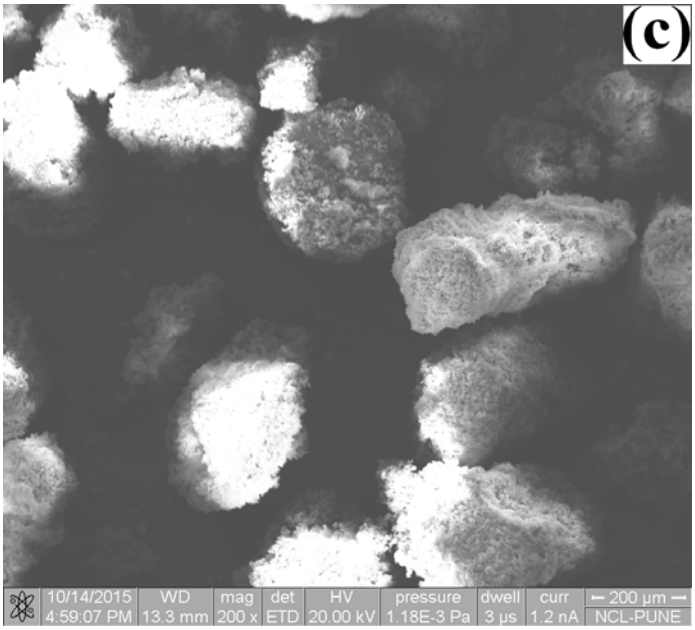
(c)
10/14/2015 4:59:07 PM
WD 13.3 mm
mag 200 x
det ETD
HV 20.00 kV
pressure 1.18E-3 Pa
dwell 3 µs
curr 1.2 nA
200 µm
NCL-PUNE

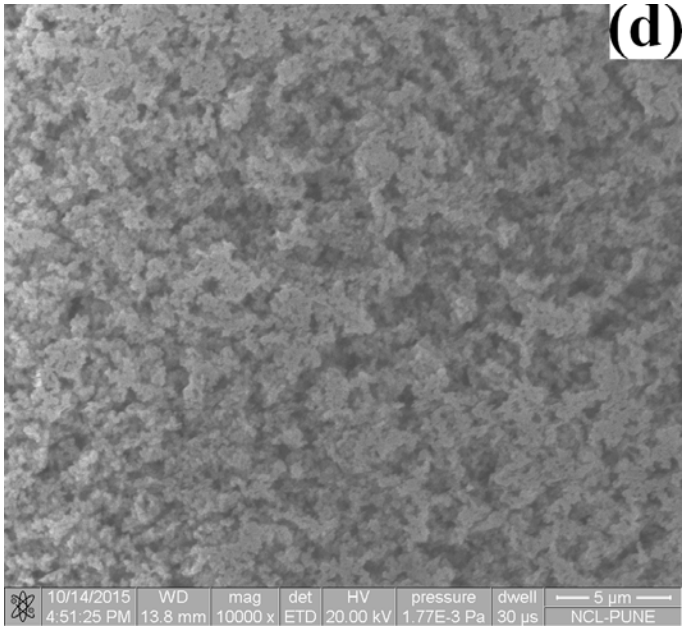
(d)
10/14/2015 4:51:25 PM
WD 13.8 mm
mag 10000 x
det ETD
HV 20.00 kV
pressure 1.77E-3 Pa
dwell 30 µs
5 µm
NCL-PUNE

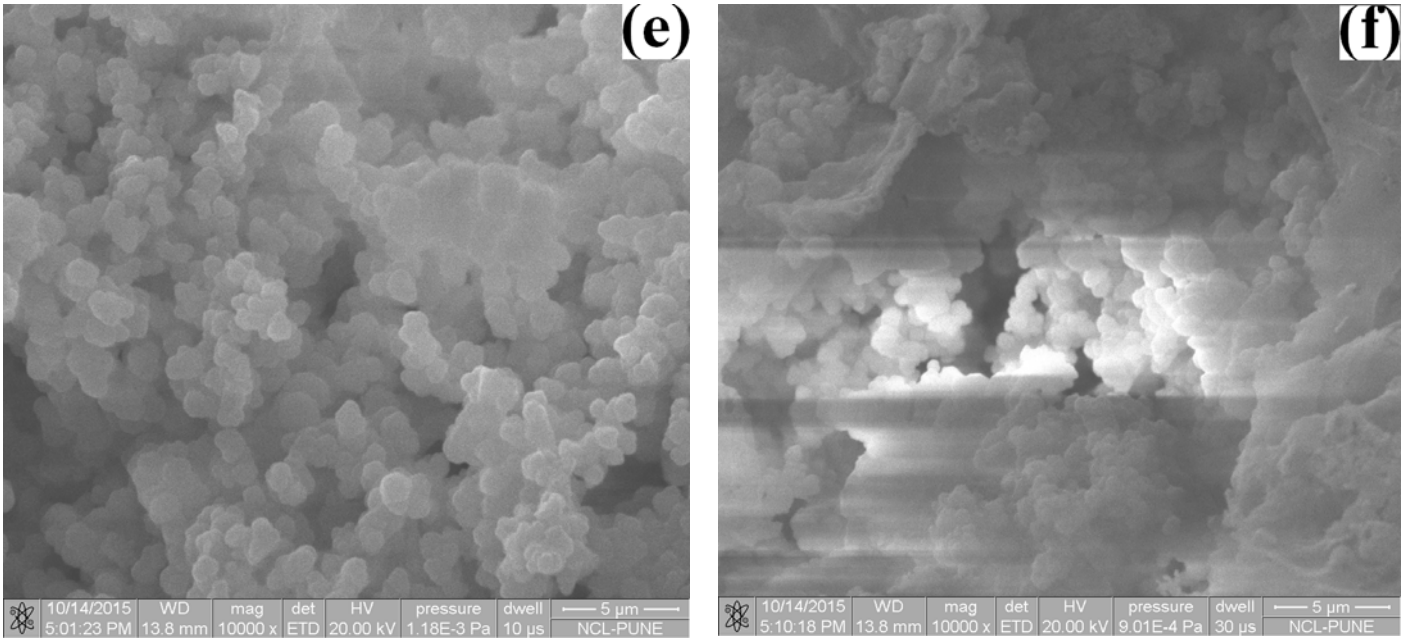

Figure 5.7. SEM micrographs of MDH-200 (1:1, 1:2, 1:3) (a, b, c) at 200x and (d, e, f) at 10000x magnification, respectively.

5.4. Conclusion

Most importantly, increasing concentration of non-solvating porogens were inversely acting on the surface area and gigaporosity of crosslinked beaded microsphere. Gigaporous microspheres were successfully synthesized bearing high pore volume and large pore size. Notably, higher concentration of non-solvating porogens led towards highly porous properties inversely small surface area. However, surface area was increased with increasing concentration of crosslinker (crosslink density). It is worth mentioning that, surface area was decreased after 150% crosslink density (CLD) for all polymer series at 1:3 monomer:porogen ratio. Poly(MMA-*co*-DVB) displayed the highest pore volume and pore size for 100% CLD (1:3 v/v) which was 3.56 cc/g and 0.68 µm, respectively. Slight change in monomer to porogen ratio led towards substantial decrease in porosity. In case of poly(MMA-*co*-EDMA), porosity was increased with higher monomer to porogen ratio in the sequence of 1:1, 1:2, and 1:3 (monomer:porogen ratio). Interestingly, average particle size of all polymer series showed the increasing particle size upto

150% CLD, above this CLD, particle size was decreased steadily. More importantly, higher rigid or lower flexible crosslinker concentration revealed the better thermal properties of a polymer. Notably, rigidity/flexibility of crosslinkers substantially attributed to the thermal properties than its concentration. Polymer-solvent interaction parameter (χ) illustrated that, polymer has lower interaction parameter with DMSO, contrary more interaction parameter with MEK. This theoretical prediction was confirmed by swelling ratio. In other words, polymer showed more swelling in DMSO than MEK as a swelling solvent. Importantly, poly(MMA-*co*-DVB) displayed the higher swelling property than poly(MMA-*co*-EDMA) in DMSO as a swelling solvent. Although, polymers obtained from n-hexanol (1:3 monomer:porogen) have gigaporous properties, however, SEM images strongly support to porous polymer beads. Especially, these polymers are inevitably essential for an enzyme immobilization, loading of catalysts, metal chelating agent, as well as in adsorption and entrapment technology.

References

[1] Li Y., Zhang W., Sun Z., Sun T., Xie Z., Huang Y., and Jing X, *Eur. Polym. J.,* 2015, **63,** 149–155.

[2] Chakraborty S., Colon Y. J., Snurr R. Q., and Nguyen, S. T., *Chem. Sci.,* 2015, **6,** 384–389.

[3] Lu W., Yuan D., Zhao D., Schilling C. I., Plietzsch O., Muller T., Brase S., Guenther J., Blumel J., Krishna R., Li Z., and Zhou H. C., *Chem. Mater.,* 2010, **22,** 5964–5972.

[4] Mane S., Ponrathnam S., and Chavan N., *Eur. Polym. J.,* 2014, **59,** 46–58.

[5] Mohamed M. H., and Wilson L. D., *Nanomaterials,* 2012, **2,** 163–186.

[6] He H., Averick S., Mandal P., Ding H., Li S., Gelb J., Kotwal N., Merkle A., Litster S., and Matyjaszewski K., *Adv. Sci.,* 2015, **1500069,** 1–6.

[7] Quast M. J., Argall A. D., Hager C. J., and Muller A., *J. Polym. Sci. Part A: Polym. Chem.,* 2015, **53(16),** 1880–1894.

[8] Kotha A., Rajan C. R., Ponrathnam S., and Shewale J. G., *React. Funct. Polym.,* 1996, **28,** 227–233.

[9] Rouquerol J., Avnir D., Fairbridge C. W., Everett D. H., Haynes J. M., Pernicone N., Ramsay J. D. F., Sing K. S. W., and Unger K. K., *Pure Appl. Chem.,* 1994, **66,** 1739–1758.

[10] Bao M. D., Barreiro R., Miranda J. M., Cepeda A., and Regal P., *Chromatography,* 2015, **2,** 79–95.

[11] Nesterenko E. P., Burke M., Bosset C., Passutto P., Malafosse C., and Collins D. A., *RSC. Adv.,* 2015, **5,** 7890–7896.

[12] Seidl J., Malinsky J., Dusek K., and Heitz W., Adv. *Polym. Sci.,* 1967, **5,** 113–213.

[13] Kubin M., Spacek P., and Chromecek R., *Coll. Czechosl. Chem. Commun.,* 1967, **32,** 3881–3887.

[14] Maciejewska M. J., *Therm. Anal. Calorim.,* 2015, **121,** 1333–1343.

[15] Sherrington D. C., *Chem. Commun.,* 1998, 2275–2286.

[16] Schafer C., Mhadgut S. C., Kugyela N., Torok M., and Torok B., *Catal. Sci. Technol.,* 2015, **5,** 716–723.

[17] Shunmughanathan M., Puthiaraj P., and Pitchumani K., *Chem. Cat. Chem.,* 2015, **7,** 666–673.

[18] Okuno Y., Isomura S., Kamakura T., Sano F., Tamahori K., Goto T., Hayashida T., Kitagawa Y., Fukuhara A., and Takeda K., *Chem. Sus. Chem.,* 2015, **8(10),** 1711–1715.

[19] Rahman A. U., Iqbal M., Rahman F. U., Dayan F. D., Yaseen M. L. Y., Omer M., Garver M., Yang L., and Tan T., *J. Appl. Polym. Sci.,* 2012, **124,** 915–926.

[20] Luque de Castro M. D., and Garco a-Ayuso L. E., *Anal. Chim. Acta,* 1998, **369,** 1–10.

[21] Bartholin M., *Macromol. Chem.,* 1981, **182,** 2075–2085.

[22] Okay O., *Prog. Polym. Sci.,* 2000, **25,** 711–779.

[23] Galia M., Svec F., and Frechet J. M. J., *J. Polym. Sci. A: Polym. Chem.,* 1994, **32,** 2169–2175.

[24] Si T., Wanga Y., Wei W., Lv P., Ma G., and Su Z., *React. Funct. Polym.,* 2011, **71,** 728–

735.

[25] Sing K. S. W., Everett D. H., Haul R. A. W., Moscou L., Pierotti R. A., Rouquerol J., and Siemieniewska T., *Pure Appl. Chem.,* 1985, **57,** 603–619.

[26] Gu T., Zhou W., Ma G., and Su Z., *China Particulogy,* 2005, **3,** 349–353.

[27] Shea K. J., Stoddard G. J., Shavelle D. M., Wakui F., and Choate R. M., *Macromolecules,* 1990, **23,** 4497–4507.

[28] Svec F., Hradil J., Coupek J., and Kalal J., *Angew. Makromol. Chem.,* 1975, **48,** 135–143.

[29] Xie S., Svec F., and Frechet J. M. J., *J. Polym. Sci. A: Polym. Chem.,* 1997, **35,** 1013–1021.

[30] Bennett D. J., Burford R. P., Davis T. P., and Tilley H. J., *Polym. Int.,* 1995, **36,** 219–226.

[31] Costae C. N., Costa M. A. S., De L. C., and Maria S., *Polymer,* 2012, **22,** 409–415.

[32] Gooch J. W., Emulsification and polymerization of alkyd resins. *Springer,* New York. 2002, **XXII,** PP 28.

[33] ASM International characterization and failure analysis of plastics. The material information society 2003, **#06978G,** PP 15.

[34] Cooper A. I., Hems W. P., and Holmes A. B., *Macromolecules,* 1999, **32,** 2156–2166.

[35] Barlkani M., and Hepburn C., *Iran. J. Polym. Sci. Tech.,* 1992, **1,** 1–5.

[36] Yildiz U., and Hazer B., *Macromol. Chem. Phys.,* 1998, **199,** 163–168.

[37] Brundha B. A., and Pazhanisamy P., *Int. J. Chem. Tech. Res.,* 2010, **2,** 2192–2197.

[38] Clarisse M., Queiros Y., Barbosa C., Barbosa L., and Lucas E., *Chem. Chem. Technol.,* 2012, **6,** 145–152.

RACEMIC DRUG RESOLUTION

6.1. Introduction

Over the last two decades polymers have been extensively used as a solid support in different fields.[1-4] Less reactive sites is the major concern with crosslinked (insoluble) polymers due to most of the functional groups being buried into the polymer matrix and are not available for indented application purpose. To overcome this difficulty, present study is devoted to the synthesis of more reactive, insoluble polymers exhibiting uniform and spherical beads to utilize the concept of core-shell polymers. In solid phase synthesis, polymers were widely used in their debut as a support[5] for substrate, reagents, catalysts, enzymes, scavenger, protecting groups, and photosensitizers. Although, these moieties can be immobilized onto the support by covalent, ionic, adsorption, or entrapment method,[6] industrially, the use of polymer as a support in asymmetric synthesis[7] and chiral resolution[8] became more successful. In 2012, Todorovic *et al.*[9] synthesized the methyl methacrylate copolymer having surface area in the range of 9 – 17 m^2/g. This low surface area of polymer is not suitable for modification with chiral selector, as column material, biomedical and any other applications since polymer efficiency decreases due to small surface area. In addition, highly porous polymer decreases mechanical strength which creates problem during application. In the present study, methyl methacrylate copolymers were successfully synthesized exhibiting higher surface area (554 m^2/g) and better strength as a core polymer.

In human body, biomolecules such as proteins (L-form of enzymes), sugars (D-form), and nucleic acids are existing in the chirally pure form. This approach suggests that, human body is highly chiral selective.[10] Racemic form of drug contains both enantiomeric forms. One isomer produces therapeutic effect while other enantiomer may be inactive or has teratogenic effect. As a result, USFDA (1992) issued a guideline to bring the only therapeutically active isomer in the market. Therefore, to make the drug chirally pure become essential. Nowadays, number of methods such as crystallization, chromatographic resolution, enzymatic resolution, capillary electrophoresis, membrane technology, supercritical fluid extraction, and liquid-liquid extraction methods[11,12] are commonly used to make the drug chirally pure. Mostly, crystallization and chromatography techniques are widely used and nearly 80% of drugs were resolved by these

techniques. However, chromatographic technique is industrially favorable due to its recycle and reuse characteristics.

Number of chiral selector such as crown ether,[13] cyclodextrin,[14,15] protein,[16] chiral surfactant,[17] metal-chiral amino acid complexes,[18] and antibiotics[19] are available in their native or derivatised form are possibly used in chiral separations. Indeed, inexpensive tartaric acids, amino acids or their derivatives have not been evaluated as chiral selectors. Furthermore, type of and concentration[20] of chiral selector as well as pH of mobile phase attributes for resolution of racemic drugs. Lin *et al.*[21] used the molecularly imprinted polymer for resolution wherein the effect of particle size on resolution is demonstrated. The present study is related to the applications of core-shell polymer for resolution of β_2-adrenergic receptor i.e. salbutamol. In 1957, thalidomide (n-phthalyl-glutamic acid imide) had been widely used in the treatment of nausea in pregnant women. Later on, widespread use of thalidomide led to tragedy due to existence of sedative and teratogenic isomer being together. Unfortunately, 10,000 children were born with phocomelia congenital disorder. This is mainly because of 'S' enantiomer of thalidomide obligates to teratogenic effect whereas 'R' enantiomer contains desirable sedative properties.[22]This tragedy underlines the importance of pure enantiomer compounds.

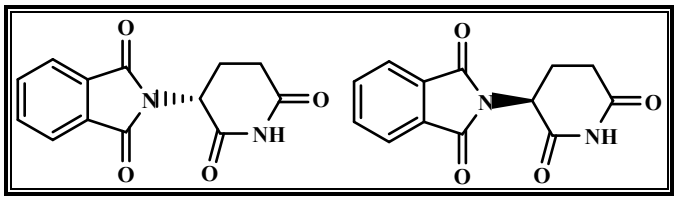

R-Thalidomide (Sedative) **S-Thalidomide (Teratogen)**

Undertaken study not only promises to provide more reactive sites but also high surface area and uniform particles sized polymer which is suitable as a column material as well for biomedical and pharmaceuticals applications. Salbutamol is a β_2 adrenergic receptor agonist[23] and commonly used to prevent and cure the asthma disease. Salbutamol is also used to treat the bronchospam and chronic obstructive pulmonary disease. The headache, anxiety and muscle crampling are some side effects with salbutamol. Structure of salbutamol drug used for resolution is given below.

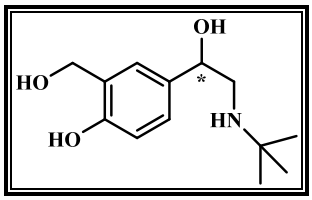

(±)Salbutamol

6.2. Experimental

6.2.1. Materials

Methanol (HPLC grade):- Make: Loba Chemie; Molecular formula: CH_4O; Molecular weight (g/mol): 32.04; Specific gravity/density (g/cm^3): 0.7918; Boiling point (^{o}C): 34.7; Physical state: colorless liquid.

Acetonitrile (HPLC grade):- Make: Loba Chemie; Molecular formula (g/mol): C_2H_3N; Molecular weight: 41.05; Specific gravity/density (g/cm^3): 0.982; Boiling point (^{o}C): 81–82; Physical state: colorless liquid.

Glycidyl methacrylate:- Make: Sigma-Aldrich; Molecular formula: $C_7H_{10}O_3$; Molecular weight (g/mol): 142.1546; Specific gravity/density (g/cm^3): 1.07; Boiling point (^{o}C): 189; Physical state: colorless liquid.

Methyl ethyl ketone:- Make: Loba Chemie; Molecular formula (g/mol): C_4H_8O; Molecular weight: 72.11; Specific gravity/density (g/cm^3): 0.805; Boiling point (^{o}C): 79.64; Physical state: colorless liquid.

2,2'-Azobisisobutyronitrile:- Make: AVRA synthesis Pvt. Ltd. Hyderabad, India; Molecular formula: $C_8H_{12}N_4$; Molecular weight (g/mol): 164.21; Specific gravity/density (g/cm^3): 1.1; Melting point (^{o}C): 103–105; Physical state: white crystals.

1,6-hexamethylenediamine:- Make: Koch-light Laboratories Ltd.; Molecular formula (g/mol): $C_6H_{16}N_2$; Molecular weight: 116.20; Specific gravity/density (g/cm^3): 0.84; Melting point (^{o}C): 39-42; Boiling point (^{o}C): 205; Physical state: yellow solid.

D-(-)-Dibenzoyl tartaric acid:- Make: Spectrochem, Mumbai; Molecular formula (g/mol): $C_{18}H_{14}O_8$; Molecular weight: 358.30; Melting point (^oC):154–156; Physical state: White powder; Chiral selector form used: S-isomer (-).

Poly(vinylpyrrolidone) K90 Powder:- Make: Fluka; Molecular formula (g/mol): $(C_6H_9NO)_n$; Molecular weight (g/mol): 360,000; Physical state: white powder.

Salbutamol sulphate:- Make: Neuland Laboratories Ltd., Hyderabad, Andhra Pradesh, India – 500 016; Molecular formula: $C_{13}H_{21}NO_3$; Molecular weight (g/mol): 239.311; Melting point (^oC): 157–158; B.P. (^oC): 433.5; Physical state: white powder; Pharmaceutical form: R-(+) form; Adverse form: S-(-) form (inactive form).

6.2.2. Synthesis of poly(MMA-co-EDMA) and poly(MMA-co-DVB) by suspension polymerization

Suspension polymerization[24] was carried out in a specially designed double walled cylindrical glass reactor equipped with a condenser, nitrogen inlet, and overhead stirrer. Oil (discontinuous) phase comprising monomer (methyl methacrylate), crosslinker (ethylene dimethacrylate/divinylbenzene), initiator (2,2'-azobisisobutyronitrile), and porogen (1,2-dichlorobenzene/1,1,2,2,-tetrachloroethane) were added to the polymerization reactor containing 100 mL of aqueous (continuous) phase of 5 wt% poly(vinylpyrrolidone) as a protective colloid in distilled water with constant stirring speed of 500 rotations per minute. After complete addition of oil phase to the aqueous phase, reactor temperature was raised to 70^{o}C and maintained for 3 h to carry out the polymerization. On completion of the reaction time, product obtained in the form of beads were cooled, filtered, and washed 2–3 times with water, methanol, and dried in oven at 60^{o}C under reduced pressure for 8 h. Copolymers obtained by suspension polymerization were purified in methanol by a soxhlet extractor.[25] Poly(MMA-*co*-EDMA) and poly(MMA-*co*-DVB) having differing CLDs were synthesized. Polymer synthesis is shown in **Schemes 6.1 and 6.2.**

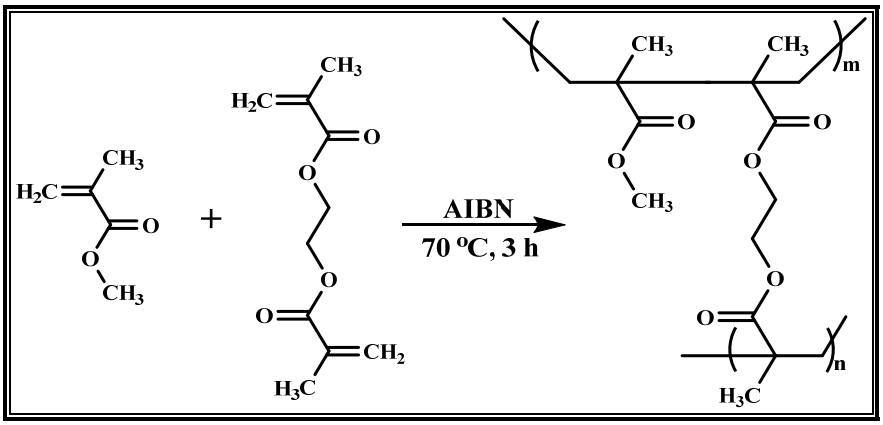

Methyl methacrylate **Ethylene dimethacrylate** **Poly(MMA-*co*-EDMA)**

Scheme 6.1. Synthesis of Poly(MMA-*co*-EDMA) by suspension polymerization

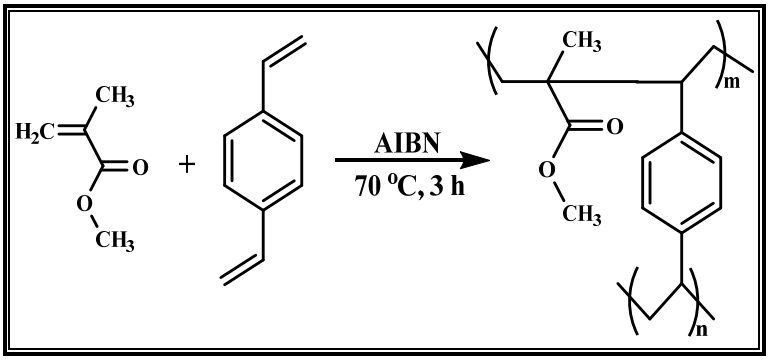

Methyl methacrylate **Divinylbenzene** **Poly(MMA-*co*-DVB)**

Scheme 6.2. Synthesis of poly(MMA-*co*-DVB) by suspension polymerization

6.2.3. Synthesis of poly(glycidyl methacrylate) by solution polymerization

In most of the cases, shell part is always solid in core-shell technology. In the present work, poly(GMA) was used as a shell which was obtained by solution polymerization.[26] To a 250 mL of double walled cylindrical glass reactor, equipped with a mechanical stirrer and thermostat, 20 g of glycidyl methacrylate, 2 mol% of AIBN, 20 mL of methyl ethyl ketone were added and reaction mixture was stirred at 70°C for 5 h. On completion of reaction time, polymeric solution was precipitated in methanol, filtered, and dried in oven under reduced pressure at 60ºC for 8 h.

Molecular weight of poly(GMA) was 24,600 g/mol which was determined by gel permeation chromatography. Shell polymer synthesis is depicted in **Scheme 6.3.**

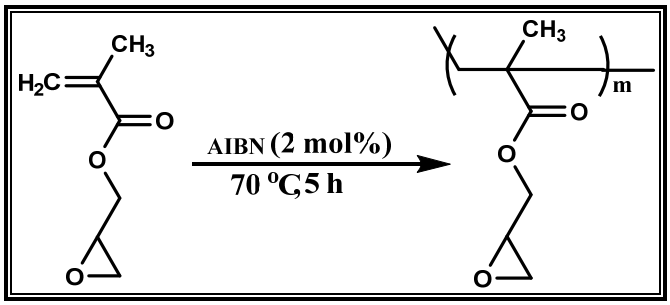

Glycidyl methacrylate **Poly(GMA)**

Scheme 6.3. Synthesis of poly(GMA) by solution polymerization

6.2.4. Synthesis of core-shell polymer

Nowadays, less reactive sites are the major concern with crosslinked (insoluble) polymer support which decreases the efficiency of polymer functionality. Inversely, homopolymer increases the reactive sites but is soluble in number of solvents, consequently, it could not be used as a solid support. To overcome these difficulties, core-shell is one of the ways which increases reactive sites as well as insoluble property. Core-shell[27] polymer was synthesized using high surface area crosslinked polymer as a core obtained by suspension polymerization and homopolymer as a shell obtained by solution polymerization.

In a stoppered conical flask, 5 g of poly(GMA) was weighed. To this, 50 mL of 1,4-dioxane was added. Poly(GMA) solution was placed for 3 days to obtain polymer dissolution. In a stoppered conical flask, 20 g of the crosslinked polymer beads prepared by suspension polymerization were weighed. To this, 40 mL of poly(GMA) in 1,4-dioxane solution was added and placed for 2 days at room temperature. Then, polymers were dried in oven under reduced pressure at 70^{o}C for 24 h to obtain an epoxy coated porous crosslinked beads. Adsorbed poly(GMA) in porous matrix of core polymers (14 g) were further treated with 7 mL of 1,6-hexamethylenediamine solution in methanol (1.47 g of 1,6-hexamethylenediamine was dissolved in 100 mL of methanol) and stirred for 24 h at room temperature to react amino groups with 5%

epoxy functionality available on the surface of the core-shell polymer. Furthermore, this core-shell polymer was washed with methanol. Subsequently, dried in oven under reduced pressure at 60^{o}C for 8 h. Synthesis of core-shell polymer is represented in **Scheme 6.4.**

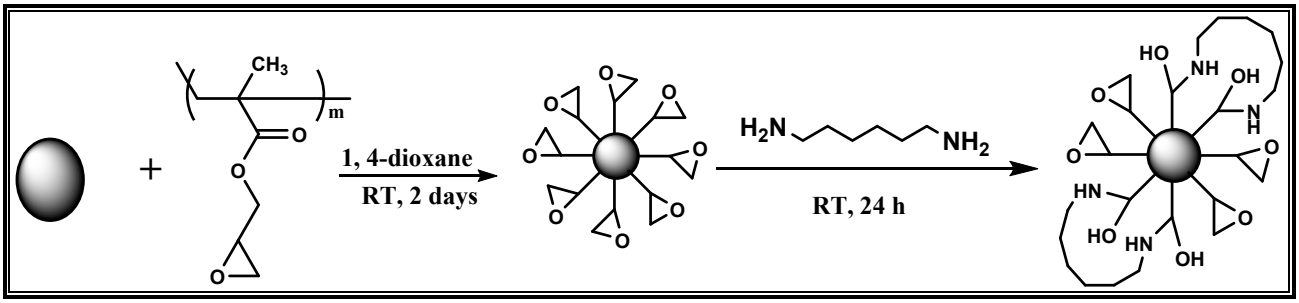

Poly(MMA-*co*-DVB) porous beads **Poly(GMA)** **Adsorption of poly(GMA) in porous poly(MMA-*co*-DVB)** **Core-shell polymer**

Scheme 6.4. Synthesis of core-shell polymer

6.2.5. Core-shell polymer modification with chiral selector D-(-)-dibenzoyl tartaric acid

Core-shell polymer (5 g, 11.81 mmol) was taken in a stoppered conical flask to which D-(-)-dibenzoyl tartaric acid (5.076 g, 14.17 mmol) was dissolved in 10 mL of methanol and reaction flak was placed at ambient temperature for a period of 30 h. On completion of the reaction time, modified polymers were washed with 10 mL of methanol and filtered. Subsequently, polymers were dried under reduced pressure at 60^{o}C for 8 h. Some abbreviations used in the present work are mentioned here. Poly(MMA-*co*-EDMA) was obtained using 1,1,2,2-tetrachloroethane/1,2-dichlorobenzene are abbreviated as **MET** and **MED,** respectively. In another, poly(MMA-*co*-DVB) was obtained using 1,1,2,2-tetrachloroethane/1,2-dichlorobenzene are abbreviated as **MDT** and **MDD,** respectively. Poly(MMA-*co*-DVB) for 200% crosslink density was used as a core polymer is abbreviated as **core.** Adsorption of poly(GMA) on the surface of core polymer is abbreviated as **CE.** Then, epoxy functionality crosslinking of **CE** with 1,6-hexamethylene diamine is abbreviated as **CED.** Covalent modification of **CED** with D-(-)-dibenzoyl tartaric acid is abbreviated as **CEDB.** Synthesis of core-shell polymer supported D-(-)-dibenzoyl tartaric acid is depicted in **Schemes 6.5.**

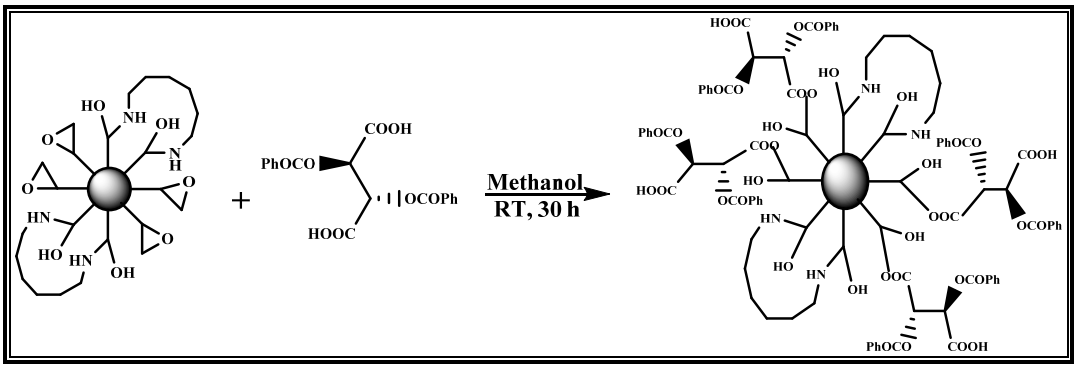

Core-shell polymer **D-(-)-dibenzoyl tartaric acid** **Core-shell polymer supported D-(-)-dibenzoyl tartaric acid**

Scheme 6.5. Synthesis of core-shell polymer supported D-(-)-dibenzoyl tartaric acid

6.2.6. Characterization

Polymers obtained by suspension polymerization, purified by soxhlet extraction and dried at 60^{o}C under reduced pressure for 6 h were used for characterization. FT-IR spectra were recorded on Perkin Elmer instrument wherein number of scans was 10 with 4 cm^{-1} resolution and 1 interval. Model was Spectrum GX. Polymer surface area was determined by NOVA 2000e, Quantachrome instruments, Boynton, FL-33426. Average particle sizes were determined using an Accusizer 780 (Model: LE 2500-20) PSS.NICOMP Particle sizing system, Santa Barbara, California, USA. Molecular weight of poly(GMA) was evaluated in chloroform using a gel permission chromatography (Viscotek 200 + RALLS, Model-Viscotek model 250, Column-3X mix B). External morphology and particle size visualization was analyzed by scanning electron microscope (Quanta 200 3D, dual beam ESEM microscope). Electron source was thermionic emission tungsten filament. ^{13}C NMR spectra of core-shell polymer and its modification with chiral selectors were recorded in adamantane ($C_{10}H_{16}$) as an internal standard (JEOL-400 MHz). An enantiomeric excess was determined by high performance liquid chromatography (Alliance, Waters e2695 separations module) and detector was waters 2998 photodiode array detector. Epoxy content was evaluated by HCl in dioxane method whereas acid content was determined by KOH in methanol method, titrimetrically.

6.3. Results and discussion

Monomer-crosslinker feed composition used for reaction is tabulated in **Table 6.1.** Concentration of monomer and crosslinker at different crosslink density (CLD) were determined by **equation (3.1).**

Table 6.1. Monomer-crosslinker feed composition of polymers synthesized by suspension polymerization at different crosslink density

Monomer system	Units	Crosslink density (%)					
		25	50	75	100	150	200
MMA:EDMA	mol	0.049: 0.015	0.042 :0.020	0.032 : 0.024	0.027 : 0.027	0.021: 0.031	0.017: 0.033
	g	4.921: 2.923	4.236 : 3.955	3.234 : 4.803	2.717 : 5.379	2.086 : 6.114	1.657: 6.561
MMA:DVB	mol	0.056: 0.014	0.045 : 0.022	0.037 : 0.028	0.032 : 0.032	0.025: 0.038	0.020 : 0.041
	g	5.649 : 1.836	4.515 : 2.935	3.760 : 3.667	3.222 : 4.189	2.504 : 4.884	2.048 : 5.326

Reaction conditions: Batch size: 8 mL; 2,2'-azobisisobutyronitrile: 2.5 mol%; stirring speed: 500 rpm; reaction time: 3 h; outer phase: H_2O; protective colloid: poly(vinylpyrrolidone); protective colloid concentration: 5 wt%; porogen: 24 mL (monomer: porogen ratio, 1:3 v/v); temp.: 70^oC.

6.3.1. Fourier transform infrared (FT-IR) spectroscopy

FT-IR spectroscopy is a well-established technique to confirm polymer synthesis (insoluble solid samples) and their modification. FT-IR analysis was carried out using Perkin Elmer (spectrum GX) instrument. FT-IR samples were prepared in the form of KBr pellet after drying the sample

at 80 °C under reduced pressure for 8 h. FT-IR spectrum (cm^{-1}) demonstrated the peak of core polymer at 1731 (–C(O)–C), 797 (aromatic C–H out-of-plane bending), 905 (disubstituted benzene) and 835 (para disubstituted benzene ring).[29] In addition to the core polymer peaks, core-coated poly(GMA) (CED) and core–shell (CE) polymer revealed the appearance of confirmative peaks. FT-IR spectrum of core-coated poly(GMA) illustrated the appearance of peaks at 907 and 840 (epoxy C–O bonds) while 2990–2854 (C–H sym. and asymm. str. vib.). Moreover, core–shell polymer showed the peak at 3628 and 795 (N–H), 1149 (C–N str.) whereas 907 and 840 (epoxy str.). Presence of these confirmative peaks strongly support to successful synthesis of core–shell polymer. Synthesis of the core polymer, core-coated poly(GMA) (CED), and core–shell polymer (CE) were confirmed by FT-IR spectroscopy (KBr pellet) and depicted in **Figure 6.1.**

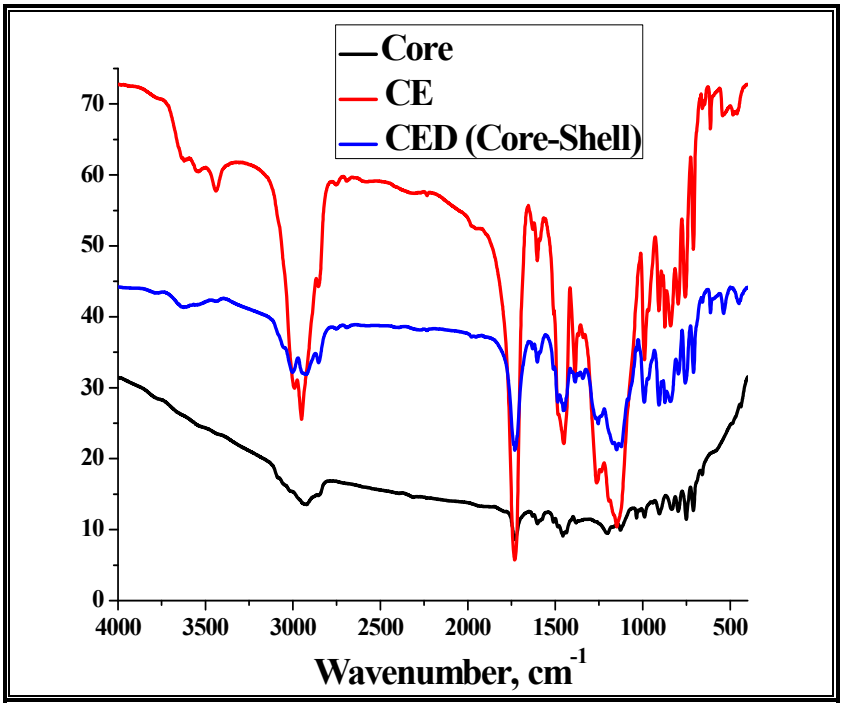

Figure 6.1. FT-IR spectrum of core, CE, and CED polymers

FT-IR spectrum (KBr pellet, cm^{-1}) of polymer supported D-(-)-dibenzoyl tartaric acid (CEDB) revealed the peak at 1733 which confirms that ester and acid are overlapped with peak broadening, 904 corresponds to the presence of disubstituted benzene and not for the epoxy stretching.[29] Presence of –OH of carboxylic acid is indicated by 1453. Besides, 3625 assigned for

the presence of –OH bend group. However, an absence of peak at 907 indicates the absence of epoxy functionality after chiral selector modification. FT-IR spectrum of D-(-)-dibenzoyl tartaric acid modified polymer is represented in **Figure 6.2.**

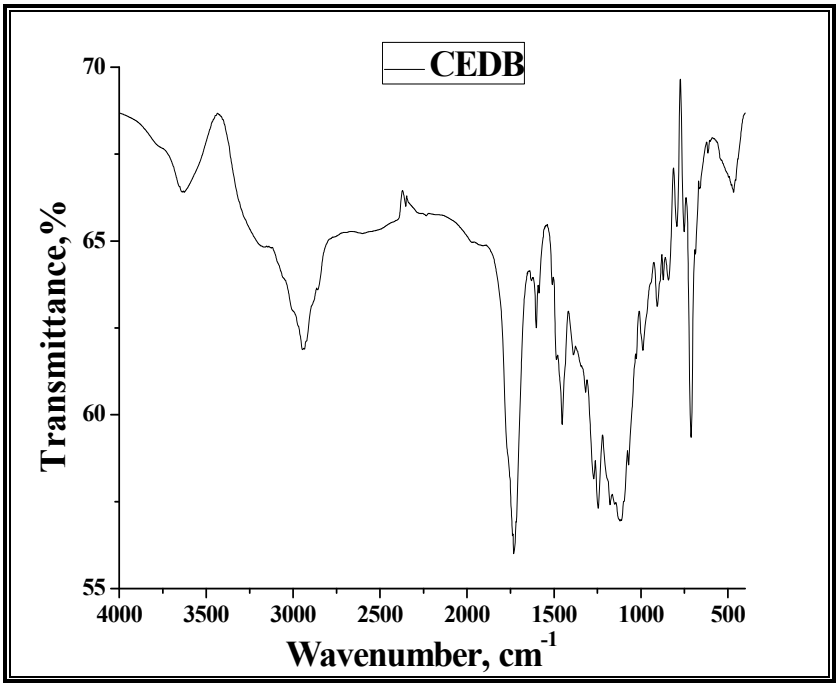

Figure 6.2. FT-IR spectrum of CEDB polymer

6.3.2. ^{13}C solid state NMR spectroscopy

Synthesis of core-shell polymer and its modification were confirmed by FT-IR spectroscopy. Moreover, ^{13}C NMR is also one of the most important tools to confirm polymer synthesis in case of solid/insoluble samples. ^{13}C solid state NMR of 400 MHz was used for analysis of base, CE, CED, and CEDB samples. In most cases, ^{13}C spectra were recorded in adamantane ($C_{10}H_{16}$) as an internal standard[30] containing two carbon peaks (29.23, 40.89 ppm). ^{13}C NMR ($C_{10}H_{16}$, 400 MHz): base (core) polymer containing peaks of methyl methacrylate and divinylbenzene, MMA: δ 17.9, 51.28, 145.83, 177.78; DVB: δ 113.46, 128.42, 138.07; CE: δ 17.01, 67.77; CED: δ 16.95, 67.89; and CEDB: δ 67.65, 73.02, 166.42. ^{13}C NMR spectrum of core polymer, CE, and CED (core-shell) is represented in **Figure 6.3,** whereas core-shell polymer supported D-(-)-dibenzoyl tartaric acid (CEDB) is represented in **Figure 6.4.**

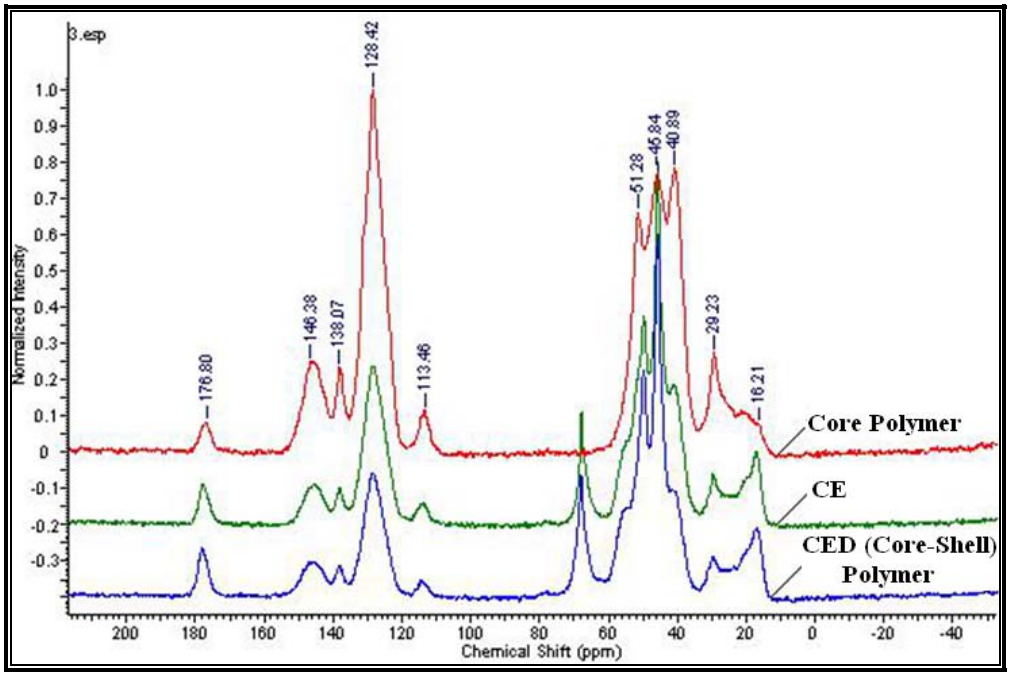

Figure 6.3. Solid state ^{13}C NMR ($C_{10}H_{16}$, 400 MHz) spectra of core, CE, and CED polymers

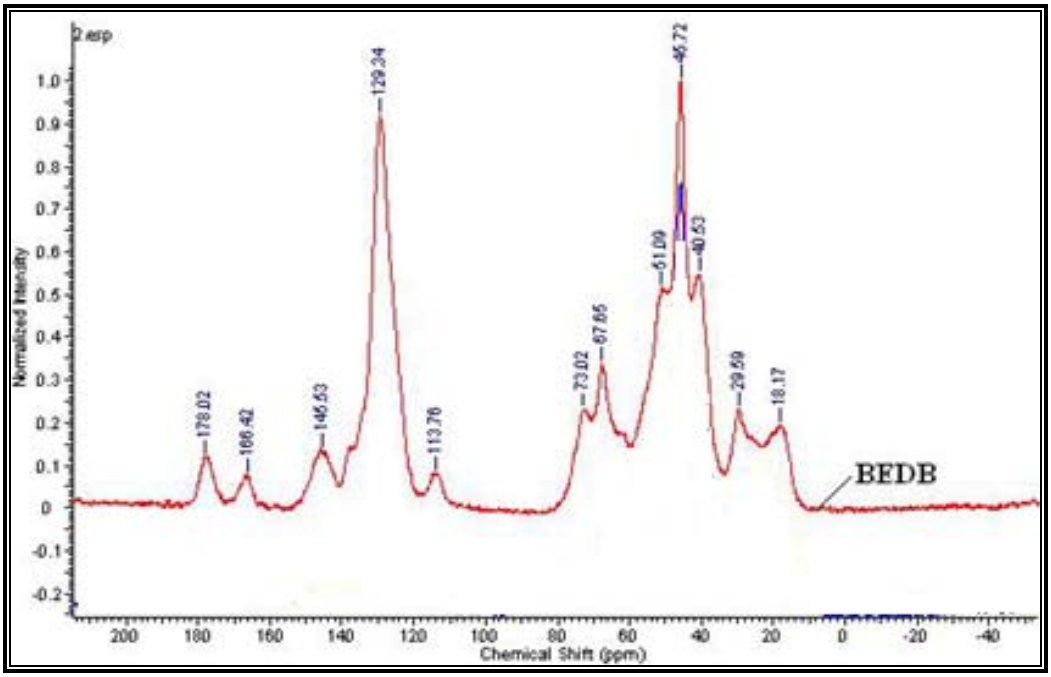

Figure 6.4. Solid state ^{13}C NMR ($C_{10}H_{16}$, 400 MHz) spectrum of CEDB polymer

6.3.3. Surface area

Surface area is the most important parameter that attributes to polymer efficiency. However, effects of several parameters were studied as a function of crosslinker, concentration of crosslinkers, and type of porogens on surface area of polymer. Crosslinkers (ethylene dimethacrylate/divinylbenzene) and porogens (1,1,2,2-tetrachloroethane/1,2-dichlorobenzene) were selected. Three types[31] of porogens can be used to generate the surface area in the polymer. i.e. solvating (SOL), non-solvating (NONSOL), and polymeric (POLY) porogen. Surface area varies according to type of porogen. Mostly, SOL porogen is used to generate the high surface area polymers. Generally, surface area decreased by porogens in the sequences of SOL, NONSOL, to POLY porogens.

6.3.3.1. Effect of crosslinkers

Four different series of methyl methacrylate monomer were obtained using two different crosslinkers (EDMA/DVB) and two different porogens (1,1,2,2-terachloroethane/1,2-dichlorobenzene). Crosslinker is the major parameter that attributes to polymer properties like surface area and particle size. Surface area was increased with increase in crosslink density (CLD).[32] Polymer series MET, MDT, and MDD revealed an increased surface area with increasing crosslink density. However, MED series demonstrated the decreased surface area after 100% crosslink density. This is possibly due to the polar EDMA crosslinker and less polar 1,2-dichlorebenzene porogen pass through a critical concentration ratio which allowed to decrease the surface area. Interestingly, it was observed that, polymer containing divinylbenzene crosslinker displayed the higher surface area than polymer containing ethylene dimethacrylate as a crosslinker. Both, MDT and MDD have higher surface area than MET and MED series. This is due to the polar and hydrophilic property of EDMA has more affinity towards an aqueous phase whereas DVB has more affinity towards an organic phase. This is because of solubility of ethylene dimethacrylate in water (1.086 g/L) is much higher than solubility of divinylbenzene (0.005 g/L) at 20^{o}C. This causes due to compatibility of DVB with organic phase resulting high surface area polymer whereas EDMA has compatibility with aqueous phase resulting lower surface area polymer. This phenomenon creates an interfacial tension[33,34] between aqueous and organic phase. Nevertheless, interfacial tension for MMA-EDMA is lower than MMA-DVB

monomer system. Notably, highest surface area obtained in the present work is 554 m^2/g with poly(MMA-*co*-DVB) for 200% crosslink density and this high surface area polymer was used as a core polymer in the present study.

6.3.3.2. Effect of porogen

Recently, Clarisse *et al.*[35] reported the surface area of poly(MMA-*co*-DVB) using the mixture of porogens. However, present study revealed the higher surface area with a single porogen instead of mixture of porogens. Poly(MMA-*co*-DVB) revealed the high surface area with 1,2-dichlorobenzene than 1,1,2,2-tetrachloroethane. Maximum surface area was observed in MDD series, 554 m^2/g, while for MDT series, it was 333 m^2/g for 200% crosslink density. In the case of poly(MMA-*co*-EDMA), maximum surface area was obtained with 1,1,2,2-tetrachloroethane than 1,2-dichlorobenzene. Thus, MET series displayed the higher surface area of 253 m^2/g whereas MED series exhibited 121 m^2/g for 200% crosslink density. Surface area of core polymers is shown in **Table 6.2** and **Figure 6.5.**

Table 6.2. Surface area of poly(MMA-*co*-EDMA) and poly(MMA-*co*-DVB) at different crosslink density

Copolymer	Polymer code	Crosslink density (%)					
		25	50	75	100	150	200
Poly(MMA-*co*-EDMA)	MET	41.5	69.6	164.4	171.8	248.5	253.5
	MED	2.84	153.0	159.8	435.6	129.9	121.2
Poly(MMA-*co*-DVB)	MDT	2.82	77.70	120.0	155.6	255.6	333.2
	MDD	146.2	168.1	271.9	489.5	536.1	554.9

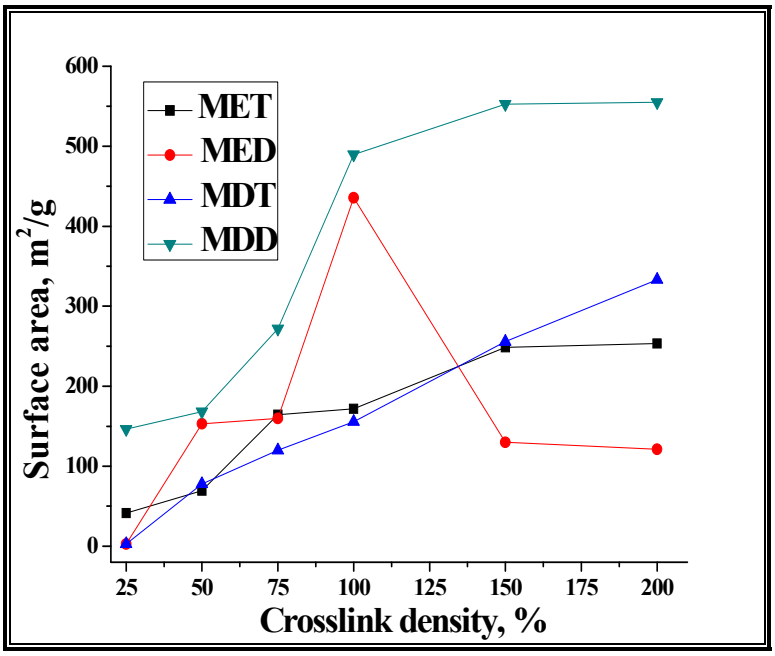

Figure 6.5. Surface area of poly(MMA-*co*-EDMA) and poly(MMA-*co*-DVB) for different crosslink density

Surface area of core polymer selected for core-shell approach was 554 m^2/g while polymer surface area after poly(GMA) shell adsorption was 410 m^2/g. This decrease in surface area from 554 to 410 m^2/g is due to poly(GMA) adsorption. Core-shell polymer implied the surface area of 332 m^2/g. Thus, surface area again decreased from 410 to 332 m^2/g mainly due to crosslinking of epoxy functionality. Besides, core-shell polymer supported D-(-)-dibenzoyl tartaric acid demonstrated the surface area of 262 m^2/g. In fact, this decrease[36] in surface area is due to the covalent modification of a core-shell polymer with chiral selectors.

6.3.4. Porosity determination

Pore volume is a measure of fraction of the volume of voids over the total volume of polymer matrix. Porosity is also one of the most crucial parameter for core polymer that significantly influences to shell immobilization. Result illustrated that, higher crosslink density polymers have more pore volume as well as porosity. Interestingly, pore volume revealed a similar observation like surface area result. Notably, highest pore volume was observed with MDD series followed by MDT, MED, and MET series. This is because of crosslinker (DVB) and

porogen (1,2-dichlorobenzene) have comparatively less hydrophilic property and more affinity towards an organic phase that allowed increasing pore volume resulting in higher porosity in MDD series. However, more hydrophilicity of crosslinker (EDMA) and porogen (1,1,2,2-tetrachloroethane) decreased the pore volume as well as porosity due to more affinity towards an aqueous phase. Owing to much higher surface area (554 m^2/g), pore volume (1.44 cc/g) and porosity (64.85%) of MDD polymer for 200% crosslink density was selected as a core polymer. This is because of high surface area and porosity of core polymer substantially attributes to core-shell polymer efficiency. In addition, core-shell polymer demonstrated the higher pore volume (1.06 cc/g) and porosity (41.99%) which illustrated the transcendent porous properties of core-shell polymer matrix. The pore volume and porosity of the core polymer synthesized by suspension polymerization for 25 and 200% crosslink density are illustrated in **Table 6.3.**

Table 6.3. Pore volume (cc/g) and porosity (%) of poly(MMA-*co*-EDMA) and poly (MMA-*co*-DVB) at different CLD

Polymer code	MET		MED		MDT		MDD	
Crosslink density (%)	25	200	25	200	25	200	25	200
Pore volume (cc/g)	0.75	0.75	0.66	0.75	0.55	0.84	0.57	1.44
Porosity (%)	50.9	55.1	50.5	60	39.5	51.3	39.4	64.9

6.3.5. Particle size distribution

Generally, suspension polymerization is well-known polymerization method to obtain the polymer having particle size is in the range of 5–200 μm. Various parameters like crosslinkers and porogens significantly affects to the particle size. Obviously, solvating porogens are able to impart small sized particles compared with non-solvating porogens. In the present study 1,1,2,2-tetrachloreethane and 1,2-dichlorobenzene were used as a solvating porogens. Average particle size of poly(MMA-*co*-EDMA) and poly(MMA-*co*-DVB) synthesized at 70^oC for 3 h were studied as a function of crosslink densities, crosslinkers, and porogens.

The result clearly showed that, particle size was slightly increased with increasing crosslink density.[37,38] Remarkably, average particle size of the polymers synthesized by suspension polymerization were in the range of 15 – 70 μm. There is small difference in average particle size with respect to crosslinker and porogen. Both, poly(MMA-*co*-EDMA) and poly(MMA-*co*-DVB) series displayed the larger particle sizes with dichlorobenzene than tetrachloroethane porogen. Polymer containing divinylbenzene revealed the larger average particle size with same monomer (methyl methacrylate) and porogen (1,1,2,2-tetrachloroethane/1,2-dichlorobenzene). Indeed, DVB has more compatibility with 1,2-dichlorobenzene than 1,1,2,2-tetrachloroethane resulting smaller particles size in MDD series and larger particle size in MDT series. However, poly(MMA-*co*-EDMA) elucidated the higher average particle size than poly(MMA-*co*-DVB). Average particle size of polymer is illustrated in **Table 6.4** and **Figure 6.6.**

Table 6.4. Average particle size of poly(MMA-*co*-EDMA) and poly(MMA-*co*-DVB) at different crosslink density

Copolymer	Polymer code	Crosslink density (%)					
		25	50	75	100	150	200
Poly(MMA-*co*-EDMA)	MET	17.45	25.25	26.42	31.99	42.70	63.27
	MED	22.88	26.84	34.26	36.73	37.07	48.73
Poly(MMA-*co*-DVB)	MDT	18.60	27.21	28.45	30.75	39.17	42.21
	MDD	18.16	18.78	20.35	24.66	29.51	33.39

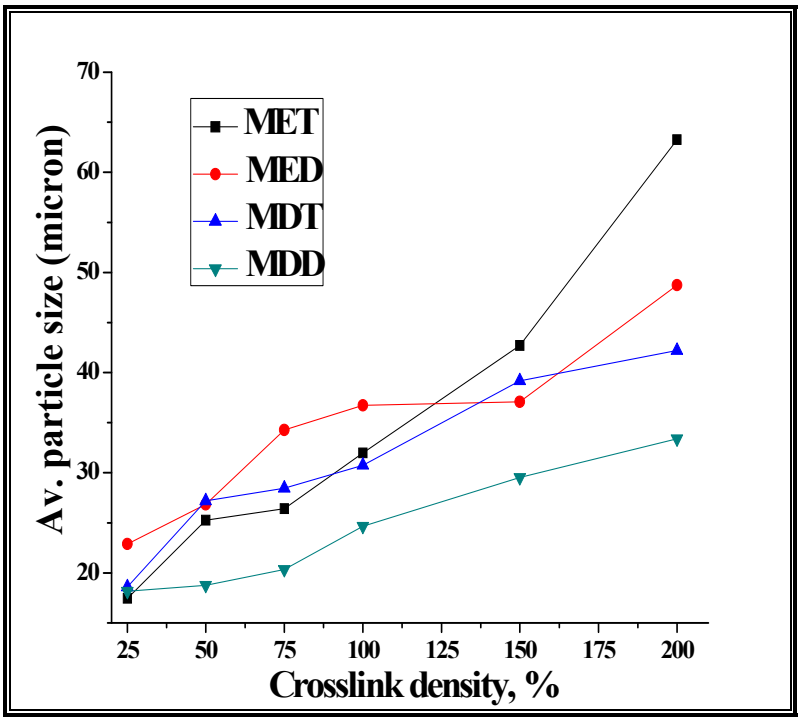

Figure 6.6. Average particle size of poly(MMA-*co*-EDMA) and poly(MMA-*co*-DVB) for different crosslink density

6.3.6. Titrimetric determination of epoxy and acid content

Epoxy content (EC) of core-shell polymers were analyzed for quantitative determination of epoxy functionality. EC determines the polymer reactivity which attributes for polymer efficiency. Epoxy content[39] of adsorbed poly(GMA) (before crosslinking) was determined using HCl-dioxane method, titrimetrically and it was 2.48 mmol/g. Subsequently, core-shell polymer was obtained and dried at 60^{o}C for 6 h. Epoxy content (after crosslinking) of these polymers were evaluated by titrimetric determination. Epoxy content of dried core-shell polymer was evaluated to be 2.35 mmol/g, titrimetrically. These core-shell polymers were used for modification with chiral selectors as aforementioned in experimental section 6.2.5. Later on, acid content[40] of polymer supported chiral selector was determined by KOH in methanol, titrimetrically. The observed acid content was 1.70 mmol/g. This characterized core-shell polymer supported chiral selector was used for racemic drug resolution using 1:0.9 chiral

selector to drug (mmol) ratio. Quantitative determination of epoxy and acid content are tabulated in **Table 6.5.**

Table 6.5. Epoxy and acid content determination by titrimetric method

Content determined	Epoxy/Acid content (mmol/g)
Epoxy content (before crosslinking)	2.48
Epoxy content (after crosslinking)	2.35
D-(-)-dibenzoyl tartaric acid	1.70

6.3.7. Scanning electron microscopy: external morphology study

Scanning electron microscopy (SEM) images is the visual observation tool that helps to confirm size, shape, porosity, and modification of beads (morphology). SEM images were scanned under 500X magnification. Figure **a** describes the SEM image of poly(MMA-*co*-DVB) core polymer beads prepared by suspension polymerization. It was observed that, spherical, quite smooth and non-agglomerated beads were formed.[41] Figure **b** describes the SEM image of core polymer coated with poly(GMA), and remarkable observation is that, SEM clearly demonstrated the surface of core is covered with thin layer of poly(GMA) in the form of ring. Figure **c** illustrated the SEM image of core-shell polymer beads crosslinked with 1,6-hexamethylenediamine. However, it was clearly observed that polymer beads were agglomerated and coupled together. Interestingly, this morphology is obviously different than Figures **a** and **b** due to the covalent modification. Figure **d** describes the SEM image of modified core-shell polymer with chiral selector D-(-)-dibenzoyl tartaric acid which also revealed the polymer beads are conglomerated, coupled together, and observed in clusters. In the present study, solvating porogens were used to obtain methyl methacrylate copolymer. It was observed that, polymer obtained from solvating porogen acquired a high surface, spherical and non-conglomerated beads. However, non-solvating porogen is able to impart[9,42] non-spherical and conglomerated properties to the polymer. Overall, it can conclude that, before modification, polymeric beads are spherical and isolated whereas modified polymeric beads also have spherical shape but are slightly conglomerated. SEM images of base and modified polymers are represented in **Figure 6.7 (a-d).**

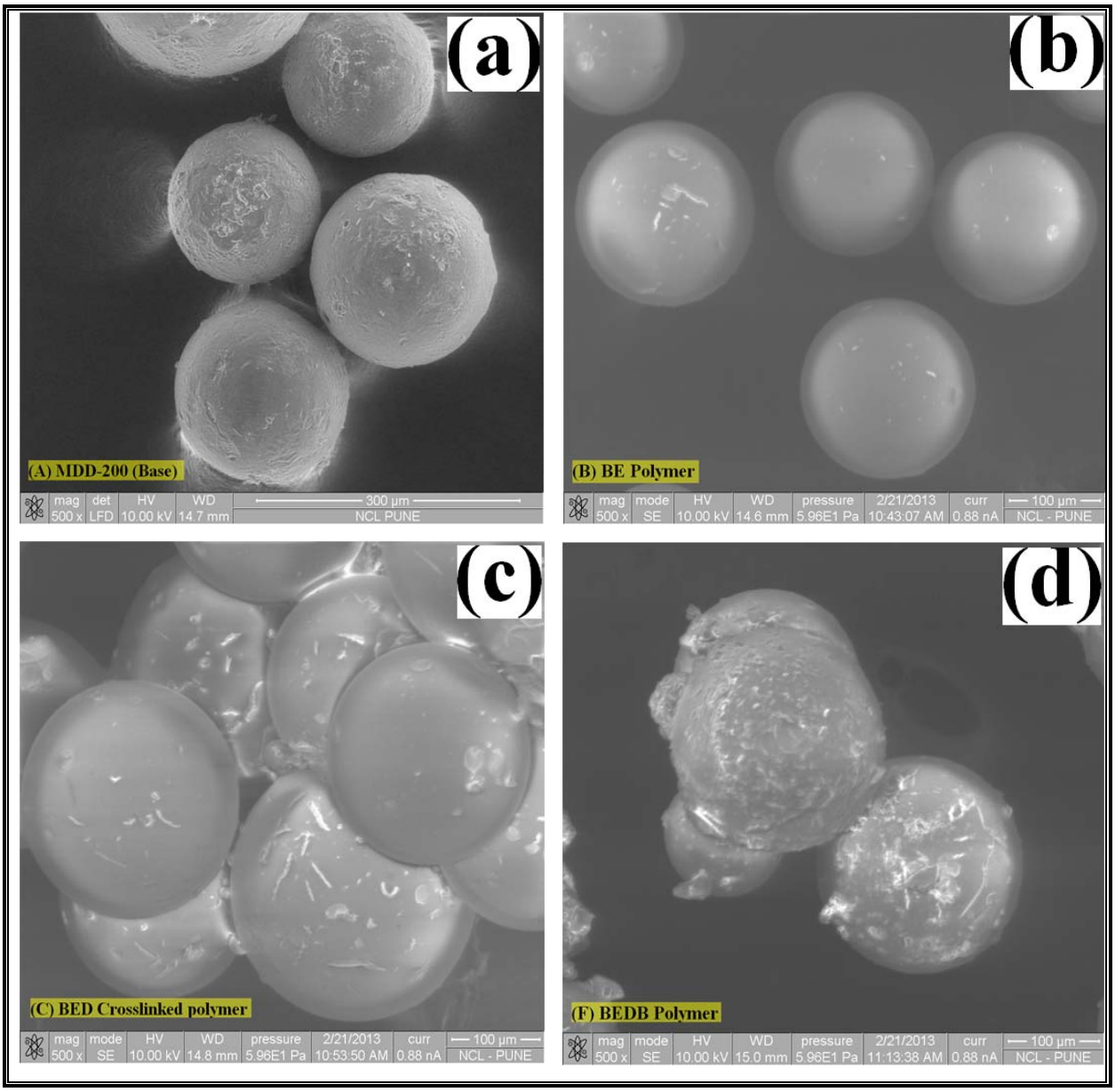

Figure 6.7. Scanning electron micrographs of (a) core, (b) CE, (c) CED, and (d) CEDB polymers

6.3.8. Enantiomeric excess determination by high performance liquid chromatography

Number of drugs is existed in the form of racemic mixture. Unfortunately, racemic drug contains one isomer resides therapeutically activity while opposite isomer may be pharmacologically inactive or produces worst effect. As a result, it is an essential to make the

drug optically pure. Obviously, polymer supported chiral selector is the major tool to make drug optically pure. Drug can be made chirally pure by different techniques like capillary electrophoresis (CE), high performance liquid chromatography (HPLC), and so on. Mostly, HPLC is a widely used technique. There are two main approaches for chiral HPLC analysis, direct and indirect. In the present investigation, direct approach was used to analyze enantiomeric excess of salbutamol drug for a period 24 h. D-(-)-dibenzoyl tartaric acid was selected as a chiral selector for racemic drug resolution. This polymer supported chiral selector was used to resolve a racemic drug, (±)-salbutamol. Concentration of chiral selector to drug ratio was 1:0.9 mmol as reported in **Table 6.6.**

Table 6.6. Polymer supported chiral selector to drug ratio used for drug resolution

Chiral selectors	Chiral selectors, (1 mmol/g)	(±) Salbutamol (g) (0.9 mmol /g)
D-(-)-dibenzoyl tartaric acid	1.70	0.5489 (1.53)

This study was carried out for a period of 24 h to analyze the efficiency of D-(-)-dibenzoyl tartaric acid. Number of factors attributes to transient diastereomer formation between racemic drug and polymer supported chiral selector such as drug solubility, transient diastereomer stability and an adsorption characteristics between chiral selector and drug.[43] Core-shell polymer supported 'S' isomer of chiral selector (1 g) was allowed to interact with racemic salbutamol drug solution in methanol. The 'S' isomer of chiral selector forms three point interaction with 'S' isomer of racemic drug allowing more stable transient diastereomer formation.[44] Inversely, 'S' isomer of chiral selector forms two point interaction with 'R' isomer of drug allowing less stable transient diastereomer formation resulting into an enantiomeric excess of 'R' isomer of the racemic drug. Due to this reason, salbutamol revealed the enantiomeric excess of 'R' isomer. Drug enantiomeric excess at different time intervals were analysed using high performance liquid chromatography for a period of 24 h. Mobile phase[45] MeOH:ACN:AA:TEA (93:7:0.045:0.055) was used for the resolution of racemic salbutamol. In case of salbutamol, 'R' enantiomer elutes at a retention time of 11.99 min followed by 'S' isomer at 15.33 min.[46] **Figure 6.8** demonstrated that, salbutamol revealed the exponentially increase in an enantiomeric excess (ee, 52%) for a period of 24 h. This is probably due to more number of

loosely bound lone pair and π electrons in DBTA make interaction in addition to three point interaction between chiral selector and drug. Enantiomeric excess of salbutamol using polymer supported D-(-)-dibenzoyl tartaric acid is illustrated in **Table 6.7** and depicted in **Figure 6.8.**

Table 6.7. Enantiomeric excess of (±) salbutamol using polymer supported chiral selector

Time, h	Core-shell polymer supported D-(-)-DBTA
	ee (%)
0	0
2	19.69
6	21.95
12	30.30
24	52.13

HPLC conditions: Chiral selector – D-(-)-dibenzoyl tartaric acid, chiral selector**:** drug ratio – 1:0.9 mmol, column – Chirobiotic T (Teicoplanin), mobile phase (v/v) – MeOH**:**ACN**:**AA**:**TEA (93**:**7**:**0.045**:**0.055), flow rate – 1 mL/min, wavelength – 270 nm.

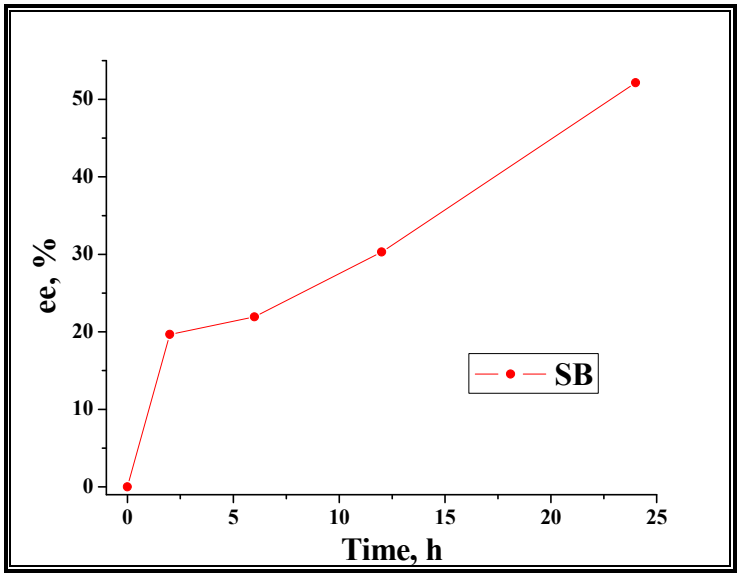

Figure 6.8. Enantiomeric excess of (±)-salbutamol

6.4. Conclusion

In conclusion, core-shell polymer was successfully obtained as a support to be used as chiral selector with enhanced polymer properties. The core-shell polymer increased the reactive sites yielding higher polymer efficiency that formed as a support material. It is worth noting that, core polymer was obtained having high surface area (554 m^2/g) that substantially attribute to more coating of shell polymer onto the surface of core polymer. Despite of insoluble, more reactive, uniform, spherical, and high surface area, evaluated epoxy content of core-shell polymer was 2.35 mmol/g. Core-shell polymer revealed the high surface area (332 m^2/g), pore volume (1.056 cc/g), and porosity (41.99%) which led to higher polymer efficiency. Overall, synthesized core-shell polymers have high reactivity, surface area, and porosity. SEM images strongly support to the spherical nature of core-shell polymer with slight conglomeration. Racemic salbutamol was resolved using core-shell polymer supported D-(-)-dibenzoyl tartaric acid as a chiral selector over a period of 24 h. It is noteworthy that, D-(-)-dibenzoyl tartaric acid demonstrated the exponential increase in enantiomeric excess even in 24 h (52%). This implied the better efficiency of tartaric acid derivatives as a chiral selector. Moreover, reactive core-shell polymer attributes to more loading of catalysts, reactants, substrate, photosensitizer, resolving agent, and chelating agent for applications in solid phase synthesis and biomedical perspectives. Thus, highly reactive, more surface area and excellent porosity of core-shell polymer was obtained. Owing to recover, recycle, and reuse properties of the core-shell polymer support, its use becomes industrially economical and environmentally benign.

References

[1] Guillier F., Orain D. and Bradley M., Review, *Chem. Rev.,* 2000, **100,** 2091–2157.

[2] Ley S.V., Baxendale I. R., Brusotti G. M., Caldarelli M., Massi A. and Nesi M., Review *IL Farmaco,* 2002, **57,** 321–330.

[3] Malachowski L., Stair J. L. and Holcombe J. A., *Pure Appl. Chem.*, 2004, **76(4),** 777–787.

[4] Clapham B., Reger T. S. and Janda, K. M., *Tetrahedron,* 2001, **57,** 4637–4662.

[5] Kim B. M. and Sharpless K. B., *Tetrahedron Lett.,* 1990, **31(21),** 3003–3006.

[6] Oehme I., Prattes S., Wolfbeis O. S. and Mohr G. J., *Talanta,*1998, **47,** 595–604.

[7] Baker G. L., Fritschel S.C., Stille J. R. and Stille J. K., *J. Org. Chem.,* 1981, **46,** 2954–2960.

[8] Gubitz G. and Schmid M. G., Review *Electrophoresis,* 2004, **23,** 3981–3996.

[9] Todorovic Z. S., Nikolic L. B., Nikolic V. D., Vukovic Z. M., Mladenovic-Ranisavljevic I. I. and Takic L. M., *Adv. Technol.,* 2012, **1(2),** 11–19.

[10] Patocka J. and Dvorak A., *J. Appl. Biomed.,* 2004, 95–100.

[11] Sekhon B. S., *Int. J. Pharm. Tech. Res.,* 2010, **2(2),** 1584–1594.

[12] Pickering P. J., and Chaudhuri J. B., *Chirality,* 1997, **9,** 261–267.

[13] Kuhn R., Stoecklin F. and Erni F., *Chromatographia,* 1992, **33(1/2),** 32–36.

[14] Aturki Z., Desiderio C., Mannia L. and Fanali S., *J. Chromatogr. A,* 1998, **17,** 91–104.

[15] Wang H., Gu J. L., Hu H. F., Dai R. J., Ding T. H. and Fu R. N., *Anal. Chem. Acta,* 1998, **359,** 39–46.

[16] Arai T., Ichinose M., Kuroda H. and Kinoshita T., *Anal. Biochem.,* 1994, **217,** 7–11.

[17] Cole R. O., Sepaniak M. J. and Hinze W. L., *J. High Resolut. Chromatogr. A,* 1990, **13(8),** 579–582.

[18] Gassman E., Kuo J. E. and Zare R. N., *Science,* 1985, **230,** 813–814.

[19] Armstrong D. W., Gasper M. P. and Rundlett K. L., *J. Chromatogr. A,* 1995, **689,** 285–304.

[20] Wei Y., Li J., Zhu, C., Hao A. and Zhao M., *Anal. Sci.,* 2005, **21,** 959–962.

[21] Lin J. M., Nakagama T., Uchiyama K. and Hobo T., *Chromatographia,* 1996, **43(11),**

585–591.

[22] Aboul-enein H.Y., and Islam, M. R., *J. Liq. Chromatogr.,* 1991, **14(4),** 667–673.

[23] Poller U., Fuchs B., Gorf A., Jakubetz J., Radke J., Ponicke K. and Brodde O. E., *Cardiovasc. Res.,* 1998, **40,** 211–222.

[24] Lu L., Jiang C., Xiufang, W., Pihui P. and Zhuoru, Y., *Chinese J. Chem. Eng.,* 2006, **14(4),** 471–477.

[25] Paukkeri R. and Lehtinen A., *Polymer,* 1994, **35(8),** 1673–1679.

[26] Ravve A. and Khamis J. T., *J. Macromol. Sci. Chem.,* 1967, **Al (8),** 1423–1431.

[27] Jin L., Deng Y., Hu J. and Wang C., *J. Polym. Sci: Part A: Polym. Chem.,* 2004, **42,** 6081–6088.

[28] Safa K. D., Bahadori A., Tofangdarzadeh S. and Nasirtabrizi M. H., *J. Iran. Chem. Soc.,* 2008, **5(1),** 37–47.

[29] Bartholin M., *Makromol. Chem.,* 1981, **182,** 2075–2085.

[30] Morcombe C. R. and Zilm, K. W., *J. Magn. Reson.,* 2003, **162,** 479–486.

[31] Seidl J., Malinsky J., Dusek K. and Heitz W., *Adv. Polym. Sci.,* 1967, **5(2),** 113–213.

[32 Kotha A., Rajan C. R., Ponrathnam S., Kumar K. and Shewale J. G., *Appl. Biochem. Biotechnol.,* 1998, **74,** 191–203.

[33] Okay O., *Prog. Polym. Sci.,* 2000, **25,** 711–779.

[34 Donahue D. J. and Bartell F. E., *J. Phys. Chem.,* 1952, **56(4),** 480–484.

[35] Clarisse M., Queiros Y., Barbosa C., Barbosa L. and Lucas E., *Chem. Chem. Tech.,* 2012, **6(2),** 145–152.

[36] Norzilah A. H., Fakhru'l-Razi A., Choong T. S. Y. and Chuah A. L., *J. Nanomater.,*

2011, **495676,** 1–18.

[37] Gooch, J. W., Emulsification and polymerization of alkyd resins. Springer, 2002, **XXII,** PP. 28.

[38] Gong T. and Wang C. C., *J. Mater. Sci.,* 2008, **43,** 1926–1932.

[39] Vogel A. I., Elementary practical organic chemistry part III quantitative organic analysis, CRC press, Lond., 1958, **XXXVIII, 2,** PP. 825–826.

[40] Vogel A. I., Elementary practical organic chemistry part III quantitative organic analysis, CRC press, Lond., 1958, **XXII.2,** PP. 711–712.

[41] Hwang M. L., Lee Y. S., Kim T. G., Yang G. G., Park T. S. and Lee Y. S., *Bull. Korean Chem. Soc.,* 2010, **31(8),** 2395–2398.

[42] Yu S., Ng F. L., Ma K. C. C., Mon A. A., Ng F. L. and Ng Y. Y., *J. Appl. Polym. Sci.,* 2013, **127,** 2641–2647.

[43] Chankvetadze B., Capillary electrophoresis in chiral analysis, *John Wiley and Sons,* 1997, **Chapter 2,** 74.

[44] Sahoo S. C., and Ray M., *Chem. Eur. J.,* 2010, **16,** 5004–5007.

[45] Carlsson E., Wikstrom H. and Owens R. K., *Chromatographia,* 2001, **53,** 419–424.

[46] Luo W., Zhu L., Deng J., Liu A., Guo B., Tan W. and Dai R., *J. Pharm. Biomed. Anal.,* 2010, **52,** 227–231.

DRUG ADSORPTION STUDY

7.1. Introduction

Much attention has been paid on gold nanoparticle research related to biomedical applications.[1–5] Gold stabilized on high surface area as well as hydrophilic polymer has received an attractive area of research. Due to higher electronegativity of gold than any other transition metal, polymer supported gold was used for drug loading kinetics evaluation.[6–8] Other factors attribute to drug loading are porosity, particle size, surface area, as well as polymer reactivity. Polymer supported gold currently used for biomedical applications especially has immense potential in drug loading.[9] Out of the transition metals, Fe, Zn, Cu, Co, Ni, Ag and Au have shown great promises in biomedical applications.[10] Polymer supported metals have recently received great attention due to interesting properties and wide applicability.[11–13] In addition to this, polymer properties are highly tunable by changing physico-chemical parameters.[14]

In 2011, Fayaz *et al.*[15] biologically synthesized the gold nanoparticles using a non-pathogenic fungus *Trichoderma viride* at room temperature and they showed the ionic interaction during vancomycin binding to the surface of gold nanoparticles. Indeed, binding site of drugs may be covalent or coordinate which depends on the nature of drug that significantly influences the drug loading. Mostly, gold nanoparticles are widely used in drug delivery and cancer detection.[16–18] Besides, gold stabilized nanoparticles have advantages like non-toxicity to human cell and biocompatibility over other metals, except the cost is the major drawback in the use of gold metal for such applications. Drug loading is one of the most active research areas in modern polymer science.[19] In oral drug administration, polar drug dissolve quickly and spread throughout the body, consequently, loss of drug as well as affect whole body instead of body part. Nevertheless, polar drug can be delivered by hydrophilic polymer modified gold having more drug loading property. Polymer supported gold is extensively used in industry, agriculture, pharmaceuticals and medical research. Polymer supported metals are industrially economical and environmentally benign[20] due to its recovery, recycle, and reuse properties.

Nowadays, metal stabilized highly porous, crosslinked, and hydrophilic polymers have received a considerable attraction in drug adsorption profiling studies. In general, nanoparticles in the range between 10–200 nm have disadvantages of aggregation or agglomeration over micron sized particles during application time.[21,22] Unfortunately, the influence of drug polarity

and theoretical predictions such as adsorption isotherm and adsorption kinetics of drug loading studies are rather limited. This work is devoted to investigate the influence of drug polarity on drug loading profile. Moreover, adsorption isotherm and kinetics were also investigated. Comparative study revealed that, pantoprazole sodium has exponential adsorption rate with gold than chloroquine. Drugs used for adsorption profiling are represented below.

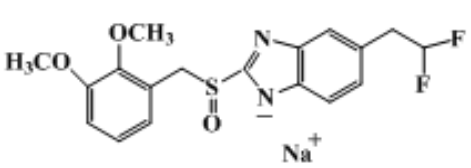

Pantoprazole sodium

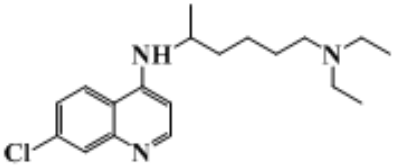

Chloroquine

7.2. Experimental

7.2.1. Materials

Acrylic acid:- Make: Merck; Molecular formula: $C_3H_4O_2$; Molecular weight (g/mol): 72.06; Specific gravity/density (g/cm^3): 1.051; Melting point (^{o}C): 14; Boiling point (^{o}C): 141; Physical state: colorless liquid.

Trimethylolpropane triacrylate:- Make: Sigma-Aldrich; Molecular formula: $C_{15}H_{20}O_6$; Molecular weight (g/mol): 296.32; Specific gravity/density (g/cm^3): 1.1; Boiling point (^{o}C): 316; Physical state: colorless liquid.

Chlorobenzene:- Make: Loba Chemie; Molecular formula: C_6H_5Cl; Molecular weight (g/mol): 112.56; Specific gravity/density (g/cm^3): 1.11; Melting point (^{o}C): (-)45; Boiling point (^{o}C): 131; Physical state: colorless liquid.

Chloroauric acid:- Make: S.D. Fine; Molecular formula: $HAuCl_4$; Molecular weight (g/mol): 339.785; Specific gravity/density (g/cm^3): 3.9; Melting point (^{o}C): 254; Physical state: orange-yellow needle-like crystals.

Sodium borohydride:- Make: Loba Chemie; Molecular formula: $NaBH_4$; Molecular weight (g/mol): 37.83; Specific gravity/density (g/cm^3): 1.07; Melting point (^oC): 400; Boiling point (^oC): 500; Physical state: white crystals.

2,2'-Azobisisobutyronitrile:- Make: AVRA synthesis Pvt. Ltd. Hyderabad, India; Molecular formula: $C_8H_{12}N_4$; Molecular weight (g/mol): 164.21; Specific gravity/density (g/cm^3): 1.1; Melting point (^oC): 103–105; Physical state: white crystals.

Poly(vinyl pyrrolidone) K90 powder:- Make: Fluka; Linear formula: $(C_6H_9NO)_n$; Molecular weight (g/mol): 360,000; Physical state: white powder.

Pantoprazole sodium:- Make: RPG Life Sciences Ltd., Mumbai, India – 400025; Molecular formula: $C_{16}H_{15}F_2N_3O_4S$; Molecular weight (g/mol): 383.371; Physical state: white powder.

Chloroquine:- Make: Ipca Laboratories Ltd., Sejavta, Ratlam 457 002, Madhya Pradesh, India; Molecular formula: $C_{18}H_{26}ClN_3$; Molecular weight (g/mol): 319.872; Physical state: white powder.

7.2.2. Synthesis of polymer

The polymer synthesis was carried out by well-known suspension polymerization method. In the present work, aqueous phase (1 wt %) was prepared by dissolving the protective colloid (PVP) in deionised water. Subsequently, organic phase was prepared by mixing monomer (acrylic acid), crosslinker (trimethylolpropane triacrylate), initiator (2,2'-azobisisobutyronitrile) and pore generating solvent (chlorobenzene) in a nitrogen inert atmosphere at room temperature. Synthesis of polymers was conducted in a specially designed double walled cylindrical glass reactor. The reactor was equipped with a constant temperature water bath (thermostat), mechanical stirrer, reflux condenser, and nitrogen gas inlet. Organic (discontinuous) phase was added to the aqueous (continuous) phase and reactants were stirred at 500 rpm under nitrogen overlay. The reaction temperature was raised to 70^{o}C and stirred for 3 h. Polymer beads obtained by suspension polymerization method were thoroughly washed with water, methanol, finally with acetone, and dried at 60^{o}C under reduced pressure. Copolymer beads were synthesized by suspension polymerization was further purified using methanol in a soxhlet extractor and dried at 60^{o}C for 8 h under reduced pressure. Poly(acrylic acid-*co*-trimethylolpropane triacrylate) series

was synthesized using chlorobenzene as a porogen and abbreviated as ATCB with crosslink density (CLD) ranging from 10 to 25%.

7.2.3. Synthesis of polymer supported gold

In the present study, polymer synthesized by suspension polymerization at 10% crosslink density (CLD) was modified with gold by simple aqueous reduction method. In a stoppered glass bottle, 200 mg of $HAuCl_4$ was dissolved in 5 mL of deionised water. This aqueous metal ion solution was added to 2 g of polymer. This mixture was placed for 30 h for uniform adsorption of chloroauric acid at room temperature. Subsequently, 500 mg of sodium borohydride was dissolved in 3 mL of deionised water. Aqueous solution of sodium borohydride was added dropwise to the polymer-chloroauric acid solution for reduction under nitrogen atmosphere for 1 h at room temperature.[23,24] Then, mixture was placed in shaker bath for 5 h. Thereafter, polymer mixture was filtered and washed with deionised water till neutral pH of the filtrate. Poly(AA-*co*-TMPTA) was obtained using chlorobenzene and abbreviated as **ATCB** having crosslink density (CLD) ranges from 10 to 25%. Furthermore, polymer embedded gold was abbreviated as **ATCBAU** for 10 and 25% CLD. The polymer synthesis and its gold modification are shown in **Schemes 7.1 and 7.2**.

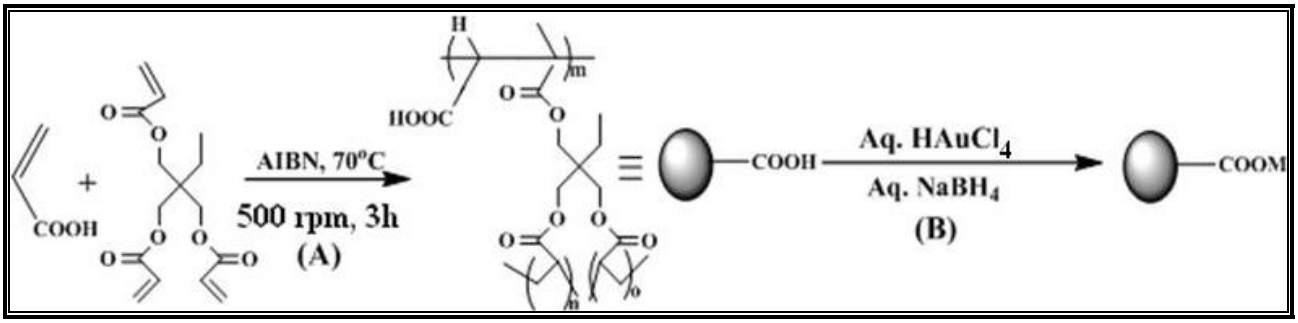

M=Au

Acrylic acid	Trimethylolpropane triacrylate	Poly(AA-*co*-TMPTA)	Hydrophilic poly(AA-*co*-TMPTA) embedded gold

Scheme 7.1. Synthesis of poly(AA-*co*-TMPTA) by suspension polymerization and polymer supported gold

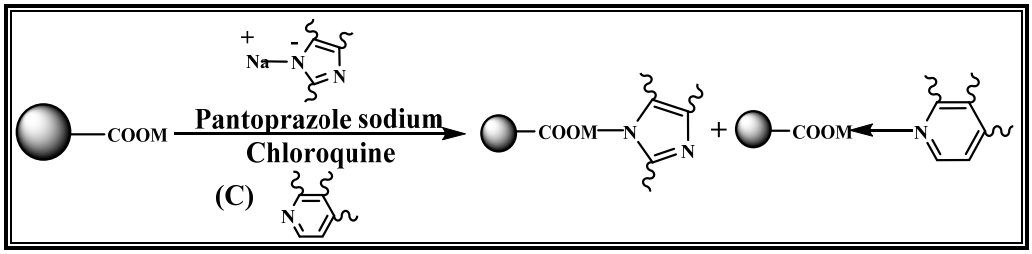

Poly(AA-*co*-TMPTA) embedded gold Drug loading on poly(AA-*co*-TMPTA) embedded gold

Scheme 7.2. Plausible covalent bonding between gold-pantoprazole sodium and coordinate bonding between gold-chloroquine

7.2.4. Characterization

FT-IR spectra were recorded on Perkin Elmer spectrophotometer having spectrum GX model. The samples in the form of KBr pellets were prepared after drying the polymers at 80^{o}C for 8 h under reduced pressure. Surface area of polymers was determined by Brunauer-Emmett-Teller (BET, nitrogen adsorption) method using a surface analyzer NOVA 2000e, Quantachrome. Average particle diameter was determined using an Accusizer 780 (model LE 2500-20) PSS.NICOMP Particle sizing system, Santa Barbara, California, USA. Acid content was determined by KOH using titrimetric method. Thermal stability of the polymers was studied using a simultaneous thermal analysis (STA, Perkin Elmer), while glass transition temperature was determined by a differential scanning calorimetry Q10 (Thermal Analysis). Scanning electron microscopy (SEM) was used to observe the external morphology, and particle visualization. Furthermore, EDX analysis was performed on Quanta 200-3D, dual beam ESEM microscope wherein an electron source was thermionic emission tungsten filament.

7.3. Results and discussion

In 1963, Merrifield published the new route of synthesis termed as solid phase synthesis.[25] In the last two decades, exhaustive work was published by researchers on the synthesis of polymers with desirable properties and its applications. In this work, hydrophilic polymer was synthesized for application in drug loading study. In our investigation, poly(AA-*co*-

TMPTA) was synthesized by suspension polymerization varying crosslink density to obtain beaded microsphere. Chlorobenzene was used as a pore generating solvent. Crosslink density is defined as the percent moles of crosslinking agent (TMPTA) relative to the moles of monomer (acrylic acid). Monomer-crosslinker feed composition of synthesized polymers at different crosslink density is presented in **Table 7.1**. Concentration of monomer and crosslinker was determined by **equation (3.1).**

Table 7.1. Monomer-crosslinker feed composition of poly(AA-*co*-TMPTA) synthesized by suspension polymerization at different crosslink density

Monomer System	Units	Crosslink density (%)			
		10	15	20	25
Acrylic acid: Trimethylolpropane triacrylate	mol	0.0995: 0.0099	0.0859: 0.0129	0.0755: 0.0151	0.0674: 0.0168
	g	7.1710: 3.3676	6.1881: 4.3589	5.4421: 5.1113	4.8566: 5.7018

Reaction conditions: Batch size: 16 mL; 2,2'-azobisisobutyronitrile: 2.5 mol%; stirring speed: 500 rpm; reaction time: 3 h; outer phase: H_2O; protective colloid: poly(vinylpyrrolidone); protective colloid conc.: 1 wt%; porogen: chlorobenzene; porogen concentration: 48 mL (monomer: porogen ratio, 1:3 v/v).

7.3.1. Fourier transform infrared (FT-IR) spectroscopy

FT-IR (KBr pellet, cm^{-1}) analysis of poly(AA-*co*-TMPTA) base polymer and polymer modified gold was carried to confirm the synthesis of base polymer and its gold modification. FT-IR spectrum of poly(AA-*co*-TMPTA) clearly shows that, broad peak at 3415 corresponds to C–OH, 2983 assigned to –C–H vib. and 1722 corresponds to carboxylic acid functionality. Peaks observed at 1171 and 963 are assigned to C-O-C str. and C–OH vib., respectively. The spectrum of polymer supported gold demonstrates the decreased absorbance or increased transmittance due to decreasing the C–OH concentration at 3400–3500. This increase in transmittance indicated polymer acid functionality gets modified with gold. Nevertheless, spectrum

demonstrated slight absorbance in the range of 3400–3500 obviously due to acid functionality buried in polymer matrix available for FT-IR analysis contrary unavailable for modification. This shifting[26] of carboxylic acid peak towards 1737 and decrease in C–OH absorbance peak of –COOH confirms the successful modification. FT-IR spectrum of poly(AA-*co*-TMPTA) and its gold modification is shown in **Figure 7.1.**

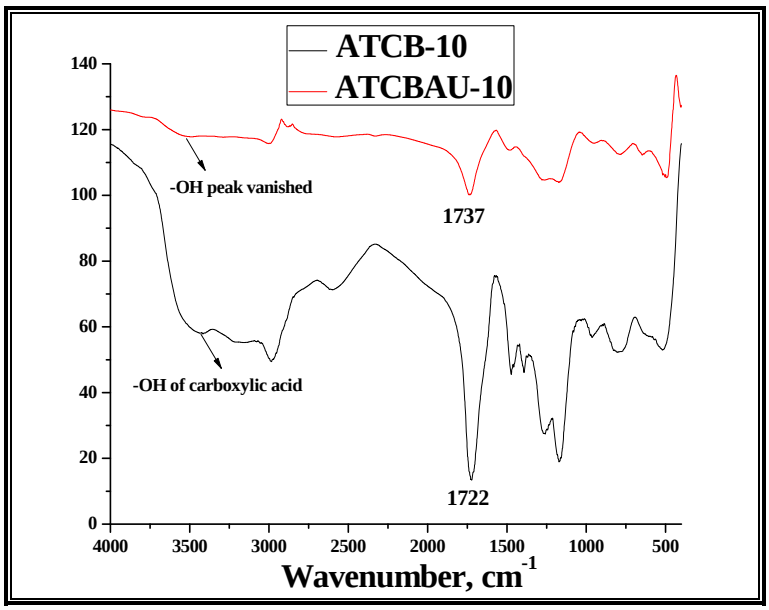

Figure 7.1. FT-IR spectrum of base (ATCB-10) and PSG (ATCBAU-10)

7.3.2. Surface area

Surface area is the most crucial parameter in selection of more efficient polymer support for application in the areas of catalysts, reagents, drug loading, column material, and metal recovery. The surface area of poly(AA-*co*-TMPTA) and PSG was evaluated for 10 and 25% crosslink density. It was observed that, base polymer has surface area of 85.67 and 287.71 m^2/g for 10 and 25% CLD, respectively. In addition, polymer supported gold (PSG) revealed the surface area of 78.87 m^2/g for 10% crosslink density. Besides, result clears that, surface area was decreased with higher CLD. This happens due to increasing CLD increases the crosslinker concentration as a result increasing micropores consequently high surface area.[27] Furthermore, polymer supported gold (PSG) demonstrated the decrease in surface area due to polymer

modification with gold. Thus, even after modification polymer demonstrated 78.87 m^2/g which is preferable for the applications.

7.3.3. Particle size

Over the past few years researchers published potential work in the applications of nanoparticles in biomedical field.[28,29] Present study was designed to synthesize the micron sized particles (15–25 μm) and its applications in drug loading study. Possible reason of better efficacy of polymer over nanoparticles is the non-conglomeration of polymer particles and ease of recovery of polymer supported compounds for recycle and reuse. In most of the cases, recovery of nanoparticle is difficult due to few nanometer sized particle may pass through filter. An objective of current work is to study the applications of polymer particles in drug adsorption profile. Average particle size of base polymer was evaluated from crosslink density 10 to 25% and polymer supported gold (PSG) for 10% crosslink density. However, base polymer (ATCB) shows that, 20.74, 20.23, 18.84, and 17.90 μm particle size for 10, 15, 20, and 25% CLD, respectively. Interestingly, particle size was decreased with increasing CLD, presumably due to higher crosslink density increased the concentration of crosslinker as result strong binding between monomer and crosslinker. On the other hand, polymer supported gold (PSG) showed very little increase in particle size (21.81 μm) perhaps due to surface modification with gold. Thus, obtained polymers were in the range of 17–21 μm. Average particle size of the base polymer is represented in **Figure 7.2.**

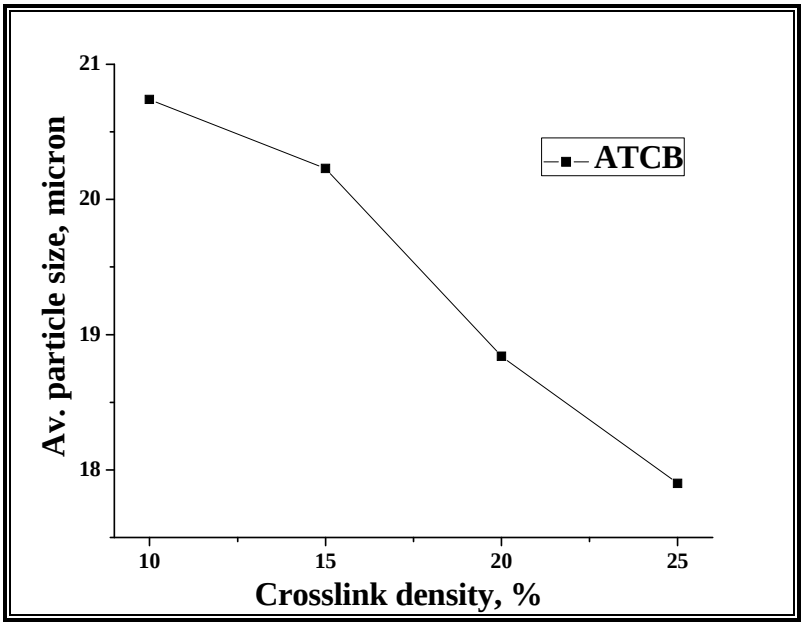

Figure 7.2. Average particle size of base polymer

7.3.4. Acid content

Acid content was evaluated to estimate the available acid content of polymer for gold modification. Acid content of synthesized base polymers were determined for 10 to 25% crosslink density by well-known KOH method, titrimetrically.[30] Dried base polymers were used for acid content determination. Theoretical acid content was determined by **equation (7.1):**

$$\text{Acid content (Theoretical)} = \frac{\text{Moles of acrylic acid}}{\text{Total wt. of acrylic acid+crosslinker}} \qquad \textbf{(7.1)}$$

It was observed that, observed acid content is much lower than theoretical. This is because of large number of acid functionality are well-buried into the polymer matrix. In addition, higher CLD lowers the observed acid content. This may happen due to concentration of acrylic acid decreased with increasing crosslink density. Result of theoretical acid content was 9.44, 8.144, 07.15, and 6.38 mmol/g whereas observed acid contents showed 3.25, 2.64, 2.20, 1.79, and 1.47 mmol/g for 10, 15, 20, and 25% crosslink density, respectively. Much higher acid content at low crosslink density implied more polymer reactivity. Theoretical and observed acid contents are reported in **Figure 7.3.**

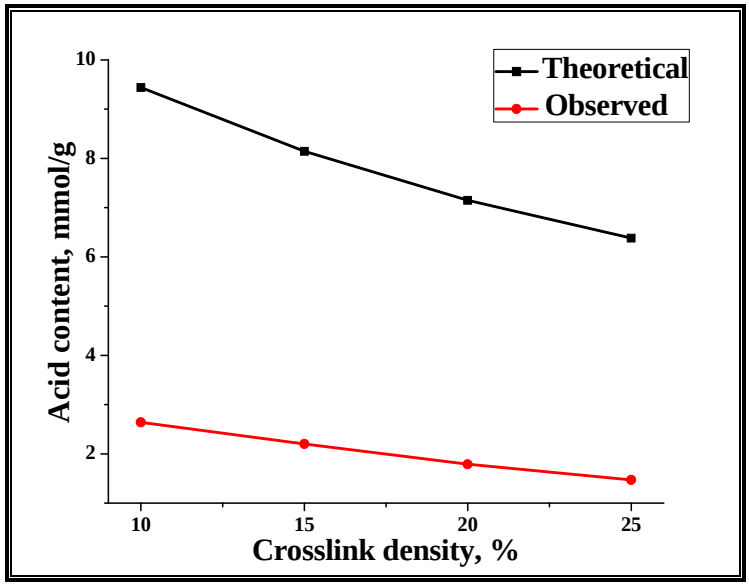

Figure 7.3. Theoretical and observed acid content (mmol/g) of base polymer (ATCB) for different crosslink density

7.3.5. Thermogravimetric analysis

Since last 20 years, polymer with controlled desired properties are attracted a lot of attention due to their potential applications in various fields. However, high surface area and hydrophilic polymer is the ubiquitous material due to vast applications of polymer as a support for catalysts, reagents or substrate for applications at room as well as high temperature reactions. Prior to use of the polymer as a support in solid phase synthesis, to understand its thermal stability is an essential. Particle size, reactivity, stiffness, hydrophilic-hydrophobic, and porosity are the ubiquitous properties along with thermostability considered during the selection of proper supporting material.[32,33] Thermostability of the synthesized polymer and polymer modified gold was analysed. Differential thermal analysis of polymer at different crosslink density (CLD) was performed by simultaneous thermal analysis (Perkin Elmer) from 50–800^{o}C temperature at heating rate of 10^{o}C/min under a nitrogen atmosphere. Differential thermogravimetry (DTG) analysis of base polymer (ATCB) for 10 and 25% crosslink densities were evaluated. DTG curve showed the Tmax of base polymer (ATCB) which was 446 and 442^{o}C for 10 and 25% CLD, respectively. This is mainly due to the concentration of flexible crosslinker increased in high CLD polymer whereas decreased in low CLD polymer. As a consequence, higher flexible

crosslinker concentration lowers the decomposition temperature. Moreover, polymer embedded gold significantly decreased the Tmax. In the present work, polymer embedded gold displayed the Tmax at 398^{o}C for 10% CLD due to gold modification. Graphical representation of DTG (Tmax) of base polymer for 10 and 25% and PSG for 10% crosslink density is represented in **Figure 7.4.**

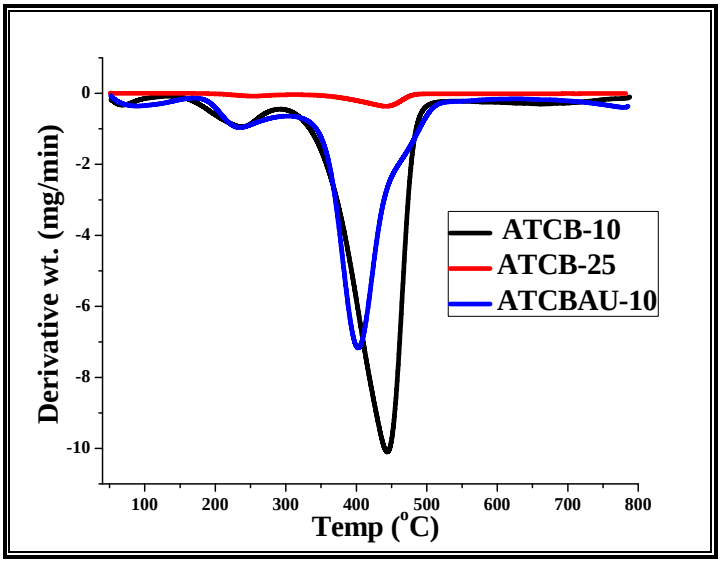

Figure 7.4. DTG thermograms of ATCB-10, ATCB-25, and ATCBAU-10

7.3.6. Differential scanning calorimetry

Much more work is presently done around the world to develop the nanoparticles for applications in different fields. This study was interested in the synthesis of TMPTA based hydrophilic polymer particles to evaluate its biomedical applications at room temperature. Indeed, both nano and micron sized particles have their own merits and demerits. Moreover, polymer should be use below glass transition temperature (Tg) to avoid interaction of polymer support with reactant or product. Thus, Tg is the crucial parameter considered during polymer support selection. In other words, Tg helps to decide safe temperature of PSG as a catalyst in an organic reactions. Industrial applications of the most electronegative gold metal in catalysis provides more efficacy due to their recovery, recycle, and reuse property.[34–36] DSC study showed that, glass transition temperature (Tg) of base polymer (ATCB) was 228 and 223^{o}C for 10 and 25% CLD, respectively whereas polymer modified gold displayed the Tg at 217^{o}C for 10%

CLD. This suggested that, polymer can be used at or below 210°C for safe temperature perspectives. The reason of difference in Tg of base polymer and polymer supported gold with crosslink density is same as aforementioned in DTG study. The DSC thermograms (Tg) of base polymer at 10 and 25% crosslink density and PSG for 10% crosslink density are depicted in **Figure 7.5.**

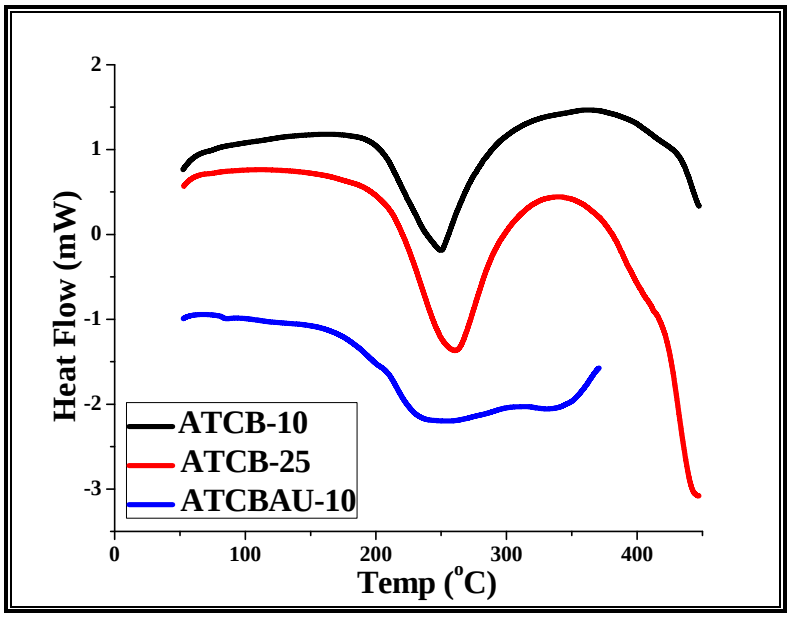

Figure 7.5. DSC thermograms of polymer ATCB-10, ATCB-25, and ATCBAU-10

7.3.7. Scanning electron microscopy

Scanning electron microscopy (SEM) is the visual observation tool that display size, shape and external surface morphology of the synthesized and modified polymer beads. SEM images of base and modified polymers were scanned for 250X magnifications. SEM images of base polymer revealed the non-conglomerated, uniform, and spherical beads. In contrast, after modification beads coupled together. It is worth mentioning that, modified beads are highly coupled together for 10% CLD than 25%. This is mainly due to more modification of reactive polymer (10% CLD) compared to less reactive polymer (25% CLD). SEM images of base and modified polymers are represented in **Figure 7.6.**

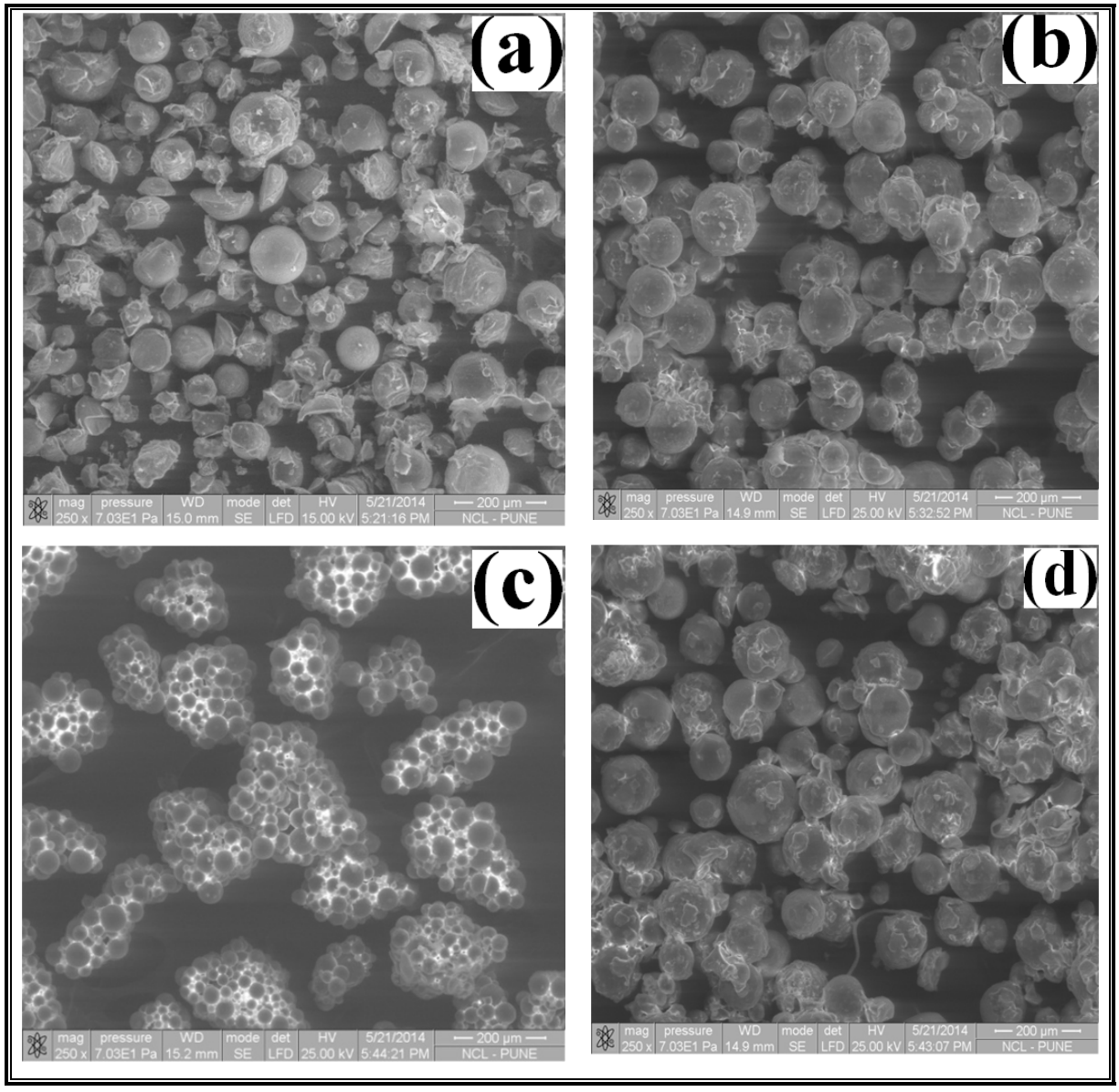

Figure 7.6. SEM images of (a) ATCB-10, (b) ATCB-25, (c) ATCBAU-10, and (d) ATCBAU-25 (250X magnification)

7.3.8. Energy dispersive X-ray (EDX) analysis

Energy dispersive X-ray spectroscopy is the well-known tool used for qualitative and quantitative determination of metal composition in the polymer matrix before and after modification. Results illustrated that, base polymer contains carbon and oxygen only. However,

polymer modified gold contains 9.17 wt% (0.69 at%) and 4.56 wt% (0.31 at%) of gold for 10 and 25% CLD, respectively along with carbon and oxygen. Unfortunately, EDX is unable to determine hydrogen content. EDX analysis revealed the higher loading of gold with lower crosslinked polymer (10%) rather than more crosslinked polymer (25%) due to the presence of more carboxylic acid functionality at low CLD compared to high CLD.

7.3.9. Drug adsorption

Nowadays, number of methods is available to study the drug loading. Still UV spectroscopy is the most accurate, convenient, and widely used method to evaluate drug loading. In order to obtain calibration curve at different concentration (5, 10, 15, 20, and 25 ppm) of pantoprazole sodium and chloroquine was prepared in deionised water and was analysed for UV absorbance. Pantoprazole sodium and chloroquine has maximum absorbance at 291 and 342 nm, respectively. The observed regression coefficient (R^2) was 0.999 and 0.998 for pantoprazole sodium and chloroquine, respectively.

7.3.9.1. Contact time effect

Contact time is a crucial parameter which substantially affects drug loading. Drug adsorption was carried out in 30 mL of glass vials wherein 20 mg of PSG was added to glass vial containing 20 mL (25 ppm) of drug solution at room temperature. Vials were placed under shaking and sample was removed after certain interval of time to analyze UV absorbance. As to be expected, adsorption of both drugs were increased with contact time.[37,38] Nevertheless, adsorption rate is exponential with pantoprazole sodium whereas gradually increased for chloroquine. Pantoprazole sodium adsorbs 72% and chloroquine adsorbs 26% in initial 2 h. Moreover, pantoprazole sodium adsorbs 91% and chloroquine 62% in 24 h. Initial 2 h is the exponential adsorption period for pantoprazole sodium whereas exponential adsorption begins after 12 h for a chloroquine. Contact time effect on drug adsorption is depicted in **Figure 7.7.**

Yet another, equilibrium adsorption of pantoprazole sodium and chloroquine was carried out using PSG (ATCBAU-10) to evaluate the maximum adsorption of drugs. Adsorption study was carried out at room temperature using 50 ppm solution of both drugs at pH 3. Experimental

procedure and conditions were same as aforementioned in contact time study. Equilibrium adsorption was studied using 50 ppm of pantoprazole sodium and chloroquine drug for 48 h at pH 3. The absorbance of a pantoprazole sodium and chloroquine was 33 and 26 mg/g of polymer, respectively.

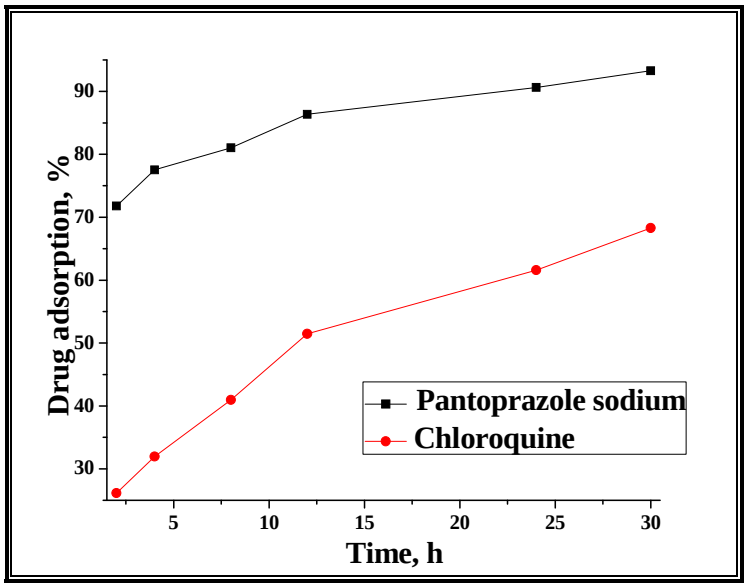

Figure 7.7. Effect of contact time on adsorption of pantoprazole sodium and chloroquine

7.3.9.2. Adsorption isotherm

Langmuir adsorption isotherm was carried out for pantoprazole sodium and chloroquine to investigate the adsorption capacity with respect to PSG at pH 3 and room temperature. Langmuir adsorption isotherm of pantoprazole sodium and chloroquine (c_e/q_e versus c_e) was well-fitted by least square method to linearly transformed Langmuir adsorption isotherm. The linear Langmuir adsorption isotherm[39,40] **equation** is presented in **(7.2):**

$$\frac{C_e}{q_e} = \frac{1}{Q_0 b} + \frac{C_e}{Q_0} \qquad \textbf{(7.2)}$$

where, C_e is the equilibrium concn. (mg/L), q_e is the amount of drug adsorbed per gram at equilibrium (mg/g), Q_0 (mg/L) and b are the Langmuir constants associated with adsorption capacity and energy of adsorption, respectively.

The results obtained by adsorption study conducted at room temperature were fitted with Langmuir linear adsorption isotherm. Both drugs obeys the Langmuir adsorption isotherm which indicates that, adsorption is monolayer and reactive of an adsorbent are homogeneous. The adsorption isotherm of c_e/q_e versus c_e is depicted in **Figure 7.8.**

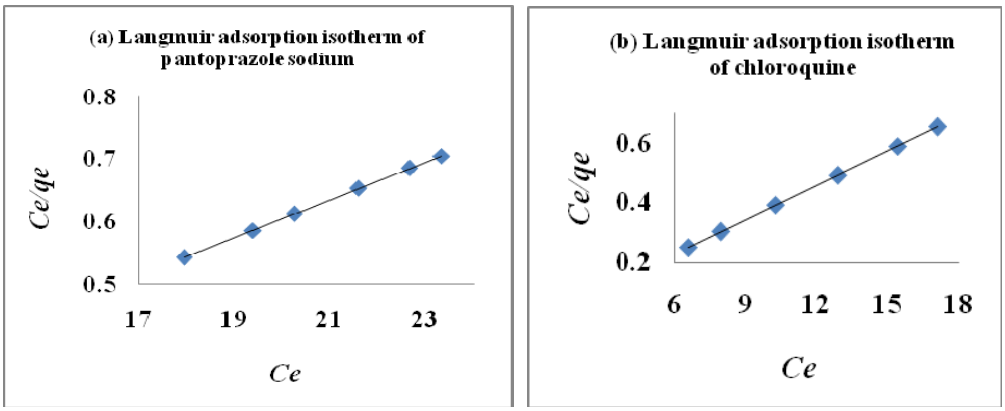

Figure 7.8. Langmuir adsorption isotherm plot of (a) pantoprazole sodium, and (b) chloroquine

7.3.9.3. Pseudo-first and pseudo-second order kinetics

In the present work, pseudo-first and pseudo-second order kinetic models were investigated. Kinetic and equilibrium adsorption are two important physico-chemical parameters considered during sorption study of metal, dye, drug and so on. Kinetic adsorption describes the relationship between contact time and drug adsorption rate whereas equilibrium adsorption describes the distribution of the drug between solid–liquid phases and determining the feasibility and capacity of the sorbent for adsorption. Pseudo-first order Lagergren kinetic[41,42] **equation (7.3)** was used to explain the adsorption mechanism.

$$log(q_e - q_t) = log q_e - \frac{K_{ad} t}{2.303} \qquad \textbf{(7.3)}$$

where, q_e is the mass of drug adsorbed at equilibrium (mg/g), q_t is the mass of drug adsorbed at time t (mg/g), K_{ad} is the first order kinetics constant (L/min), and t is the time in h.

In this model physicochemical interaction between PSG and drug solution in an aqueous medium attributes to drug removal. Pseudo-first order kinetics determines the rate of occupation of adsorption sites is proportional to the number of unoccupied sites. Plot of $log(q_e-q_t)$ versus t revealed a straight line which illustrated the application of the pseudo-first order kinetic model. Figures clearly indicated that, pseudo-first order was not exactly obeyed by both metals, obviously, demonstrates adsorption is not physisorption. Pseudo-first order kinetics carried out at ambient temperature for pantoprazole sodium and chloroquine [$log(q_e-q_t)$ versus t] is represented in **Figure 7.9.**

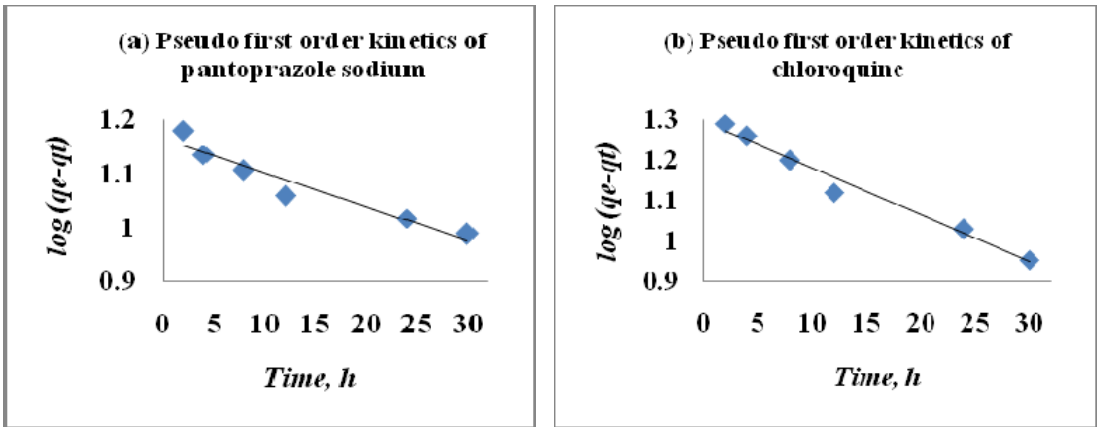

Figure 7.9. Pseudo-first order kinetic of (a) pantoprazole sodium, and (b) chloroquine

Pseudo-second order kinetic equation was applied to the present study to determine the equilibrium capacity[41–43] of PSG using **equation (7.4).**

$$\frac{t}{q_t} = \frac{1}{K_{2ad}q_e^2} + \frac{t}{q_e} \qquad \textbf{(7.4)}$$

where, K_{2ad} is the second order kinetics rate equilibrium constant (g/mg·min), q_e is the equilibrium adsorption of drug, and q_t is the adsorption of drug at time t.

The plot of t/q_t versus t was plotted for an equilibrium adsorption capacity study. An equilibrium adsorption plot of pantoprazole sodium and chloroquine implied the linear increase in the pseudo-second order kinetics and obeyed chemisorption either covalent or co-ordinate. Pseudo-second order kinetics of pantoprazole sodium and chloroquine carried out at an ambient temperature is represented in **Figure 7.10.**

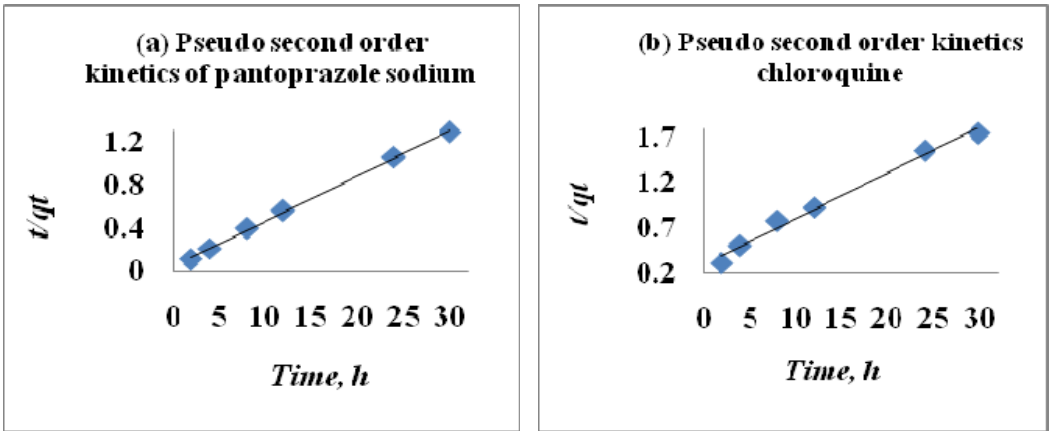

Figure 7.10. Pseudo-second order kinetic of (a) pantoprazole sodium, and (b) chloroquine

7.4. Conclusion

In conclusion, polymer modified gold was successfully synthesized for drug loading application and kinetics evaluation in acidic buffer medium. Interestingly, more polymer modification by gold obtained was 9.17 wt% for 10% crosslink density which increases drug loading efficiency. However, pantoprazole sodium revealed more adsorption than chloroquine with polymer supported gold as a consequence of more drug polarity and compatibility of pantoprazole sodium with polymer modified gold unlike chloroquine having less compatibility and polarity. Furthermore, contact time displayed 91% of pantoprazole sodium and 62% of chloroquine loading in 24 h at pH 3. Initial 2 h is the exponential adsorption period for pantoprazole sodium whereas exponential adsorption begins after 12 h for chloroquine. Langmuir adsorption isotherm was well-fitted with drug loading indicated monolayer drug adsorption. Pseudo-first and pseudo-second order kinetics showed that, drug adsorption mechanism is chemisorption either covalent or co-ordinate. Overall, hydrophilic polymer synthesized in the present work is the unique drug carrier material in an acidic buffer medium. Present work provides the high surface area, uniform, and spherical polymer that increases efficiency of polymer modified gold. In addition, thermostability was studied by DTG and DSC which is useful to select the high efficient and thermostable polymer prior to the applications in high temperature reaction as a polymer support.

References

[1] Andujar C. B., Tung L. D. and Thanh N. T. K., *Annu. Rep. Prog. Chem., Sect. A,* 2010, **106,** 553–568.

[2] Khan M. S., Vishakante G. D. and Siddaramaiah H., *Adv. Colloid Interface Sci.,* 2013, **199–200,** 44–58.

[3] Tiwari P. M., Vig K., Dennis V. A. and Singh S. R., *Nanomaterials,* 2011, **1,** 31–63.

[4] Jeong E. H., Jung G., Hong C. A. and Lee H., *Arch. Pharm. Res.,* 2014, **37,** 53–59.

[5] Parida U. K., Biswal S. K., Nayak P. L. and Bindhani B. K., *World J. Nano Sci. Technol.,* 2013, **2(1),** 47–57.

[6] Malathi S., Balakumaran M. D., Kalaichelvan P. T. and Balasubramanian S., *Adv. Mat. Lett.,* 2013, **4(12),** 933–940.

[7] Cai W., Gao T., Hong H. and Sun J., Review, *Nanotechnol. Sci. Appl.,* 2008, **1,** 17–32.

[8] Mukherjee P., Bhattacharya R., Bone N., Lee Y. K., Patra C. R., Wang S., Lu L., Secreto C., Banerjee P. C., Yaszemski M. J., Kay N. E. and Mukhopadhyay D., *J. Nanobiotechnol.,* 2007, **5,** 4.

[9] Kim J. and Lee T. R., *Drug Dev. Res.,* 2006, **67,** 61–69.

[10] Das I. and Ansari S. A., *J. Sci. Ind. Res.,* 2009, **68,** 657–667.

[11] Hossein H. and Mohsen H., *Curr. Drug Saf.,* 2009, **4(1),** 79–83.

[12] Neuse E. W., *Hindawi Pub. Corp.,* 2008, **469531,** 1–19.

[13] Shah V., Desai R. N. and Patel P. K., *Int. J. Sci. Eng. Technol.,* 2012, **1(2),** 222–228.

[14] Mohamed M. H. and Wilson L. D., *Nanomaterials,* 2012, **2,** 163–186.

[15] Fayaz A. M., Girilal M., Mahdy S. A., Somsundar S. S., Venkatesan R. and Kalaichelvan P. T., *Process Biochem.,* 2011, **46(3),** 636–641.

[16] Kumar A., Zhang X. and Liang X., *Biotechnol. Adv.,* 2013, **31(5),** 593–606.

[17] Ali M. R. K., Panikkanvalappil S. R. and El-Sayed M. A., *J. Am. Chem. Soc.,* 2014, **136,** 4464−4467.

[18] Llevot A. and Astruc D., *Chem. Soc. Rev.,* 2012, **41,** 242–257.

[19] Vinogradov S. V., *Curr. Pharm. Des.,* 2006, **12(36),** 4703–4712.

[20] Kanaoka S., Yagi N., Fukuyama Y., Aoshima S., Tsunoyama H., Tsukuda T. and Sakurai H., *J. Am. Chem. Soc.,* 2007, **129,** 12060–12061.

[21] Hondow N., Brydson R., Wang P., Holton M. D., Brown M. R., Rees P., Summers H. D. and Brown A., *J. Nanopart. Res.,* 2012, **14,** 977.

[22] Indira T. K. and Lakshmi P. K., Review, *Int. J. Pharm. Sci. Technol.,* 2010, **3(3),** 1035–1042.

[23] Voliani V., Signore G., Nifosí R, Ricci F., Luin S. and Beltram F., *Rec. Pat. Nanomed.,* 2012, **2(1),** 1–11.

[24] Low A. and Bansal V., *Biomed. Imaging Intervention J.,* 2010, **6(1),** 1–5.

[25] Merrifield R. B., *J. Am. Chem. Soc.,* 1963, **85(14)**, 2149–2154.

[26] Tu W. X., *Chin. J. Polym. Sci.,* 2008, **26(1),** 23−29.

[27] Kotha A., Rajan C. R., Ponrathnam S., Kumar K. K. and Shewale J. G., *Appl. Biochem. Biotechnol.,* 1998, **74,** 191–203.

[28] Parida U. K. and Nayak P. L., *World J. Nano Sci. Technol.,* 2012, **1(2),** 10–25.

[29] Ghosh P., Han G., De M., Kim C. K. and Rotello V. M., *Adv. Drug Delivery Rev.,* 2008, **60,** 1307–1315.

[30] Vogel A. I., Lond., 1958, **Chapter XVI,** 667–671.

[31] Alves F., Scholder P. and Nischang I., *Appl. Mater. Interfaces,* 2013, **5,** 2517−2526.

[32] Xu W., Lu T. J. and Wang F., *Int. J. Solids Struct.,* 2010, **47,** 1830–1837.

[33] Schmidt G. and Malwitz M. M., *Curr. Opin. Colloid Interface Sci.,* 2003, **8,** 103–108.

[34] Guino M., Brule E. and De Miguel Y. R., *J. Comb. Chem.,* 2003, **5**, 161–165.

[35] Bergbreiter D. E., Hobbs C. and Hongfa C., *J. Org. Chem.,* 2011, **76,** 523–533.

[36] Dalal M. K., *Int. J. Chem. Eng. Appl.,* 2012, **3(3),** 211–215.

[37] Goppert T. M. and Muller R. H., *Int. J. Pharm.,* 2005, **302(1-2),** 172–186.

[38] Selvam P., Marek S., Truman C. R., Hugh D. M. and Smyth D. C., *Aerosol Sci. Technol.,* 2011, **45,** 81–87.

[39] Zheng H., Liu D., Zheng Y., Liang S. and Liu Z., *J. Hazard. Mater.,* 2009, **167,** 141–147.

[40] Desta M. B., *J. Thermodyn.,* 2013, **375830,** 1–6.

[41] Robati D., *J. Nanostruct. Chem.,* 2013, **3,** 1–6.

[42] Ho Y. S., *Scientometrics,* 2004, **59,** 171–177.

[43] Ho Y. S. and McKay G, *Process Biochem.,* 1999, **34,** 451–465.

POLYMER SUPPORTED LEWIS ACIDS: RECYCLABLE CATALYSTS

8.1. Introduction

In 1877, Charles Friedel and James Crafts developed the reaction to attach the substituent to the aromatic ring via electrophilic substitution reaction.[1] This reaction is generally carried out in non-aromatic solvents such as ethanol, acetone, THF, diethyl ether, and chloroform. Over the last decade, Lewis acids have been generally used in Friedel-Craft alkylation, acylation, dealkylation of tertiary butyl group, hydroxylation, and sulfonylation.[2–5] However, Lewis acids are mostly used in Friedel-Craft alkylation and acylation reactions. Friedel-Craft reaction using Lewis acid is oldest method for C–C bond formation but is still attractive.[6] Polymer supported Lewis acid (PSLA) catalysts are used attractively in acylation,[8] hydroxylation,[9] and sulfonylation.[10–12] In recent years, homopolymer as well as crosslinked polymer support is a growing research area in polymer supported Lewis acids. The number of methods are available to anchor the Lewis acids to polymer support include co-ordinate binding,[13] encapsulation,[14] immobilization,[15] adsorption and entrapment. These methods have their own merits and demerits. Generally, Lewis acids are used at high temperature ranging from 50–300^{o}C depending on the reaction conditions.[16,17] Most of the organic reactions carried out in an organic solvents, as a result polymer support should have hydrophobic properties to obtain better results. In high temperature reactions, thermostability of PSLA is an important. Consequently, thermostable polymer is an essential criterion of solid support in high temperature reactions. The Alder-Ene reaction requires high temperature[18] ranging from 200–600^{o}C. Therefore, study of thermal stability of base polymer support and supported Lewis acid is an important prior to use in solid phase synthesis.

Lewis acids used in organic reactions are difficult to separate after completion of reaction. Another problem is that, unsupported Lewis acid can be used only once and has to be discarded after use. Undoubtedly, the polymer supported Lewis acids (PSLAs) can eliminate both above problems. In other words, polymer supported catalysts can be easily recovered by filtration and can be regenerated and reused for number of cycles.[19] Last decade researchers have extensively studied the synthesis of polymer with desirable properties and polymer supported catalysts.[20–23] In the past, Lewis acids used largely in an organic synthesis are $AlCl_3$,[24] $SnCl_2$,[25] $HgCl_2$,[26,27] BF_3,[28] $TiCl_4$[2] etc. The crucial problem is the less catalyst loading and leakage of a

catalyst during its application that affects the yield and purity of the product in an organic synthesis[29]. Currently, the low loading of catalyst, reagent, substrate, and protecting groups is the major concern with solid support. However, more reactive and primary amine based poly(allylamine-*co*-divinylbenzene) synthesized for modification with Lewis acid offers a possible solution.

Our investigation resolves the problem of catalyst leakage using strong co-ordinate bonding between amine functionality of polymer matrix and electron deficient metal halides. Poly(allylamine-*co*-divinylbenzene) as hydrophobic polymer was obtained for the applications in an organic solvents. Owing to ease of separation, reusability, high Lewis acid loading and non-leaking of Lewis acid are some advantages of PSLAs over the conventional Lewis acid catalysts during application. The properties of polymer supported Lewis acids such as surface area, average particle size, thermal analysis, swelling, and morphology were also evaluated. These polymers were successfully used in poly(imine) synthesis and recovered for recycle and reuse perspectives. Recycling and reuse make them industrially economical and environmentally benign.

8.2. Experimental

8.2.1. Materials

Allylamine: Make:- Spectrochem; Molecular formula: C_3H_7N; Molecular weight (g/mol): 57.09; Specific gravity/density (g/cm^3): 0.7630; Boiling point (^{o}C): 55–58; Physical state: colorless liquid.

Divinylbenzene (80%):- Make: Loba Chemie; Molecular formula: $C_{10}H_{10}$; Molecular weight (g/mol): 130.19; Specific gravity/density (g/cm^3): 0.914; Boiling point (^{o}C): 195; Physical state: colorless liquid.

Cyclohexanol:- Make: Loba Chemie; Molecular formula: $C_6H_{12}O$; Molecular weight (g/mol): 100.16; Specific gravity/density (g/cm^3): 0.9624; Boiling point (^{o}C): 162; Physical state: colorless, viscous liquid, hygroscopic.

Ethanol:- Make: Loba Chemie; Molecular formula: C_2H_6O; Molecular weight (g/mol): 46.07; Specific gravity/density (g/cm^3): 0.789; Boiling point (^{o}C): 78.37; Physical state: volatile, flammable, colorless liquid.

Acetonitrile:- Make: Loba Chemie; Molecular formula: C_2H_3N; Molecular weight (g/mol): 41.05; Specific gravity/density (g/cm^3): 0.786; Boiling point (^{o}C): 82; Physical state: colorless liquid.

1,4-Dioxane:- Make: Loba Chemie; Molecular formula: $C_4H_8O_2$; Molecular weight (g/mol): 88.11; Specific gravity/density (g/cm^3): 1.033; Boiling point (^{o}C): 101.1; Physical state: colorless liquid.

2,2'-Azobisisobutyronitrile:- Make: SAS Chemicals (Mumbai, India); Molecular formula: $C_8H_{12}N_4$; Molecular weight (g/mol): 164.21; Specific gravity/density (g/cm^3): 1.1; Melting point (^{o}C): 103–105; Physical state: white crystals.

Poly(vinyl pyrrolidone) K90 powder:- Make: Fluka; Molecular formula: $(C_6H_9NO)_{n;}$ Molecular weight (g/mol): 360,000; Physical state: white powder.

Aluminium(III)chloride anhydrous:- Make: Merck; Molecular formula: $AlCl_3$; Molecular weight (g/mol): 133.34; Specific gravity/density (g/cm^3): 2.48; Melting point (^{o}C): 192.4; Physical state: white or pale yellow solid.

Stannous(II)chloride:- Make: Merck; Molecular formula: $SnCl_2.2H_2O$; Molecular weight (g/mol): 225.63; Specific gravity/density (g/cm^3): 2.71; Melting point: 37.7; Boiling point (^{o}C): 623 (decomp.); Physical state: white crystalline solid.

Mercury(II)chloride:- Make: Merck; Molecular formula: $HgCl_2$; Molecular weight (g/mol): 271.52; Specific gravity/density (g/cm^3): 5.43; Melting point (^{o}C): 276; Boiling point (^{o}C): 304; Physical state: white crystalline solid.

4,4'-Diacetylbiphenyl:- Make: Sigma-Aldrich; Molecular formula: $C_{16}H_{14}O_2$; Molecular weight (g/mol): 238.28; Melting point (^{o}C): 193–195; Physical state: white crystals.

Para-phenylene diamine:- Make: Merck; Molecular formula: $C_6H_8N_2$; Molecular weight (g/mol): 108.14; Melting point (^oC): 145; Boiling point (^oC): 267; Physical state: white crystalline solid darkens upon exposure to light.

N-methyl-2-pyrrolidone:- Make: Merck; Molecular formula: C_5H_9NO; Molecular weight (g/mol): 99.13; Specific gravity/density (g/cm^3): 1.028; Boiling point (^oC): 202–204; Physical state: colorless liquid.

8.2.2. Polymer synthesis

An aqueous phase (5 wt%) was prepared by dissolving the protective colloid poly(vinyl) pyrrolidone in deionized water. Organic phase was prepared by mixing a monomer (allylamine), crosslinker (divinylbenzene), an initiator (2,2'-azobisisobutyronitrile) and pore generating solvent (cyclohexanol) in a nitrogen atmosphere at room temperature. The synthesis of polymers was conducted in a specially designed polymerization reactor. The reactor was equipped with a constant temperature water bath (thermostat), mechanical stirrer, reflux condenser and a nitrogen gas inlet. Organic (discontinuous) phase was added to the aqueous (continuous) phase with stirring at 500 rpm in a nitrogen overlay. The reaction temperature was raised to 70^{o}C and stirred for 3 h. The obtained polymer beads were thoroughly washed with water, methanol and finally with acetone, and dried at 60^{o}C under reduced pressure. The polymers obtained by suspension polymerization were further purified by soxhlet extraction method.[30]

8.2.3. Preparation of polymer supported Lewis acid

Soxhlet purified polymers were used for modification with Lewis acids. For this, poly(AA-*co*-DVB) having crosslink density (CLD) of 5, 10, 15, 20, and 25% were modified with commonly used Lewis acids such as aluminium chloride ($AlCl_3$), stannous chloride ($SnCl_2$), and mercury chloride ($HgCl_2$). Later on, $AlCl_3$ (5 g) was dissolved in 50 mL of ethanol and placed at room temperature for 2 days to obtain complete dissolution. Furthermore, 2 g of ADC (5 to 25% crosslink density) polymers were taken separately in glass vials. To this, 10 mL of Lewis acid solution was added to each crosslink density polymer. These modified polymers were placed for 2 days at ambient temperature to obtain uniform polymer modification. These polymers were

then washed with ethanol for 3–4 times to remove unreacted Lewis acid and were dried at 70°C under pressure for 8 h. Dried polymers were used for characterization. Aforementioned procedure was followed to modify polymers with stannous chloride and mercury chloride. The poly(allylamine-*co*-DVB) before modification is labeled as **ADC** (base polymer) whereas base polymer supported Lewis acids, $AlCl_3$, $SnCl_2$, and $HgCl_2$ are labeled as **ADCA, ADCS,** and **ADCH,** respectively. The synthesis of polymers by suspension polymerization and its modification with Lewis acids are represented in **Scheme 8.1.**

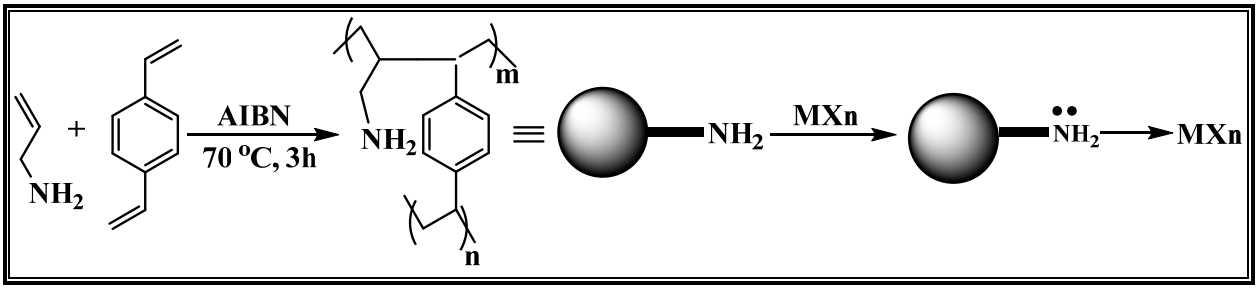

MXn: $AlCl_3/SnCl_2/HgCl_2$

Scheme 8.1. Synthesis of poly(allylamine-*co*-DVB) and its modification with Lewis acid by coordinate bonding

8.2.4. Synthesis of poly(imine) using polymer supported Lewis acid

Polymer application was evaluated to analyze polymer efficiency. For instance, PSLAs were used in poly(imine) synthesis. For this, 100 mL of three necked flask was equipped with a constant temperature oil bath, mechanical stirrer, and nitrogen gas inlet. To this, 4,4'-diacetylbiphenyl (1 g, 4.1967 mmol), N-methyl-2-pyrrolidone (5 mL), and poly(AA-*co*-DVB) supported $AlCl_3/SnCl_2$ (1 g) was added and stirred for 10 min. Subsequently, *para*-phenylene diamine (0.454 g, 4.5845 mmol) was added and stirred for 3 h at 90°C. After completion of reaction time, the reaction mixture was filtered to recover polymer supported $AlCl_3/SnCl_2$. The clear filtrate was poured in methanol and placed for overnight to precipitate the polymer. Then, precipitate was filtered, washed with methanol and dried at 70°C for 8 h under reduced pressure. Yield of the product was 1.31 g, 90.1%. Recovered polymer supported catalysts can be reused to

study the reuse efficiency. Synthesis of poly(imine) using polymer supported Lewis acid is demonstrated in **Scheme 8.2.**

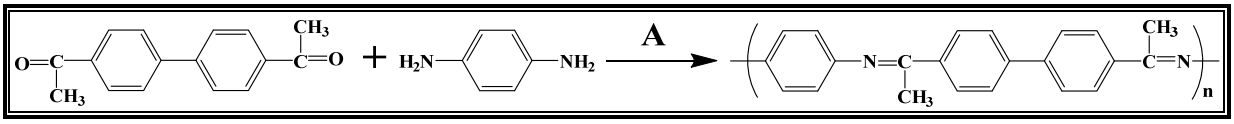

4,4'-Diacetylbiphenyl *para*-diphenyl diamine Poly(imine)

A: Polymer supported Lewis acids ($AlCl_3/SnCl_2/HgCl_2$)/100^oC/3 h

Scheme 8.2. Synthesis of poly(imine) using polymer supported Lewis acid

8.2.5. Characterization

The polymers obtained by suspension polymerization were purified by soxhlet extraction to remove unreacted ingredients. In the present work, both, base and modified polymers were characterizad by different techniques. FT-IR spectra were recorded on Perkin Elmer spectrophotometer to confirm the polymer synthesis using model spectrum GX. The samples were prepared after drying the polymers at 80^oC for 8 h. Surface area of polymers was determined by BET method using a surface analyzer NOVA 2000e, Quantachrome. Average particle diameter was determined using an Accusizer 780 (model LE 2500-20) PSS.NICOMP Particle sizing system, Santa Barbara, California, USA. Amine content was determined by acetic anhydride in pyridine using titrimetric method. Thermal stability (DTG) of polymer was evaluated using simultaneous thermal analysis (STA, Perkin Elmer) while glass transition temperature was studied by differential scanning calorimetry Q10 (Thermal analysis). Swelling ratio of polymers was determined by wt/wt ratio. Scanning electron microscopy was used for external morphology and particle visualization which were performed using Quanta 200-3D, dual beam ESEM microscope wherein an electron source was thermionic emission tungsten filament.

8.3. Results and discussion

Poly(allylamine-*co*-divinylbenzene) was synthesized by suspension polymerization by varying different crosslink density using cyclohexanol as a porogen. Monomer-crosslinker feed composition was determined by **equation 3.1.** Feed composition of monomer-crosslinker and reaction conditions of poly(AA-*co*-DVB) synthesis used in suspension polymerization is shown in **Table 8.1.**

Table 8.1. Monomer-crosslinker feed composition of poly(allylamine-*co*-divinylbenzene) synthesized by suspension polymerization at different crosslink density

Monomer system	CLD (%)	Allylamine		Divinylbenzene	
		mol	g	mol	g
Allylamine: Divinylbenzene	5	0.195	11.147	0.001	1.271
	10	0.180	10.256	0.018	2.339
	15	0.166	9.496	0.025	3.248
	20	0.155	8.842	0.031	4.033
	25	0.145	8.271	0.036	4.716

Reaction conditions: Batch size: 16 mL; 2,2'-azobisisobutyronitrile: 2.5 mol%; stirring speed: 500 rpm; reaction time: 3 h; outer phase: H_2O; protective colloid: poly(vinylpyrrolidone); protective colloid conc.: 1 wt%; porogen: cyclohexanol, porogen concentration: 48 mL (monomer:porogen ratio, 1:3 v/v).

8.3.1. Fourier transform infrared (FT-IR) spectroscopy

In the present work, poly(allylamine-*co*-divinylbenzene) was synthesized by suspension polymerization and modified with various Lewis acids such as aluminium chloride ($AlCl_3$), stannous chloride ($SnCl_2$), and mercury chloride ($HgCl_2$). The synthesis of polymer and its modification was confirmed by Fourier transform infrared (KBr pellet, cm^{-1}) spectroscopy. FT-IR illustrated that, peak appeared at 3367 assigned to primary amine in the polymer matrix.

Moreover, peaks observed at 2937, 1727, 1455, and 1250 correspond to aliphatic –C–H str., ester functionality, methyl C–H asymm. bend., and C–O–C str., respectively. Then, peaks at 906 and 797 were assigned to aromatic –C–H out-of-plane bending and disubstituted ring at *para* position[31] assigned by 832. Yet another, PSLAs revealed, $AlCl_3$ (1603, 1446) $SnCl_2$ (1603, 1447) and $HgCl_2$ (1602, 1445) peaks corresponds to Lewis acids[32] in addition to base polymer peak. FT-IR spectra of base polymer and PSLAs are illustrated in **Figure 8.1.**

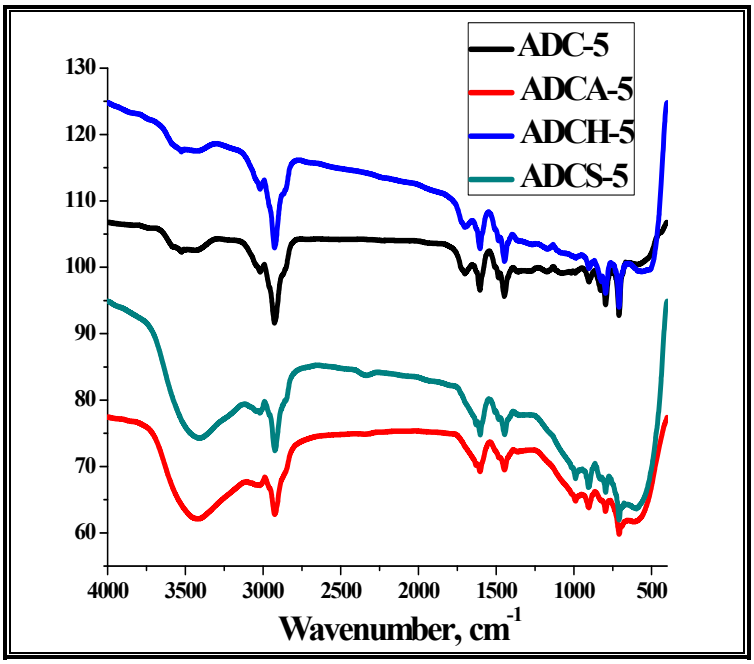

Figure 8.1. FT-IR spectrum of base polymer and PSLAs.

8.3.2. Surface area

Polymer efficiency is influenced by various properties including surface area, particle size, shape, and morphology of beaded polymers.[33] In general, solvating and non-solvating porogens have the property to impart micro and macroporous structure to the polymer matrix, respectively. In the present work, solvating porogen (cyclohexanol) was used to obtain micropores structure which attributes to high surface area. However, poly(allylamine-*co*-divinylbenzene) obtained by suspension polymerization for 5 and 25% crosslink density were used for surface area evaluation. Surface area was determined by nitrogen adsorption-desorption BET method. The result showed that, base polymers have a surface area of 80.78 and 165.41

m^2/g for 5 and 25% crosslink density respectively. It seems that, surface area was increased with increase in crosslink density.[34,35] However, polymer supported $AlCl_3$, $HgCl_2$, and $SnCl_2$ demonstrated the surface area of (76.39, 77.42), (62.28, 65.35), and (53.32, 57.54) for 5 and 25% crosslink density, respectively. It is worth noting that, surface area was decreased after modification with Lewis acids. At lower concentration of crosslinker, higher meso and macropores structure formation takes place resulting in lower surface area. In contrast, at higher amount of crosslinker, micropores slightly fused together which led towards increase in surface area. Thus, high surface area was obtained at higher crosslink density polymer and decreased with decrease in crosslink density.[36]

8.3.3. Amine content

Poly(allylamine-*co*-divinylbenzene) was synthesized by suspension polymerization from 5 to 25% crosslink density. The amine content of polymer was evaluated by well-known acetic anhydride in pyridine method, titrimetrically.[37] It was observed that, theoretical amine content was 15.7, 14.3, 13.0, 12.0, and 11.2 mmol/g whereas observed amine content was 4.0, 3.1, 2.7, 2.2, and 1.9 mmol/g for 5, 10, 15, 20, and 25% CLD, respectively. Results clearly revealed that, amine content was attenuated with increasing CLD because allylamine concentration was decreased with increasing CLD in copolymer composition. Furthermore, observed amine content is much lower compared to theoretical amine content. This is mainly due to amine functionality is well-buried into the polymer matrix consequently not available for titrimetric determination. Theoretical and observed amine content of poly(allyl-*co*-divinylbenzene) is depicted in **Figure 8.2.**

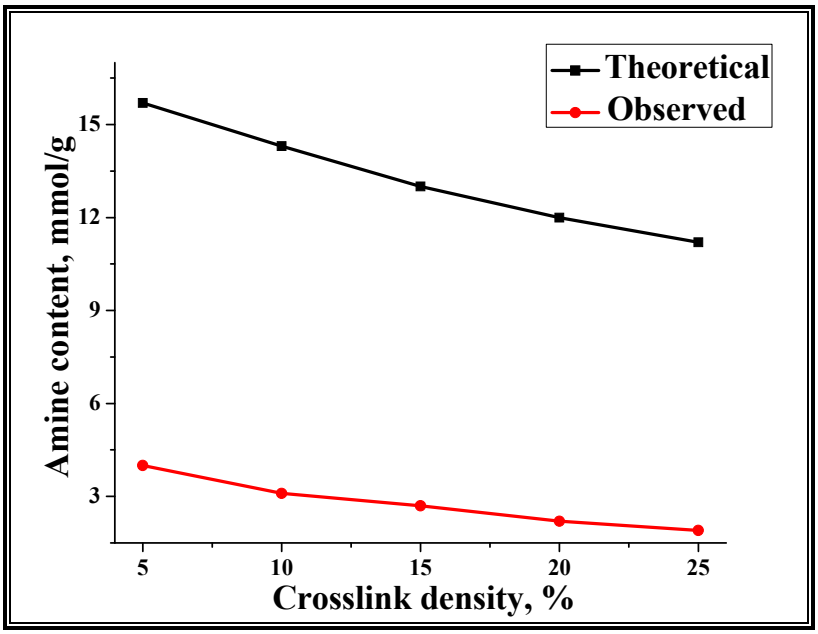

Figure 8.2. Theoretical and observed amine content of poly(AA-*co*-DVB)

8.3.4. Particle size

In reality, number of factors attribute to particle size. However, polymerization method is the major, and reaction parameters are the minor parameter that influences the particle sizes of polymers. In the present work, polymer was obtained by well-known suspension polymerization method. Undoubtedly, suspension polymerization is able to provide particle size in the range of 10–200 μm. Moreover, emulsion and dispersion polymerization techniques can provide nano sized polymer particles. However, some minor parameters including stirring speed, porogen (solvating/non-solvating), and porogen concentration also affect the polymer particle size. In this work, poly(allylamine-*co*-divinylbenzene) beads having 5 to 25% crosslink densities were obtained by suspension polymerization using a solvating porogen (cyclohexanol). Particle size of base polymers and PSLAs were evaluated. Results demonstrated that, particle sizes were slightly decreased with increasing crosslink density.[38] This phenomenon was observed perhaps due to highly crosslinked polymer has strong bonding between monomer and crosslinker. It must be pointed out that, polymer supported Lewis acids revealed slightly increased particle size due to surface modification with Lewis acids. Beads obtained by suspension polymerization have

particle size in the range 15–35 μm. The average particle sizes of base polymer and PSLAs are depicted in **Figure 8.3.**

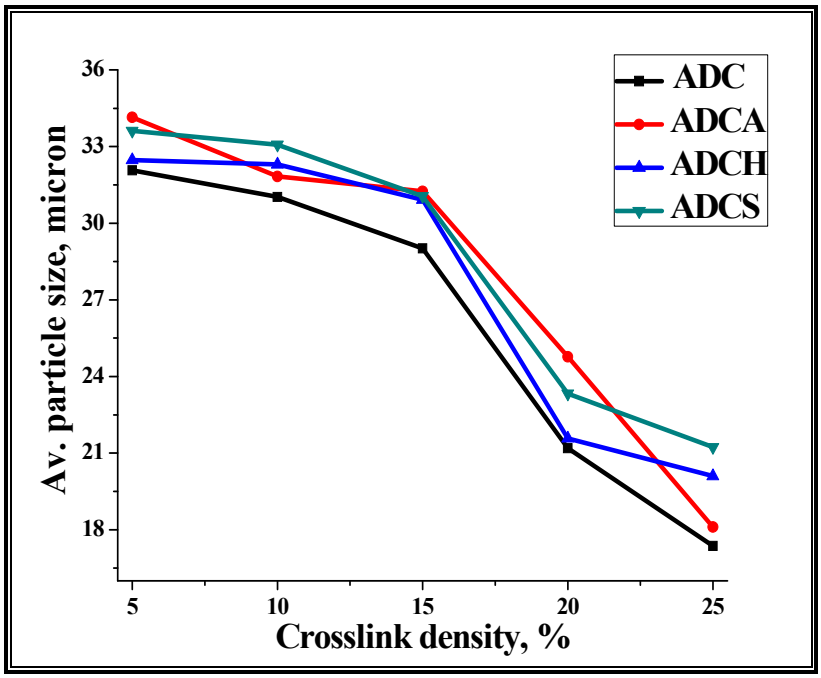

Figure 8.3. Average particle size of base polymer and PSLAs

8.3.5. Thermogravimetric analysis

Lewis acids were widely used in different organic reactions such as alkylation, acylation, sulfonylation, and dealkylation of tertiary butyl group.[39,40] However, Lewis acids are not only used at room temperature but also used in high temperature reactions. The temperature depends on the reaction conditions. Prior to use of the polymer supported catalysts in a reaction, thermostability study of PSLAs is an essential. Thermogravimetric analysis was carried out in the temperature range of 250–700^{o}C in a nitrogen overlay by simultaneous thermal analysis (STA, Perkin Elmer). Results clearly revealed that, degradation temperature (T_{dc}) of ADC (446, 435), ADCA (448, 435), ADCS (447, 444) and ADCH (448, 444) for 5 and 25% crosslink density, respectively. It is noteworthy that, T_{dc} of both base polymer and PSLAs was in the range of 430–450^{o}C. This is mainly due to small difference in crosslink density led to little difference

in T_{dc}. Decomposition temperature (T_{dc}) of base polymer as well as PSLAs are reported in **Figure 8.4.**

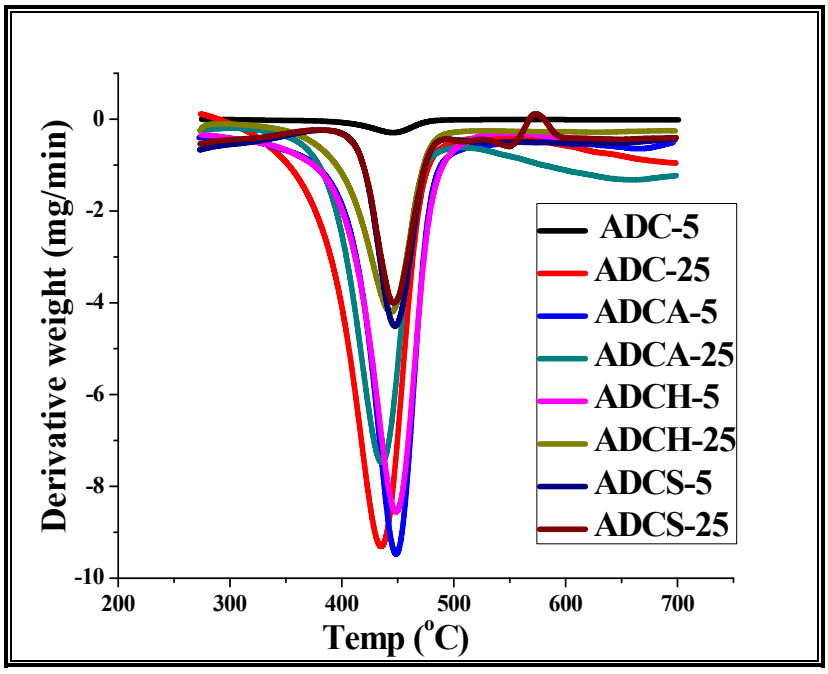

Figure 8.4. DTG curve of base polymer and PSLAs

8.3.6. Swelling ratio

Swelling ratio provides an essential information regarding the selection of the swelling solvent in solid phase synthesis. Generally, Lewis acids are used in non-aromatic solvents. Hence, non-aromatic solvents were selected for swelling purpose. Hildbrand solubility parameter of poly(AA-*co*-DVB) was calculated whereas solubility parameter of solvents were referred.[41] The solubility parameter was used to calculate polymer-solvent interaction parameter. Polymer-solvent interaction parameter is the theoretically prediction of swelling capacity of solvent to the polymer. Generally, each solvent can swell the polymer to a certain extent. This extent of swelling depends on the polymer-swelling solvent interaction parameter, polymer crosslink density, and porosity of polymer. The solubility parameter of polymers (calculated) and solvents (referred) are reported in **Table 8.2.** Solvents for swelling ratio study were selected according to

the solubility parameter of polymer. Solubility parameter of poly(AA-DVB) was determined[42] by the **equation (3.3).**

Table 8.2. Solubility parameter of polymer and different swelling solvents

Copolymer/Swelling solvent	Solubility parameter (δ) $(cal/cm^3)^{1/2}$
Poly(AA-*co*-DVB)	9.41
Ethanol	12.7
Acetonitrile	11.9
1,4-Dioxane	10.0

Polymer-solvent interaction parameter (χ) is directly proportional to molar volume of solvent and square of difference between solubility parameter of solvent and polymer. The calculated polymer-solvent interaction parameter is reported in **Table 8.3.** The polymer-solvent interaction parameter (χ) was determined[43] by Bristo and Watson semi empirical **equation (3.4).**

Table 8.3. Polymer-solvent interaction parameter

Copolymer	Solvent	Polymer-solvent interaction parameter (χ)
Poly(AA-*co*-DVB)	Ethanol	0.5934
	Acetonitrile	0.4698
	1, 4-dioxane	0.3519

Swelling measurements[44] were carried out by storing 0.5 g of polymer matrix in 20 mL of ethanol/acetonitrile/1,4-dioxane at room temperature for 24 h to obtain equilibrium swelling. The swelling ratio of crosslinked polymer was determined by measuring the weight of the polymer after equilibrium swelling in solvent (W_s) and after drying (W_d) of polymers. Swelling ratio was calculated[45] by the following mass swell ratio **equation (3.5).**

Swelling ratio was measured as a function of polymer-solvent interaction parameter and crosslink density of polymer. Polymer-solvent interaction parameter difference between poly(AA-*co*-DVB) and 1,4-dioxane is closer while difference was increased for acetonitrile and

further for ethanol. Results clearly indicated that, smaller the polymer-solvent interaction parameter more is the polymer swelling and vice-versa because at small interaction parameter difference there is no force to oppose the solvent to penetrate into the polymer matrix. Swelling ratio also depends on the polymer crosslink density. Swelling ratio was decreased with increasing crosslink density because small chains in high crosslink density polymer difficult to swell the polymer, contrary, long chain length in low crosslink density polymer easily expand and swell the polymer.[46,47] Thus, swelling ratio is the measure of crosslink density. The observed swelling ratio is represented in **Figure 8.5.**

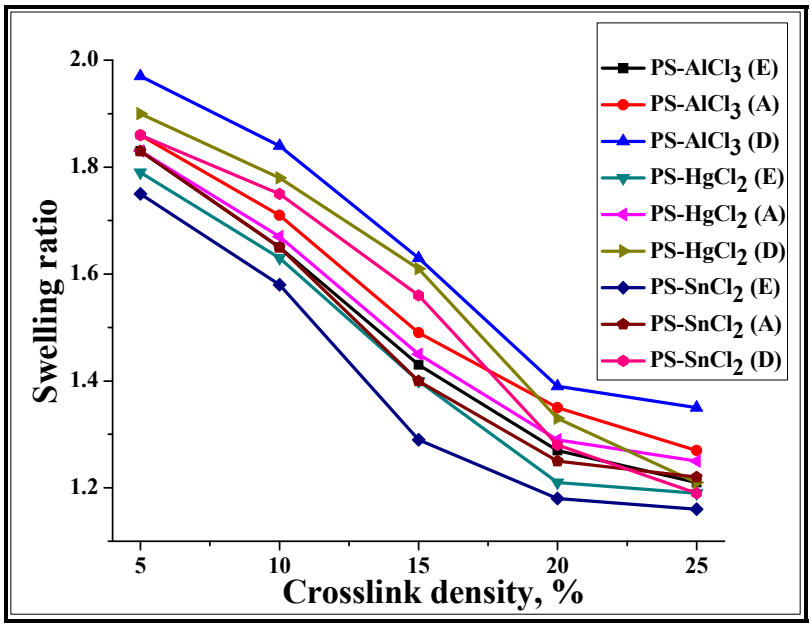

Figure 8.5. Swelling ratio of PSLAs

8.3.7. External morphology

SEM images of base polymer and PSLAs were scanned for 5 and 25% crosslink density polymers. For this, polymer beads were mounted on copper grid. This grid was placed below electron beam to observe the surface morphology of polymers. The polymers were conglomerated before and after polymer modification with Lewis acids. There is difference in surface morphology of base and polymer modified Lewis acid catalysts.[48,49] SEM images of base and PSLAs at 2500X magnification is represented in **Figure 8.6.**

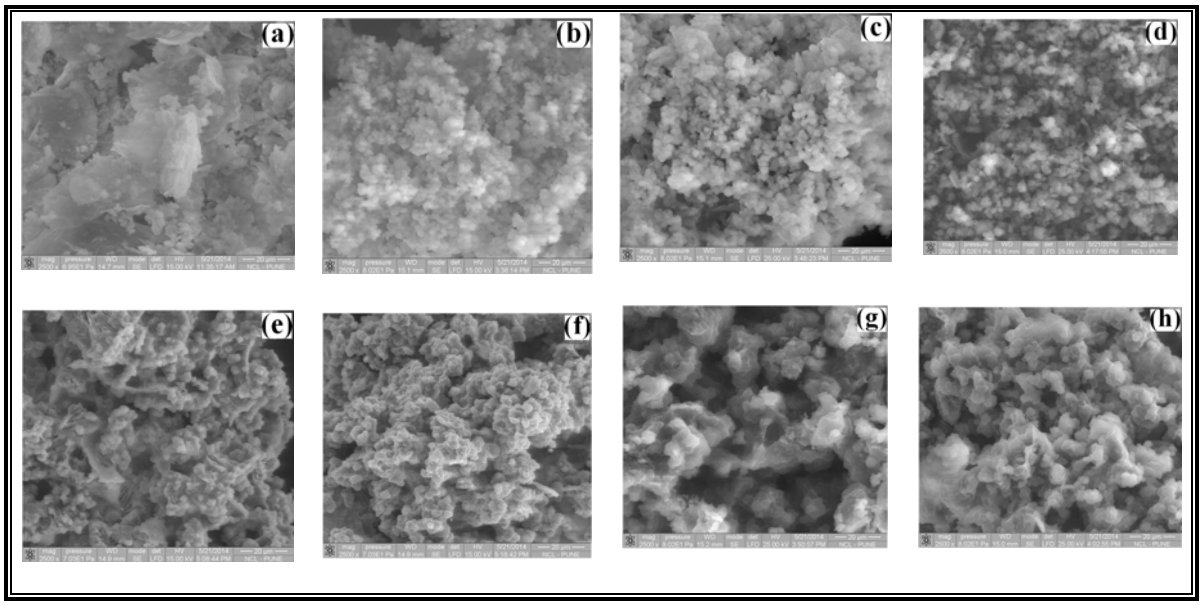

Figure 8.6. SEM images of base polymer ADC (a, b), and PSLAs of ADCA (c, d), ADCS (e, f), ADCH (g, h) for 5 and 25% crosslink density (2500X magnification)

8.3.8. Energy dispersive X-ray (EDX) analysis

Energy dispersive X-ray (EDX) analysis is the most important and well-known tool to evaluate the qualitative and quantitative determination of an element. In the present study, EDX analysis of base polymer and PSLAs were performed by Quanta 200-3D, dual beam ESEM microscope with thermionic emission tungsten filament as an electron source. The base polymer shows that, polymer contains carbon and nitrogen only. PSLA demonstrated the presence of aluminium, mercury, tin, and chlorine in their respective polymers. It was observed that, percentage of aluminium, mercury, and tin decreased with higher crosslink density. More metal modification was observed for 5% crosslink density. Results of polymer modification revealed that, aluminium 10 (5.18), mercury 31.01 (2.88), and tin 33.02 wt% (5.30 at%). Another interesting observation is that, more co-ordinate complex was formed between polymer and tin and decreased to mercury and further for aluminium. Hydrogen in the polymer is not detected due to an instrument limitation. EDX analysis (metal composition) of base and PSLA in wt and at% is depicted in **Figure 8.7.**

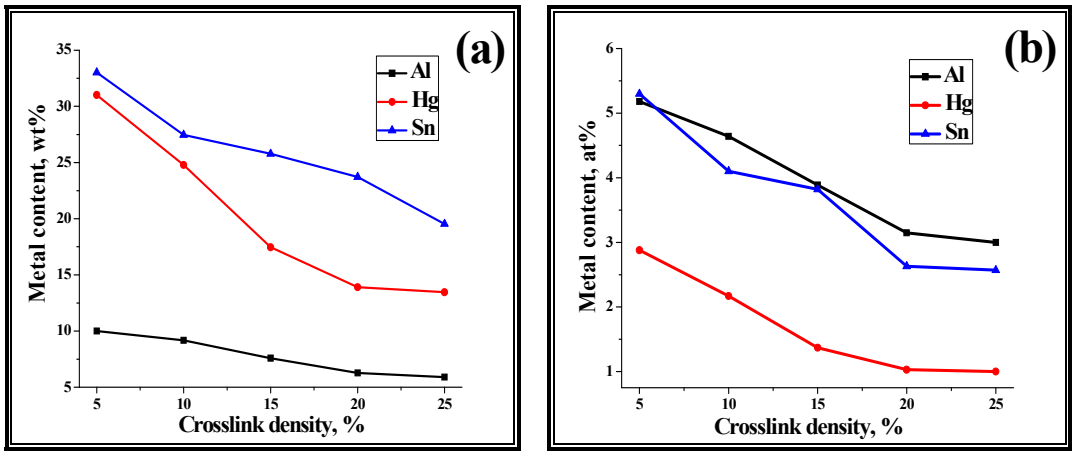

Figure 8.7. EDX analysis of PSLAs (a) wt%, and (b) at%

8.3.9. Application of poly(AA-co-DVB) supported Lewis acids in poly(imine) synthesis

In recent years, there has been potential use of PSLAs due to ease of recovery, recycle, and reuse properties. Consequently, use of PSLAs became industrially economical and environmentally benign. Polymer efficiency was evaluated using PSLAs in poly(imine) synthesis. Poly(imine) was synthesized using aforementioned procedure in section 8.2.4 and was confirmed by ^{1}H NMR (200 MHz, $CDCl_3$+TMS) which demonstrates δ 8.04 – 8.08 (8H, d), δ 7.70 – 7.74 (8H,d), and δ 2.65 (6H,S). More importantly, $–NH_2$ protons are absent. ^{1}H NMR of poly(imine) ($CDCl_3$+TMS, 200 MHz) is represented in **Figure 8.8.** Subsequently, thermal stability was also evaluated to confirm polymer synthesis. Differential thermogravimetric (DTG) analysis was performed by simultaneous thermal analysis (STA, Perkin Elmer) in the temperature range of 50–650^{o}C under nitrogen overlay at a heating rate of 10^{o}C/min. Thermal property evaluation demonstrated that, maximum decomposition temperature (Tmax) of poly(imine) was 291^{o}C and is illustrated in **Figure 8.9.**

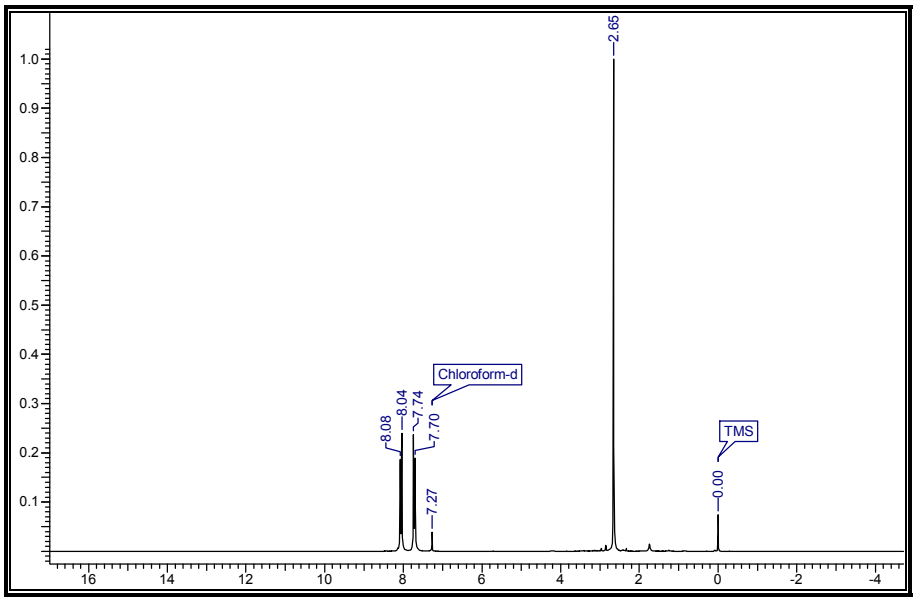

Figure 8.8. ^{1}H NMR of poly(imine)

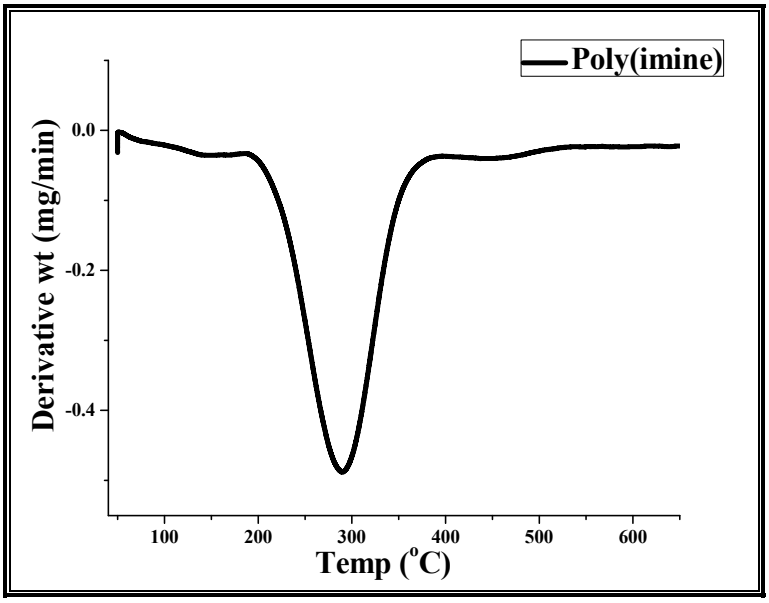

Figure 8.9. Differential thermogravimetric (DTG) analysis of poly(imine)

8.4. Conclusion

Hydrophobic poly(allylamine-*co*-divinylbenzene) was synthesized and modified with various Lewis acids for applications in an organic reactions. Average particle size of base and polymer supported Lewis acids (PSLAs) were in the range of 15–35 μm. Differential thermal analysis demonstrated that, maximum decomposition temperature is below 430^{o}C. Acid content revealed polymer reactivity whereas swelling ratio decides the suitable solvent for the polymer applications. High Lewis acid loading was observed with less crosslinked polymer than higher crosslinked polymer. Lewis acid leakage problem was possibly solved since highly reactive primary amine functionality binds Lewis acid strongly, consequently, polymer also promises for high efficiency of recovered PSLAs on the basis of strong co-ordinate bonding. PSLAs were successfully used in poly(imine) synthesis and the polymer recovered after completion of reaction which revealed recovery, recycle, and reuse properties of a polymer which would led to industrially economical and environmentally benign features. Obviously, polymers obtained in the present work not only promises to support the Lewis acids but also can be used to support various catalysts, reagents, substrates, scavengers and so on.

References

[1] Friedel C. and Craft J. M., *Compt. Rend.,* 1877, **84,** 1392–1395 and 1450–1454.

[2] Ran R. C. and Shen J., *J. Macromol. Sci. Chem.,* 1988, **A25(8),** 923–933.

[3] Rueping M. and Nachtsheim B. J., *Beilstein J. Org. Chem.,* 2010, **6,** 6. DOI:10.3.3762/bjoc.6.6.

[4] Kim Y. D., Kim J. H., Sim S. J., Woo K., Choi G. J. and Cho Y. S., *J. Ind. Eng. Chem.,* 1998, **4(4),** 329–333.

[5] Smith A. G. and Johnson J. S., *Org. Lett.,* 2010, **12(8),** 1784–1787.

[6] Prajapati S., Mishra A. P. and Srivastava A., *Int. J. Pharm. Chem. Biol. Sci.,* 2012, **2(1),** 52–62.

[7] Corma A. and Garcia H., *Chem. Rev.,* 2003, **103,** 4307−4365.

[8] Kawamura M., Cui D. M., Hayashi T. and Shimada S., *Tetrahedron Lett.,* 2003, **44,** 7715–7717.

[9] Fuson R. C., Weinstock H. H. and Ullyot G. E., *J. Am. Chem. Soc.,* 1935, **57(10),** 1803–

1804.

[10] Truce W. E. and Vriesen C. W., *J. Am. Chem. Soc.,* 1953, **75(20),** 5032–5036.

[11] Repichet S., Le R. C., Hernandez P., Dubac J. and Desmurs J. R., *J. Org. Chem.,* 1999, **64(17),** 6479–6482.

[12] Truce W. E. and Milionis J. P., *J. Am. Chem. Soc.,* 1952, **74(4),** 974–977.

[13] Qin Y. and Jakle F., *J. Inorg. Organomet. Polym. Mater.,* 2007, **17(1),** 149–157.

[14] Srirattnai K., Damronglerd S., Omi S., Roengsumran S., Petsomc A. and Ma G. H., *Tetrahedron Lett.,* 2002, **43,** 4555–4557.

[15] Chiang C. T., Lewis acid catalysts supported on porous polymer substrate. Patent No. US 05,770,539, 1998.

[16] Spitler E. L. and Dichtel W. R., *Nat. Chem.,* 2010, **2(672),** 672–677.

[17] Liao C. C. and Zhu J. L., *J. Org. Chem.,* 2009, **74,** 7873–7884.

[18] Dias L. C., *J. Braz. Chem. Soc.,* 1997, **8(4),** 289–332.

[19] Masoud M. and Masoumeh R. N., *Iran. J. Chem. Chem. Eng.,* 2013, **32(1),** 43–48.

[20] Bandini M., Fagioli M., Melloni A. and Umani-Ronchi A., *Adv. Synth. Catal.,* 2004, **346,** 573–578.

[21] Luis S. V., Burguete M. I., Ramireza N., Mayoral J. A., Cativiela C. and Royo A. J., *React. Polym.,* 1992, **18,** 237–248.

[22] Kobayashi S. and Nagayama S., *J. Am. Chem. Soc.,* 1998, **120,** 2985–2986.

[23] Clapham B., Reger T. S. and Janda K. D., *Tetrahedron,* 2001, **57,** 4637–4662.

[24] Ma H., Bao Z., Bai L. and Cao W., *Int. J. Org. Chem.,* 2012, **2,** 21–25.

[25] Ruicheng R. A. N. and Diankui F. U., *Chin. J. Polym. Sci.,* 1991, **9(1),** 79–85.

[26] Ma S. and Wang L., *J. Org. Chem.,* 1998, **63,** 3497–3498.

[27] Adams R. and Adams E. W., *Org. Synth.,* 1941, **1,** 459. DOI:10.15227/orgsyn.005.0087.

[28] Suzuki K., *Pure Appl. Chem.,* 1994, **66(7),** 1557–1564.

[29] Lee K. Y., Kawthekar R. B. and Kim G. J., *Bull. Korean Chem. Soc.,* 2007, **28(9),** 1553–1561.

[30] Foreman E., Puskas J. E., Fray M. E., Prowans P. and Piątek M., *Polym. Prepr.,* 2008, **49(1),** 822–823.

[31] Bartholin M., *Makromol. Chem.,* 1981, **182,** 2075–2085.

[32] Djomgoue P. and Njopwouo D., *J. Surf. Eng. Mater. Adv. Technol.*, 2013, **3,** 275–282.

[33] Hwang M. L., Lee Y. S., Kim T. G., Yang G. S., Park T. S. and Lee Y. S., *Bull. Korean Chem. Soc.,* 2010, **31(8),** 2395–2398.

[34] Pujari N. S., Vishwakarma A. S., Pathak T. S., Kotha A. M. and Ponrathnam S., *Bull. Mater. Sci.,* 2004, **27(6),** 529–535.

[35] Mane S., Ponrathnam S. and Chavan N., *Eur. Polym. J.,* 2014, 59, 46–58.

[36] Okay O., *Prog. Polym. Sci.,* 2000, **25,** 711–779.

[37] Vogel A. I., Elementary Practical Organic Chemistry, Part-III, Quantitative Organic Analysis, (Lond.), Chapter XIX, 1958, **2,** 697.

[38] Banerjee S., Chaurasia G., Pal D., Ghosh A. K., Ghosh A. and Kaity S., *J. Sci. Ind. Res.,* 2010, **69,** 777–784.

[39] Rueping M. and Nachtsheim B. J., *Beilstein J. Org. Chem.,* 2010, **6(6),** 1–24.

[40] Kawamura M., Cui D. M., Hayashi T. and Shimada S., *Tetrahedron Lett.,* 2003, **44,** 7715–7717.

[41] Paik U., Lee S. and Park J. G., *J. Semicond. Technol. Sci.,* 2008, **8(1),** 46–50.

[42] Weast R. C., CRC Handbook of Chemistry and Physics, CRC Press, Inc. U.S.A. 56th Edition C-725 (D), 1974–75.

[43] Barlkani M. and Hepburn C., *Iran. J. Polym. Sci. Tech.,* 1992, **1(1),** 1–5.

[44] Yildiz U. and Hazer B., *Macromol. Chem. Phys.,* 1998, **199,** 163–16.

[45] Brundha B. A. and Pazhanisamy P., *Int. J. Chem. Tech. Res.,* 2010, **2(4),** 2192–2197.

[46] Varga I., Gilanyi T., Meszaros R., Filipcsei G. and Zrınyi M., *J. Phys. Chem. B,* 2001, **105,** 9071–9076.

[47] Lee W. F. and Lin Y. H., *J. Mater. Sci.,* 2006, 41, 7333–7340.

[48] Hong L. S. and Lai J. H. T., *J. Chin. Inst. Chem. Engrs.,* 1999, **30(3),** 189–197.

[49] Wei X., Wang Z. J. Wang and Wang S., *Membr. Water Treat.,* 2012, **3(1),** 35–49.

SUMMARY & CONCLUSION

9.1. Summary and conclusion

Prime aim of this work was to synthesize the porous polymers having potential applications in various fields. Hydroxyl functionalized microporous and high surface area (564 m^2/g) crosslinked poly(HEMA-*co*-EDMA) and poly(HEMA-*co*-DVB) were synthesized successfully. Average particle size of polymer beads were in the range of 15–80 μm and this particle size promises for application in column chromatography as well as support for catalysts, reagents, and scavengers. Swelling ratio was useful to select a suitable solvent for solid phase synthesis. The thermogravimetric analysis (TGA) and differential scanning calorimetry (DSC) study helps to screen the polymer as a support in high temperature solid phase synthesis. This study implied that, surface area was increased and hydroxyl content was decreased with increasing crosslink density. Poly(HEMA-*co*-DVB) showed higher swelling ratio in toluene and DMF than poly(HEMA-*co*-EDMA) due to closer polymer-solvent interaction parameter and hydrophobic property of poly(HEMA-*co*-DVB) compared to poly(HEMA-*co*-EDMA). Thus, poly(HEMA-*co*-DVB) for 200% crosslink density is a suitable polymer support for adsorption and entrapment technology due to its high surface area, higher thermostability, and hydrophobic properties. Consequently, low crosslink density polymers are suitable polymer supports for further modification by covalent binding with catalysts, reagents, or substrates whereas high crosslink density polymers having large pore size are useful for entrapment of an enzymes as a polymer supported catalyst.

Megaporous acrylate based poly(MMA-*co*-EDMA) and poly(MMA-*co*-DVB) was synthesized using non-solvating porogens. It is worth noting that, surface area was decreased inversely pore volume and pore size was increased with increasing carbon content in the porogen. Surface area is higher for polymers obtained by cyclohexanol and decreased for n-octanol and further for n-decanol. In contrast, pore volume and pore size is higher for polymers obtained by n-decanol and decreased for n-octanol and further for cyclohexanol. Poly(MMA-*co*-EDMA) revealed the surface area of 94.7 and 294.5 m^2/g whereas poly(MMA-*co*-DVB) showed the surface area of 94.3 and 196.3 m^2/g for 25 and 200% crosslink density, respectively with cyclohexanol porogen which were significantly decreased for n-octanol and further for n-decanol. Interestingly, much higher pore size (5.47 μm) and pore volume (5.52 cc/g) was obtained with inexpensive n-decanol porogen whereas porous properties significantly decreased

for n-octanol and further for cyclohexanol. Higher rigidity of crosslinker (DVB) and its concentration increased the decomposition temperature of polymers. Opposite to this, higher flexibility of crosslinker (EDMA) and its concentration decreased the decomposition temperature as well as glass transition temperature of the microbeads. Observation revealed that, smaller the difference between polymer – solvent interaction parameter higher is the swelling ratio of polymer and vice-versa. However, polymer demonstrated the higher swelling in methanol compared to acetone. Owing to less crosslinking, small crosslink density polymer showed the higher degree of swelling compared to high crosslinked microbeads. Scanning electron microscopy images clearly revealed the porous nature of polymer beads. More importantly, cyclohexanol is a porogen which generates pores with high surface area and volume.

Effect of concentration of non-solvating porogen was also evaluated with poly(MMA-*co*-EDMA) and poly(MMA-*co*-DVB). Gigaporous microspheres were successfully synthesized bearing high pore volume and large pore size. Notably, higher concentration of non-solvating porogens led to more porous properties inversely small surface area. Surface area was increased with increasing concentration of crosslinker (crosslink density). It is worth mentioning that, surface area was decreased after 150% crosslink density (CLD) for all polymer series at 1:3 (monomer:porogen) ratio. Poly(MMA-*co*-DVB) displayed the highest pore volume and pore size for 100% CLD (1:3 v/v) which was 3.56 cc/g and 0.68 μm, respectively. Slight change in monomer to porogen ratio led towards substantial decrease in porosity. In case of poly(MMA-*co*-EDMA), porosity was increased with higher monomer to porogen ratio in the sequence of 1:1, 1:2, and 1:3. Average particle size of all polymer series showed the increased particle size upto 150% CLD, above this CLD, particle size was decreased steadily. Higher rigid or lower flexible crosslinker concentration revealed the better thermal properties of a polymer. Polymer-solvent interaction parameter (χ) illustrated that, polymer has less interaction with DMSO, contrary more interaction with MEK. This theoretical prediction was confirmed by swelling ratio. In other words, polymer showed more swelling in DMSO than MEK as a swelling solvent. Importantly, poly(MMA-*co*-DVB) displayed the higher swelling property than poly(MMA-*co*-EDMA) in DMSO as a swelling solvent. Although, polymers obtained from n-hexanol (1:3 monomer:porogen) have gigaporous properties. Especially, these polymers are an essential for

enzyme immobilization, loading of catalysts, metal chelating agent, as well as in adsorption and entrapment technology.

In conclusion, core-shell polymer was successfully synthesized bearing high surface area and porous properties. Core-shell polymer has the greater reactive sites resulting in more efficient polymer and consequently can be recognized as a versatile polymer support. Notably, core polymer was obtained bearing high surface area (554 m^2/g) which substantially attributes to more coating of shell polymer onto the surface of core polymer. Overall, synthesized core-shell polymer has more reactivity, high surface area and porosity. SEM images demonstrated the spherical nature of core-shell polymer with slight conglomeration. Racemic salbutamol was resolved using polymer supported D-(-)-dibenzoyl tartaric acid as a chiral selector for a period of 24 h. Salbutamol showed an enantiomeric excess of 52% in 24 h. In still another aspect, reactive core-shell polymer attributes to more loading of catalyst, reagent substrate, photosensitizer, resolving agent and chelating agent for solid phase synthesis and extraction. Thus, more reactive, high surface area and excellent porosity of core-shell polymer was obtained. Owing to recover, recycle, and reuse properties of a core-shell polymer, its use offers an economical and environmentally benign feature.

Poly(acrylic acid-*co*-trimethylolpropane triacrylate) was obtained for drug loading application in an acidic buffer medium. It was observed that, polymer supported gold has more adsorption capacity and selectivity with pantoprazole sodium than chloroquine as a consequence of more drug polarity and compatibility of pantoprazole sodium with polymer modified gold unlike chloroquine having less compatibility and polarity. Contact time displayed 91% of pantoprazole sodium and 62% of chloroquine loading in 24 h at pH 3. Initial 2 h is an exponential adsorption period for pantoprazole sodium whereas exponential adsorption begins after 12 h for chloroquine. Langmuir adsorption isotherm was well-fitted with drug loading which indicates monolayer drug adsorption. Pseudo-first and pseudo-second order kinetics showed the drug removal mechanism and physicochemical parameter are an attributing factor. Overall, polymer synthesized in the present work is the best drug carrier in an acidic buffer medium. This work also provided the high surface area, uniform and spherical polymer which increases efficiency of a modified polymer. In addition, thermostability was studied by TGA and

DSC which is useful to select the more efficient and thermostable polymer prior to the applications in high temperature reactions as a polymer support.

Moreover, hydrophobic poly(allylamine-*co*-divinylbenzene) was obtained synthesized and modified with various Lewis acids for applications in an organic synthesis. Average particle sizes of base and polymer modified Lewis acids were in the range of 15 – 35 μm. Differential thermal analysis demonstrated the decomposition temperature was below 430^{o}C. Acid content illustrates the polymer reactivity whereas swelling ratio decides the suitable solvent for polymer applications. High Lewis acid loading was observed with low crosslink density polymer than high crosslinked polymer. Lewis acid leakage problem was possibly solved since highly reactive primary amine functionality binds Lewis acid strongly. As a result, polymer also promises for more recycle and reuse efficiency on the basis of strong co-ordinate bonding. Polymer supported Lewis acids were successfully used in a poly(imine) synthesis and recovered after completion of reaction that implied recover, recycle and reuse properties of polymer and led towards industrially economical and environmentally benign. Obviously, polymers obtained in the present work not only promises to support Lewis acids but to support various catalysts, reagents, substrates, scavengers and protecting groups.

9.2. PUBLICATIONS

1. **Sachin Mane,** Surendra Ponrathnam, Nayaku Chavan, Synthesis and characterization of hypercrosslinked hydroxyl functionalized co-polymer beads. **Eur. Polym. J. 2014, 59, 46–58.**
2. **Sachin Mane,** Surendra Ponrathnam, Nayaku Chavan, Role of interfacial tension of solvating diluents and hydrophilic-hydrophobic cross-linkers in hyper-cross-linked solid supports**. ACS - Ind. Eng. Chem. Res. 2015, 54(27), 6893–6901.**
3. **Sachin Mane,** Surendra Ponrathnam, Nayaku Chavan, Design and synthesis of cauliflower-shaped hydroxyl functionalized core-shell polymer. **Des. Monomers Polym. 2015, 18(8), 723–733.**
4. **Sachin Mane,** Surendra Ponrathnam, Nayaku Chavan, Selective solid-phase extraction of metal for water decontamination. **J. Appl. Polym. Sci. 2016, 132(1), 42849.**
5. **Sachin Mane,** Surendra Ponrathnam, Nayaku Chavan, Synthesis and characterization of thermotropic liquid crystalline polyimides. **Bull. Mater. Sci., 2005, 38(6), 1553–1559.**
6. **Sachin Mane,** Surendra Ponrathnam, Nayaku Chavan, Hyperhydrophilic three-dimensional crosslinked beads as an effective drug carrier in acidic medium: adsorption isotherm and kinetics appraisal. **New J. Chem. 2015, 3835–3844.**
7. **Sachin Mane,** Surendra Ponrathnam, Nayaku Chavan, Interfacial tension approach toward drug loading with two-dimensional crosslinked polymer embedded gold: Adsorption kinetics evaluation. **Int. J. Polym. Mater. Polym. Biomater. 2015, DOI: 10.1080/00914037.2015.1074911.**
8. **Sachin Mane,** Surendra Ponrathnam, Nayaku Chavan, Crosslinked Polymer Embedded Cu/Ag for Comparative Drug Adsorption and Kinetics Evaluation**. Int. J. Polym. Mater. Polym. Biomater., 2015, DOI: 10.1080/00914037.2015.1119684.**
9. **Sachin Mane,** Surendra Ponrathnam, C. R. Rajan, Manohar Badiger, Nayaku Chavan, Role of aliphatic hydrocarbon content in non-solvating porogens toward abnormal porosity of cross-linked microbeads. **Revision Submitted, Polymer 2015, Polymer-15-1735.**
10. **Sachin Mane,** Surendra Ponrathnam, Nayaku Chavan, Synthesis and characterization of moisture-insensitive polymer anchored acidic catalysts for anhydrous solid phase synthesis, **Revision Submitted, Can. Chem. Trans., 2015, CCT-2015-0247.**

11. **Sachin Mane,** Surendra Ponrathnam, Nayaku Chavan, Role of interfacial tension of non-solvating diluents towards surface area and gigaporosity of beaded microsphere. **Under Review, Polymer, 2015.**
12. **Sachin Mane,** Surendra Ponrathnam, Nayaku Chavan, Solvent-free one-pot condensation reaction using hyper-branched silica grafted polyphosphoric acid: Synthesis of 9-(4-nitrophenyl)-9*H*-xanthene derivatives. **Ready for submission, J. Nanoparticle Res., 2015.**

9.3. REVIEWS

1. **Sachin Mane,** Surendra Ponrathnam, Nayaku Chavan,* A review on designing of controlling parameter for desired functional, porous, and crosslinked polymer properties. **Under Review, Polym Eng. Sci., 2015, PES-15-1329.**
2. **Sachin Mane,** Surendra Ponrathnam, Nayaku Chavan,* A review on effect of chemical crosslinking on desired polymer properties. **Revision Submitted, Can. Chem. Trans., 2015, CCT-2015-0245.**

9.4. PATENTS

1. **Sachin Mane,** Siona Daniels, Sarika Deokar, Smita Mule, Surendra Ponrathnam, Nayaku Chavan, Racemic drug resolution using polymer supported chiral selectors **[WO2015029072A2].**
2. **Sachin Mane,** Nayaku Chavan, Surendra Ponrathnam, Metal embedded hydrophilic polymer for drug delivery applications **[PCT/IN2015/050118].**
3. **Sachin Mane,** Nayaku Chavan, Surendra Ponrathnam, Selective solid phase extraction of heavy metal ions using crown ether anchored polymer support **[Provisional filing: 2724/DEL/2014].**
4. **Sachin Mane,** Nayaku Chavan, Surendra Ponrathnam, Hydrophobic polymer supported Lewis acid: recyclable catalyst **[Provisional filing: 0128/DEL/2015].**

9.5. CONFERENCES / SYMPOSIUMS / WORKSHOPS PRESENTATIONS

1. **Sachin Mane,** Surendra Ponrathnam, Nayaku Chavan, "Racemic drug resolution using polymer supported chiral selectors" APA international conference on **"Polymers: Vision and Innovations"** in Indian Institute of Technology (IIT), New Delhi, Feb-2014.

2. **Sachin Mane,** Surendra Ponrathnam, Nayaku Chavan, Conferences on Racemic drug resolution using polymer supported chiral selector" **"Advances in Polymers and Coatings-Rangotsav"** in Institute of Chemical Technology (ICT), Mumbai, Jan-2014.

3. **Sachin Mane,** Surendra Ponrathnam, Nayaku Chavan, "Synthesis, characterization, and applications of Polymer supported chiral selectors in chiral drugs resolution" poster presented in International conferences on **"Global Opportunities for Latest Developments in Chemistry and Technology"** in North Maharashtra University, Jalgaon, Feb-2014.

4. **Sachin Mane,** Surendra Ponrathnam, Nayaku Chavan, "Study of various effects on heavy metal ion chelation using polymer supported DB18C6 by spectrophotometric method" International conference on **"Solid Waste Management and Technology"** in Bharati Vidyapeeth University, Pune, Jan-2014.

5. **Sachin Mane,** Surendra Ponrathnam, Nayaku Chavan, Racemic drug separation using chiral selectors" International conference on **"Herbal and Synthetic Drug Studies"** in Abeda Inamdar Senior College, Pune, Feb-2014.

6. **Sachin Mane,** Surendra Ponrathnam, Nayaku Chavan, "*In vitro* metal responsive controlled drug release using hydrophilic metal nanoparticles" International conference **"NANOCON-014"** in Bharati Vidyapeeth University, Pune in Oct-2014.

7. **Sachin Mane,** Surendra Ponrathnam, Nayaku Chavan, "Drug polarity approach towards effective drug loading with hyperhydrophilic gold imprisoned polymer matrix: Adsorption isotherm and kinetics evaluation" International symposium **"MACRO-2015"** in Indian Association for Cultivation Science, Kolkata in Jan-2015.

8. **Sachin Mane,** Surendra Ponrathnam, Nayaku Chavan, International meet on **"Advances in Polymer Sciences"** in National Chemical Laboratory Oct-2014.

9. **Sachin Mane,** Surendra Ponrathnam, Nayaku Chavan, International conference on **"Recent Advances in Chemistry"** in Solapur University, Nov-2013.

10. **Sachin Mane,** Participated in 17th CRSI **"National Symposium in Chemistry-2015"** in

National Chemical Laboratory.

11. **Sachin Mane,** Surendra Ponrathnam, Nayaku Chavan, "Synthesis and characterization of high surface area polymers" poster presented in "**National Science Day"** Programme in Feb-2013, National Chemical Laboratory, Pune.

12. **Sachin Mane,** Surendra Ponrathnam, Nayaku Chavan, "Racemic drug resolution using polymer supported chiral selector" poster presented in **"National Science Day"** Programme in Feb-2013, National Chemical Laboratory, Pune.

13. **Sachin Mane,** Surendra Ponrathnam, Nayaku Chavan, "Heavy metal ion chelation using crown ether anchored polymer support" work presented in **"National Science Day"** Programme in Feb-2014, National Chemical Laboratory, Pune.

14. **Sachin Mane,** participated in the workshop of "Particle size and colloidal stability using Dynamic Light Scattering: Nano to Micro".

15. **Sachin Mane,** participated in "Patent certificate course for scientist and engineers" conducted collaboratively by Venture center, IPFACE and National Chemical Laboratory in Feb-2014.

16. **Sachin Mane,** participated in three month "Patent Agent Course-2014" conducted by Venture Center, National Chemical Laboratory, Pune.